STRUCTURAL TUNING OF MONTMORILLONITE CLAYS BY PILLARING: DESIGNING OF SHAPE SELECTIVE SOLID ACID CATALYSTS AND PANI - MONTMORILLONITE NANOCOMPOSITES

Thesis submitted to

Cochin University of Science and Technology

In partial fulfillment of the requirements for the degree of

DOCTOR OF PHILOSOPHY

IN

CHEMISTRY

In the Faculty of Science

By

BINITHA N N

Department of Applied Chemistry

Cochin University of Science and Technology

Kochi-22

OCTOBER 2006

In memory of my loving father

…..who dreamt a lot about me

DEPARTMENT OF APPLIED CHEMISTRY

COCHIN UNIVERSITY OF SCIENCE AND TECHNOLOGY

KOCHI - 682 022, INDIA

Phone : 0484-2575804, Telex : 885-5019 CU IN, Grams : CUSAT
Fax : 91-484-2577595, E-mail : chem@cusat.ac.in Web: www.cusat.ac.in/dac

CERTIFICATE

Certified that the present work entitled **"Structural tuning of Montmorillonite clays by pillaring: Designing of shape selective solid acid catalysts and PANI - Montmorillonite nanocomposites"**, submitted by Ms. Binitha N.N is an authentic record of research work carried out by her under my supervision at the Department of Applied Chemistry in partial fulfillment of the requirements for the degree of Doctor of Philosophy in Chemistry of the Cochin University of Science and Technology and has not been included in any other thesis submitted previously for the award of any degree.

Professor Dr.S. Sugunan
(Supervising Guide)
Department of Applied Chemistry
Cochin University of Science and Technology
Kochi- 682022.

Kochi-22
11-10-2006

DECLARATION

I hereby declare that the present work entitled **"Structural tuning of Montmorillonite clays by pillaring: Designing of shape selective solid acid catalysts and PANI - Montmorillonite nanocomposites"** is based on the original work done by me under the guidance of Dr.S. Sugunan, Professor in Physical Chemistry, Department of Applied Chemistry, Cochin University of science and Technology and has not been included in any other thesis submitted previously for the award of any other degree.

Binitha N N

BINITHA N N

Kochi-22

11-10-2006

The two-dimensional Montmorillonite clay structures can be made as thermally stable three-dimensional solid by intercalating the clay with inorganic polycations and that result in increase in the fraction of internal surface area available for adsorption and eventually for catalytic processes. In addition, pillaring provides acidity to the material. The pillared clays (PILCs) are an interesting alternative to zeolites in catalytic processes and have attracted considerable attention in basic research.

Friedel-Crafts alkylation of aromatics is an important reaction used in the synthesis of fine chemicals and/or intermediates for the preparation of fine chemicals in pharmaceutical and other chemical industries. The conventional method adopts homogeneous catalysts that pose several environmental and separation problems. Development of reusable solid acid catalysts having high activity is, therefore, of great practical importance in this era of Green Chemistry. Clays, due to the interlayer microenvironment are effective heterogeneous shape selective catalysts for a wide variety of organic reactions.

Polymer nanocomposites are a class of hybrid materials composed of an organic polymer matrix that is imbedded with inorganic particles which have at least one dimension in the nanometer size range. At this scale, they can strongly impact the macroscopic properties of the polymer. The small particle size, layer structure, high aspect ratio and ease of ionic modification of clays permit the formation of clay/polymer nanocomposites that are typical examples

of nanotechnology. The subject of hybrids based on layered inorganic compounds such as clays has been studied for a considerable time, but the area is enjoying a resurgence of interest and activity as a result of the exceptional properties which can be realized from such nanocomposites.

The present study deals with PILCs. Ti, Zr, Al and Cr single and mixed pillared montmorillonites are prepared. A number of techniques have been used to get valuable information on PILC structure, acidity, porosity, surface area, etc. These PILCs are efficiently used as solid acid alternatives for homogeneous Friedel-Crafts catalysts. The reactions selected are isopropylation of benzene and toluene, ethylation of benzene, toluene methylation as well as Linear Alkyl Benzene synthesis. In-situ polymerization of aniline is done inside the pillared clay matrix where the non-swellable PILC confined matrix allowed efficient polymerization that leads to high polymer order, crystallinity and nanofibrous morphology.

Here the thesis is structured into twelve chapters. The first three chapters deals with the introduction, materials, methods and PILC characterization. Fourth chapter explores the need of solid acid PILC catalysts for Friedel-Crafts alkylation reactions. Then the following five chapters describe the reactions selected. Tenth chapter introduces polyaniline, its nanocomposites, the materials used and the methods adopted for the composite preparation and characterization. The results and discussion of the obtained polyaniline/PILC nanofibers are displayed in the eleventh chapter. Last chapter summarizes and concludes the present work with a brief future outlook.

Acknowledgement

It seems to me shallow and arrogant for any man in these times to claim he is completely self-made, that he owes all his success to his own unaided efforts. Many hands and hearts and minds generally contribute to anyone's notable achievements.

Walt Disney

I wish to express my gratitude to a number of people who made this thesis possible and an unforgettable experience for me. Before that, let me thank God almighty, for all the blessings showered upon me till now.

With deep sense of gratitude, I express my obligation towards my supervising guide, Prof. Dr.S. Sugunan, for his excellent guidance, timely suggestions and the freedom in discussing problems. He provided a motivating, enthusiastic, and critical atmosphere during the many discussions we had. His smiling confidence towards students gave great pleasure to me to conduct my research work under his supervision.

I thank Prof Dr.M.R. Prathapachandra Kurup, Head, Department of Applied Chemistry for providing the necessary facilities for the research work.

I remember with gratitude my MSc teachers, Prof Dr.K.K. Mohammed Yusuff, Dr.K. Sreekumar, Dr.S. Prathapan, Dr.K. Girish Kumar, Dr.P.A. Unnikrishnan, Dr.P.V. Mohanan, Dr.A.G. Ramachandran Nair and Dr.S. Sreedevi. We the students cannot forget Dr. Nalini Chakraborthy for her wise counsels and she is living in our memories.

My fascination towards research and clay science started during MSc project period at Clays and Clay Minerals Division, RRL, Thiruvananthapuram, under the firing guidance of Dr.D. Bahulayan, (presently, Research Fellow, Department of Chemistry, National University of Singpore). His valuable suggestions, constructive comments and encouragement maintained confidence in perplexed situations of the

research work. The technical helps, in doing clay characterization are also acknowledged.

Blessings from Sr. Robin, Ms. Shoshamma, other teachers and friends at Little Flower college, Guruvayoor are my strength during the difficult situations of life at CUSAT. The mental support from Jainy for the last 12 years is a great relief in troublesome moments. She encouraged me to grow and to expand my thinking. I am lucky to have such a good friend.

The peaceful and loving moments shared by the non teaching staffs of the Department of Applied Chemistry, CUSAT, is always a relaxation during the continuous hours spent in the lab. I thank Usha chechi, Sreerekha chechi, Saradha chechi, Bharathy chichi, Indira devi SO chechi, Molykkutty SO chechi, Ammini chechi Valsala madam, Uma, Jisha, Bindhu, Vineetha chechi, Ajitha chechi, Radhakrishnettan, Manojettan, Krishnankutty chettan and other present and former non-teaching staffs of the department.

I thank Mr.S. Shylesh, NCL, Pune, for his selfless support, encouragement and helps extended in literature collection. I acknowledge with thanks the helps rendered from Dr.M.R. Anantharaman, Lecturer, Department of Physics, CUSAT and Dr.S. Lokesh, Dept of Inorganic & Physical Chemistry, IISC, Bangalore, in doing conductivity studies. Helps from Aravindettan in literature collection is very useful during thesis writing. Special thanks to Sebastain chettan, Iswarya and Sreeja P. B for helping in literature collection.

The cheerful moments shared by Seema, Subhadra, Reshmi, Saritha, Jaya, Sreerekha, Abha, Nandhini, Aparna, sajisha and Radha during my stay at Aiswarya Hostel, CUSAT is unforgettable. My gratitude for their care and precious friendship. The hours spent with my MSc juniors, Mary, Ani, Raji, Thena, Zurumiya and Priya was a relief from the hazardous starting period of research work. I would like to thank my senior lab mates Dr. Suja Haridas, Dr. Deepa C.S, Dr. Manju Kurian, Dr. Sunaja Devi K.R, Dr. Fincy Jose, Dr. Sanjay Gopinath and Dr. Bejoy Thomas for the

many comments and advice. The smiling and caring moments shared with Dr. Rehna K Shamsudheen, Dr. Sreeja Rani. K, Dr. Renuka. N.K and Dr. Nishamol Kannat is ever memorable.

I thank my MSc classmates Ambily, Rekha, Raji, Neil, Sukesh, Kannan and Pavi for still keeping our relationship fresh. I place on record here my sincere gratitude to Rekha for the initial guidance in doing computers. I thank Roshni, Daly, Mini, Pearl, Annu, Sreesha, Bessy, Boli, Suni chechi, Seena, Serina, Leji, Rema chechi, Vidya chechi, Mangala, John, Arun, Manoj, Anoop, Rajesh and all other research scholars of the department for their love and companionship.

I take this opportunity to thank Mr. Kashmiri and Jose Sir of USIC, CUSAT, Suresh and Kumar, Service engineers of Chemito, Shibu Eapen, Adarsh, Saji, Aneesh and Prem of SAIF, STIC, CUSAT, for the technical helps extended in during various analyses. I extend my special thanks to Indraneel, IIT Madras, Saravanan, Veena, Swapna, Vijitha, Beena and other friends in the Department of Physics for their readiness to help on various occasions. Helps from Arun in doing DRS Analysis, John in FTIR Analysis and Rani in TGA is remembered with gratitude. STIC (CUSAT), SAIF (IITB, CDRI, Lucknow and IISc Bangalore) are acknowledged for carrying out clay and composite characterization.

I feel privileged to have been able to work with Shali, Maya and Salini. The mental support provided by them in times of shade is ever memorable. Radhika, Kochurani, Ajitha teacher and Reshmi were always there to help me immensely by giving encouragement and friendship. Thanks a lot, Joyes teacher for your language corrections in the final draft of this thesis. Suraj and Ramu were there to keep the spirit of pooram, elephant, etc at Thrissur - the cultural capital of kerala, even in the stressful hours of lab work.

Character develops at home, all good qualities in me is a result of the love, affection and caring from my parents. The expectation of my mother is the basis of all my achievements. I studied cooperation from my siblings. I am glad to be one of them.

Acknowledgement

I take this opportunity to express the profound gratitude from my deep heart to my beloved parents, grandparents, and my siblings for their love and continuous support – both spiritually and materially. I believe I owe deepest thanks to my in laws for the moral support extended throughout my research work. The cute and tender moments with appu, ammu, aju, pappi and my unnimol is a nice feeling in situations of frustration.

This thesis could not have been accomplished without my husband who is always with me no matter how dubious my decisions are. He always gives me warm encouragement and love in every situation. Words are inadequate when I wish to express my appreciation towards him without whose constant support I could not have completed my lab work successfully. He was always ready to suffer any difficulties for the completion of my Ph. D work. I apologise him for the hours he spent in helping me in computers, for his university visits etc, in spite of all the domestic affairs. It may be easy to get a loving husband but rare to get one who considers the partner's work satisfaction. He is certainly the main contributor of all the best in my life for the last three years; I thank God for the extraordinary chance of having him as my husband, friend and companion.

The financial support granted by CSIR, New Delhi is gratefully acknowledged.

Binitha N.N.

CONTENTS

Chapter 1 CLAYS: INTRODUCTION AND LITERATURE SURVEY

Chapter 1

CLAYS: INTRODUCTION AND LITERATURE SURVEY

The natural abundance and eco-friendliness makes clays important in this era of Green Chemistry. In addition to conventional industrial applications the layered structure introduces clays into the field of catalysis as well as nanotechnology. The process of pillaring props the layers apart and converts clays to thermally stable structure. The enhancement in layer distance allows shape selective catalysis and polymer/clay nanocomposite formation within the matrix due to the increased insertion of reactant molecule and monomers. The confined matrix leads to well ordered polymer chain formation. In this chapter introduction to clays and its applications in catalysis as well as polymer/clay nanocomposites are described. The process of pillaring with detailed description of the available pillaring agents and the improvement in structural properties are also given.

1.1 CLAY MINERALS

Clay minerals are the most important chemical weathering product of the soil. They are formed by the alteration of existing minerals or by synthesis from elements when minerals weather to their elemental form. In general the term clay implies a natural, earthy, fine - grained material, which develops plasticity when mixed with a limited amount of water (Grim, 1968). Clays and clay minerals occur under a fairly limited range of geologic conditions. The environments of formation include soil horizons, continental and marine sediments, geothermal fields, volcanic deposits, and weathering rock formations. Most clay minerals are formed when rocks come into contact with water, air, or steam. Examples of these situations include weathering boulders on a hill side, sediments on sea or lake bottoms, deeply buried sediments containing pore water, and rocks in contact with water heated by magma (molten rock). All of these environments may cause the formation of clay minerals from preexisting minerals. Extensive alteration of rocks to clay minerals can produce relatively pure clay deposits that are of economic interest.

Clay minerals are distinguished from other colloidal materials by the highly anisometric and often irregular particle shape, the broad particle size distribution, the flexibility of the layers, the different types of charges (permanent charges on the faces, P^H- dependent charges at the edges), the heterogeneity of the layer charges, the pronounced cation exchange capacity, the disarticulation (in smectites) and the different modes of aggregation.

Chemically clays are microcrystalline, hydrous aluminium (occasionally Mg and/or Fe) silicates. Majority of these minerals have layer structures and therefore are called phyllosilicates, but some have chain structures and these are called inosilicates.

1.2 STRUCTURE OF CLAYS

The term clay generally refers to aluminosilicates where the particle size is in the micron range and which exhibit cation exchange capacity. This broad definition encompasses zeolites, but the term is normally used in connection with sheet silicates only. The atomic structure of the clay mineral consists of two types of structural units. These are the SiO_4 tetrahedron and $Al(OH)_3$ gibbsite or $Mg(OH)_2$ brucite octahedral unit, both of which form sheet or layer structure (figure 1.2.1).

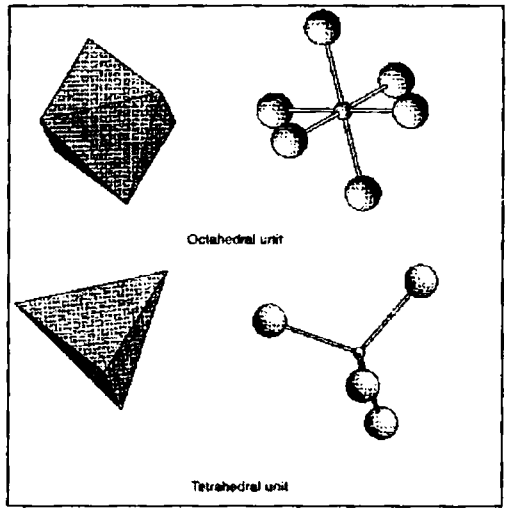

Figure 1.2.1 Tetrahedral as well as octahedral structural units of clay minerals

Tetrahedral layers consist of continuous sheets of silica tetrahedra linked via three corners to form a hexagonal mesh and the fourth corner of each tetrahedron (normal to the plane of the sheet) is shared with octahedral in adjacent layers. Octahedral layers in clay mineral, on the other hand consist of flat layers of edge – sharing octahedra, each formally containing cations at its center (usually Al^{3+} or Mg^{2+}) and OH^- or O^{2-} at its apices[1] (figure 1.2.2).

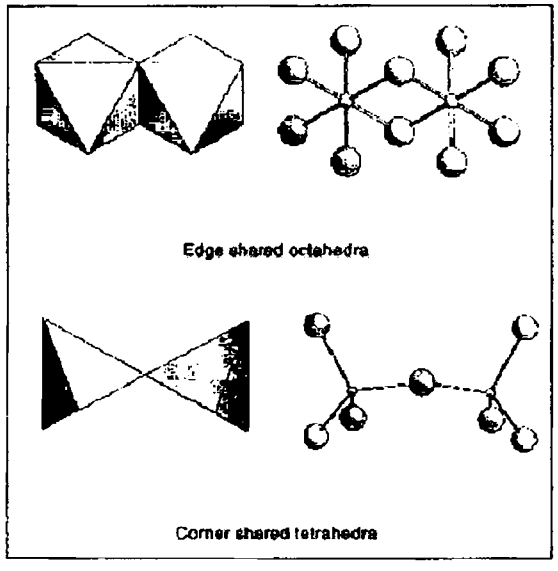

Figure 1.2.2 Edge shared octahedra and corner shared tetrahedra forming clay layers

The general structural scheme of clay minerals is generated by the combination of sheets of tetrahedral and octahedral units (figure 1.2.3). The apical oxygens of the tetrahedral layers replace 2/3 of the hydroxyls in one plane of the octahedral layer. The remaining OH^- ions in this layer are in the

centers of the hexagons formed by the oxygens of the tetrahedral layer. The different arrangement of tetrahedral and octahedral layers leads to different classes of clay minerals.

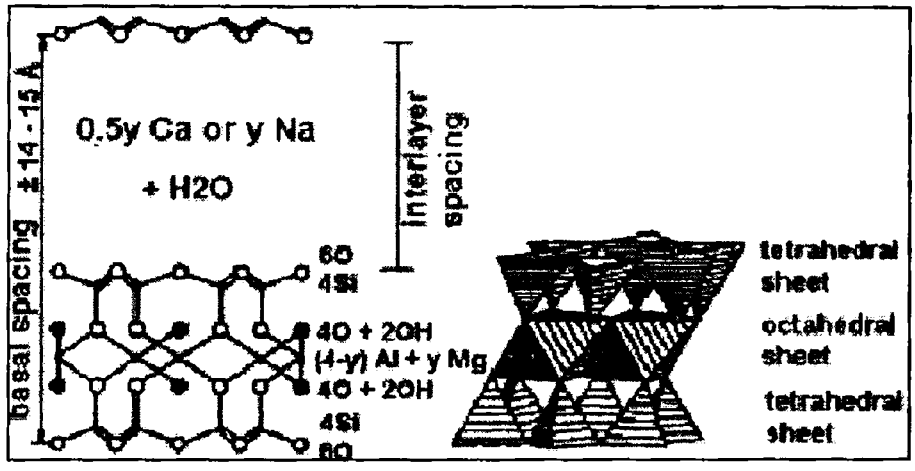

Figure 1.2.3 One of the possible combinations of tetrahedral and octahedral layers

When trivalent aluminium is the dominant cation in the octahedral layer, only 2/3 of the octahedral sites are occupied. Such a structure is described as "dioctahedral" and there are two octahedral cations per unit cell. When a divalent cation such as Mg^{2+}, is dominant in the octahedral layer, all the available sites are filled. In this type of structure there are three octahedral cations per half unit cell and the structure is described as "trioctahedral" (figure 1.2.4).

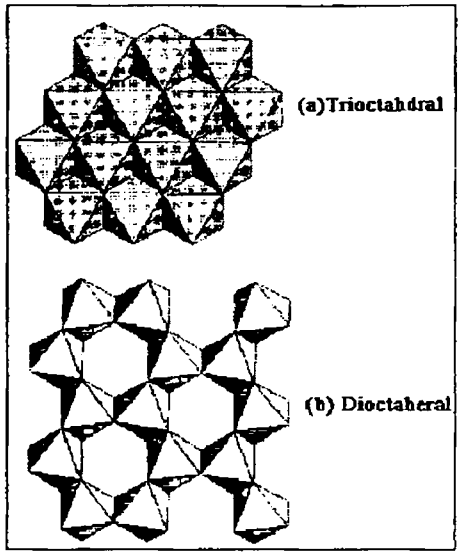

Figure 1.2.4 Octahedral sheets for the trioctahedral (a) and dioctahedral (b) cases. Note that the existence of the vacant octahedral site (b) creates distortions in the remaining octahedral sites and an enlargement of the octahedral site, which is missing the cation

The different classes of clay minerals have a different arrangement of tetrahedral and octahedral layers and are named as 1:1, 2:1, 2:1:1 etc. Structural units of clays therefore consists of either

(a) Alternating tetrahedral or octahedral sheets (OT or 1:1 structure) e.g. Kaolinite group.

(b) A sandwich of one octahedral sheet between two tetrahedral sheets (TOT or 2:1 structure) e.g. Smectite clays

(c) An arrangement in which the three layers TOT units alternate with a brucite layer (2:1:1 structure) e.g. Chlorite.

1.3 ISOMORPHOUS SUBSTITUTION IN LAYERS

Si^{4+} mainly occupies tetrahedral sites in clay minerals. However, isomorphous substitution by Al^{3+} is also common. In the case of trioctahedral, Mg^{2+} generally occupies octahedral sites. Isomorphous substitution by other divalent cations such as Fe^{2+} or Ni^{2+} or by univalent cations such as Li^{+} is common. In the case of dioctahedral clay minerals, octahedral sites are predominantly occupied by Al^{3+} and isomorphous substitution by other trivalent cations like Fe^{3+}, Cr^{3+} or divalent cations like Mg^{2+} or Fe^{2+} are common.

As a result of isomorphous substitution, in some clay the valencies of coordinated oxygens are no longer saturated and thus the layer acquires a net negative charge.

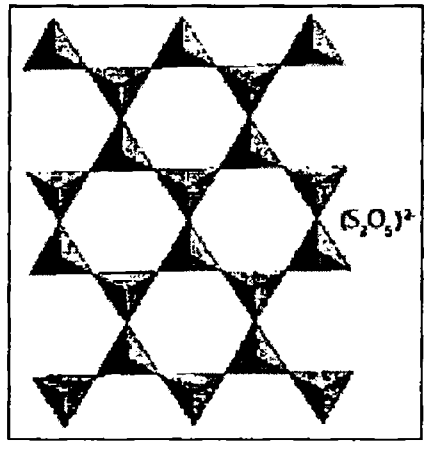

Figure 1.3.1 Two dimensional tetrahedral sheet of composition $(S_2O_5)^{2-}$

In order for electro neutrality to be maintained, cations come into the interlamellar space. The current working definition of clay is a phyllosilicate consisting of two - dimensional tetrahedral sheets fused to octahedral sheets and, if necessary for charge neutrality, coordinated to charge balancing cations. Phylosilicates are themselves defined as consisting of sheets of fused tetrahedra of composition $(S_2O_5)^{2-}$, $(S = Si, Al, Fe etc)^2$ as shown in figure 1.3.1.

Most clays but by no means, all swell upon by the intake of water and other, generally polar solvents such as ethanol or glycerol. Clays are one class of a large number of distinct structural types, which are possible using the SiO_4 tetrahedron as building block. The mineral kingdom contains many more structures derived from SiO_4 than any other unit.

1.4 COMPOSITION AND FABRIC OF CLAYS

The composition and fabric of important clay minerals are given below.

1.4.1 Kaolinite group

Structure: 1:1 dioctahedral

Composition: $Al_4Si_4O_{10}(OH)_8$

The mineral species: Kaolinite, nacrite, dickite, halloysite, anauxite.

Here the charges within the structural unit are balanced. There is a slight substitution of Ti and Fe for Al. Halloysite is the hydrous form of

kaolinite. The presence of interlayer water in halloysite makes the bonds rather weak. Halloysite occurs in tubes whereas the rest of the minerals in this group are tabular.

1.4.2 Serpentine Group

Structure: 1:1 trioctahedral

Composition: $Mg_6Si_4O_{10}(OH)_8$

The mineral species: chrysotile-fibrous, lizardite-platy, antigorite-fibrous

Variety of atomic substitutions can take place. The following substitutions are possible:

Tetrahedral: Si^{4+}, Al^{3+}, and Fe^{3+}

Octahedral: Al^{3+}, Mg^{2+}, Fe^{2+}, Fe^{3+}, Co^{2+}, Mn^{2+}, Ni^{2+}, and Cr^{3+}

1.4.3 Montmorillonite or Smectite group

Structure: 2:1 dioctahedral or trioctahedral

Composition: $Mx_{/n}.YH_2O[Al_{4.0-x}Mg_x]Si_8O_{20}(OH)_4$

The mineral species is either a dioctahedral smectites such as montmorillonite, beidellite and nontronite or trioctahedral smectites such as hectorite, saponite, sauconite etc. They have a charge deficiency either in the octahedral or tetrahedral layer.

1.4.4 Pyrophyllite Group

Structure: 2:1 dioctahedral

Composition: $Mg_3Si_4O_{10}(OH)_2$

Layers are electrically neutral so that no interlayer cation is present. If alumina replaces silica, the structure is no more neutral. To balance it K^+ may be added, which produces muscovite.

1.4.5 Talc

Structure: 2:1 dioctahedral

Composition: $Al_2Si_4O_{10}(OH)_2$

The bonds are held together with Van der Waals forces so it gives a greasy feeling to talc. Layers are electrically neutral, thus no interlayer cation is present.

1.4.6 Mica Group

Structure: 2:1 dioctahedral or trioctahedral

Composition: $X_2Y_{4-6}Si_6Al_2O_{20}(OH)_4$;

(X = K and/or Na, Y = Al and/or Fe and/or Mg)

The mineral species includes dioctahedral micas; muscovite, paragonite, phengite, leucophyllite etc and trioctahedral micas such as biotite, phylogopite, lepidolite, taeniolite etc. Most commonly the mineral illite (dioctahedral) is closely related to muscovite though it contains less potassium and more water and shows structural variability. Glauconite may be regared as an iron rich

illite that has larger amounts of ferric iron than aluminium in the octahedral layer.

1.4.7 Chlorite

Structure: 2:2 trioctahedral

Composition: $(mg_{6-y-x}Fe_yAl_xSi_{4-x})O_{10}(OH)_8$

Isomorphous substitutions. There are many mineral names for compositionally distinct members of the group and extensive solid solutions occur by ionic substitution between members

1.5 STRUCTURAL FORMULA FOR CLAYS

The composition of any clay-type could be written relative to the proportion of oxides. For e.g., composition of kaolinite as $Al_2O_3.2SiO_2.2H_2O$, but this is virtually devoid of structural information. It is better to take the unit cell as the basic quantity, and then the above formula can be expressed as $(Si_4)^{IV}(Al_4)^{VI}O_{10}(OH)_8$. This gives the cation occupancy of the tetrahedral sheet (superscript IV) and the octahedral sheet (superscript VI). All the 1:1 clay mineral will have the same anionic group, $O_{10}(OH)_8$. Similarly, the anionic group for all 2:1 minerals is $O_{20}(OH)_4$. The unit cell formula for dioctahedral 2:1 type is $(Si_8)^{IV}(Al_4)^{VI}O_{20}(OH)_4$. Here out of the six octahedral sites, only four are occupied and is by Al. 2:1 trioctahedral type in which tetrahedral cations are Si^{4+} and octahedral cations are Mg^{2+} have unit cell representation as

$(Si_8)(Mg_6)^{VI}O_{20}(OH)_4$. Table 1.5.1 shows the structural formulae for some dioctahedral and trioctahedral 2:1 phyllosilicates.

Table 1.5.1 Idealized structural formulae for some dioctahedral and trioctahedral 2:1 phyllosilicates

Layers	Trioctahedral	Dioctahedral
Octahedral only	Brucite, $Mg(OH)_2$	Gibbsite, $Al(OH)_3$
T-O	Serpentine group $Mg_3Si_2O_5(OH)_4$	Kaolinite group $Al_2Si_2O_5(OH)_4$
T-O-T	Talc group $Mg_3Si_4O_{10}(OH)_2$	Pyrophyllite, smectite group $Al_2Si_4O_{10}(OH)_2$
T-O-T with interlayer cations (e.g., K^+)	Phlogopite micas $K(Mg, Fe^{2+})_3(Si_3AlO_{10})(OH)_2$	Muscovite micas, illite clays $K_2(Al)_2(Si_3AlO_{10})(OH)_2$

1.6 MIXED LAYER CLAY

Mixed layer clays are common and consist of clays that change from one type to another through a stacking sequence. The sequences can be ordered and regular, or highly disordered and irregular. For example montmorillonite layers

can alternate with illite layers in an ordered way, or there can be several layers of montmorillonite with random layers of illite (figure 1.6.1).

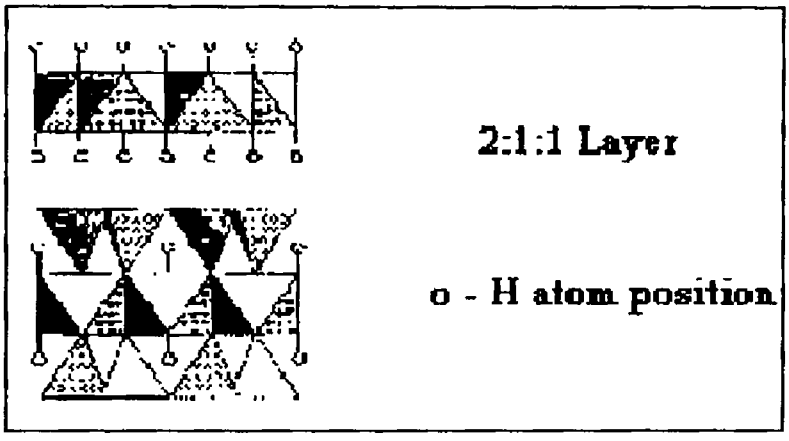

Figure 1.6.1 Mixed layers clay with a repeating 2:1:1 structure

1.7 SMECTITE CLAYS

Smectite minerals are components of many soils and sediments and often are found as large, mineralogically pure deposites[3]. They have either 2:1 dioctahedral or 2:1 trioctahedral structure. In the layer lattice structure, a central $MO_4(OH)_2$ octahedral sheet is symmetrically cross linked above and below to two tetrahedral MO_4 sheets. Al, Mg, Fe and sometimes Li occupy the octahedral sites whereas Si and in part Al occupy the tetrahedral sites. When substitution occurs between elements of unlike charge, deficit or excess charge develops on the corresponding points of the structure. The deficit charges are compensated by monovalent and divalent cations, especially Na^+, K^+ and Ca^{2+}, sorbed in the interlamellar space. The members of smectite group of clay are

distinguished by the type and location of cations in the oxygen framework. In a unit cell formed from 20 oxygens and 4 hydroxyl groups there are eight tetrahedral sites and six octahedral sites. Thus the primary structure of smectites is lamellar, with parallel layers of tetrahedral silicate and octahedral aluminate sheets. Secondary structure stems from valence deficiencies in primary structure. The tertiary structure is a consequence of secondary structure. This is a result of interstitial cations that are trapped as freely moving ions between the negatively charged layers. The nature of cations filling the octahedral and tetrahedral sites in the 2:1 layers distinguishes the various members of the smectite clay family. Montmorillonite, Beidllite, Nortronite etc belong to dioctahedral smectite group while Hectorite, Saponite, Sauconite etc are included in the trioctahedral group of smectite clays.

In smectites, the charge on the layers is intermediate between the talc group where layers are electrically neutral and mica groups where layers bear a net negative charge of two electrons per unit cell. The difference in layer charge results in physical and chemical properties not found for talc and mica groups. Typically the positive charge deficiency in the layers of smectites ranges from 0.4 to 1.2 e˙s/ unit cell.

1.8 PROPERTIES OF SMECTITES

Smectites are nanomaterials. The elementary platelets are a few tenths to a few hundreds of nanometer wide and long and 0.96 – 1.50 nm in thickness. The exact thickness depends on the number of adsorbed water layers. As already mentioned isomorphous substitution results in negative

charge to the elementary platelets, thus corresponding charge neutralizing and exchangeable cations together with one or two water layers are located in the interlamellar space between the elementary particles.

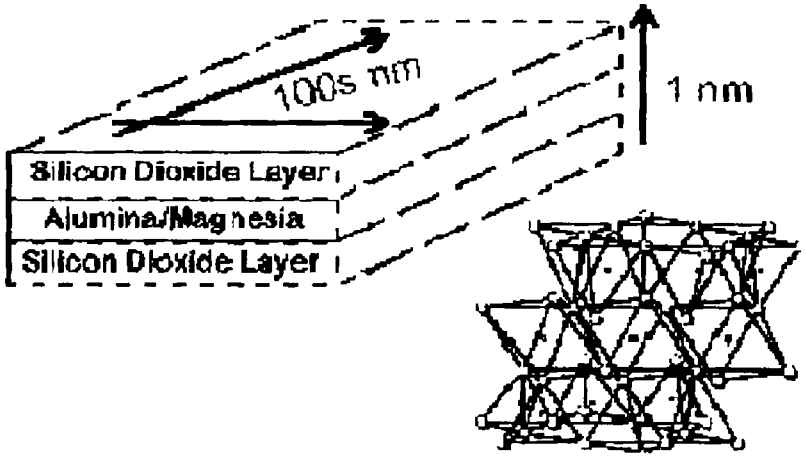

A single smectite platelet is composed of a central alumina or magnesia layer joined to silica layers. The particle is one nm thick and up to several hundred nanometer across.

A group of elementary platelets form a clay particle. As a result of these structural characteristics, smectite clays possess a combination of cation exchange, intercalation and swelling properties, which make them unique[4].

1.8.1 Cation exchange capacity

Cation exchange refers to the capacity of smectites to change the cations adsorbed on the surface. Exchange of Na^{+}, Ca^{2+}, etc ions in smectite

clays can be done with hydrated transition metal ions, rare earth metal ions as well as robust cations. The essence of this phenomenon is that the cations of the interlamellar space, that neutralizes the net negative charges of the layers, have no fixed sites in the lattice and hence if the mineral is immersed in an electrolyte, exchanges governed by the principle of equivalence will take place between the external and internal cations[5] i.e. the hydrated cations of the interlamellar surface of the native minerals can be replaced with almost any desired cation by utilizing simple ion exchange methods.

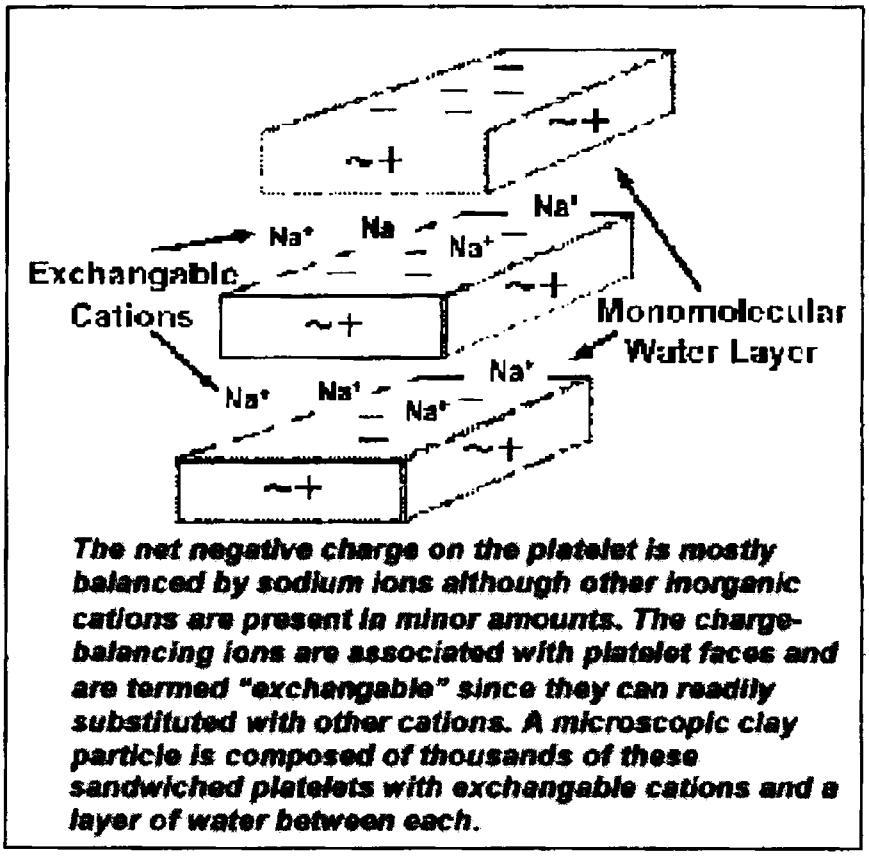

The net negative charge on the platelet is mostly balanced by sodium ions although other inorganic cations are present in minor amounts. The charge-balancing ions are associated with platelet faces and are termed "exchangable" since they can readily substituted with other cations. A microscopic clay particle is composed of thousands of these sandwiched platelets with exchangable cations and a layer of water between each.

With large complex cations, the extent of ion replacement may be size limited[6]. Table 1.8.1 shows the CEC of some clay minerals. From the table it is evident that the CEC of smectites is large compared to other type of clays.

Table 1.8.1 CEC of clay minerals

Clay mineral	CEC (meq/100g)
Kaolinite	3 - 15
Halloysite.$2H_2O$	5 - 10
Halloysite.$4H_2O$	40 - 50
Illite	10 - 40
Chlorite	10 - 40
Pyrophyllite	0
Talc	0
Smectites	
Montmorillonite	80 - 150
Vermiculite	100 - 150
Beidilite	60 - 120
Nontronite	60 - 120
Hectorite	60 - 120
Saponite	60 - 120

1.8.2 Intercalation

Intercalation in clays refers to the insertion of guest species within the layers. As already mentioned the hydrated cations on the interlamellar surfaces of the native minerals can be replaced with any desired cation by ion exchange. Neutral molecules other than water also can be intercalated between the silicate layers of smectites. Because of the ability of smectites to imbibe a variety of cations and neutral molecules, an almost limitless number of intercalates are possible with the retention of the layer structure. Several binding mechanisms may operate in the intercalation process[6-8]. One particularly important mechanism involves complex formation between exchange cation and the intercalant. Such a mechanism operates in the binding of pyridine (py) to Cu^{2+} exchanged form of smectites[9] where the horizontal lines symbolize the silicate layers.

$$[Cu(H_2O)_x]^{2+} + py \xrightarrow{-H_2O} [Cu(py)_4]^{2+}$$

The reaction of the hydrated cation functioning as a Brønsted acid and the intercalant acting as a base is another important intercalation mechanism. Ammonia, for e.g., binds as ammonium ion in Mg^{2+}-Montmorillonite[10].

$$[Mg(H_2O)_x]^{2+} + NH_3 \longrightarrow [Mg(OH)(H_2O)_{x-1}]^{+} + NH_4^{+}$$

1.8.3 Swelling

The ability of smectites to expand beyond a single molecular layer of intercalant is very important. Many clay minerals absorb water between their layers, which moves apart, and the clay swells. Swelling is a reversible process that occurs, essentially from the extra hydration of the interlamellar cations. The extent of interlayer swelling depends on the nature of the swelling agent, the exchange cation, the layer charge and the location of the layer charge.

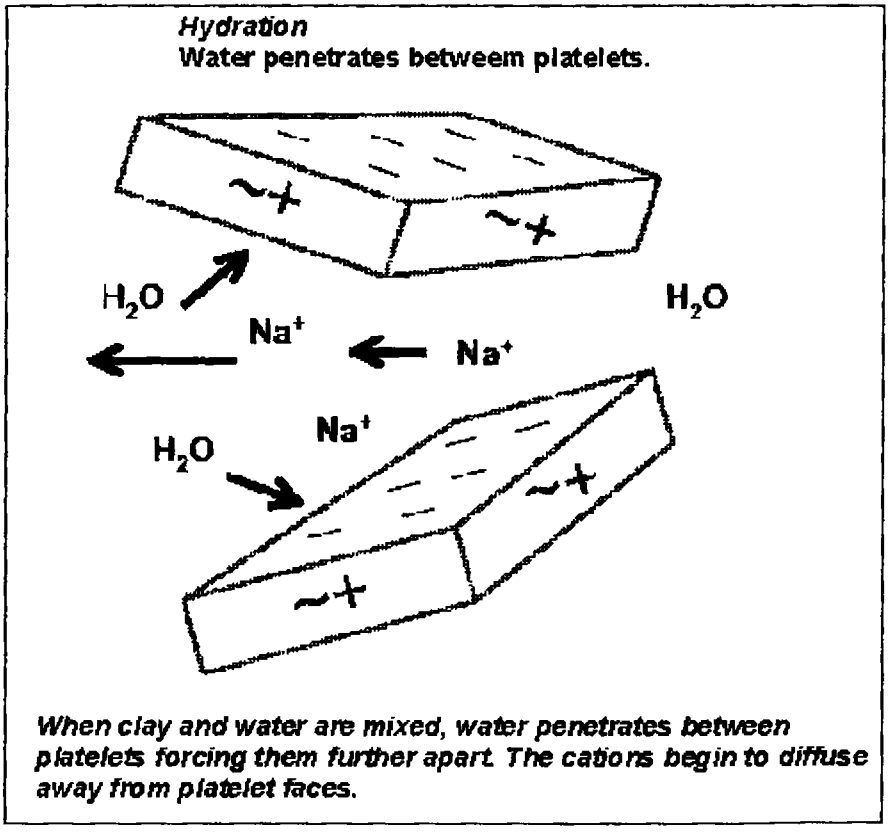

When clay and water are mixed, water penetrates between platelets forcing them further apart. The cations begin to diffuse away from platelet faces.

For efficient swelling, the energy released by cations and/or layer solvation must be sufficient to overcome the attractive forces (such as H-bonding) between the adjacent layers. In 1:1 (OT) clay minerals, water forms strong H- bonding with hydroxyl groups on hydrophilic octahedral layers, allowing swelling to occur.

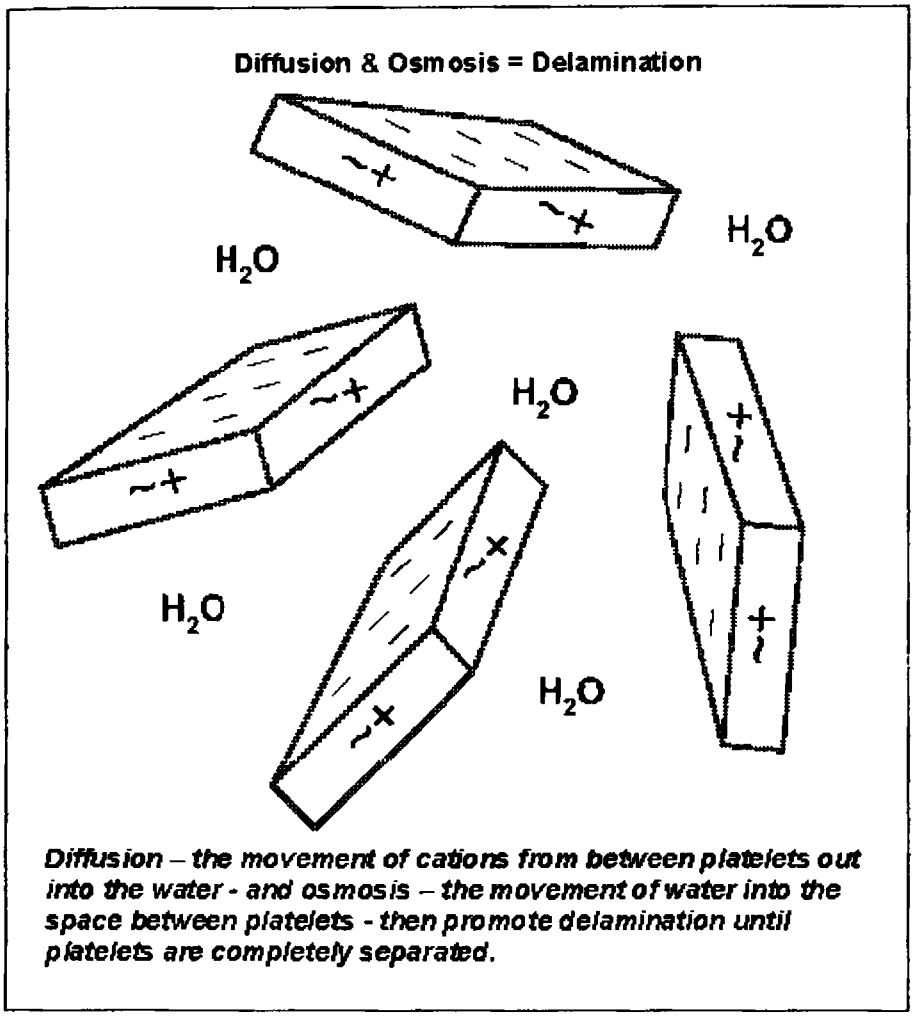

Diffusion – the movement of cations from between platelets out into the water - and osmosis – the movement of water into the space between platelets - then promote delamination until platelets are completely separated.

With 2:1 (TOT) clay minerals, the ability to swell depends on the solvation of the interlayer cations and layer charge. Clays with 2:1 structures and low layer charge (e.g. talc and pyrophyllite) have very low concentration of interlayer cations and therefore do not swell readily. At the other extreme, those with very high layer charges (e.g. mica) have strong electrostatic forces holding alternate anionic layers and the interlayer cations swell most readily and with divalent, trivalent and polyvalent cation swelling decreases accordingly. Thus Li^{+} and Na^{+} exchanged forms of the minerals are particularly susceptible to swelling by water[11-13].

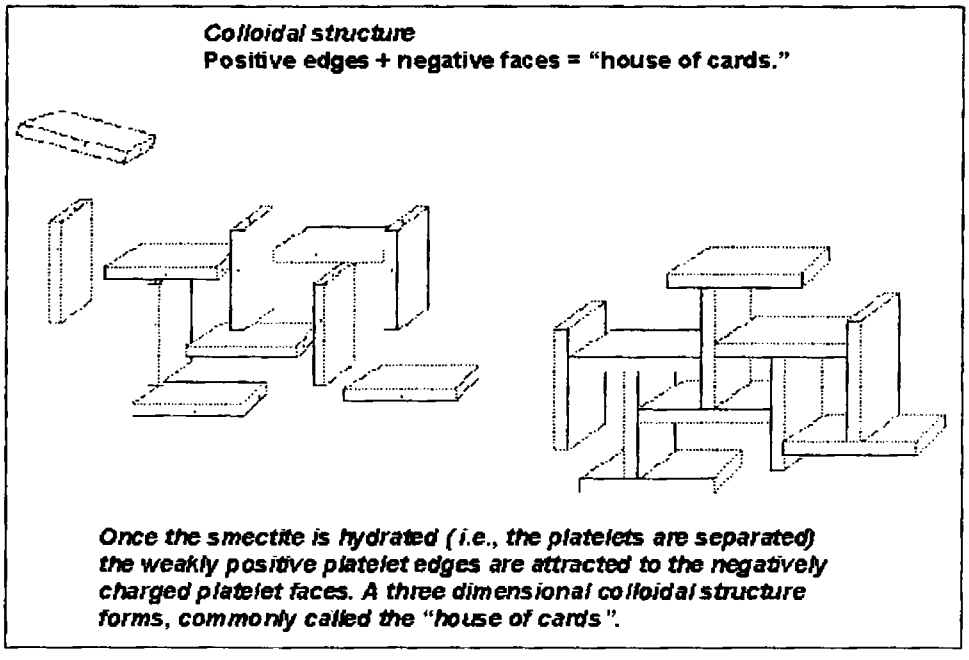

As the interlayer water content of Na^{+}-smectites is increased with increasing partial pressure, a more or less constant interlayer spacing

corresponding to monolayer formation is observed. After this, the spacing jumps abruptly to a value corresponding to two intercalated water layers. The stepping of the interlayer spacing is especially well behaved in beidellite and saponite[11]. Further swelling of interlayer due to osmotic forces is observed when the minerals are immersed in liquid water.

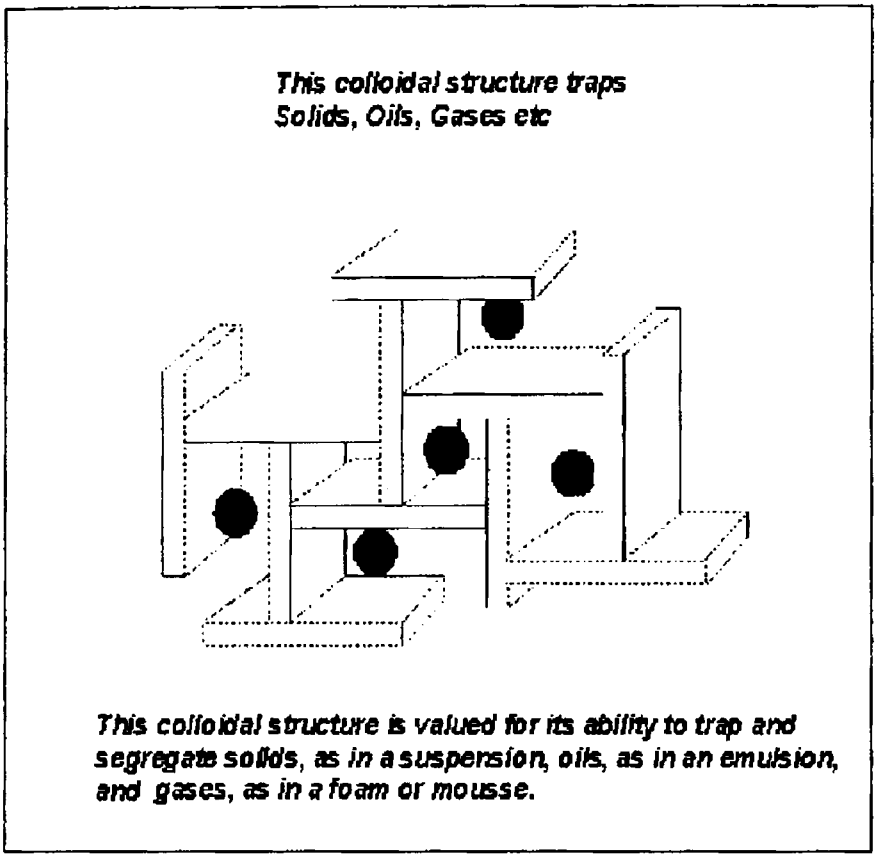

The osmotic swelling of smectite clays can be quite spectacular. Under appropriate conditions the silicate layers can be separated by hundreds of

angstroms of water. In fact, the silicate layers of Na^+ - montmorillonite in dilute aqueous suspensions are completely dispersed (delaminated). As the concentration of the dispersion is increased, gelation occurs. The gelation phenomenon, which occurs at a concentration as low as 2% clay by weight is believed to result from layer edge - to face – interactions, which generates a "house - of - cards" structure[14].

1.8.4 Acidity

The interlayer cations contribute to the acidity of clay minerals. Some of these cations may be protons or polarizing cations (e.g. Al^{3+}), which give rise to strong Brønsted acidity. The higher the electronegativity of M^+, the stronger the acidic sites generated. H_3O^+ associated with the negatively charged octahedral layers acts as a Brønsted acid site. Brønsted acidity also stems from the terminal hydroxyl groups and from the bridging oxygen atoms. In addition, clay minerals have layer surface and edge defects, which would result in weaker Brønsted and/or Lewis acidity generally at low concentrations, i.e. Al in three fold coordination, perhaps occurring at an edge, or arising from a Si-O-Al rupturing. Dehydroxylation of Brønsted site would correspond to a Lewis site (figure 1.8.1). An octahedral Al^{3+} located at a platelet edge after thorough dehydration, will be electron pair acceptors and will function as acids in the Lewis sense. Obviously, water will convert the Lewis site into Brønsted site, a fact that limits the study of Lewis sites to relatively anhydrous systems.

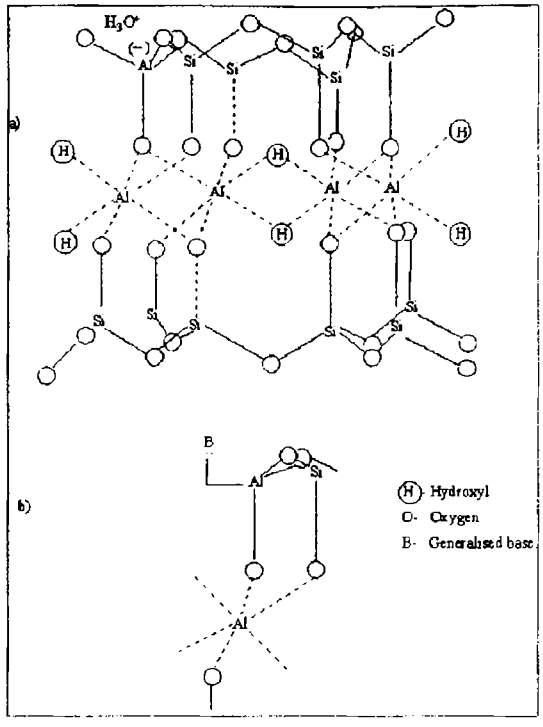

Figure 1.8.1 a) Off axis projection of a 2:1 dioctahedral mineral with Brønsted acid sites. b) Possible configuration of a Lewis acid site

1.9 MONTMORILLONITE CLAYS

Montmorillonite, the most important smectite is composed of units made up of two SiO_2 tetrahedra sheets and one Al_2O_3 octahedral sheets. The inter sheet layer include, exchangeable metal ions, neutralizing the net negative charges, which are generated by the partial substitution of Al^{3+} with Mg^{2+} at the octahedral sites. To a lesser extend some tetrahedral sites also might be occupied by ions other than Si^{4+}. These characteristics explain the high cation

exchange capacity (CEC) and good swelling properties that provides wide applications.

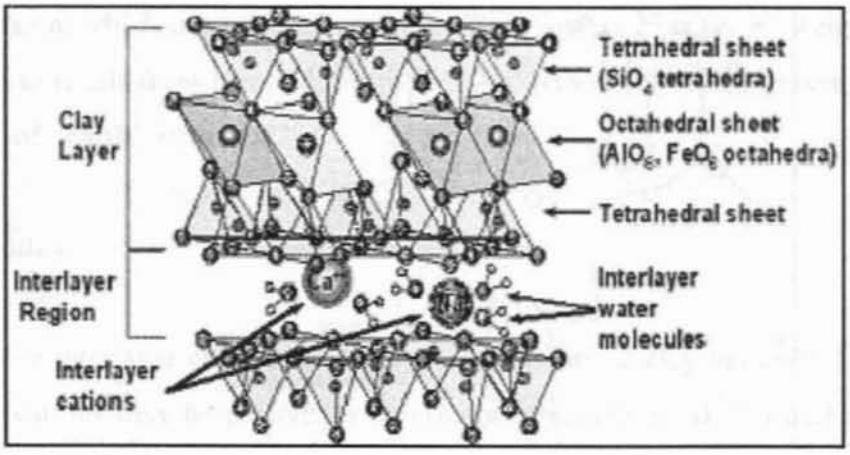

Figure 1.9.1 Structure of montmorillonite clay

Calcium is the commonest interlayer cation but when sodium is the exchangeable ion, the mineral swells more when placed in contact with water. Replacement of interlayer cation by potassium resembles montmorillonite with illite, but does not lose its ability to take up water. Structure is shown in figure1.9.1. Mineral data of montmorillonite is given in the table 1.9.1

Table 1.9.1 Montmorillonite: mineral data

Montmorillonite:	$(Na, Ca)_{0\text{-}3}(Al; Mg)_2Si_4O_{10}(OH)_2 . nH_2O$
Crystal Data:	Monoclinic. Point Group: 2/m: Tiny scaly crystals, tabular on {001}; as lamellar or globular

	microcrystalline aggregates; clayey, compact, massive.
Physical Properties:	Cleavage: {001}, perfect. Fracture: Uneven. Hardness = 1-2. D(meas.) = 2-3 D(calc.) = n.d. Positive identification of minerals in the smectite group may need data from DTA curves, dehydration curves, and X-ray powder patterns before and after treatment by heating and with organic liquids.
Optical Properties:	Translucent. Colour: White, pale pink, buff, yellow, red, green. Luster: Dull, earthy. Optical Class: Biaxial (-). Pleochroism: X = colourless to pale brown, yellow-green; Y = dark brown to yellow-green, olive-green, pale yellow; Z = brown to olive-green, pale yellow. Orientation: X ~ c; Y = b; Z ~ a. α = 1.492 - 1.503 β = 1.513 -1.534 γ = 1.513 - 1.534 2V(meas.) = 10°-25°
Cell Data:	Space Group: C2/m. a = 5.17(2) b = 8.94(2) c = 9.95(6) β = n.d Z = 1
X-ray Powder Pattern:	Chambers, Arizona, USA; Na and glycerol saturated. 17.6 (10), 4.49 (8), 1.50 (6), 9.00 (5), 3.58 (4), 2.57 (4b), 2.99 (3)
Polymorphism & Series:	Interstratifies with chlorite, muscovite, illite, cookeite, kaolinite.
Mineral Group:	Smectite group.

Occurrence: An alteration product of volcanic tuff and ash, forming bentonite beds, and of pegmatite dikes and wall rocks bordering hydrothermal mineral deposits. Forms under alkaline conditions of poor drainage, with Mg, Ca, Na, and K remaining in the soil.

Chemistry: (1) Montmorillon, France; corresponds to $(Ca_{0.14}Na_{0:02})_{\Sigma=0.16}(Al_{1.68}Mg_{0:36}Fe_{0.04})_{\Sigma=2:08}(Si_{3.90}Al_{0:10})_{\Sigma=4.00}O_{10}(OH)_2.1.02H_2O$.

(1)

SiO_2	51.14
Al_2O_3	19.76
Fe_2O_3	0.83
MgO	3.22
CaO	1.62
Na_2O	0.11
K_2O	0.04
H_2O^+	7.99
H_2O^-	14.81
Total	99.52

Association: Cristobalite, zeolites, biotite, quartz, orthoclase, dolomite, amphiboles, pyroxenes, olivine, calcite, gypsum, pyrite, limonite.

Distribution: A common clay mineral, with numerous localities

worldwide. From Montmorillon, Vienne, France. In the USA, material considered as standards from Bayard and Santa Rita, Grant Co., New Mexico; near Chambers, Apache Co., Arizona; at Belle Fourche, Butte Co., South Dakota; in Wyoming, on the John C. Lane tract, Upton, Weston Co., at Clay Spur, near Newcastle, Crook Co., and elsewhere. In the Itawamba mine, Itawamba Co., and in mines around Polkville, Simpson Co., Mississippi; at Strasburg, Shenandoah Co., Virginia.

Name: After the occurrence at Montmorillon, France.

1.10 APPLICATION OF CLAYS

Clays and clay minerals have been mined since the Stone Age; today they are among the most important minerals used by manufacturing and environmental industries. Clay has been used since the very beginning of civilization, for making cooking pots, bricks, porcelain, and also drainage pipes. Both brick clays and other clays are used for other purposes, such as the manufacture of clay pipes, and for floor and wall tiles. Fireclays are used for more refractory purposes such as heat-resistant tiles or bricks. Ball clays are used for ceramics. China clay, predominantly kaolinite, is used in ceramics, as filler and in drug manufacture. Expanded clays are used as a lightweight aggregate in the manufacture of expanded clay blocks used for insulation.

However, the major use of clay, after brick manufacture, is in the manufacture of cement.

Highly absorbent, bentonite is much used in foundry work for facing the moulds and preparing the molding sands for casting metals. The less absorbent bentonites are used chiefly in the oil industry, e.g., as filtering and deodorizing agents in the refining of petroleum and, mixed with other materials, as drilling muds to protect the cutting bit while drilling. Other uses are in the making of fillers, sizings, and dressings in construction, in clarifying water and wine, in purifying sewage, and in the paper, ceramics, plastics, and rubber industries.

The U.S. Geological Survey (USGS) supports studies of the properties of clays, the mechanisms of clay formation, and the behavior of clays during weathering. These studies can tell us how and where these minerals form and provide industry and land-planning agencies with the information necessary to decide how and where clay and clay mineral deposits can be developed safely with minimum effects on the environment. Clays are further more used as decolourisation agents and ion exchangers.

In the year 1865, Von Liebeg described the properties of china clay that could catalyze the formation of water from oxygen and hydrogen at a pressure and temperature at which they are usually unreactive. Then the use of clays as catalysts became widespread. The small particle size and layer structure permits the formation of clay/polymer nanocomposites that are typical

examples of nanotechnology. This class of materials uses smectite type clays, such as hectorite, montmorillonite and synthetic mica as fillers to enhance the properties of polymers.

1.11 MODIFICATION ON CLAYS

Clay modifications are done mainly for the use in catalysis. Naturally occurring clays may not be efficient catalysts. Modifications are needed to improve the acidity, porosity, thermal stability, mechanical strength etc for variety of applications for e.g. in acid catalyzed as well as shape selective reactions. The important methods of modifications include acid activation, cation exchange, intercalation, pillaring etc.

1.11.1 Acid Activation

This modification involves the treatment of clay with mineral acids, which replaces the interlamellar cations with protons. When the phyllosilicate clay minerals are treated with dilute acids, the H^+ ions attack the silicate layers via the interlayer region and exposed edges, thus displacing the octahedral ions such as Al^{3+} and Mg^{2+}, which then occupy the interlayer sites. Acid activation causes little damage to the silicate layers where the structure for the center of the platelet remains intact. The rate of dissolution of the octahedral sheet increases with the concentration of the acid, temperature, contact time and increasing Mg content in the octahedral sheet[15,16]. Dealumination develops mesoporosity in the layers and contribute to high surface area. The protons exchanged for the interlamellar ions and the leached hydrated alumina occupying the cation exchange sites contribute to the enhanced acidity[17].

However, prolonged acid activation usually leads to a complete dealumination resulting in a silica matrix.

1.11.2 Cation exchange

The interlamellar cations as already mentioned are exchangeable and thus cations, neutral molecules etc can be entered between the layers and this leads to the modifications, intercalation as well as pillaring. Cation exchanged montmorillonite clays are useful for a number of organic transformations. The exchanged cations favour the properties such as acidity etc.

1.11.3 Intercalation

Montmorillonite can efficiently adsorb various organic compounds, ionic or neutral, within its interlayers. The intercalation is quite easy accomplished by magnetic stirring of the clay dispersed aqueous solution with an appropriated amount of guest ions dissolved in water or sometimes added directly as a powder. Such intercalation can be utilized as a probe for identification of 2:1 type clay minerals[18,19]. Due to the ionic exchange with the exchangeable alkali ions, generally, more that 95% of the guest ions are incorporated on the basis of the CEC of the clay[20,21]. Also non ionic guests with large dipole moments such as ketones and nitriles can be adsorbed to the exchangeable metallic ions within the layers according to their coordination with the ionic sites in the interlayers.

In general, clays act as catalysts by intercalating organic molecules, which are then activated by interaction with the internal surface acid sites that

are part of the walls of the interlamellar region. For this reason, the understanding of the process of intercalation is fundamental in the study of catalysis by clays. A large variety of organic molecules are intercalated by the so called displacement method[22]. This amounts to intercalating a small molecule in the first instance, such as ammonium acetate, which is then displaced by a second, usually larger or less polar entity, such as glycol. The degree of swelling as a result of intercalation is governed in part by the nature of the interlamellar cation.

The adsorption property in clays permits the mutual interaction of the incorporated guests that form self assembling molecular aggregates due to the two-dimensional layer surface, which is in contrast to silica colloidal surfaces[23]. It is possible to obtain detailed information on the higher dimensional structure of the guest molecules by various methods such as X-ray diffraction, neutron scattering or high resolution electron microscopy, nuclear magnetic resonance (NMR)[24], electron spin resonance (ESR)[25] etc.

The intercalation of polymers into clay minerals is also an important area of research since hybridization may produce unique material with moisture adsorbing properties. In order to make a polymer clay hybrid material, for e.g., polymerization of the alkenes, were conducted in the layers of the clay in the presence of an initiator after the adsorption of the alkenes as monomers.

1.12 PILLARED CLAYS (PILCs)

The beautiful and so flexible architecture of the natural smectites seemed excluded in the harsh conditions of most catalytical reactions. Pillaring is the process by which a layered compound is transformed into a thermally stable micro and/or mesoporous material with retention of the layer structure. Dehydration and collapse of the clay structure occurs even at temperatures such as 200°C, are severe problems associated with the clays. Pillaring solves this problem of thermal stability to a great extent and these porous materials are used as catalysts, catalyst supports, sensors or adsorbents[26].

Barrer and Mac Leod[27] in 1955 first introduced the concept of transforming a lamellar solid into a porous structure by inserting laterally spaced molecular props between the layers of smectite clay mineral. They used organic compound, tetraalkyl ammonium ions to develop porosity. However, organic and organometallic intercalating or pillaring agents decompose at relatively modest temperatures causing the PILC structure to collapse. The terms 'pillared' and 'pillaring' originates from the work of Brindley and Semples[28] and Vaughan and Lussier[29] in 1970 on smectite type clay minerals. They found that thermally stable, robust inorganic moieties could be intercalated between the individual clay platelets of the stack or aggregate of clay lamellae. These materials are referred to as pillared interlayered clays (PILCs). Nowadays, the range of materials that can be pillared has expanded beyond smectite type clay minerals.

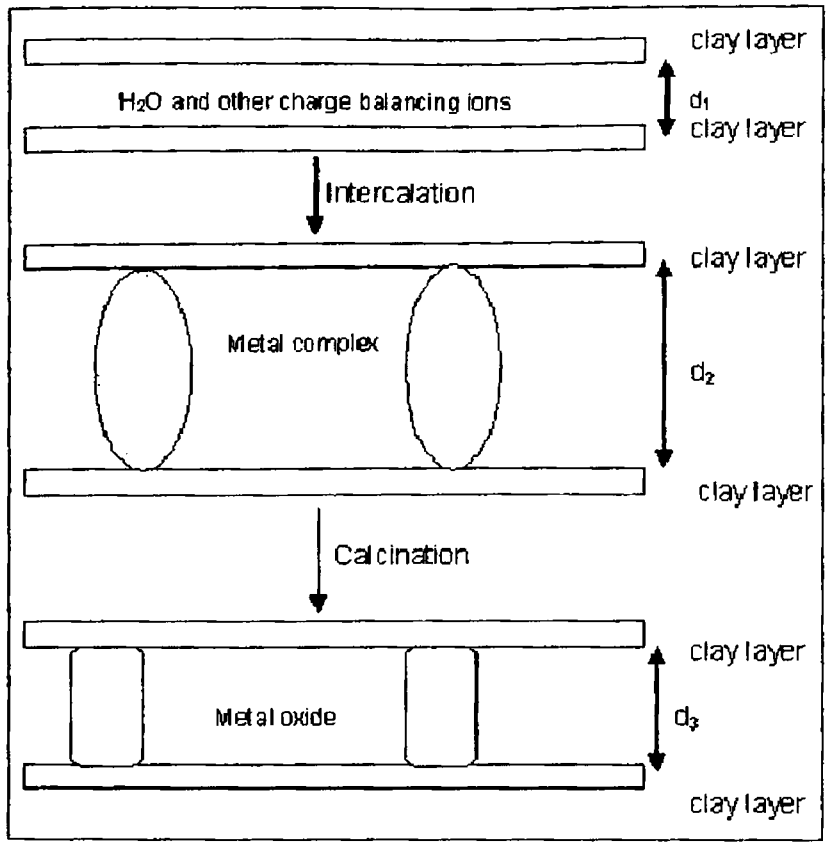

Figure 1.12.1 Schematic representation of pillaring

Cation exchange in the interlayer by bulky (polyoxo) cationic species (oligomer) that acts as props to keep the structure open is the basic phenomenon involved in the pillaring process. Thus swelling clay minerals capable of cation exchange can be pillared. We can represent the cation exchange process as

$$M\,Na_v + P_n^{v+} \longrightarrow MP_n + VNa^+$$

where Na^+ is the common interlamellar cation and P_n^{v+} is the pillaring cationic oligomer that has high charge and large size. The cationic oligomer results from partial hydroxylation of salts or condensation reaction.

$$nP^{z+} \longrightarrow P_n^{v+} + (nz - v)H^+ + x\,H_2O(n)$$

The careful processing of the intercalated solid transforms the clay structure into a thermally stable porous structure. Dehydration and dehydroxylation of the polycation occurs upon thermal activation (calcination) to get stable oxide cluster as a pillar (converting the hydroxide pillars) between the layers.

Calcination shifts the bonding between interlayer species and clay layers from ionic to covalent. After pillaring the enhanced spacing between the adjacent layers remains stable, upon introduction and removal of the solvent, thermal treatment etc. On pillaring the thermal stability can be enhanced up to 750°C[30]. All PILCs are stable in the temperature range 400 -500°C.

The schematic representation of pillaring is shown above (figure 1.12.1). The d spacing ranges from 15 - 30 Å depending on the pillar metal, pillaring agent and the treatments after the intercalation. The pore size is thus determined by the size of the pillars and the spacing between the pillars in the layer, i.e. the interlayer spacing depends on chemical nature and height of intercalating species. On the other hand, interpillar distance is mainly related to the density of pillars, which in turn depends strongly on the extent, and distribution of charge density on clay layers and also on size of pillars.

1.12.1 Pillaring agents

The use of organic reactants has been recently reviewed by Barrer[31]. Pinnavaia has reviewed the intercalation of smectites by organometallic complexes. The stability of these structures hardly reaches 450°C. Polynuclear hydroxy metal cations yield high free spacings with reasonable stability at high temperatures.

In principle, any positively charged ion can be used. Thus oxidic pillaring usually proceeds via insertion of hydroxy oligomeric cationic species between aluminosilicate layers and stabilization by heat treatment[32]. Another method is the insertion of organocationic complexes into interlamellar space, followed by heating which removes the organic part leaving oxidic micro pillars[33].

Much effort has been expanded in finding various pillaring polyoxocations. The formation of poly nuclear cations was first recognized by Bjerrum[34] in his study on the hydrolysis of Cr^{3+} and later for metal ions such as Al^{3+}, Be^{2+}, Ni^{2+}, Pb^{2+}, Zr^{4+}, Hf^{4+}, Ti^{4+}, Fe^{3+} and Ce^{4+} by other workers[35]. The various types of polynuclear hydroxy metal cations for pillaring smectites include those of Al[36], Zr[37], Ti[38], Si[39], Fe[40], Cr[41], Nb[42], Ga[43], Ni[44], U[45], Bi[46] and organometallics. Mixed metal oxide pillars containing two or more cations have also been prepared.

1.12.2 Aluminium PILCs

Most of the research on PILCs has been focused on alumina PILCs which uses Al_{13} polyoxocation as the pillaring agent. Solutions containing this complex are prepared through partial hydrolysis of aluminium salts.

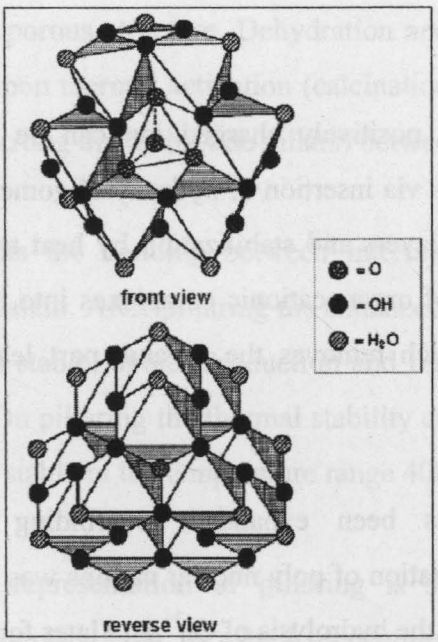

Figure 1.12.2 Structure of Al_{13} complex

Forced hydrolysis is done either by addition of a base (hydroxide, carbonate etc) to aluminium chloride or aluminium nitrate solutions up to an OH/Al molar ratio of 2.5[47] or by dissolving Al powder in $AlCl_3$ (i.e. aluminium chlorohydrate or aluminium chlorhydrol; ACH). From ^{27}Al NMR and XRD[48] analysis, the structure of the complex is found to be the tridecamer

$[AlO_4Al_{12}(OH)_{24}(H_2O)_{12}]^{7+}$, a keggin structure[49] (figure 1.12.2). On partial hydrolysis species other than Al_{13} polyoxocation exist that exchange for the clay interlayer cation[50].

To obtain PILCs, partially hydrolyzed aluminium solutions with an effective charge of approximately +0.5/Al need to be mixed in a dilute form with dilute clay suspension followed by careful washing[51]. Schoonheydt and Leeman[52] succeeded in pillaring saponites in concentrated partially hydrolyzed Al solutions in which the species were different from Al_{13} polyoxocation. The main disadvantages of this route are (1) the time consuming preparation of the solution and clay suspension and (2) the large quantities of water to be handled.

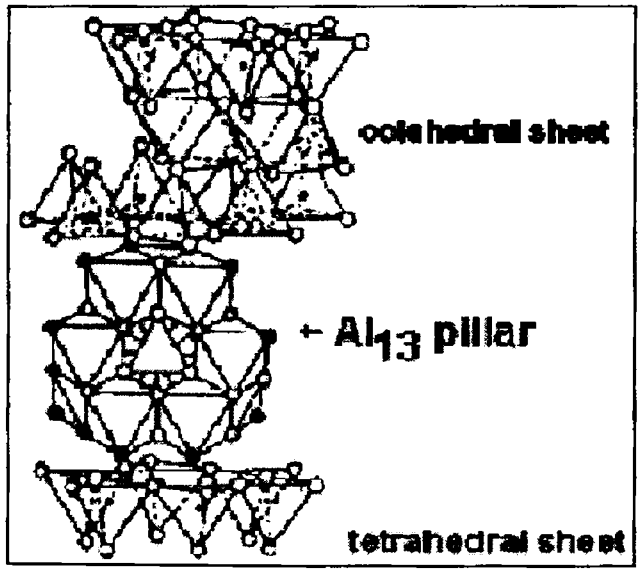

Figure 1.12.3 Aluminium pillared montmorillonite

The amount of aluminum bound in the interlayer per unit cell varies only within a small range (2.78 - 3.07) equivalent to approximately one Al_{13}/4.6 to 6 unit cells and no correlation with the charge of the layer. This suggests a more or less uniform monolayer of hydrated Al polyoxocation to be present in the interlayer. Bergaovi et al[53] indicated that the amount of Al never exceeds one Al_{13}/6 unit cell due to steric constraints at the solid – liquid interface. The layer charge plays role in the competition between flocculation and intercalation. Pillaring results in an effective reduction of the initial CEC of the starting clay[54]. Acid activation of montmorillonite prior to pillaring results in a higher surface acidity and pore volume/diameter compared to normal pillared montmorillonite, but here the surface area is found to be small[55]. The surface area ranges from 220 -380 m^2/g and basal spacing 17 - 20 Å.

Plee et al[56] have used ^{27}Al and ^{29}Si MAS NMR techniques to study the thermal transformation of the pillars and their linkage with the clay sheets. Aluminium pillared montmorillonite is shown in figure 1.12.3.

The dehydroxylation during calcination is by the reaction

$$[AlO_4Al_{12}(OH)_{24}(H_2O)_{12}] \longrightarrow 6.5\ Al_2O_3 + 7H^+ + 20.5\ H_2O$$

Depending on the drying conditions, Kodama and Singh[57,58] obtained three types of Al pillared montmorillonites. Extremely dry conditions led to a phase exhibiting a basal spacing of 18.8 Å. An intermediate phase was formed under ambient conditions. Both phases transformed to a third phase displaying

a basal spacings of 28 Å upon aging. The phase of basal spacing of 18.8 Å converted to the phase of basal spacing of 28 Å upon heating at 700°C. The phase of basal spacing of 28 Å is a relatively regular interstratified structure of non expanding layers of spacing of 9.6 Å and expandable layers of a spacing of 18.8 Å in a ratio of 0.46: 0.54.

1.12.3 Zirconium PILCs

Zr polyoxocations of the type $[Zr_4(OH)_{16-n}(H_2O)_{n+8}]^{n+}$ or $[Zr_4(OH)_8(H_2O)_{16}(Cl,Br)_x]^{(8-x)+}$ (figure 1.12.4), have been formed by the dissolution and ageing of zirconyl chloride, $ZrO_2Cl_2.8H_2O$[59-63]. The degree of polymerization is affected by not only ageing but also by concentration and pH.

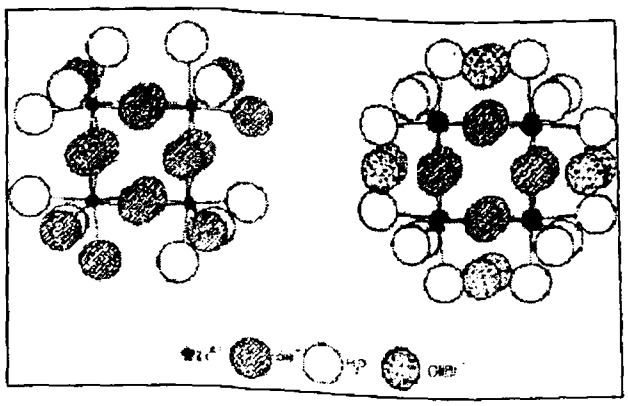

Figure 1.12.4 Zirconium pillar polyoxocation

The basal spacings showed a rather large variation with values between 13.4 and 19.3 Å, depending on the exact preparation method. Similar differences were observed for the surface areas. Addition of bases like NaOH

accelerates the polymerization and increases the stability of the Zr-PILCs due to a higher pillar density[64].

Controlled polymerization offers the possibility to prepare PILCs with different interlayer distances and surface areas[65]. Hydrolytic polymerization can be induced by refluxing of the pillaring solution and/or the PILC suspension[66-68]. Ohtsuka et al.[66] observed two different phases after refluxing. Clays pillared with a solution containing less than 1 M zirconyl chloride exhibited a basal spacing of 23.3 Å, whereas pillaring with a solution containing a higher zirconyl chloride concentration had a basal spacing of 21.3 Å. Burch and Warburton[67] interpreted from their data that the insertion of single Zr tetramers parallel to the clay layer surface form the low basal spacings of approximately 13–14 Å. This in contrast to Yamanaka and Brindley[69] who observed basal spacings around 19.6 Å, which they interpreted as being formed by either the same tetramers standing perpendicular to the clay layer surface or by stacking of two tetramers on top of each other. The difference might be explained by the much higher amount of Zr taken up in the second case. However, there seems to be no clear evidence for this type of pillar positioning. The larger basal spacings between 19 and 24 Å are interpreted as being due to either the formation of larger polymeric cations or by overlap due to mismatch between cations adsorbed on opposite clay layers. The observed high thermal stability (700-800°C) favors the first option.

FTIR studies on pyridine adsorption on Zr-PILCs showed that the Lewis acid sites were only located on the pillars, while the Brønsted acid sites were associated with the exposed clay surface and the pillar-clay bonding[70].

1.12.3 Titanium PILCs

Titanium is known to form polymeric species in solution for quite some time[71,72]. In general two different methods to create Ti complexes (figure 1.12.5) suitable for pillaring processes were reported in the literature. The first method to form Ti complexes in solution is the addition of $TiCl_4$ to 5 or 6 M HCl followed by dilution with distilled water and ageing from 3 hours up to as long as 20 days prior to their use as pillaring agents[73-75]. A drawback of this preparation route is the highly acidic conditions one has to work in, resulting in leaching of small amounts of Al and Si from the clay structure[74,75].

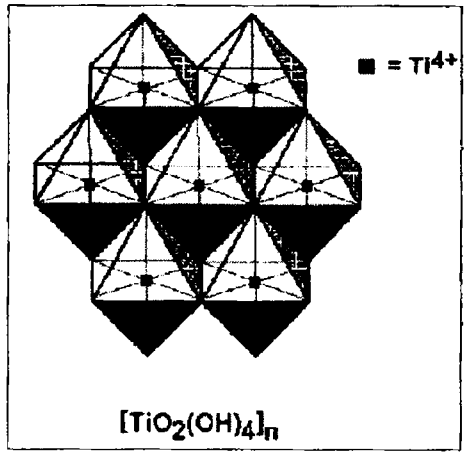

Figure 1.12.5 Titanium pillar complex

The second route is based on the hydrolysis of various Ti alkoxides (e.g., tetra-ethoxide, tetra-n-propoxide, tetra-isopropoxide, tetra-n-butoxide) under much milder acidic conditions (mostly 1 M HCl)[76-80]. The basal spacing $d_{(001)}$ has been shown to increase generally to values around 24-25Å following both hydrolysis methods (although Yang et al[73] reported an unexplained value of 28.3 Å after calcination at 300°C). Consequently the specific surface area increased to values between 250 and 350 m^2/g depending on the precise preparation conditions and calcination temperature. In the work of Bernier et al.[75], which follows the initial work of Sterte[74], it is proven that the experimental conditions like Ti concentration, temperature and pH of the Ti complexes-clay suspension are critical to the morphology and texture of the final PILCs.

XRD patterns of the PILCs given in some studies[75,81] show a relatively large amount of unexpanded clay. This portion may consist of either unreacted clay or clay exchanged with some type of monomeric Ti species. This amount decreases with increasing $TiCl_4$ concentration and lower acidity. Such large amounts of unexpanded clays were not reported in other papers. Sterte[74] inferred from the decrease in surface area with increasing amounts of Ti added, while the pore volume and actual uptake of Ti remained constant.

Malla et al.[76] observed that with increasing calcination temperatures the nitrogen surface areas remained more or less constant, whereas the water surface areas decreased continuously indicating that the pores become more hydrophobic upon calcination. Temperature-programmed desorption (TPD) of

ammonia and pyridine adsorption/desorption experiments revealed that the acid sites or mainly strong Lewis acid sites, must be located at the interphase between pillar and the siloxane surface[75] because (1) TiO_2 itself has no significant acidity and (2) the observed acidity differs strongly from the acidity of the starting clay. Sychev et al.[79] state that the increased acidity is due to the dealumination during the synthesis of the Ti-PILCs.

1.12.4 Chromium PILCs

Cr is one of the few cations in addition to Al which can be hydrolyzed extensively to form large polyoxycations. Cr polyoxocations can be prepared by base hydrolysis analogous to that used for Al[81-85]. Chromium nitrate solutions have a red-purple colour, which changes upon increasing basicity to bluish-green and finally to deep green. The polymerization reaction is rather slow at room temperature[86] but quite rapid at 100°C[86,87] and the deep green species were attributed to higher polymers like the trimer[86,88] and others[89,90]. Brindley and Yamanaka[81] were one of the first to attempt to synthesize Cr-PILCs by exchange with partially hydrolyzed chromium nitrate solutions prepared at room temperature. They observed an increased basal spacing of 16.8 Å. However, the expanded clay was rather unstable and totally collapsed at 300°C. Chemical and thermogravimetric analyses indicated that the OH/Cr ratio in the clay interlayer was higher than the initial solution, which may be explained by partial dissociation of water adjacent to Cr^{3+} ions in the interlayer and a continued reaction

$$Cr^{3+} + H_2O \longrightarrow Cr(OH)^{2+\,b}$$

Dubbin et al.[91] observed an additional basal spacing at 19.2 Å in addition to the main basal spacing at 16.7 Å. They argued that this additional spacing might be due to some type of Cr Keggin structure or a linear trimer of three octahedra. XPS binding energies of Cr in the clay however were essentially the same as those in $CrCl_3.6H_2O$ and indicative of Cr^{3+}. Due to the fact that the central cation in the Keggin structure is tetrahedrally coordinated to oxygen and this is only observed for higher oxidation states of Cr, the presence of a Keggin structure in the clay interlayer region can be ruled out. A linear trimer as pillaring species is therefore thought to have caused the basal spacing of 19.2 Å. Pinnavaia et al.[83] and Tzou and Pinnavaia[92] showed that increasing the hydrolysis temperature from 25°C, as used by Brindley and Yamanaka[81], to 95°C resulted in larger polymers, giving PILCs with basal spacings near 27 Å instead of 17 Å and an increased thermal stability up to 500°C (basal spacing of 21 Å). Increasing the Cr content in the interlayer region did not result in significantly different basal spacing although the surface area diminished. This has to be interpreted in terms of rod- or disk-shape chromic aggregation oriented in the interlayer region with the axis parallel to the tetrahedral layers of the clay.

1.12.5 Other Metal PILCs

Pillaring using other metals which forms polyoxocations are also reported among which pillaring using metals like Fe, V, Si etc are common.

There are many reports for Fe PILCs from the partial hydrolysis of $FeCl_3$[93,94], $Fe(NO_3)_3$[95], $Fe(ClO_4)_3$, $Fe(SO_4)_3$[96]. In many other reports[97-99], the

complete collapse of clay occurs after calcination. Another route attempted to prepare Fe-PILCs makes use of organic cage like structures such as Fe(II)-1,10-phenantroline[100] and trinuclear aceto Fe(III) ions[101-103].

Studies concerning the hydrolysis of gallium have shown that a keggin structure similar to the Al_{13} can be formed[104-106]. Bradely and Coworkers[107-109] extensively described the synthesis of Ga-PILCs. V-PILC is prepared by refluxing a chloro-montmorillonite with NH_4VO_3 in dry acetone for 12 h[110]. Montmorillonite on refluxing with $VOCl_3$ in dry benzene is another method[111]. Endo et al[112] prepared Si-PILCs by in-situ hydrolysis of tris(acetyl acetonato silicon cations). Lewis et al[113] used organo silicon monomers as intercalating agents.

Bi-PILCs were prepared by Yamanaka et al[46]. Yamanaka and Brindley and Brindley and Kao[114] prepared Ni and Mg – PILCs. La-PILCs are prepared by Lavados and Pomonis[115] and Skaribas et al[116]. Other PILCs known are those of Pb[117] by the addition of lead nitrate solution to the clay suspension followed by hydrothermal treatment.

1.13 MIXED PILCS

The thermal stability, porosity etc of single oxide PILCs can be improved by incorporating a second component into pillars. Various metals have been described in combination with the Al polyoxycation, the most

important of them being Fe, Ga, Si, and Zr. Table 1.13.1 summarizes the most important data for mixed PILCs[118].

Table 1.13.1 Different mixed pillars with d spacing

Pillar type	d(001) (Å) calcined	SA (m^2/g)	Remarks
	9.6 (500)*		Fe/Al ratio 1/9
		240	Fe/Al ratio 3/1
	18.8 (400)	255	
Fe/Al	16.1 (400)	280	Fe/Al ratio 1/1
	14.8 (400)	240	Fe/Al ratio 3/1
	13.7 (400)	190	Alloy Al_{12}:$5Fe_{0:5}O_4(OH)_{24}$
	10.2-18.2 (500)	170 –237	Depending on ratio and preparation Route
	±16 (400)		Fe/Al ratio's 1/9, 1/8, 1/7
	±16 (700)	245	Pillar comparable to $Al_{13}GaO_4Al_{12}(OH)_{24}(H_2O)_{12}]7^+$
Ga/Al	16.4-17.3 (600)	200 –235	Depending on Ga/Al ratio
	17.7 (500)	136 –288	SA strongly depending on

			Ga/Al ratio
		125	Strong decrease in SA due to Agglomeration
	18.8 (400)	212	Langmuir SA
Si/Al		278 –458	Route A, Al added to Si
		343-499	Route B, Si added to Al
	17.5–18.3 (500)	267	2 basal reflections at temperatures below 400°C
	17.3 (400)	315	Langmuir SA at 400°C pillared Montmorillonite
Zr/Al			
	16.0 (400)	260-300	Ideal as above but pillared hectorite
UO_2Al		390	Photoluminescence suggest incorporation of UO_2 in Al pillar
B/Zr/Al	18.0 (700)	331	
B/Si/Al	17.0 (700)	327	

* Between parentheses calcination temperature

1.14 CHARACTERISTICS OF PILCS

The PILCs have created tremendous potential for adsorption and catalysis because of high surface area and permanent localized porosity in the large micropore region. Also introduction of Brønsted and Lewis acidity, improved thermal stability and increased pore width open a wide scope for the PILCs in its utility in various organic transformations and adsorption.

The preparation conditions used, pillaring metal selected, pillaring solution preparation, drying conditions and the calcination temperature play important role in the layer expansion and surface area - pore volume increase (figure 1.14.1). Thus designing of structure to the required level can be attained. Pillaring transforms the bond between the clay layers from Van der Vaals, or ionic to near covalent, stabilizing the porous net work from structural collapse. Generally pillaring makes the layer distance between 14 – 30 Å from 9.8 Å. The density of pillars and the pillar distribution is important in addition to the pillar size for structural modifications.

From previous discussions we reach in the conclusion that, on pillaring we are getting thermally stable clay with high porosity, surface area, acidity etc which can be tuned to a number of industrial applications. The eco-friendly society demands solid acid catalysts, whereas the enhanced porosity offers shape selective catalysis. The interlamellar space of clays, capable of the uptake of organic molecules allows intercalation and the polymerization of

monomers when allowed inside the matrix drives the application of clays as nanocomposites.

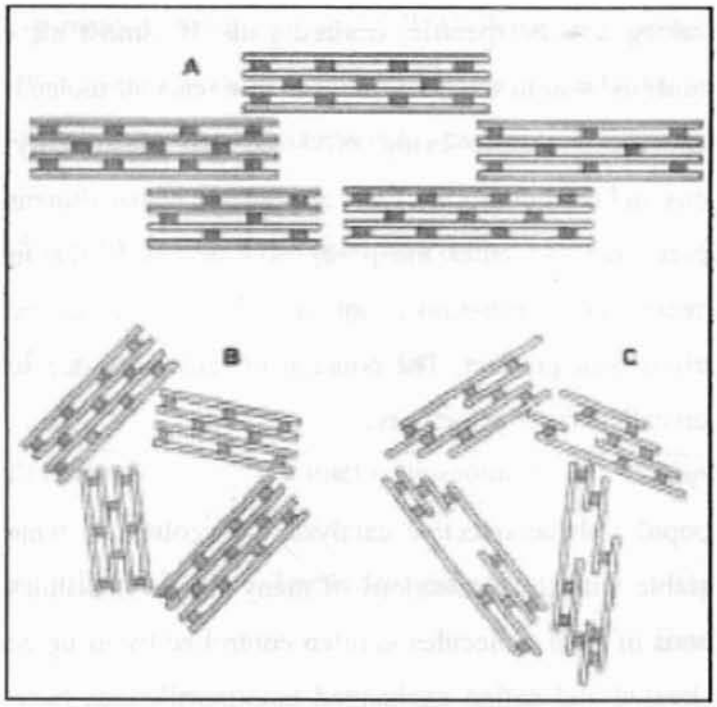

Figure 1.14.1 Different forms of precursor association: A. air-dried; B. freeze-dried; C. with platelet cutting

We in the present study monitor the structural tuning of montmorillonite clays by pillaring for the applications as shape selective solid acid catalysts as well as in the development of polymer/clay nanocomposites.

1.15 SHAPE SELECTIVE ACID CATALYSIS BY PILCS

The most important role of a catalyst is to provide selectivity to direct a chemical reaction along a very specific, desired path. If almost all of the catalytic sites are confined within the pore, the fate of a reactant molecule and probability of a specific molecule being produced are affected by their molecular dimensions and configurations. Only a molecule whose dimension is smaller than the pore size can enter the pore, have access to the internal catalytic sites and react there. Furthermore, only a molecule that can leave the pore can appear in the final product. The concept in selectivity due to such steric effect has been called shape selectivity.

The most popular shape-selective catalysts are zeolites in which the pore size is comparable with the dimensions of many simple molecules. The selectivity of reactions of such molecules is often controlled by using zeolites as catalysts. Acid treated and cation exchanged montmorillonites have been shown to possess an ability to promote organic reactions as acid catalysts, as was reviewed by Ballantine[119]. Clay catalysts were used as industrial catalysts for petroleum cracking although they were superseded by amorphous silica-alumina and zeolites because of the lack of thermal stability at high temperatures. PILCs having high thermal stability and surface area have provided a new class of molecular sieves which are structurally different from zeolites. As pillars prop open the clay layers, the accessibility of reactant molecules to the interlamellar catalytic sites increases, resulting in a high catalytic activity. Simultaneously, the pillar can exert a shape-selective effect

which controls diffusion rates of reactants and products or formation of reaction intermediates. Thus, PILCs have awoken a lot of interest in their application for shape-selective catalysts, and they have been used as practical catalysts in many organic reactions. PILCs have been investigated as acid catalysts for various reactions. Table 1.15.1 lists several PILC catalysts and the reactions which they have been reported to catalyze[120-124].

Table 1.15.1 Acid catalyzed reactions on PILCs

Clay	Pillar	Reaction
Montmorillonite	Tetramethylammonium	Oligomerization
Montmorillonite	Triethylene diamine	Hydration Esterification
Montmorillonite Hectorite Bentonite	Al, Zr, (Al / Zr)	Cracking
Montmorillonite	Al, Zr	Disproportionation
Montmorillonite Saponite Bentonite	Al	Alkylation

Montmorillonite	Al, Zr	Methanol conversion
Bentonite	Al, (Al / Zr)	Oligomerization
Montmorillonite Bentonite	Al	Hydroisomerization

1.16 CLAY/POLYMER NANOCOMPOSTIES

The mystery of the 'nano-world' has been progressively exposed in recent years. The real interest in nanotechnology is to create revolutionary properties and functions by tailoring materials and designing devices on the nanometer scale.

Clay/polymer nanocomposites are typical examples of nanotechnology. This class of material uses smectite type clays, such as rectorite, montmorillonite and synthetic mica as fillers to enhance the properties of polymers. In clays, as already mentioned, hundreds or thousands of layers are stacked together with weak Van der Waals forces (approximately 1nm thick and 30 nm to several microns or larger diameter) to form a clay particle. Thus it is possible to tailor clays into various different structures in a polymer.

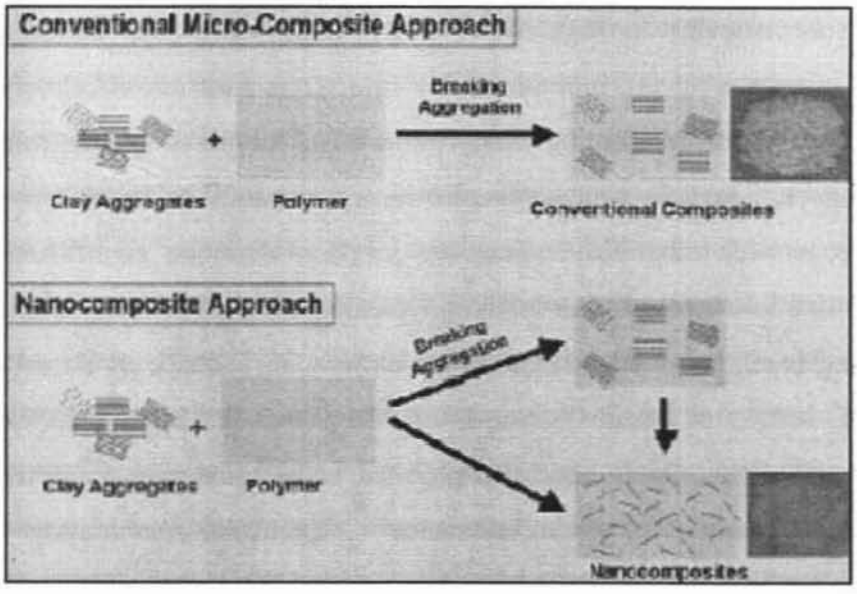

Figure 1.16.1 Diagrammatic representation of polymer/clay composites

In the past, the major interest in using clays for polymer enhancement was to break down clay particle aggregates into individual particles to form micro-sized filler reinforced polymers, as shown in figure 1.16.1. It can be imagined that the excellent mechanical properties of each individual layer in clay particles cannot function effectively in such a system. The weak interlayer bonding may act as damage initiation sites in applications. It is common to use high clay loading to achieve adequate improvement of the modulus, while strength and toughness of the polymer are reduced.

The principle used in clay/polymer nanocomposites is to separate not only clay aggregates but also individual silicate layers in a polymer, as

illustrated schematically in figure.1.16.1. By doing this, the excellent mechanical properties of the individual clay layers can function effectively, while the number of reinforcing components also increases dramatically because each clay particle contains hundreds or thousands of layers. As a consequence, a wide range of engineering properties can be significantly improved with a low level of filler loading, typically less than 5 wt%. At such a low loading level, polymers such as nylon-6 show an increase in Young's modulus of 103%, in tensile strength of 49%, and in heat distortion temperature of 146%[7]. Other improved physical and engineering properties include fire retardancy[125,126], barrier resistance[127-129], and ion conductivity[130-131]. Other method to produce nanocomposites includes doing the polymerization of monomers inside the clay layers. Here efficient distribution of polymers occurs within the layers. Another advantage of clay/polymer nanocomposites is that the optical properties of the polymer are not significantly affected. The thickness of individual clay layers is much smaller than the wavelength of visible light so that well exfoliated clay/polymer nanocomposites should be optically clear. The images of micro-and nanocomposites shown in figure were produced using the same clay and polypropylene mixture and applying a rapid cooling process to minimize the crystallization effect. The conventional microcomposites appear brown and opaque, while the nanocomposites are almost transparent.

It is clear from this evidence that clay/polymer nanocomposites are a good demonstration of nanotechnology. By tailoring the clay structure in polymers on the nanometer scale, novel material properties have been found.

Another interest in developing clay/polymer nanocomposites is that the technology can be applied immediately for commercial applications. The first commercial application of these materials was the use of clay/nylon-6 nanocomposites as timing belt covers for Toyota cars, in collaboration with Ube in 1991[132]. Shortly after this, Unitika introduced nylon-6 nanocomposites for engine covers on Mitsubishi's GDI engines[132]. In August 2001, General Motors and Basell announced the application of clay/polyolefin nanocomposites as a step assistant component for GMC Safari and Chevrolet Astro vans[133]. This was followed by the application of these nanocomposites in the doors of Chevrolet Impalas. More recently, Noble Polymers has developed clay/polypropylene nanocomposites for structural seat backs in the Honda Acura[134], while Ube is developing clay/nylon-12 nanocomposites for automotive fuel lines and fuel system components.

The era of clay/polymer nanotechnology can truly be said to have begun with Toyota's work on the exfoliation of clay in nylon-6 in the latter part of the 1980s and the beginning of the 1990s[135-137]. It was this work that demonstrated a significant improvement in a wide range of engineering properties by reinforcing polymers with clay on the nanometer scale[138,139]. Since then, extensive research in this field has been carried out globally. At present, development has been widened into almost every engineering polymer including polypropylene (PP), polyethylene, polystyrene, polyvinylchloride, acrylonitrile butadiene styrene (ABS) polymer, polymethylmethacrylate, PET, ethylene-vinyl acetate copolymer (EVA), polyacrylonitrile, polycarbonate, Polyaniline, polyethylene oxide (PEO), epoxy resin, polyimide, polylactide,

polycaprolactone, phenolic resin, poly p-phenylene vinylene, polypyrrole, rubber, starch, polyurethane, and polyvinylpyridine (PVP)[140-161].

Several methods have been developed to produce clay/polymer nanocomposites. Three methods were developed in the early stages of this field and have been applied widely. These are: in situ polymerization, solution induced intercalation[162], and melt processing[163]. In situ polymerization involves inserting a polymer precursor between clay layers and then expanding and dispersing the clay layers into the matrix by polymerization. The initial work in this area was carried out by the Toyota Research Group to produce clay/nylon-6 nanocomposites[164,165]. This method is capable of producing well-exfoliated nanocomposites and has been applied to a wide range of polymer systems. The technology is suitable for raw polymer manufacturers to produce clay/polymer nanocomposites in polymer synthetic processes and is also particularly useful for thermosetting polymers. The solution-induced intercalation method applies solvents to swell and disperse clays into a polymer solution. This approach poses difficulties for the commercial production of nanocomposites for most engineering polymers because of the high costs of the solvents required and the phase separation of the synthesized products from those solvents. There are also health and safety concerns associated with the application of this technology. However, solution- induced intercalation is applicable to water-soluble polymers, because of the low cost of using water as a solvent and its low health and safety risks, and can be used in the commercial production of nanocomposites. The melt processing method induces the intercalation of clays and polymers during melt. The efficiency of

intercalation using this method may not be as high as that of in situ polymerization[166] and often the composites produced contain a partially exfoliated layered structure. However, the approach can be applied by the polymer processing industry to produce nanocomposites based on traditional polymer processing techniques, such as extrusion and injection molding. Therefore, the technology has played an important role in speeding up the progress of the commercial production of clay/polymer nanocomposites. In addition to these three major processing methods, other fabrication techniques have been also developed. These include solid intercalation[167], co-vulcanization[168], and the sol- gel method[169]. Some of these methods are in the early stages of development and have not yet been widely applied.

1.17 OBJECTIVES OF THE PRESENT WORK

The main objective of the present work includes

- Structural tuning of montmorillonite clays by single as well as mixed pillaring using polyoxocations of Titanium, Zirconium, Aluminium and Chromium.
- Physico-chemical characterization using various techniques such as CEC measurements, elemental analysis, BET surface area and pore volume measurements, XRD, FTIR, ^{27}Al NMR, ^{29}Si NMR, UV-DRS, TG/DTA and SEM analysis to know the improvement upon modification.

- Note the acidity using three independent methods i.e. TPD of NH_3, Pyridine IR and test reactions cumene cracking as well as cyclohexanol decomposition.
- Monitoring the catalytic efficiency towards industrially as well as pharmaceutically important organic transformations, by selecting some Friedel-Crafts Alkylation reactions such as isopropylation of benzene and toluene, ethylation of benzene, methylation of toluene and LAB synthesis using 1-octene, 1-decene and 1-dodecene as the alkylating agents.
- To check the intercalating properties to form PANI/Montmorillonite nanocomposites in the presence of initiator oxidant $(NH_4)_2S_2O_8$.

REFERENCES:

1. M. Balogh, P. Laszlo, Organic Chemistry Using Clays, Springer, Berlin, 1993.
2. R.S. Varma, Tetrahedron 58 (2002) 1235.
3. E. Grim, Clay Minerology, Mc Graw-Hill, New York. ed. 2. 1968, Ch. 14.
4. T. J. Pinnavaia, Sci. 220 (1983) 365.
5. A. Azzouz, D. Messad, D. Niston, C. Catrinescu, A. Zvolinaschi, A. Asaftei, Appl. Catal. A: Geen. 241 (2003) 1.
6. M.M. Mortland, Adv. Agron. 22 (1970) 75.

7. M.M. Mortland, Trans. 9th Int. Congr. Soil Sci. 1 (1968) 691.
8. B.K.G. Theng, The Chemistry of Clay Organic Reactions, Wiley, New York 1974.
9. V. Berkheiser, M.M. Mortland, Clays Clay Miner. 25 (1977) 105.
10. K.V. Raman, M.M. Mortland, Ibid. 16 (1968) 393.
11. H. Suquet, C. de la Calle, H. Pezerat, Clays Clay Miner. 23 (1975) 1.
12. D.M. Mac Ewan, M.J. Wilson, Crystal Structures of Clay Minerals and Their X-ray Identification, G.W. Brindley, G. Brawn, (eds), Mineralogical society, London, 1980, Ch. 3.
13. R. Glaeser, J. Mering, C.R. Acod, Sci. Cer. D 267 (1968) 463.
14. H. Van Olphen, An Intreoduction to Clay Colloid Chemistry, Willy, New York, ed. 2, 1977, Ch. 7.
15. D.A. Morgen, D.B. Shaw, M.J. Sidebottom, T.C. Soon, R.C. Taylor, J. Am. Oil Chem. Soc. 62 (1985) 292.
16. W. Cranquit, G.S. Gardner, Clays Clay Miner. (1952) 292.
17. C.R. Theocharis, K.J. Jacob, A.C. Gray, J. Chem. Soc. Faraday Trans. 1 (1988) 1509.
18. R.E. Grim, Clay Mineralogy, McGraw-Hill, New York, 1953.
19. S.L. Swarten-Allen, E. Matijevic, Chem. Rev. 74 (1974) 385.
20. I. Sissoko, E.T. Iyagba, R. sahai, J. Biloen, Solid State Chem. 60 (1985) 283.
21. R. Thevenot, R. Szymanski, P. Chaumette, Clays Clay Miner. 37 (1989) 396.
22. G. Lagaly, Phil Trans. Roy. Soc. Lond. A311 (1984) 315.
23. L.R. Synder, J.W. Ward, J. Phys. Chem. 70 (1966) 3941.

24. D.O. Hary, Chem. Soc. Rev. (1992) 19.
25. R.M. Kim, J.E. Pillon, D.A. Burwell, J.T Groves, M.E. Thompsom, Inorg. Chem. 32 (1993) 4509.
26. F. Berjaya, N. Hassoun, L. Gatineau, J. Barrault, Preparation of Catalysts, G. Poncelot (ed), Elsevier Science Publishers B.V, Amsterdam, 1991, p. 329.
27. R.M. Barrer, D.M. McLeod, Trans Faraday Soc. 51 (1955) 1290.
28. G.W. Brindley, R.E. Sempels, Clay Minerals 12 (1977) 229.
29. D.E.W. Vaughan, R.J. Lussier, in Proc. 5th International Conference on Zeolites, Naples, L.V.C. Rees (ed), Hyeden, London, 1980, p. 94.
30. K.M. Parida, P.K. Satapathy, A.K. Sahoo, N. N. Das, J.Coll. Interface Sci. 173 (1995) 112.
31. B.M. Choudary, V.L.K. Valli, A. D. Prasad, J. Chem. Soc. Chem. Commun. (1990) 721.
32. F. Figueras, Catal. Rev. Sci. Eng. 42 (2000) 145.
33. L. Li, X. Liu, R. Xu, J. Rocha, J. Klinowski, J. Phy. Chem. 97 (1993) 10389.
34. N. Bjerrum, Phys. Chem. 59 (1907) 349.
35. C.F. Baes, R.E. Mesmer, The Hydrolysis of Cations, Wiley, New York, 1976.
36. B. Gu, H.E. Doner, Clays Clay Miner. 38 (1990) 493.
37. G.J.J. Bartley, Catal. Today. 2 (1988) 309.
38. H. Yoneyama, S. Haga, S. Yamanaka, J. Phy. Chem. 93 (1989) 4833.
39. A.G. Vormokov, Topics in Current Chemistry, Springer Verlay, Berlin, 1982, p. 169.

40. P. Canizares, J.L. Velverde, M.R. Sunkou, C.B. Molina, Microporous Mater. 29 (1999) 267.

41. C. Volzone, Clays Clay Miner. 43 (1995) 377.

42. S.P. Christiano, J. Wang, T.J. Pinnavaia, inorg. Chem. 24 (1985) 1222.

43. S.M. Bradley, R.A. Kydd, Catal. Lett. 8 (1991) 185.

44. S.Yamanaka, G.w. Bridley, Clays Clay Miner. 26 (1978) 21.

45. S.L. Suib, J. F. Tanguay, M.L. Occelli, J. Am. Chem. Soc. 108 (1986) 6972.

46. S. Yamanaka, G. Yamashita, M. Hattori, Clays. Clay Minor. 28 (1980) 281.

47. J.T. Kloprogge, D. Seykens, J.B.H. Jansen, J.W. Geus, J. Non-Cryst. Solids 142 (1992) 94.

48. J.Y. Bottero, D. Tchoubar, J.M. Cases, F. Fiessinger, J. Phys. Chem. 86 (1982) 3667.

49. G. Johansson, Acta Chem. Scand. 14 (1960) 771.

50. J.P. Sterte, J.E. Otterstedt, in Preparation of Catalysts IV, B. Delmon, P. Grange, P.A. Jacobs, G. Poncelet (eds), (1987), p. 631.

51. R.A. Schoonheydt, J. van der Eynde, H. Tubbax, H. Leeman, M. Stuyckens, I. Lenotte, W.E.E. Stone, Clays Clay Miner. 41 (1993) 598.

52. R.A. Schoonheydt, H. Leeman, Clays Clay Miner. 27 (1992) 249.

53. L. Bergaoui, J.-F. Lambert, R. Franck, H. Suquet, J.-L. Robert, J. Chem. Soc. Faraday Trans. 91 (1995) 2229.

54. R. Keren, Clays Clay Miner. 34 (1986) 534.

55. P. Falaras, F. Lezou, G. Seiragakis, D. Petrakis, Clays Clay Miner. 48 (2000) 549.

56. D. Plee, F. Borg, L. Gatineau, J.J. Fripiat, J. Am. Chem. Soc. 107 (1985) 2362.
57. H. Kodama, S.S. Singh, Solid State Ionics 32/33 (1989) 363.
58. S.S. Singh, H. Kodama, Clays Clay Miner.36 (1988) 397.
59. M.L. Occelli, J. Mol. Catal. 35 (1986) 377.
60. M.L. Occelli, in Proc. Int. Clay Conf. Denver 1985, L.G. Schultz, H. van Olphen, F.A. Mumpton (eds), 1987, p. 319.
61. M.L. Occelli, D.H. Finseth, J. Catal. 99 (1986) 316.
62. R. Burch, C.I. Warburton, J. Catalysis 97 (1986) 503.
63. R. Burch, C.I. Warburton, J. Catalysis 97 (1986) 511.
64. E.M. Fanfan-Torres, O. Dedeycker, P. Grange, in Scientific Bases for the Preparation of Heterogeneous Catalysts, 5th Int.Symp. Louvain-La-Neuve, Belgium, 1990, Preprint, p. 469.
65. G.J.J. Bartley, Catal. Today 2 (1988) 233.
66. G.J.J. Bartley, R. Burch, Appl. Catal. 19 (1985) 175.
67. K. Ohtsuka, Y. Hayashi, M. Suda, Chem. Mater. 5 (1993) 1823.
68. E.M. Fanfan-Torres, E. Sham, P. Grange, Catal. Today 15 (1992) 515.
69. S. Yamanaka, G.W. Brindley, Clays Clay Miner. 27 (1979) 119.
70. S.A. Bagshaw, R.P. Cooney, Chem. Mater. 5 (1993) 1101.
71. B.I. Nabivanets, L.N. Kudritskaya, Russ. J. Inorg. Chem. 12 (1967) 616.
72. H. Einaga, J. Chem. Soc. Dalton Trans. (1979) 1917.
73. R.T.Yang, J.P. Chen, E.S. Kikkinides, L.S. Chen, Ind. Eng. Chem. Res. 31 (1992)1440.
74. J. Sterte, Clays Clay Miner. 34 (1986) 658.
75. A. Bernier, L.F. Admaiai, P. Grange, Appl. Catal. 77 (1991) 269.

76. P. Malla, S. Yamanaka, S. Komarneni, Solid State Ionics 32/33 (1989) 354.

77. H. Yoneyama, S. Haga, S. Yamanaka, J. Phys. Chem. 93 (1989) 4833.

78. B.M. Choudary, V.L.K. Valli, A. Durga Prasad, J. Chem. Soc., Chem. Commun. (1990) 1186.

79. M. Sychev, N. Kostoglod, A. Kosorukov, V. Goncharuk, V. Kashkovski, in Proc. Polish-German Zeolite Colloquium, M. Rozwadowski (ed), Torun, Poland, 1992, p. 63.

80. H.L. Del Castillo, P. Grange, Appl. Catal. 103 (1993) 23.

81. G.W. Brindley, S. Yamanaka, Amer. Mineral. 64 (1979) 830.

82. R.M. Carr, Clays Clay Miner. 33 (1985) 357.

83. T.J. Pinnavaia, M.-S. Tzou, S.D. Landau, J. Am.. Chem. Soc. 107 (1985) 4783.

84. P.D. Hopkins, B.L. Meyer, D.M. Van Duch, U.S. Patent 4,452,910, 1984.

85. C.F. Baes, R.E. Mesmer, The Hydrolysis of Cations, Wiley-Interscience, New York, 1976, p. 211.

86. J.A. Laswick, R.A. Plane, J. Am. Chem. Soc. 81 (1959) 3564.

87. J.E. Early, R.D. Cannon, in Transition Metal Chemistry 1, R.L. Carlin (ed) Martin Dekker, New York, 1965, p. 34.

88. J.E. Finholt, M.E. Thompson, R.E. Connick, Inorg. Chem.20 (1981) 4151.

89. H. Stunzi, W. Marty, Inorg. Chem. 22 (1983) 2145.

90. H. Stunzi, L. Spicia, R.P. Rotzinger, W. Marty, Inorg. Chem. 28 (1989) 66.

91. W.E. Dubbin, T.B. Goh, D.W. Oscarson, F.C. Hawthorne, Clays Clay Miner. 42 (1994) 331.
92. M.-S. Tzou, T.J. Pinnavaia, Catal. Today 2 (1988) 243.
93. R. Burch, C.I. Warburton, Appl. Catal. 33 (1987) 395.
94. F. Bergaya, N. Hassoun, J. Barrault, L. Gatineau, Clay Minerals 28, 109 (1993).
95. D.H. Doff, N.H.J. Gangas, J.E.M. Allan, J.M.D. Coey, Clay Miner. 23 (1988) 367.
96. M.-S. Tzou, Ph.D. Thesis, Michigan State University, 1983.
97. W.Y. Lee, B.J. Tatarchuk, Hyperfine Interactions. 41 (1988) 661.
98. W.Y. Lee, R.H. Raythatha, B.J. Tatarchuk, J. Catal. 115 (1989)159.
99. H.M. Mody, P.M. Oza, V.P. Pandya, J. Indian Chem. Soc.70 (1993) 11.
100. C.I. Warburton, Catal. Today 2 (1988) 271.
101. S. Yamanaka, T. Doi, S. Sako, M. Hattori, Mat. Res. Bull.19 (1984)161.
102. S. Yamanaka, M. Hattori, Catal. Today 2 (1988) 261.
103. M.A. Martin-Luengo, H. Martins-Carvalho, J. Ladriere, P.Grange, Clay Miner. 24 (1989) 495.
104. S.M. Bradley, R.A. Kydd, R. Yamdagni, J. Chem. Soc. Dalton Trans. (1990) 413.
105. S.M. Bradley, R.A. Kydd, R. Yamdagni, J. Chem. Soc.Dalton Trans. (1990) 2653.
106. S.M. Bradley, R.A.Kydd, R.Yamdagni, Magn. Res. Chem. 28 (1990) 746.
107. S.M. Bradley, R.A. Kydd, R. Yamdagni, in Proc. Symp. Synthesis and Properties of New Catalysts; Utilization of Novel Materials,

Components and Synthetic Techniques, Fall Meeting MRS Boston, U.S.A., E.W. Corcoran and M.J. Ledoux (ed), 1990, p. 69.

108. S.M. Bradley, R.A. Kydd, K.K. Brandt, Progress in Catalysis, (1992) 287.

109. S.M. Bradley, R.A. Kydd, J. Catal. 142 (1993) 448.

110. B.M. Choudary, V.L.K. Valli, J. Chem. Soc., Chem. Commun. (1990) 1115.

111. B.M. Choudary, V.L.K. Valli, A. Durga Prasad, J. Chem. Soc., Chem. Commun. (1990) 721.

112. T. Endo, M.M. Mortland, T.J. Pinnavaia, Clays Clay Miner. 28 (1980) 105.

113. R.M. Lewis, K.C. Ott, R.A. van Santen, U.S. Patent 4,510,257, 1985.

114. G.W. Brindley, C.-C. Kao, Clays Clay Miner. 28 (1980) 435.

115. A.K. Lavados, P.J. Pomonis, in Scientific Bases for the Preparation of Heterogeneous Catalysts, 5th Int. Symp. Louvain-La-Neuve Belgium, 1990, Preprint, p. 131.

116. S.P. Skaribas, P.J. Pomonis, P. Grange, B. Delmon, J. Chem. Soc. Faraday Trans. 88 (1992) 3217.

117. M. Uehara, A. Yamazaki, R. Otsuka, S. Tsutsumi, Clay Sci. 9 (1993) 1.

118. J.T. Kloprogge, J. Porous Mater. 5 (1998) 5.

119. J.A. Ballantine, Chemical Reactions in Organic and Inorganic Constrained System in NATO ASI Series Ser. C 165 (1985) 197.

120. A. weiss. Angew. Chem Ind. Ed. Engl. 20 (1981) 850.

121. M.M. Mortland, V. Berkheiser, Clays Clay Miner. 24 (1976) 60.

122. J. Shabtai, N. Frydman, R. Lazer, Proc. 6th Int. Congr. Catal. 1976, p.

660.

123. J. Shabtai, R. Lazer, A.G. Oblad, Proc. 7th Int. Congr. Tokyo, 1980, p. 828.

124. E. Kikuchi, T. Matsuda, R.E.P. Asahi, Glass Found. Ind. Techol. 45 (1985) 111.

125. J. W. Gilman, Appl. Clay Sci. 15 (1999) 31.

126. A.B. Morgan, J.M. Antonucci, M.R. VanLandingham, R.H. Harris, T. Kashiwagi, Polym. Mater. Sci. Eng. 83 (2000) 57.

127. Yano, K., A. Usuki, A. Okada, T. Kurauchi, O. Kamigaito, J. Polym. Sci., Part A: Polym. Chem. 31 (1993) 2493.

128. C. Nah, H.J. Ryu, W.D. Kim, S.S. Choi, Polym. Adv. Technol. 13 (2002) 649.

129. G. Gorrasi, Polym. 44 (2003) 2271.

130. R. A. Vaia, Adv. Mater. 7 (1995) 154.

131. J. C Hutchison, R. Bissessur, D.F. Shriver, Chem. Mater. 8 (1996) 1597.

132. Auto applications of drive commercialization of nanocomposites. Plastic Additives & Compounding, January 2002, 30.

133. H. Cox, et al., Nanocomposite systems for automotive applications. Presented at 4th World Congress in Nanocomposites, EMC, San Francisco, 1-3 September 2004.

134. T. Patterson, Forte™ nanocomposites – our revolutionary breakthrough. Presented at 4th World Congress in Nanocomposites, EMC, San Francisco, 1-3 September 2004.

135. A. Okada, Y. Fukushima, M. Kawasumi, S. Inagaki, A. Usuki, S. Sugiyama, T. Kurauchi, O. Kamigaito, US Patent 4,739,007, 1988.

136. M. Kawasumi, M. Kohzaki, Y. Kojima, A. Okada, O. Kamigaito, US Patent 4,810,734, 1989.

137. A. Usuki, Y. Kojima, M. Kawasumi, A. Okada, Y. Fukushima, T. Kurauchi, O. Kamigaito, J. Mater. Res. 8 (1993) 1179.

138. Y. Kojima, A. Usuki, J. Mater. Res. 8 (1993) 1185.

139. Y. Kojima, A. Usuki, M. Kawasumi, A. Okada, T. Kurauchi, O. Kamigaito, J. Appl. Polym. Sci. 49 (1993) 1259.

140. M. Kawasumi, N. Hasegawa, M. Kato, A. Usuki, A. Okada, Macromol. 30 (1997) 6333.

141. J.S. Bergman, H. Chen, E.P. Giannelis, M.G. Thomas, G.W. Coates, Chem. Commun. 21 (1999) 2179.

142. X. Fu, S. Qutubuddin, Mater. Lett. 42 (2000) 12.

143. C. Wan, X. Qiao, Y. Zhang, Y.X. Zhang, Polym. Test. 22 (2003) 453.

144. L.W. Jang, J. Polym. Sci., Part B: Polym. Phys. 39 (2001) 719.

145. M. Okamoto, A. Morita, H. Taguchi, Y.H. Kim, T. Ko-taka, H. Tateyama, Polym. 41 (2000) 3887.

146. G. Zhang, Mater. Lett. 57 (2003) 1858.

147. M. Alexandre, G. Beyer, C. Henrist, R. Cloots, A. Rulmont, R. Jérôme, Ph. Dubois, Macromol. Rapid Commun. 22 (2001) 643.

148. K. A. Carrado, L. Xu, Chem. Mater. 10 (1998) 1440.

149. X. Huang, S. Lewis, W.J Brittain, R.A Vaia, Macrom. 33 (2000) 2000.

150. W. Krawiec, L.G. Scanlon, J.P. Fellner, R.A. Vaia, E.P. Giannelis, J. Power Sources. 54 (1995) 310.

151. J. M. Brown, D. Curliss, R.A. Vaia, Chem. Mater. 12 (2000) 3376.

152. J. H. Chang, K. M. Park, Polym. Eng. Sci. 41 (2001) 2226.

153. R. S. Sinha, P. Maiti, M. Okamoto, K. Yamada, K. Ueda, Macromol. 35 (2002) 3104.
154. J. Hao, J. Appl. Polym. Sci. 86 (2002) 676.
155. M.H. Choi, I.J. Chung, J.D. Lee, Chem. Mater. 12 (2000) 2977.
156. H.C. Lee, Appl. Clay Sci. 21 (2002) 287.
157. S.H. Hong, B.H. Kim, J. Joo, J.W. Kim, H.J. Choi, Curr. Appl. Phys. 1 (2001) 447.
158. Y.P. Wu, L.Q. Zhang, Y.Q. Wang, Y. Liang, D.S. Yu, J. Appl. Polym. Sci. 82 (2001) 2842.
159. H. M. Park, X.C. Li, C.Z. Jin, C.Y. Park, W.J. Cho, C.S. Ha, Macromol. Mater. Eng. 287 (2002) 553.
160. T.K. Chen, Y.I. Tien, K.H. Wei, Polym. 41 (2000) 1345.
161. R. Dhamodharan, J.D. Jeyaprakash, S. Samuel, M.K. Rajeswari, J. Appl. Polym. Sci. 82 (2001) 555.
162. K. Yano, A. Usuki, A. Okada, T. Kurauchi, O. Kamigaito, J. Polym. Sci., Part A: Polym. Chem. 31 (1993) 2493.
163. R.A. Vaia, H. Ishii, E.P. Giannelis, Chem. Mater. 5 (1993) 1694.
164. A. Okada, M. Wakasumi, A. Usuki, Y. Kojima, T. Kurauchi, O. Kamigaito, Mater. Res. Soc. Proc. 171 (1990) 45.
165. Y. Kojima, A. Usuki, M. Kawasumi, A. Okada, T. Kurauchi, O. Kamigaito, J. Polym. Sci., Part A: Polym. Chem. 31 (1993) 983.
166. Gao, F., et al., From burning behaviour to understand the mechanisms of solution and solid intercalations in clay/PEO nanocomposites. Presented at Organic-Inorganic Hybrids II, PRA, Guildford, 28-29 May 2002.
167. F. Gao, S. Chen, J.B. Hull, J. Mater. Sci. Lett. 20 (2001) 1807.

168. A. Usuki, A. Tukigase, M. Kato, Polym. 43 (2002) 2185.

169. P. Musto, G. Ragosta, G. Scarinzi, L. Mascia, Polym. 45 (2004) 1697.

★★★★★★★★★★★★★★★★★

Chapter 2

MATERIALS AND METHODS

Eco-friendly society demands the heterogeneous catalysis, but the main problem here lies in the selectivity and the efficiency. The demand of heterogeneous catalysts is in its regenerability and reusability. Thus for efficient use of the naturally available clays the structural as well as thermal stability is to be improved, the porosity must be enhanced and additional acidic sites are required for efficient catalytic activity in acid catalyzed reactions. The porous nature increases the intercalating properties for the preparation of nanocomposites. Here the process of pillaring, which can be monitored using various characterization techniques, does the art of structural tuning of montmorillonite clays. This chapter describes the present preparation method and various experimental techniques used to prove the enhancement in the structural as well as textural properties upon pillaring. The procedure for gas phase reactions are given with the detailed description of the analytical methods adopted.

2.0 INTRODUCTION

In designing and synthesizing new solid inorganic materials used as catalysts the aims are to maximize surface area, activity, selectivity, longevity and durability. Surface area increase as a result of enlarged porosity enhances the intercalating properties in layered materials. For producing materials with large surface areas, the surface composition, structure and atomic architecture of the materials before and after modifications are incontrovertibly characterized. The optimum preparation conditions in material synthesis have to be strictly followed to get good results whose variation leads the modification less effective.

2.1 PREPARATION OF PILLARED CLAYS (PILCS)

Titanium, Zirconium, Aluminium and Chromium single PILCs are prepared. Mixed PILCs containing 2 metals as the pillars are also prepared to enhance the properties of single PILCs.

Materials	Suppliers
Titanyl Sulphate	Travancore Titanium Products, Trivandrum, 99% purity
Zirconyl oxychloride	CDH
Aluminium (III) nitrate	Merck
Chromium (III) nitrate	CDH

Liquid Ammonia	Qualigens
Nitric Acid	Merck
Sodium carbonate	Qualigens

Pillaring agent preparation is the first step of propping apart the clay layers. Ti pillaring agent is the titania sol prepared through colloidal route where Zr pillaring agent is the freshly prepared zirconyl oxychloride solution. Al and Cr pillaring agents are prepared using partial hydrolysis method.

The various steps during pillaring are

- Preparation of pillaring solution
- Intercalation of metal polyoxocations between the layers
- Washing of the reaction mixture
- Drying and Calcination

Prior to pillaring KSF is treated with 0.5 M sodium nitrate (Sd Fine Chemicals Ltd.) solution at 70°C for 24 h, then filtered, made nitrate free by washing and is dried at 110°C to get the Na^+-exchanged montmorillonite. The pillaring solution is then added to the previously swelled Na^+-exchanged montmorillonite clay with a metal to clay ratio of 10 mmol/g. The solution is stirred at 70°C for 24 h, kept overnight, filtered, washed free of nitrate/chloride ions, dried at 110°C and calcined at 500°C for 5 h to get pillared montmorillonite.

For mixed pillared systems 5 mmol of each pillaring solution is mixed to give a total of 10mmol metal/g clay.

For Al pillaring partially hydrolyzed aluminium nitrate solution (0.2 M) prepared at 70°C is used. Partial hydrolysis is done by drop wise addition of 0.3 M sodium carbonate solution with a base to metal ratio of 2 under vigorous stirring for 2 h at 70°C and is again stirred at the same temperature for 6 h. 0.2 M solution of Chromium nitrate was partially hydrolyzed by drop wise addition of 0.3 M sodium carbonate solution with a base to metal ratio of 2 under vigorous stirring for 2 h at 95°C and is again stirred at the same temperature for 6 h. Freshly prepared zirconiumoxychloride is used for Zr pillaring. Ti pillaring agent is prepared using the method reported by Sivakumar et al[1]. Titanyl sulphate is used as precursor for the synthesis of titania sol. In a typical experiment, titanyl sulphate is dissolved in 500 ml of distilled water (0.2 M) and is hydrolyzed by slow addition of ammonium hydroxide (10%) solution under constant stirring at room temperature, until the reaction mixture attained pH 7.5. The precipitate obtained is separated by filtration and is washed free of sulphate ions with distilled water. The precipitate is further dispersed in 1000 ml of hot distilled water and is peptized by addition of 10% HNO_3 solution to get titania sol which is the pillaring agent. All systems are calcined at 500°C for 5 h.

2.2 NOTATION OF CATALYSTS

XM is the notation used for single PILCs, where X is the first letter in the chemical formula of the pillar metal and M represents montmorillonite clay. XYM designates mixed PILCs, X and Y are the first letter in the chemical formula of the various metal pillars. In NM, N represents the exchanged Na^+ cations.

The different systems are notated as

M	Montmorillonite
TM	Titanium pillared Montmorillonite
ZM	Zirconium pillared Montmorillonite
AM	Aluminium pillared Montmorillonite
CM	Chromium pillared Montmorillonite
TZM	Titanium - Zirconium mixed pillared Montmorillonite
TAM	Titanium -Aluminium mixed pillared Montmorillonite
TCM	Titanium - Chromium mixed pillared Montmorillonite
AZM	Aluminium - Zirconium mixed pillared Montmorillonite
ACM	Aluminium - Chromium mixed pillared Montmorillonite
ZCM	Zirconium - Chromium mixed pillared Montmorillonite

2.3 CHARACTERIZATION TECHNIQUES

Various analytical techniques provide information about the designing of clay matrix for enhanced catalytic as well as intercalation properties. A brief description of various spectroscopic, quantitative as well as thermal analysis techniques adopted, principles and experimental aspects are given here. Except for thermal studies the systems are activated at 500°C for 2 h before subjecting to analysis.

Materials	Suppliers
Ammonium acetate	Merck
Ethyl alcohol	Merck
Sodium hydroxide	Qualigens
Hydrochloric acid	Qualigens
Sulphuric acid	Qualigens
Hydrofluric acid	Merck
Liquid nitrogen	Sterling Gases
Potassium bromide	Qualigens
Magnesium oxide	Merck

2.3.1 CATION EXCHANGE CAPACITY (CEC) MEASUREMENTS

Base exchange refers to the capacity of colloid particles to change the cations adsorbed on the surfaces. By cation exchange the permeability of clay

can be decreased and the sensitivity can be increased. The clay minerals have the property of sorbing certain anions and cations and retaining them in an exchangeable state. The exchangeable ions are held around outside of the silica alumina clay – mineral structural unit.

Compositional variation through ionic or isomorphous substitution within the clay mineral crystal lattice can leave the structural unit with a net negative charge. Substitution also reduces the crystal size and alters its shape. Exposed hydroxyl groups and broken surface bonds can also lead to a net negative charge on the structural unit. The presence of this net negative charge means that soluble cations can be attracted or adsorbed on to the surface of the clay mineral structural units without altering the basic structure of the clay mineral. The ability of clay to hold cations is termed as its cation exchange capacity. The most common soluble cations are Na^{+}, K^{+}, Ca^{2+}, and Mg^{2+}.

Pillaring polyoxocations enters the matrix by ion exchange with the exchangeable cations and remains as non-ion exchangeable metal oxide pillars after thermal treatment. Thus decrease in CEC is a measure of increase in the extent of pillaring.

The CEC is determined by stirring the sample with 3 M ammonium acetate (P^{H} = 7) solution. The mixture (1 g clay/60 ml solution) is stirred using a magnetic stirrer for 8 h at room temperature and then filtered. The resulting solid is washed with isopropyl alcohol and dried at 110°C for 4 h before use, and treated with 60% w/w NaOH in a Kjeldahl flask. The ammonia released is

collected in a 0.025 M HCl solution, and titrated with 0.025 M NaOH solution[2].

2.3.2 ELEMENTAL ANALYSIS – INDUCTIVELY COUPLED PLASMA – ATOMIC EMISSION SPECTROSCOPY

The elemental analyses of the PILC materials are done using inductively coupled plasma – atomic emission spectrometer. The advantage of ICP – AES analysis lies in its greater sensitivity and the possibility of multi element analysis. The multi element analysis offers a tremendous saving in analysis time. When heated to temperatures above 6000°C, gases such as argon form plasma – that is a gas containing a high proportion of electrons and ions. The plasma may be produced by an EC arc discharge or by inductive heating in an inductively coupled plasma (ICP) torch.

Discharge of a high voltage from a Tesla coil through flowing argon will provide free electrons, which will 'ignite' the gas to plasma. If the conducting plasma is enclosed in a high frequency electromagnetic field, then it will accelerate the ions and electrons and cause collisions with the support gas, argon, and the analyte. The temperature rises to around 10,000°C. At such temperatures, energy transfer is efficient and the plasma becomes self sustaining. It is held in place by magnetic field in the form of a fireball. The same aerosol enters the fireball at high speed and is pushed through it, becoming heated and emerging as a plumb, which contains the sample elements as atoms or ions, free of molecular association. As they cool to

around 6000 – 7000°C, they relax to their ground state and emit their characteristic spectral lines. This technique is ICP – Atomic emission spectroscopy (ICP – AES).

With ICP – AES there is little interference with ionization, since there is an excess of electrons present. The high temperature ensures that there is less interference from molecular species or from the matrix. Since a large number of elemental emission lines are excited, line overlap, though rare, may occur. By this technique up to 70 elements, both metals and non metals can be determined.

Clay samples for analysis are prepared after removing silica, which is estimated. A known weight (W_1) of the sample is taken in a beaker, treated with concentrated sulphuric acid (95%, 30 ml) and is heated until SO_3 fumes are evolved. It is cooled, diluted with water and filtered with ash less filter paper. Filtrate is collected; the residue is heated in a platinum crucible and is weighed (W_2). To the weighed high temperature treated sample 40% HF is added in drops, warmed and strongly heated to dryness. This is repeated 5-6 times, until no fumes of H_2SiF_6 are evolved. It is again incinerated to 800°C for 1 h, cooled and weighed (W_3). From the loss in weight the amount of silica present can be estimated using the equation

$$\% SiO_2 = (W_3-W_2) \times 100/W_1$$

Filtrate is diluted to a known volume and a small portion is taken for quantitative ICP – AES analysis. Analysis is done using 'GBC' Plasmalab 8440M instrument.

2.3.3 X-RAY DIFFRACTION (XRD) ANALYSIS

X-ray diffraction is an extremely important technique in the field of material characterization to obtain information on an atomic scale form both crystalline and non crystalline (amorphous) materials. XRD is also applied to derive information on the fine structure of materials – crystallite size, lattice strain, chemical composition, state of ordering etc. In a material an infinite number of lattice planes with different miller indices exist and each set of plane will have a particular separation d_{hkl}. In clays the interlayer spacing is of the d_{100} plane[3]. From Braggs equation,

$$n\lambda = 2d\sin\theta$$

d_{100} spacing is determined which is a measure of the extent of pillaring.

In powder XRD, there will be all possible orientation of the crystal. Each lattice spacing will give rise to a cone of diffraction. Each cone consists of a set of closely spaced data each one of which represents a diffraction form a single crystallite within the powder sample. Detector used in powder XRD is sensitive to X-rays. Scanning of the detector around the sample along the circumference of a circle cuts through the diffraction cones at various diffraction maxima. The intensity of X-rays detected as a function of detector angle 2θ is obtained.

The X-ray diffraction pattern of the powdered clays are obtained using a Rigaku D MAX III VC Ni-filtered Cu K alpha radiation (λ = 1.5404 Å at a scan rate of 4°/min).

2.3.4 SURFACE AREA AND PORE VOLUME MEASUREMENTS

Brunauer, Emmett and Teller developed the most common method of measuring surface area[4]. Early descriptions and evaluations are given by Emmett. In essence, the Langmuir adsorption isotherm is extended to multiplayer adsorption. The heat of adsorption of all layers except the 1st layer is assumed to be equal to the heat of liquefaction of the adsorbed gas. Summation over an infinite number of adsorbed layers gives the final expression as follows

$$P/V(P_0-P) = 1/V_mC + (C-1)P/V_mCP_0$$

Where V = volume of gas adsorbed at pressure P,

V_m = volume of gas adsorbed in monolayer, same unit as V

P_0 = saturation pressure of adsorbate gas at the experimental temperature

C = a constant related exponentially to the heats of adsorption and liquefaction of gas

$$C = e^{(q1-qL)/RT}$$

where q_1 = heat of adsorption on the first layer

q_L = heat of liquefaction of adsorbed gas on all other layers

R = the gas constant.

A graph of $P/V(P_0-P)$ Vs P/P_0 gives a straight line, the slope and intercept of which can be used to evaluate V_m and C.

Many adsorption data show very good agreement with the BET equation over values of the relative pressure P/P_0 between approximately 0.05 and 0.3 and this range is usually used for surface area measurements. The surface area of the catalyst can be calculated from V_m, if the average area occupied by an adsorbed molecule is known.

$$S.A = V_m N_0 A_m / 22414W$$

Where N_0 is the Avogadro number, A_m is the molecular cross sectional area of adsorbate and W is the weight of the sample. Adsorption of N_2 gas at its boiling point is generally used for surface area measurements using BET method. However, in microporous solids like PILCs where the interlamellar distance is of the order of a few molecular diameters, monolayer formation on clay silicate layer occurs. Thus surface areas approximated by Langmuir equation are reasonable representations of PILC surface areas[5].

The microporous surface area of the samples was calculated by the t-plot[6,7]. In this method, the adsorbed N_2 volume is plotted against statistical thickness (t) of adsorbed N_2 layer to yield micropore volume on the basis of

$$V = V_{micro} + 10^{-4} S_0 t$$

Where V_{micro} is the volume of N_2 adsorbed in micropores and S_0 is the external surface area. A universal t-curve of N_2 has been established which gives,

$$t = [13.99/ (0.034 - \log(P/P_0))]^{0.5}$$

where t is in Å. If the plot of V versus t gives a straight line passing through the origin, the test solid is considered to be free of micropores. For a microporous test solid, the t-plot shows a straight line at high t and a concave-down curve at low t; the extrapolation of the upper linear line to t = 0 gives a

slop of S_0 and an intercept of V_m. The difference between the BET surface area and the external surface area gives internal surface area, i.e., the surface area from pores. Mesopore volume is obtained by subtracting micropore volume from the total pore volume. The mean pore width is obtained from the relation dm = 2V/A, where V is the pore volume and A is the internal surface area[3].

The simultaneous determination of surface area and pore volumes of the catalyst samples was done on a micrometrics Gemini 2360 surface area analyzer. Previously activated samples were degassed at 300°C under N_2 atmosphere for 3 h and then brought to N_2 boiling point.

2.3.5 FOURIER TRANSFORM INFRARED (FTIR) SPECTROSCOPIC ANALYSIS

Infrared spectroscopy is a rapid, economical and non destructive physical method universally applicable to structural analysis. The technique is so versatile that it can be used both as a source of the physical parameters of crystal lattice determination and as a means of eliciting purely empirical quantitative relationships between specimens. It is an intrinsically simple technique that deserves to be more widely used in clay mineralogy and soil science.

The absorption of infrared radiation by clay minerals depends critically on atomic mass and length, strength and force constants of inter-atomic bonds in the structures of these minerals. It is also controlled by the constraints of the

overall symmetry of the unit cell, and the local site symmetry of each atom within the unit cell. The total number of potentially active internal vibrations is given by 3n-6, where n is the number of atoms in the unit cell. Not all of these vibrations are active in the infrared, only those that undergo a change in dipole moment during the absorption process.

The non-dispersive FTIR spectrometers, the detector continuously monitors the full wave number range of radiation emitted by the IR source, providing an inherently more sensitive system. Fourier transform instruments use interferometers, and they require a dedicated computer to transform their out put – an interferogram – into an absorption spectrum. FTIR spectrometers may be either single beam, in which the sample spectrum must be ratioed against a background, or double beam, in which ratioing against background is carried out continuously.

FTIR spectra of the powdered samples are measured by the KBr disk method over the range 4000 – 400 cm^{-1} using ABB BOMEM MB SERIES.

2.3.6 NMR SPECTRAL ANALYSIS

NMR spectroscopy is based on the absorption of energy in the radio frequency region of the electromagnetic spectrum by the nuclei of these elements that have spin angular momentum and a magnetic moment. For the nuclei of a particular element, characteristic absorption, or resonance frequencies, and other spectral features provide useful information on identity[8].

Nuclei of elements that possess spin angular momentum and generate a magnetic moment are assigned a half-integral or integral spin quantum number. This determines the number of orientations in space that can be adopted by the spinning of nuclei when subjected to an external magnetic field. Electrons also possess spin angular momentum, which generates a magnetic moment that affects the magnitude of the external field experienced by nuclei.

Nuclei of a particular element that are in different chemical environments within the same molecule generally experience slightly different applied magnetic field strength due to the shielding and deshielding effects of near by electrons. As a result, their resonance frequencies differ, and each is defined by a characteristic chemical shift value. The ^{27}Al NMR and ^{29}Si NMR gives the different environments of Al and Si present in parent as well as PILC systems.

NMR spectrometers comprise a superconducting solenoid or electromagnet to provide a powerful, stable and homogeneous magnetic field, a transmitter to generate the appropriate radiofrequencies, and a receiver coil and circuitry to monitor the detector signal. A dedicated microcomputer controls the recording of spectra and processing of data.

Solid NMR studies of materials are usually carried out by "Magic Angle Spinning (MAS)" i.e. rapid rotation of the sample about an axis subtended at an angle 54°44' with respect to magnetic field. This technique removes line broadening from dipolar interactions, chemical shift anisotropy

and quadrapolar interactions to the first order since all interactions contain the angular term ($3\cos^2\theta$ - 1) which is zero for θ = 54°44'. The number of signals in solid state NMR spectrum gives the number of different structural environment of observed nucleus in the sample while relative signal intensities correspond to relative occupancies of different environments[9]. High resolution solid state NMR provides information about bonding situation, symmetry properties and dynamic behavior of solid state structures.

^{27}Al NMR gives signals for octahedral Al at 0 ppm and tetrahedral Al at around 60 ppm. The tetrahedral Al in montmorillonite arises from pillaring species as well as leaching of octahedral Al into interlamellar sites during Na^+ ion exchange and pillaring.

In ^{29}Si NMR the resonance at –93.9 ppm is attributed to T (3Si, 1Al) units representing Si(IV) atoms linked through oxygens to three other Si(IV) and one Al(VI) (or Mg) in the clay octahedral layer. The second resonance near –112.5 ppm is attributed to SiO_2 impurities present in the parent clay.

Solid-state NMR experiments were carried out over a *Brucker DSX-300* spectrometer at resonance frequencies of 78.19 MHz for ^{27}Al and 59.63 MHz for ^{29}Si. XWINNMR software operating in a Unix environment in a silicon graphic computer was employed to acquire and retrieve the data. For all the experiments a standard 4 mm double- bearing *Brucker* MAS probe was used. The chemical shifts were referred to external standards, viz. tetramethylsilane

(TMS) for ^{29}Si studies at 0 ppm. 0.1 M aluminium nitrate solution was used as the external standard in the case of ^{27}Al.

2.3.7 UV-VIS DIFFUSED REFLECTANCE SPECTROSCOPY

Diffuse reflectance UV-visible spectroscopy is a useful probe of the electronic structure of dispersed metal oxides. A number of studies have shown that in situ UV- visible spectroscopy can probe the extent of reduction under steady state catalysis.

UV-VIS DRS spectra were taken in the range 200-800 nm on an Ocean Optics, Inc. SD 2000, Fiber Optic Spectrometer with a charged coupled device detector. The spectra were recorded at room temperature using MgO as a reference.

2.3.8 THERMAL ANALYSIS

The thermal stability of materials can be easily evaluated using thermal analysis i.e. simply by heating of the material and observe the changes that occur. While some analytical methods, such as spectrometry, give results that are very specific for the particular sample, thermal methods will respond to the totality of the effects. Anything that changes the mass at a particular temperature: evaporation, reaction or oxidation will affect the thermogravimetric measurement.

2.3.8.1 THERMOGRAVINETRY (TG)

In thermogravimetry the sample is heated, only that changes the mass of the sample will affect the measurement. The rate of change of mass, dm/dt depends on the amount of sample present and the reaction rate constant at the experimental temperature.

Thermal analysis finds widest applications in the determination of different parameters on preparation of materials, nature and composition of catalytically active phase, effect of added promoters or presence of impurities on the catalyst, dispersion of active phase and active phase support interactions, nature and heterogeneity of active sites on catalyst surface, nature of different bound states of adsorbates on catalyst surface, mechanistic aspects of the reaction under investigation, transient chemical changes that occur on surface, catalyst deactivation and regeneration. The technique can also be used for quality control and catalyst characterization through finger print spectra of different batches of the same catalyst.

A crucible containing the sample is heated in a furnace at a controlled rate and weighed continuously on a balance. Temperature and mass data are collected and preceded by a computer dedicated to the system. Control of the atmosphere surrounding the sample is important.

In more difficult cases, the reactions may overlap and then it is difficult to assess the separate temperature ranges and mass losses. An aid to this is the

derivative thermogravimetric (DTG) curves. This is produced electronically from TG trace by the computer and represents the dm/dt or occasionally the dm/dT, as a function of time or temperature.

TG analysis of the dried samples are performed in a Perkin Elmer Pyris Diamond thermogravimetric/differential thermal analyzer by heating the sample at a rate of 20°C min^{-1} from room temperature to 800°C in N_2.

2.3.8.2 DIFFERENTIAL THERMAL (DTA) ANALYSIS

This method relate to the monitoring of the heat absorbed or evolved during the heating of the sample and a reference in equivalent environments. Here the temperature difference is monitored. The measurement unit has a matched pair of temperature sensors placed in or near the sample and reference pans and heated in a temperature controlled furnace.

Physical changes that are not associated with weight loss are not detectable in TG, but give DTA signals. DTA gives signals corresponding to weight changes also. Heat capacity, which relates to the quantity of heat required to raise the sample temperature by one Kelvin is studied by DTA and physical changes such as melting and vaporization as well as crystal structure changes give peaks and some may be used to calibrate the system. Decompositions, oxidations or other reactions that may be endothermic or exothermic are also detected.

DTA is used to study pure chemicals, mixtures such as clay minerals and coal, biological samples, pharmaceuticals and especially polymers and materials. DTA of the dried samples are performed in a Perkin Elmer Pyris Diamond thermogravimetric/differential thermal analyzer by heating the sample at a rate of 20°C min^{-1} from room temperature to 800°C in N_2.

2.3.9 SCANNING ELECTRON MICROSCOPIC (SEM) ANALYSIS

Scanning electron microscopy has been used particularly for examination of the topology of catalyst surfaces and morphology of particles and crystals. Scanning electron microscopy examines the structure by bombarding the specimen with a scanning beam of electrons and then collecting slow moving secondary electrons that the specimen generates. These are collected, amplified and displayed on a cathode ray tube. The electron beam and the cathode ray tube scan synchronously so that an image of the specimen surface is formed. The samples are coated within a thin film of gold to make it conducting to prevent surface charging and to protect the material from thermal damage by electron beam[10].

The SEM images are taken in a JSM - 840 A, Scanning electron microscope, JEOL – Japan.

2.4 MEASUREMENT OF ACIDITY

Solid acid catalysis involves the largest amounts of catalysts used and the largest economical effort in the oil refining and chemical industry. Acid catalysts have the attractiveness that the nature of active sites are known and its behavior in acid catalyzed reactions can be rationalized by means of existing theories and models. Thus the surface acidity determination plays an important role in catalyst characterization[11].

The exact value of acid sites in catalysts cannot be determined directly as in solution. Also for any solid acid, a range of sites of different strengths exists. Thus it is not possible to know the exact acidity of each site. Hence, domains of acid strengths and number of sites belonging to the domain only can be defined.

Various methods have been used to find out the nature, strength and concentration of acid centers on the surface.

Materials used for surface acidity measurements are

Materials	Suppliers
Sulphuric acid	Merck
Sodium hydroxide	Qualigens
Oxalic acid	Merck

Phenolphtalein	CDH
Cumene	Aldrich
Cyclohexanol	Merck

The two independent techniques used to have a thorough knowledge of surface acidity are

1. Temperature programmed desorption of ammonia (TPDA)
2. FTIR of pyridine adsorbed samples
3. Test reactions for characterization of acid-base nature
    a) Cumene cracking reactions
    b) Cyclohexanol decomposition studies.

2.4.1 TEMPERATURE PROGRAMMED DESORPTION (TPD) OF AMMONIA

Temperature programmed desorption was first introduced by Amenomiya and Cvetanovic[12] which is a modification of flash desorption technique. It is, much simpler as it does not require any high vacuum conditions for the sample. Temperature programmed desorption of ammonia (TPDA) is widely used for the direct determination of cumulative acidity and acid site distribution. Ammonia, the important prob molecule used, can titrate acid sites of any strength and is easily accessible to even micropores due to its small size. NH_3 chemisorbs on a surface having acidic protons, electron acceptor sites and hydrogen from weakly acidic hydroxyls and thus can detect most types of acid sites[13].

The total acid site density of each of the catalyst is measured by TPDA (TPD of NH_3) using in a conventional flow-type apparatus at a heating rate of 20°C min^{-1} and in a nitrogen atmosphere[14].

The palletized samples are housed in a quartz reactor and pre heated in a flow of N_2 while heating at 20°C/min up to 300°C. After a period of 30 min at this temperature the sample is cooled to 40°C and NH_3 is injected and is saturated for 30 min. The catalyst is then allowed to equilibrate in a N_2 flow at room temperature for 30 min to remove any physisorbed one. The NH_3 is then desorbed using a linear heating rate of 20°C/min up to 600°C. The desorbed NH_3 is passed through 100 ml H_2SO_4 (0.0125) solution, to neutralize the evolved NH_3 at a temperature interval of 100°C. The excess H_2SO_4 is back titrated with NaOH (0.0125) for quantitative determination using phenolphthalein indicator. The amount desorbed at 35 - 200°C, 200 - 400°C and 400 - 600°C are assigned as weak, medium and strong acid sites respectively.

2.4.2 FTIR OF PYRIDINE ADSORBED SAMPLES

Infrared (IR) and Raman spectroscopy have been used to determine acidity of solid catalysts by studying adsorbed probe molecules[15,16]. The IR spectroscopy is a very powerful technique since it allows one to look directly at the hydroxyls present on a solid acid catalyst and consequently to see which of them can interact with basic molecules and therefore to find out which

presents Brønsted acidity and which of them are, or are not, accessible to base molecules of different sizes. In principle, the concentration of hydroxyl groups, and therefore the concentration of potential Brønsted acid sites, could be obtained from the intensity of the corresponding IR band. However, for quantitative estimation the extinction coefficients of the different types of hydroxyls contributing the IR band are required, something which is very seldom possible.

Attempts have been made to measure the surface concentration of different hydroxyl groups on the basis of the assignment of O-H stretching frequencies to specific types of hydroxyls, [17-20] with limited success in most of the cases. Then, it is not surprising that most of the information on acidity of solid catalysts obtained by IR comes from spectroscopic studies of adsorbed molecules. From this point of view two main groups of probe molecules have been used. The first one involves the adsorption of relatively strong basic molecules such as pyridine, substituted pyridines, quinoline, and diazines. Among them, 1,2- and 1-C diazines are less basic than pyridines and are more appropriate for the selective detection of very strong acid sites and for the semi quantitative measurement of Lewis and Brønsted acid sites, but they are in general less informative than pyridine. The pioneering works of Parry, Basila et al., and Hughes and White[21-23] showed that the pyridine molecule is able to simultaneously determine the concentration of Brønsted and Lewis acid sites. Moreover, when IR is combined with thermal desorption, it can provide estimation of acid strength distribution. The characteristic bands of pyridine protonated by Brønsted acid sites (pyridinium ions) appear at 1540 and 1640

cm^{-1}, while the bands from pyridine coordinated to Lewis acid sites appear at 1450 and 1620 cm^{-1}. Then, by measuring the intensity of those it is possible to calculate the number of Brønsted and Lewis acid sites.

Pyridine and NH_3 have been widely used as probe molecules, because they are quite stable and the IR spectroscopy can differentiate and quantify the amounts adsorbed on Brønsted and Lewis sites.

IR spectra of the different clays are taken after adsorbing pyridine. Samples are kept in a desicator containing pyridine where temperature is kept at 150°C for 3 h and is then cooled to room temperature and kept for 72 h. Then the samples are taken out, excess and physisorbed pyridine is degassed and is analysed using ABB BOMEM (MB Series) FTIR spectrometer.

2.4.3 TEST REACTIONS FOR ACID - BASE PROPERTIES

2.4.3.1 CUMENE CRACKING REACTIONS

Cumene cracking reaction is performed to know the catalytic activity and acid site distribution. Cumene is a convenient model compound for such catalytic studies, because it undergoes different reactions over different types of active sites. The cracking of cumene, producing benzene and propene, is generally attributed to the action of Brønsted acid sites, following a carbonium ion mechanism and it is commonly used as a model reaction for characterizing the presence of this type of site on catalyst surface. The formation of α-methyl

styrene during cumene cracking, due to dehydrogenation, has been ascribed to Lewis acidity[24,25]. Thus the present study allows the comparison of the distribution of both Brønsted as well as Lewis acid sites of the catalysts prepared.

2.4.3.2 CYCLOHEXANOL DECOMPOSITION REACTIONS

Alcohol decomposition reaction has been widely studied because it is a simple model reaction to determine the functionality of an oxide catalyst. Decomposition of isopropanol and that of cyclohexanol are the most widely studied reactions in this category. Dehydration activity is linked to the acidic property and dehydrogenation activity to the combined effects of both acidic and basic properties of the catalyst. Studies on cyclohexanol decomposition on spinel oxide have been reported[26]. Bezouha-nova and Al-Zihari[27], have recommended the dehydration activity of cyclohexanol conversion as a simple test to measure the Brønsted acid sites in a metal oxide. We are doing cyclohexanol decomposition reactions over various catalyst systems. In addition to measure the relative acidic sites it allows us to know whether there is any basic site present which makes clays as a bifunctional catalyst.

2.5 EXPERIMENTAL PROCEDURE FOR GAS PHASE REACTIONS

The catalyst was activated at 500°C for 2 hours before subjecting to the reaction. Reaction is carried out at atmospheric pressure in a fixed bed, vertical, down- flow glass reactor placed inside a double-zone furnace. Exactly

0.5 g of the sample is sandwiched between the layers of inert silica beads. A thermocouple detector monitors the temperature of the catalyst. The reactant is fed into the reactor by means of a syringe pump (Cole palmer®) at required WHSV, molar ratio (arene/alkylating agent in the case of Friedel-Crafts alkylation reactions) and temperature under a constant flow of nitrogen. The products and the unreacted reactant are condensed by means of a water condenser, collected in an ice trap and liquid samples are subjected to Gas Chromatographic analysis using Chemito GC 1000 gas chromatograph with BP1 capillary column connected to a FID detector. The reactant (alkylating agent in Friedel-Crafts alkylation reactions since we are using excess arene in all cases) conversion (weight percentage) and product selectivity (%) are noted. Initial activity is taken as the activity at 2nd hour. This is done to ensure the attainment of a steady state for the reaction over the catalysts and also to compensate effect of temperature fluctuations, if any due to the starting of the reaction.

2.6 GAS CHROMATOGRAPHY

Gas chromatography is a technique for the separation of volatile components of mixtures by differential migration through a column containing a liquid or solid stationary phase. Solutes are transported through the column by a gaseous mobile phase and are detected as they are eluted.

The mobile phase is an inert gas, generally nitrogen or helium, supplied from a cylinder via pressure and flow controls, and passing through

purification cartridges before entering the column. Gaseous, liquid and solid samples are introduced into the flowing mobile phase at the top of the column through an injection port using a micro syringe, valve or other device. Columns are either long, narrow capillary tubes with the stationary phase coated onto the inside wall, or shorter, larger diameter tubes packed with a particulate stationary phase. Stationary phases are high boiling liquids, waxes or solid sorbents. The column is enclosed in a thermostatically controlled oven that is maintained at a steady temperature or programmed to increase progressively during a separation. Solutes are detected in the mobile phase as they are eluted from the end of the column. The detector generates an electric signal that can be amplified and presented in the form of a chromatogram of solute concentration as a function of time.

A dedicated microcomputer is an integral part of a modern gas chromatograph. Software packages facilitate the control and monitoring of instrumental parameters and the display and processing of data.

Doing GC, unknown solutes can be identified by comparison of retention times, spiking samples with known substances, or using retention indices. Quantitative information is obtained from peak area measurements and calibration graphs using internal or external standards, or by standard addition or internal normalization. The analyses of the products whose standards are not available are done using a Shimadzu QP 2010- GCMS with 30 m universal capillary column of cross linked 5% phenylmethylsilicon. The MS detector voltage was 1KV. The m/z values and relative intensity (%) are indicated for

the significant peaks (Column temperature: 50 - 260°C and heating rate was 10°C/min, injector temperature: 240°C and detector temperature: 290°C).

Gas Chromatographic analysis is done using Chemito GC 1000 gas chromatograph with BP1 capillary column connected to a FID detector. The details of the analysis are given in table 2.6.1.

Table 2.6.1 Analysis conditions of various catalytic reactions

Catalytic reaction	Analysis conditions		
	Temperature programme*	Injector (°C)	Detector (°C)
Cumene cracking	60°C-8-20°C-200°C-2	200	200
Cyclohexanol decomposition	60°C- 5-20°C-230°C-2	200	200
Benzene isopropylation	60°C-5-10°C-250°C-2	220	220
Toluene isopropylation	60°C-5-10°C-250°C-2	230	230
Benzene ethylation	60°C-4-20°C-220°C-2	230	230
Toluene methylation	60°C-3-10°C-230°C-2	230	230

Linear Alkyl Benzene synthesis	110°C-3-10°C-275°C-5	250	250

*Initial temperature-duration in minutes-rate of increase-final temperature-duration in minutes

REFERENCES:

1. S. Sivakumar, C.P. Sibu, P. Mukundan, P. Krishna Pillai, K.G.K. Warrier, Mat. Lett. 58 (2004) 2664.
2. K.P. Kitsopoulos, Clays Clay Miner. 47 (1999) 688.
3. H.Y. Zhu, E.F. Vasant, J.A. Xia, G.Q. Lu, J. Porous Mater. 4 (1997) 17.
4. S. Brunauer, P.H. Emmett, E. Teller, J. Am. Chem. Soc. 60 (1938) 309.
5. M.L. Occelli, J.A. Bertrand, S.A.C.Gould, J.M. Dominguez, Microporous Mater. 34 (2000) 195.
6. J.M. de Boer, B.C. Lippens, B.G. Linsen, J.C.P. Broekhoff, A. Van der Heuvel, Th. Osinga, J. Colloid Interface Sci. 21 (1966) 405.
7. D.W. Rutherford, C.T. Chiou, D.D. Eberl, Clays Clay Miner. 45 (1997) 534.
8. J.M. Thomas, J. Klinowski, Adv. Catal. 33 (1985) 199.
9. E.R. Andrew, Intern. Rev. Phys. Chem. 1 (1981) 195.
10. R.A. Jonathan, N. Pervaiz, A.K. Cheetham, M.W. Anderson, J. Am. Chem. Soc. 120 (1998) 10754.
11. A. Coma, Chem. Rev. 95 (1995) 559414.
12. Y. Amenomiya, R.J. Cvetanovic, J. Phys. Chem. 67 (1963) 144.

13. F. Lonyi, J. Valyon, Micro Meso Mater. 47 (2001) 293.
14. M. Kurian, S. Sugunan, Indian. J. Chem. 42A (2003) 2480.
15. M.W. Anderson, J. Klinowski, Zeolites 6 (1986) 455.
16. U. Lohse, E. Loffler, M. Hunger, J. Stockner, V. Patzelova, Zeolites 7 (1987) 11.
17. J. Klinowski, H. Hamdan, A. Corma, V. Fornes, M. Hunger, D. Freud, Catal. Lett. 3 (1989) 263.
18. D. Dombrowski, J. Hoffman, J. Fruwert, T. Stock, J. Chem. Soc., Faraday Trans. 1 81 (1985) 2257.
19. J. Dwyer, K. Karim, W. Kayali, D.O. Milward, P.J. Malley, J. Chem. Soc., Chem. Commun. (1988) 594.
20. U. Lohse, E. Loffler, M. Hunger, J. Stockner, V. Patzelova, Zeolites. 7 (1987) 11.
21. E.P. Parry, J. Catal. 2 (1963) 371.
22. M.R. Basila, T.R. Kantner, K.H. Rhee, J. Phys. Chem. 68 (1964) 3197.
23. T.R. Hughes, H.M. White, J. Phys. Chem. 71 (1967) 2192.
24. J.T. Richardson, J. Catal. 9 (1967) 182.
25. E.T. Shao, E.M.C. Innich, J. Catal. 4 (1965) 586.
26. C.G. Ramankutty, S. Sugunan, B. Thomas, J. Mol. Catal. A: Chem. 187 (2002) 105.
27. C.P. Bezouhanova, M.A. Al-Zihari, Catal. Lett. 11 (1991) 245.

★★★★★★★★★★★★★★★

Chapter 3

PHYSICO - CHEMICAL CHARACTERIZATION: STRUCTURAL AND TEXTURAL MODIFICATIONS

In recent years a considerable interest has been focused on heterogeneous catalysis of organic reactions by montmorillonite clays, a member of dioctahedral smectite group, which are new classes of eco-friendly shape selective solid acid catalysts. Increase in the intercalating properties increases the accessibility of host molecules with in the matrix and is attained as a result of increase in the interlayer distance by pillaring with metal polyoxocations. This will give better shape selectivity in catalysis and one-dimensional nanoscale structural formation in clay/polymer composites. The catalytic conversion and selectivity is regulated by controlling the structural as well as textural properties to the required level where characterization methods becomes important. Knowledge about the increase in interlayer distance is needed to know the efficiency of nanocomposite formation where an organic species is inserted between inorganic clay layers. Present chapter discuses the detailed characterization of the prepared pillared clays.

3.0 INTRODUCTION

In an attempt to improve upon the limited pore size range available to zeolites, there has been renewed interest in the preparation of novel, two dimensional, molecular sieve-type materials based on clays. These materials are known as pillared interlayer clays or pillared clays (PILCs). The pillar influences interlayer spacing, whilst the frequency of pillars influences pore width. Pore dimensions varying from 0.22 to >2 nm can be achieved which are larger than those for zeolites (0.2 – 0.8 nm). Pillared smectites are generally prepared by cation exchange of the clay with polynuclear cations large enough to permanently prop open the clay structure, leaving part of the interlayer region open for adsorption and catalysis. Polynuclear cations suitable for this purpose are formed upon hydrolysis of a number of metal cations. Present study uses Ti, Zr, Al and Cr metals as the pillars. The acidity and other properties of PILC which is prepared by incorporating pillars into clay's interlayer space are by no means simple summations of those properties of the pillar and the original clay material. The influence of pillaring on surface area, pore volume, interlayer spacing basic clay layer structure, acidity, stability etc should be investigated in this chapter.

3.1 CEC MEASUREMENTS

The ion – exchange capacity of clay minerals, in particular, smectites, influence their unique physical properties, such as the cation retention and diffusion processes of charged and uncharged molecules. These processes influence cation and molecular migration through clay – rich barriers in nature.

The numerical value of this property is described by cation exchange capacity (CEC).

Table 3.1.1 CEC measurements of various systems

Clay	CEC (mmol/g)	Residual CEC (%)
M	0.96	89.2
NM	1.02	100.0
TM	0.83	81.5
ZM	0.28	27.5
AM	0.68	66.7
CM	0.74	72.5
TZM	0.20	19.6
TAM	0.36	35.3
TCM	0.38	37.3
AZM	0.32	31.4
ACM	0.54	52.9
ZCM	0.42	41.2

Upon calcinations of a PILC precursor around 500°C, the dehydration of the intercalated oxo-hydroxy cations liberate protons. Although most of these protons stay in the interlayer space, some migrate through hexagonal cavities formed by the basal SiO_2 tetrahedra towards the octahedral sheet that carries the negative charges[1]. As a result, in the thus prepared PILCs, the CEC

is dramatically lower than that of its precursor. This is in addition to the reduction in CEC, as a result of the exchange of exchangeable cations by unexchangable pillar species.

The CEC of NM is greater than the parent montmorillonite M because during ion exchange process leaching of octahedral Al in the layers occurs which increases the net negative charge of clay layers. Pillaring is done on the Na^+-exchanged montmorillonite, thus the initial CEC taken is that of NM. On pillaring the CEC decreases because of the presence of charge compensating pillar oligomers. The residual CEC of various systems are shown in table 3.1.1. The percentage cation exchanged during various pillaring process is shown. It is found that mixed Ti – Zr pillaring solution is most effective in exchanging the cations. Thus TZM is assumed to have higher surface area, pore volume, acidity etc, since it props apart the layer and thus exposes active sites, most effectively. The decreased CEC may be due to the entrance of maximum amount of total pillar metals at the expense of exchangeable cations. TM is having the highest CEC among the present pillared systems, which may be due to the presence of low amount of pillar metal and leaching out of layer octahedral Al.

The residual CEC of various PILC systems follows the order NM> M> TM> CM> AM> ACM> ZCM> TCM> TAM> AZM> ZM> TZM. Both Cr and Al pillaring is assumed to be less effective in pillaring process as evident from their high residual CEC values. All mixed pillared systems shows good exchangeable capacity and is found to be an effective way for pillaring when

compared to single metal pillaring. The presence of residual CEC implies that the PILCs can further exchange cations with other cations or with any similar species. Poncelef et al measured residual CEC of Al, Zr and mixed Al-Zr pillared species and 16-35% of original CEC is retained. Present study follows the same trend except that for single alumina pillared species. Same authors found that residual CEC of Al PILCs lies between 43-82% of original CEC and the CEC of AM lies in this range. Zr single as well as Zr and Ti mixed pillared systems are found to be effective in pillaring process from their low CEC values.

3.2 ELEMENTAL ANALYSIS (ICP-AES)

Elemental analysis is done using ICP-AES after the quantitative separation of SiO_2. The data shown in table 3.2.1 gives the amount of pillar metal present and thus the extent of pillaring and as well as the amount of cations present after pillaring which is related to the residual CEC. In the table X represents the firtst pillar metal for e.g., Ti in the case of TZM where Y represents the second pillar metal i.e., Cr in ACM, etc.

Na^+-exchange replaces a portion of other exchangeable cations present. Pillaring results in further reduction of these metals as well as Na^+ ions. Total pillar metal is found to be highest for Zr containing clays which support their low residual CEC values showing that pillar metal enters at the expense of exchangeable cations.

Table 3.2.1 Elemental analysis data of different clays

Clay	Element (%)										Si/Al
	Na	Mg	Al	Si	K	Ca	Fe	Pillar Metal			
								XM	YM	PM*	
M	2.18	2.81	17.74	56.47	4.11	5.01	11.67	-	-	-	3.18
NM	5.56	2.69	15.52	58.85	3.80	2.08	11.50	-	-	-	3.79
TM	2.76	2.23	14.72	57.42	2.47	1.53	9.90	8.97	-	8.97	3.90
ZM	1.31	1.86	13.1	52.24	1.14	-	4.95	25.40	-	25.40	3.98
AM	2.50	2.21	23.69	61.16	2.28	-	8.16	-	-	8.17	2.58
CM	2.69	2.74	14.32	54.08	3.28	-	8.36	14.35	-	14.35	3.78
TZM	0.05	1.44	10.80	50.25	2.15	-	7.47	4.13	23.71	27.84	4.65
TAM	0.88	1.86	19.14	58.48	3.42	0.26	7.82	8.13	-	11.63	3.06
TCM	-	1.30	13.20	56.23	2.00	0.43	5.58	11.74	9.52	21.26	4.26
AZM	3.65	2.20	22.49	53.00	3.61	-	4.71	-	13.02	17.47	2.36
ACM	-	1.31	19.42	53.76	3.30	1.27	8.04		12.23	16.13	2.77
ZCM	1.17	1.39	13.07	51.79	3.11	0.83	4.54	21.35	2.74	24.09	3.96

PM* - Total pillar metal

Si/Al ratio increases slightly as a result of ion exchange due to leaching out of Al. The value is very high upon Ti pillaring showing further leaching due to the acidic nature of pillaring agent used. But the increase is not to a large extent that can cause structural alterations to the framework of clay. Al

single and mixed pillaring decreases the value due to the additional introduction of Al from the pillar.

We tried to correlate the amount of total pillar metal present with that of (100- residual CEC), which is a measure of pillar metal incorporated where we get a perfect correlation supporting the assumption that pillar metal enters at the expense of exchangeable cations (figure 3.2.1).

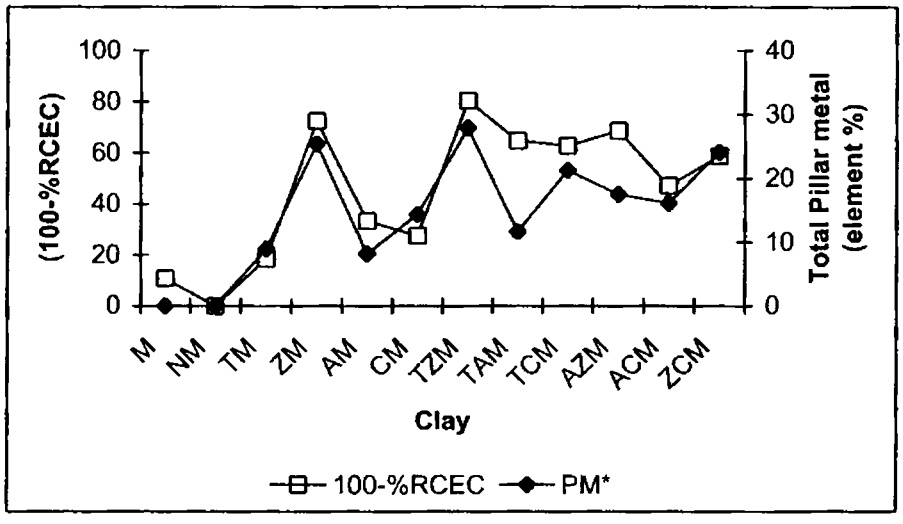

Figure 3.2.1 correlation diagram of (100 - % residual CEC) versus total pillar metal present

3. 3 SURFACE AREA AND PORE VOLUME MEASUREMENTS

During pillaring process stable metal oxide clusters are incorporated into interlayer space of swellable clays. Thus a three dimensional porous

network is generated which results in increased surface area and pore volume. This makes surface area pore volume determination particularly important in the case of PILCs, which is directly related to the extent of pillaring. The BET and Langmuir surface areas of various systems are given in table 3.3.1. The range of validity of BET equation for these materials is usually between P/P_0 = 0.01 and 0.1. However, in microporous solids like PILCs where the interlamellar distance is of the order of a few molecular diameters, monolayer formation on clay silicate layers occurs. Thus surface areas approximated by Langmuir equation are reasonable representations of PILC surface areas[2].

The high temperature calcination reduces the surface area and pore volume of parent montmorillonite (BET surface area = 7.9 m^2/g) due to the structural collapse. Na^+-ion exchange delaminates the clay layers partially and thus porosity as well as surface area gets increased. Delamination is an outstanding property of dispersed montmorillonite particles that happens when the counter ions are alkali cations, preferentially of lithium and sodium, and the salt concentration is sufficiently small (approximately <0.2 mol/L for Na^+ ions)[3]. Present study adopts 0.5 M solution of Na^+ ions for ion exchange, thus only partial delamination is expected.

Table 3.3.1 surface area – pore volume data

Clay	BET Surface area (m^2/g)	Pore volume ($\times 10^{-6} m^3/g$)	Langmuir Surface area (m^2/g)

M	7.90	0.0116	11.32
NM	51.64	0.0512	81.34
TM	132.25	0.1235	196.81
ZM	131.82	0.1090	191.00
AM	119.84	0.1183	177.20
CM	117.43	0.1162	174.25
TZM	162.08	0.1461	235.84
TAM	122.12	0.1221	181.09
TCM	137.04	0.1365	203.82
AZM	136.52	0.1236	200.08
ACM	121.53	0.1201	180.24
ZCM	125.42	0.1107	183.58

In the present study we are pillaring montmorillonite KSF that is acid activated. As already reported, here the pillaring process is less efficient when compared to untreated clays[4]. Surface area of different PILCs lies between 117 – 162 m^2/g. Among the single metal PILCs Ti and Zr pillars increase the surface area more when compared to single Al and Cr pillars. The mixed pillared systems follow this trend. Thus in the present systems TZM possess maximum surface area and pore volume data which is supported from its lowest CEC values. Except in the case of ZCM and TAM, all mixed pillared systems have surface area values higher than the surface area of individual single metal PILCs. In ZCM surface area is found to be higher than CM showing the efficiency of mixed pillaring. Similar is the case of TAM where surface area is higher than AM. Al and Cr single pillared systems show

increase in surface area upon mixed pillaring. Thus from the above discussions it is clear that mixed pillaring is more effective than single pillaring.

3.4 X-RAY DIFFRACTION (XRD) ANALYSIS

The crystalline structure of the montmorillonite clay is known to be comprised of sheets formed by stacking two tetrahedral Al-Si-O networks. The tetrahedron faces form the exterior surfaces of the sheets. The vertexes of upper and lower tetrahedrons are turned to each other forming between them an octahedral network. Cations Si^{4+} and Al^{3+} fill the tetrahedrons, while two thirds of the octahedrons are occupied by Al^{3+} and Mg^{2+} cations. Exchangeable hydrated cations and water molecules fill the space between the sheets.

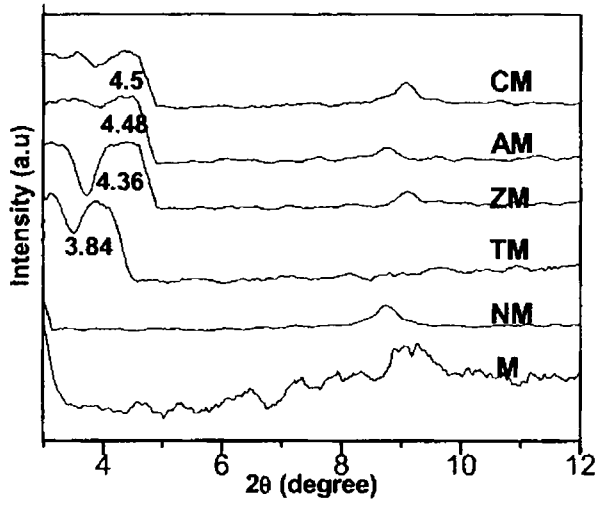

Figure 3.4.1 XRD pattern of M, NM and single PILCs

The easiest way to determine whether pillar intercalation has been successful is to record an X-ray diffraction pattern of the PILC. The position of the diffraction peak of the (100) plane defined the interlayer space. In parent clay the 2θ value corresponding to the (100) plane lies at ~8.9°, with a basal spacing of 9.8 Å[5] (for calcined parent montmorillonite KSF, since 9.6 Å is the reference value for completely dehydrated parent montmorillonite) calculated from Bragg equation. Pillaring process results in shift of this 2θ value towards left indicating increase in the d-spacing.

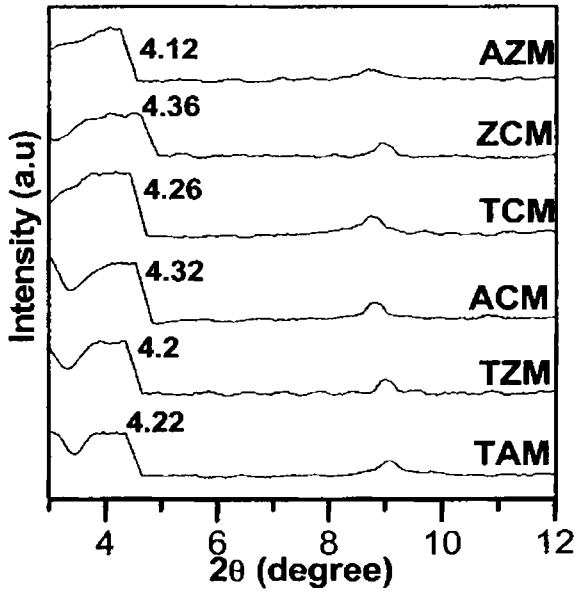

Figure 3.4.2 XRD pattern of mixed PILCs

The basal spacing of different PILCs calcined at 500°C lies between 19.6 - 23.0 Å. The d-spacing increase results from the incorporation of bulkier

polyoxocations between the layers that transform to stable metal oxide clusters upon calcinations that prop the layers apart. The XRD patterns are shown in figure 3.4.1 and 3.4.2; the corresponding basal spacings are given in table 3.4.1.

Table 3.4.1 d-spacing values of PILCs

Clay	d-spacing (Å)	Clay	d-spacing (Å)
M	9.8	TZM	21.0
NM	9.8	TAM	20.9
TM	23.0	TCM	20.7
ZM	20.4	AZM	21.4
AM	19.7	ACM	20.2
CM	19.6	ZCM	20.4

The parent montmorillonite M and Na^+-exchanged one NM, shows relatively sharp intense reflection. Upon pillaring except in the case of TM, we get broadened reflection which indicates partial destruction of the layer structure[6]. This severe disorder in the layer structure may be due to the high calcination temperature. Appreciable expansion is noted in all the cases. The absence of highly delaminated structure[7] of TM as in the case of other reports is the reason for the characteristic peak of well oriented and pillared structure. The relative intensity of the peaks, i.e. the ratio of intensity of peak at 8.9° and the newly originated one upon pillaring gives measure of the extent of

pillaring. In all cases high intensity is there for the peak corresponding to pillaring when compared to that at 8.9° which indicates that here pillaring is efficient in propping apart the clay layers.

It is reported that compared with single metal oxide PILCs, intercalation of clay layers by mixed oxide pillared is an efficient method to increase the d- spacing[8]. Present systems except TM, shows the same trend. Ti single pillared system, as in agreement with previous reports shows high d-spacing[9].

3.5 POROUS STRUCTURE

PILCs are microporous materials. For an ideal PILC, the micropore is defined by the interlayer distance, which is the space between the clay layers, and lateral distance, which is the space between the metal oxide pillars, as illustrated in figure 3.5.1(a). Generally PILCs exhibit bimodal pore size distribution with pore size bigger than zeolites, which show advantages in reactions with larger molecules. In the acid catalytic applications, the porous structure of PILCs, always associated with the surface acidity, will determine the type of reactions and also the total conversion and product selectivity. The pore size of PILCs can be varied from 5 Å to over 60 Å, depending on the synthesis conditions, such as type of the starting clay materials[10], cation exchange capacity (CEC) of clays[11], type of the metal oxide pillars[12], and thermal treatment temperature[13].

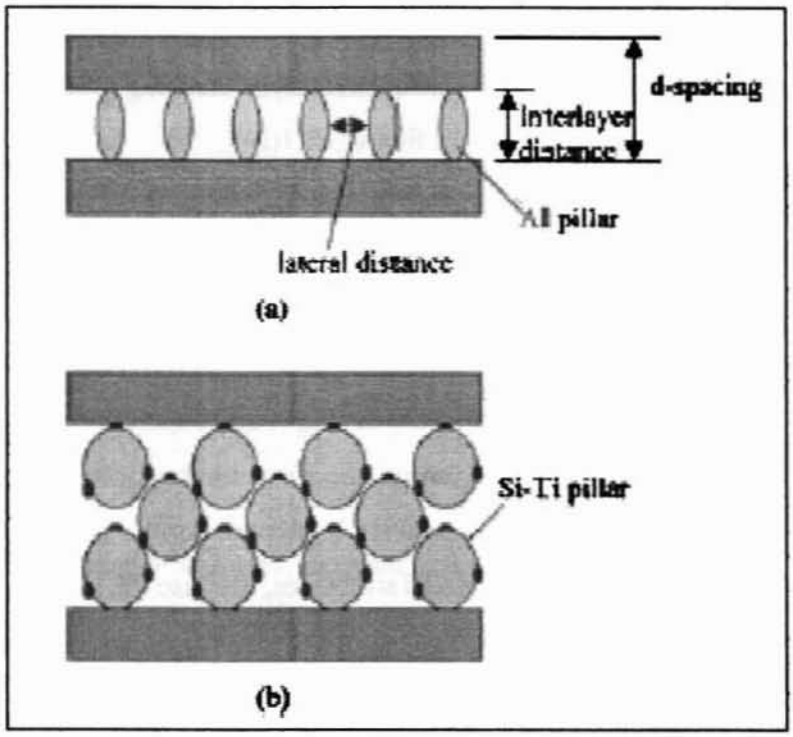

Figure 3.5.1 Schematic structures of the single and mixed metal oxide PILCs with various d-spacings. (a) Al-PILC; (b) Si/Ti-PILC

The d-spacings, determined by X-Ray Diffraction (XRD) measurement, of various single and mixed metal oxide PILCs are summarized in the recent reviews by Kloprogge[14] and Gil et al[15]. It is reported that compared with single metal oxide PILCs, intercalation of clay layers by mixed oxide pillars is an efficient method to increase the d-spacing[16-18]. Recent reports show d-spacing as high as 60 Å can be obtained on some composite PILCs, such as Si/Ti-PILC (60 Å)[19], Si/Cr-PILC (47 Å)[20], Si/Fe-PILC (63 Å)[21], etc. However, detailed surface area analysis indicated that for these PILCs, d-spacing measured by

XRD is always much larger than the average pore size. The reason is that the mixed metal oxide pillars are present as multilayer stacking nano particles between the silicate layers, as shown in figure 3.5.1(b).

Apart from adjusting pore openings by different pillar species and organic templates, the drying process, which transforms wet PILCs into dry solid, is another important factor. Treating same PILC by different drying methods, such as normal air-drying, freeze drying[22], and supercritical drying[23], will lead to different porous structures. The first method often produces laminated pillared structure, while the PILCs prepared from the latter two methods show more random/ delaminated structures, because the silicate layers from both the methods favour the edge-to-face and edge-to-edge stacking. Therefore, the average pore size of PILCs will increase in the order of air-drying, freeze drying and supercritical drying. In the present work we had adopted air drying of the PILCs and a laminated structure is expected.

Table 3.5.1 Pore volume data of PILCs

Clay	External Surface area (m^2/g)	Internal Surface area (m^2/g)	Micropore volume ($\times 10^{-6} m^3/g$)	Mesopore volume ($\times 10^{-6} m^3/g$)	Mean pore size (Å)	d-spacing (Å)
M	-	-	-	-	-	9.8
NM	22.05	29.59	0.0280	0.0232	3.5	9.8
TM	27.00	105.84	0.0660	0.0575	23.3	23.0
ZM	20.45	111.37	0.0630	0.0460	19.6	20.4

AM	24.14	95.70	0.0596	0.0587	22.8	19.7
CM	20.00	97.43	0.0606	0.0556	23.9	19.6
TZM	24.52	137.56	0.0808	0.0653	21.2	21.0
TAM	12.11	110.01	0.0804	0.0417	22.2	20.9
TCM	18.56	118.48	0.0741	0.0624	23.0	20.7
AZM	24.14	112.38	0.0642	0.0594	21.2	21.4
ACM	19.64	101.89	0.0620	0.0581	23.6	20.2
ZCM	15.56	109.86	0.0665	0.0442	20.2	20.4

The micropore volumes, external and internal surface area of the clays are calculated from t - plot[24]. The data in table 3.5.1 reveals the porous structure of present PILCs. The clays possess both micro and mesopores as expected. The mean pore size of various systems did not show the same trend as that of interlayer spacing which indicates that in addition to interlayer spacing other factors also contributes porosity.

3.6 FOURIER TRANSFORM INFRARED (FTIR) SPECTROSCOPIC ANALYSIS

FTIR reveals the bonding and the changes upon modifications. Thus this technique is very useful to study any structural changes that occurred during pillaring.

Figures 3.6.1 and 3.6.2 show the FTIR spectra of the parent, ion exchanged and pillared montmorillonites. The two bands around 3,500 cm^{-1}, in

the –OH stretching region are attributed to silanol groups (3740 cm^{-1}) of the external layer and a broader band due to Al_2OH group (3650 cm^{-1}) of the octahedral layer[25]. Stretching vibrations of water molecules may also contribute to –OH peaks (3500 cm^{-1}). On pillaring the band broadens due to the introduction of more –OH groups of the pillar, which is interpreted as an effect of pillaring[26]. The decrease in intensity arises from the dehydration and dehydroxylation steps during pillaring.

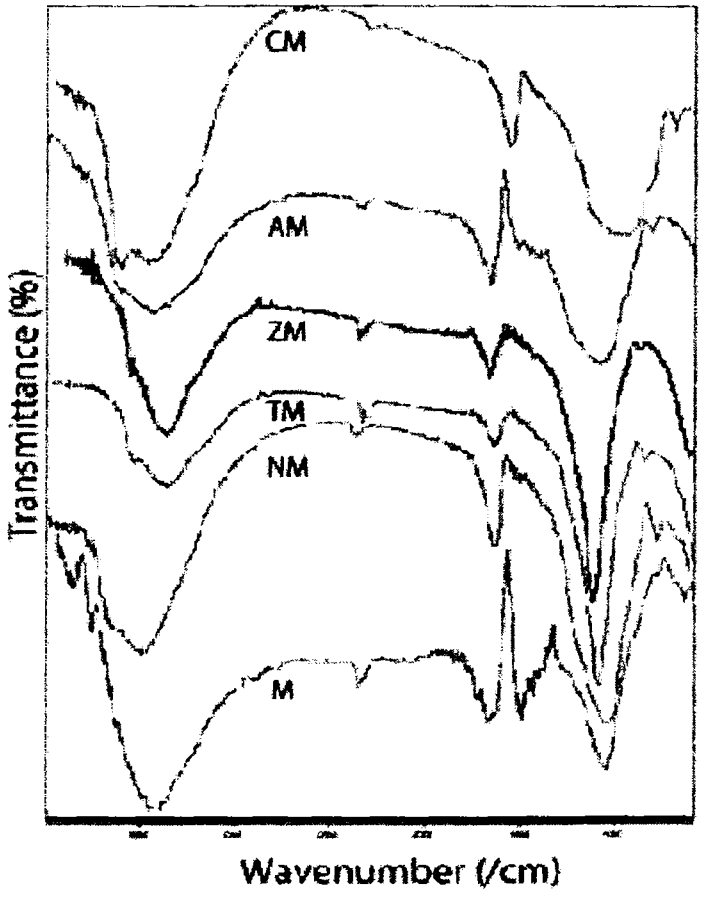

Figure 3.6.1 FTIR spectra of M, NM and single PILCs

Peak at around 1600 cm^{-1} is due to bending vibrations of water. Pillaring process replaces a large amount of interlayer cations that generally exists as hydrated, decreases the intensity of -OH peaks. PILCs have low amount of adsorbed/coordinated water due to the non-swellable nature.

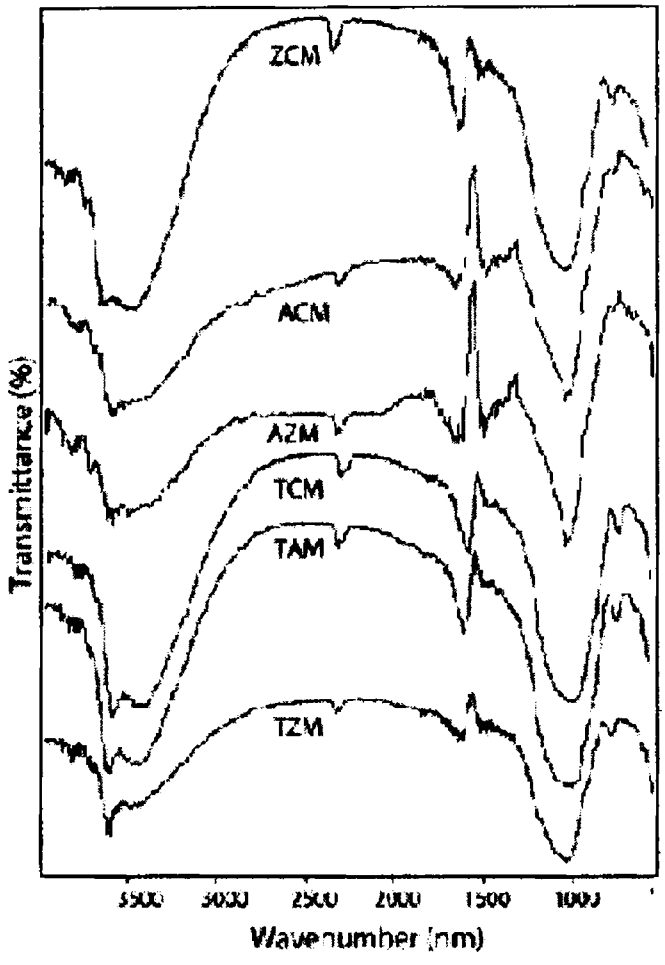

Figure 3.6.2 FTIR spectra of mixed PILCs

Thus as a result of pillaring intensity of band around 1600 cm^{-1} also decreases[27]. The band around 1060 cm^{-1} is due to asymmetric stretching vibrations of SiO_2 tetrahedra. A band around 800 cm^{-1} is due to stretching vibration of Al^{IV} tetrahedra and absorption at 526- 471 cm^{-1} is due to bending of Si-O vibration. The retention of all peaks as in parent montmorillonite in the framework region clearly shows that the basic clay layer structure remains unaffected on pillaring.

3.7 NMR ANALYSIS

The structural rearrangements that occur during the calcinations and the exact nature of metal oxide clusters that form the pillars in PILCs remain a subject of discussion. In the case of alumina pillaring it has been proposed that heating causes the dehydroxylation of the keggin ions with the formation of alumina and water as well as protons that migrate to the octahedral layer vacant $O_4(OH)_2$ sites to charge compensate for the presence of divalent ions[28].

$$[Al_{13}(O)_4(OH)_{24}(H_2O)_2]^{7+} \longrightarrow 13/2\ Al_2O_3 + 41/2\ H_2O + 7\ H^+$$

It is believed that the dehydration reactions at 500°C forming heat stable Al_{13} blocks, 0.98nm x 1.09nm x 0.84nm in size, is better represented by:

$$[Al_{13}(O)_4(OH)_{24}(H_2O)_{12}]^{7+} \longrightarrow [Al_{13}O_{13}(OH)_{13}] + 14H_2O + 7\ H^+$$

in which 13 AlOOH units connect to form the Al_{13} – pillar. Moreover protons instead of bonding with oxides or hydroxides in the clay AlO_6 layer could react With the silicate layers to form silanol and Si–O-Al(VI)$_P$ groups scheme (3.7.1).

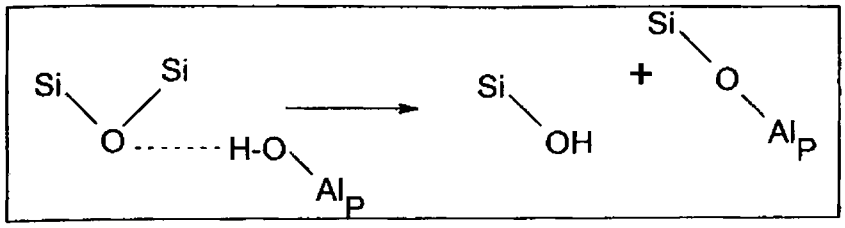

Scheme 3.7.1 Formation of Si-O-pillar group

This can be generalized as Si-O-M_P; where M is any pillar metal (M = Al, Zr, Ti or Cr in the present work). Proton attack of the siloxane layers could be facilitated by the stretching of Si-O bonds observed by AFM in Al_{13}-PILC samples[29]. As a result, the pillar composition may not be as indicated because of protonation reactions with the Si-O-Si bond and because of different [O/OH] ratios within the pillars.

The ^{29}Si NMR and ^{27}Al NMR spectral analysis gives idea about the nature of pillars and the influence of pillars on the clay layers. Pillaring solution of Zr contains $[Zr_4(OH)_{16-n}(H_2O)_{n+8}]^{n+}$ or $[Zr_4(OH)_8(H_2O)_{16}(Cl, Br)_x]^{(8-x)+}$. Ti pillaring polyoxocations consists of $[TiO_2(OH)_4]_n^{m+}$ species where Cr pillaring solution consists of a trimer and higher polymers. Plee et al.[30] have used ^{27}Al and ^{29}Si solid state nuclear magnetic resonance (MAS NMR) techniques to study the linkage of pillars with the clay sheets.

3.7.1 ^{29}SI NMR SPECTRA

Figure 3.7.1 shows the ^{29}Si NMR spectra of parent montmorillonite and PILCs. In agreement with published results[31,32], the spectrum of parent

montmorillonite contains two resonances. The one at –95.56 ppm is attributed to T (3Si, 1Al) units representing Si^{IV} atoms linked through oxygen to three other Si^{IV} and to one Al^{VI} (or Mg) in the clay octahedral layer. The second resonance near -110.20 ppm is due to silica impurities present in the parent clay. On pillaring the T (3Si, 1Al) resonance shifts and broadens considerably. This upfield shift has been attributed to the diffusion of the charge compensating protons generated during calcination to the clay octahedral layer[31]. The presence of Si-O-M_{pillar} site may be responsible for the broadened resonance observed in the spectrum of PILC[33]. The δ ppm values of different systems are shown in table 3.7.1

Table 3.7.1 δ ppm values of T (3Si, 1Al)

Clay	δ ppm	Clay	δ ppm
M	95.56	TZM	96.64
NM	94.80	TAM	96.34
TM	96.12	TCM	96.28
ZM	96.02	AZM	97.66
AM	95.98	ACM	96.07
CM	95.77	ZCM	96.05

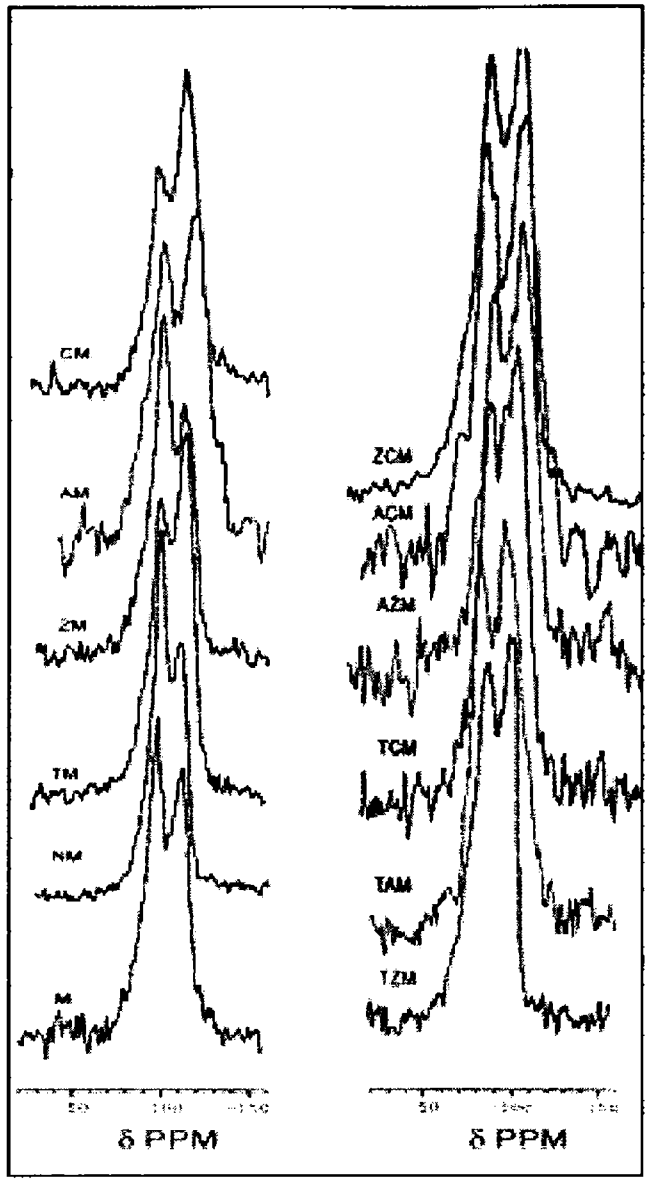

Figure 3.7.1 ^{29}Si NMR spectra of present clay systems

3.7.2 ^{27}Al NMR SPECTRA

^{27}Al NMR can detect the cordination of Al atoms in clays containing as little as 0.26% of Al_2O_3 and thus is of particular utility in studying octahedral and tetrahedral sites.

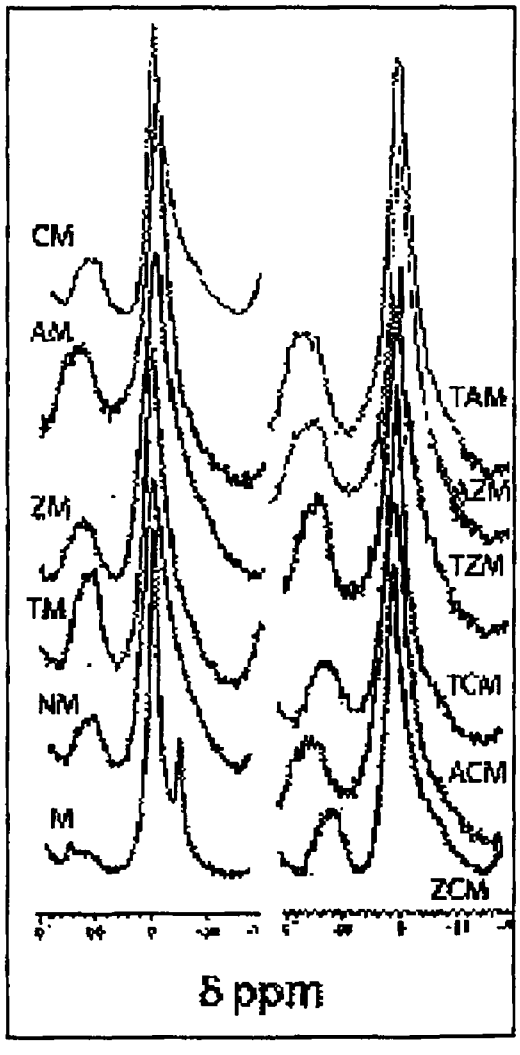

Figure 3.7.2 ^{27}Al NMR spectra of different clays

The resonance of montmorillonite at –0.8 ppm is due to the octahedral aluminium and the one around 60.0 ppm is attributable to tetrahedrally co-ordinated Al atoms. The peak of Al^{IV} is present in Na^{+}-exchanged and pillared systems, which is due to the leaching of octahedral Al and is very weak in parent montmorillonite. During ion exchange, treatment with sodium nitrate at 70°C for 24 h may leads to the leaching of some octahedral layer Al^{VI} to interlamellar space where it exists as tetrahedral Al^{IV}. Increased intensity of Al^{IV} peak of PILCs is due to the leaching of Al at 70°C and acidic conditions of pillaring solution. For pillared sample small change in δ ppm value for octahedral Al atoms may be due to the bonding of M_{pillar} atoms of intercalating polymer via oxygen atoms with layer metals. Eventhough there is leaching of octahedral Al and some Al occupies in interlamellar region as tetrahedral Al (figure 3.7.2), the basic clay layer structure is retained. The peak of tetrahedral Al is broad and intense in Al pillared systems (single and mixed PILCs) due to the presence of Al^{IV} in the center of keggin cation of the Al_{13} pillar.

3.8 UV-VIS DIFFUSED REFLECTANCE SPECTROSCOPY

The UV–vis-diffuse reflectance spectroscopy is a suitable technique to study solids, particularly dispersed oxides[34] and metal ions in constrained environment such as MCM, zeolites and clay materials[35-37] to obtain information on the coordination environment, oxidation state of the embedded transition and rare earth metal ions. We have employed this method to study the chemical environment, location and interaction of Cr^{3+} ions in the microenvironment of the single Cr-PILC as well as in mixed PILCs.

Figure 3.8.1 shows the UV–Vis-DRS spectra of parent, ion exchanged and single PILCs. The parent clay without the Cr^{3+} ion did not display any characteristic band above 250 nm (figure 3.8.2 shows the DRS of mixed pillared systems).

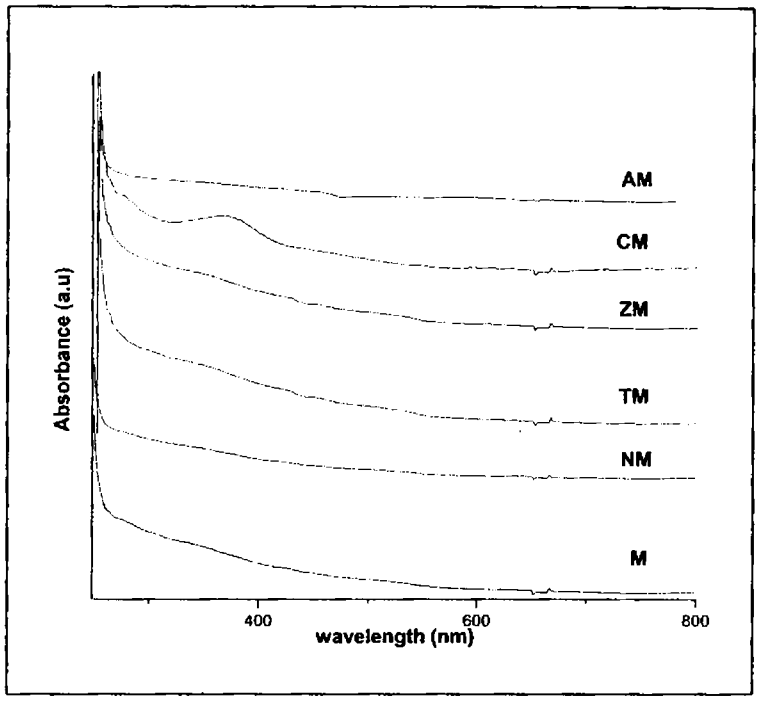

Figure 3.8.1 UV–Vis-DRS spectra of parent, ion exchanged and single PILCs

This broad band centered at 242 nm (not shown in figure) is assigned to ($Fe^{3+} \leftarrow O^{2-}$, OH^- or OH_2) charge transfer band for iron present in the octahedral layer of the clay mineral[38] and is common to modified as well as parent montmorillonite clays. The basic structural SiO_4 units of tetrahedral silicate layers in the clay lattice do not absorb light in the range of 200–800 nm

except when the transition metal ions are exchanged in the interlayers or present in the silicate structure. In the present case, the montmorillonite used in this study contains Fe^{3+} ions isomorphously substituted in the octahedral layer. These metal ions account for the strong absorption in the UV region of the clay materials. The incorporation of Cr^{3+} ion in the pillar position leads to characteristic absorption of light in the UV region of the DRS spectra. The Cr^{3+} ion with $3d^3$ configuration is known to exhibit strong optical absorption in the UV region of the electronic spectrum. In the present study, the clay samples containing Cr pillar species show new absorption bands in the UV region of the DRS spectra.

Alumina is a direct band gap insulator which does not absorb light in the UV-region of the spectrum. The Al_2O_3 pillars formed after the heat treatment of the Al-PILCs samples thus do not contribute any additional feature to the DRS spectrum of Al-PILCs as evident from the figures[39].

Intercalation of the Zr pillars into the clay structure results a broad absorption feature extending up to 400 nm. Such absorption feature has been observed for ZrO_2 samples with structural disorder and defect centers[40]. Zirconium dioxide is a direct band gap insulator which shows interband transitions at ~230 nm with an absorption edge at 250 nm. However, the presence of structural disorder and defect centers shift the adsorption edge to higher wavelength due to the presence of localized states between the valence and conduction band[40].

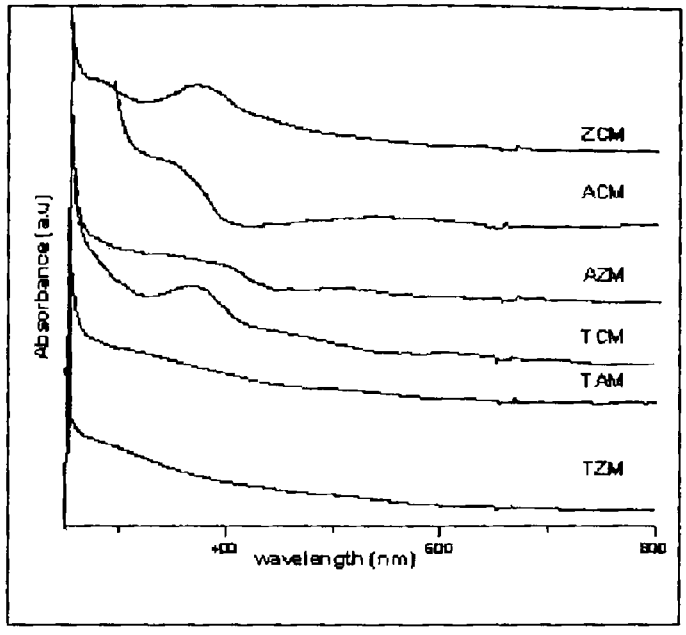

Figure 3.8.2 DRS of mixed PILCs

The Zr nanosized pillars in the Zr-PILCs can contain defect sites and can contribute to the broad absorption feature in the higher wavelength side of the spectrum. But calcination at 500°C results in loss of intensity of the higher wavelength absorption feature. This is due to the fact that annihilation of the defect centres takes place at higher temperatures. Moreover, coalition of the Zr-pillars to bigger Zr clusters can also take place upon heat treatment. Montmorillonite clay, used in this study is a dioctahedral clay mineral in which most of the layer charge originates from the octahedral layer and is considered to be delocalized[41]. The charge delocalization helps in the mobility of the Zr-pillars in the interlayer and upon heat treatment the Zr-pillars coalesce to form

bigger clusters. Thus Zr containing PILCs did not show any characteristics absorption of Zr.

Ti containing PILCs did not show any characteristic peak for Ti which may be due to the very low concentration and efficient distribution of Ti in the PILCs.

3.9 THERMAL ANALYSIS

Pillaring is the only clay modification method that gives thermal stability. Thermal stability is an important parameter that makes clays suitable for high temperature applications. Therefore thermal analysis plays a major role in clay characterization. In general the porous structure of PILCs can be stable up to 400-500°C[42]. Further increase in the heating temperature will lead to the collapse of clay layers due to the sintering of the pillars and the dehydroxylation of clay sheets. Both the nature of the clay materials and type of metal oxide pillars will affect the thermal stability of the resulting PILCs.

3.9.1 THERMOGRAVINETRY (TG)

Figures 3.9.1 and 3.9.2 show the loss of weight as a function of temperature for different clays. The weight loss up to 200°C is a result of the loss of surface - adsorbed water. In M and NM a high temperature weight loss is a result of water removal originated from dehydration of the layers. This structural collapse continues even up to 800°C. In the pillar polyoxocation

intercalated clay samples a less pronounced slope is present in the dehydration segment of the TGA curve.

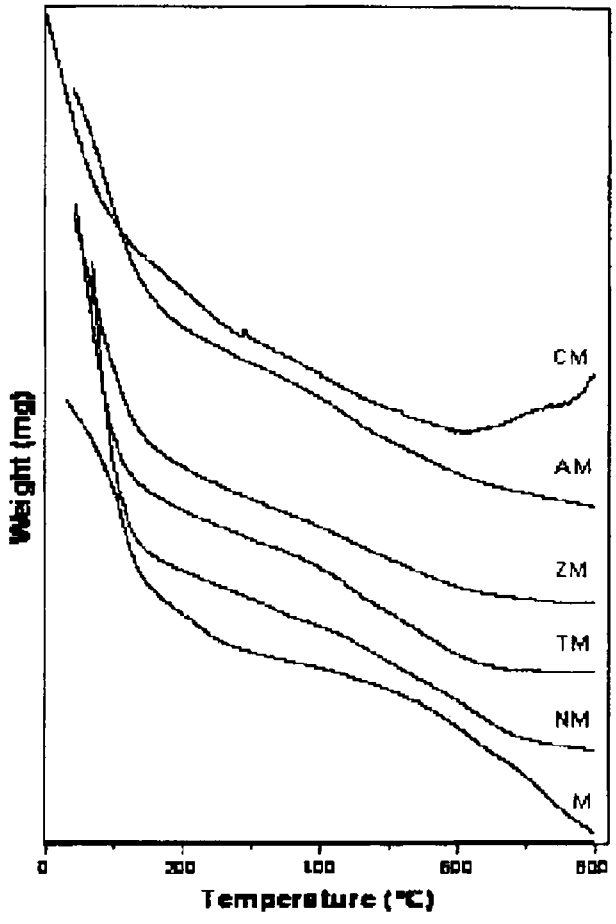

Figure 3.9.1 TGA curves of M, NM and single PILCs

This is interpreted as an overlapping of the weight loss produced by water removal from the surface, the micropores, and the dehydroxylation of hydroxy metal oligomers of the pillars. The new inflections at around 400°C present in the PILCs may have been due to the transformation of metal oxyhydroxide to

metal oxide in the pillars[43]. The weight loss becomes absent at temperature above 650°C in PILCs which may be due to the additional stability obtained to montmorillonite upon pillaring.

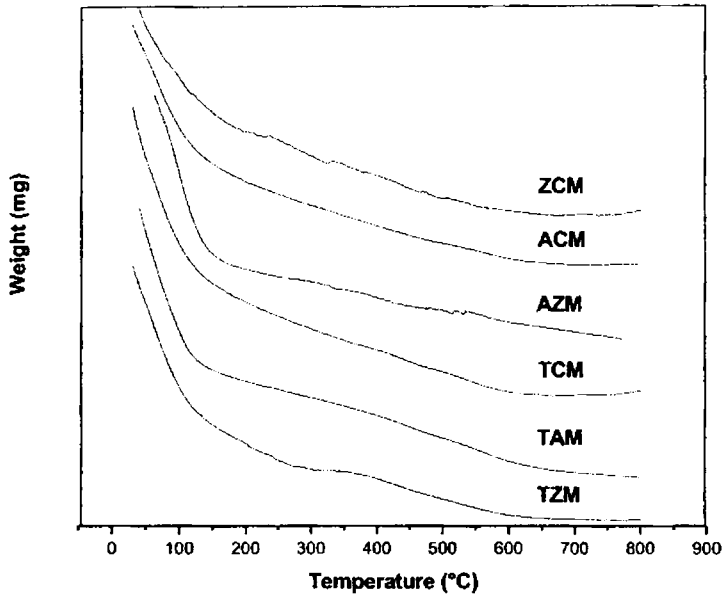

Figure 3.9.2 TGA curves of mixed PILCs

3.9.2 DIFFERENTIAL THERMAL (DTA) ANALYSIS

DTA was also used to investigate the thermal stability of PILCs. As shown in Figures 3.9.3 and 3.9.4 two endothermic peaks are obtained. PILC products show one small endothermic peak at about 600°C assigned to dehydroxylation of any remaining hydroxide pillars besides one endotherm near 100°C induced by dehydration[44].

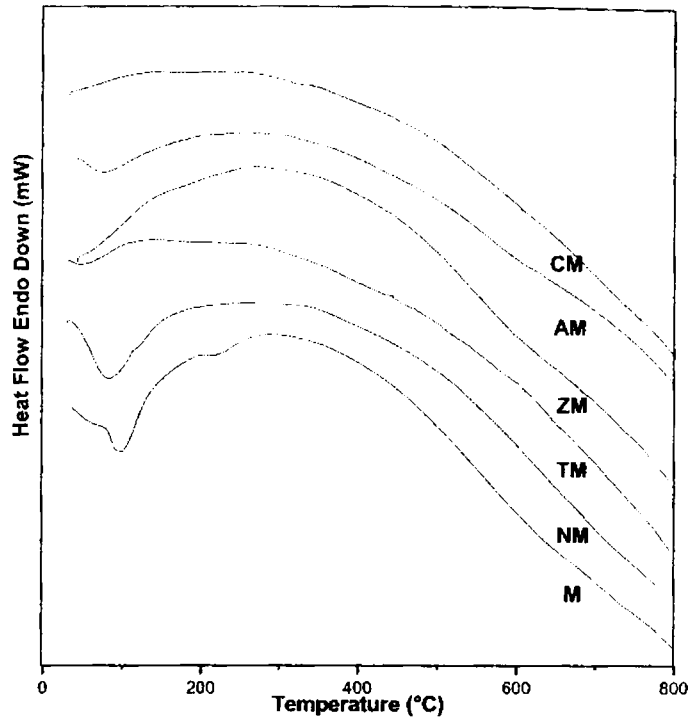

Figure 3.9.3 DTA profiles of M, NM and single PILCs

Endothermic peak at about 300-400°C is assigned to dehydroxylation of metal hydroxide pillars to metal oxide.

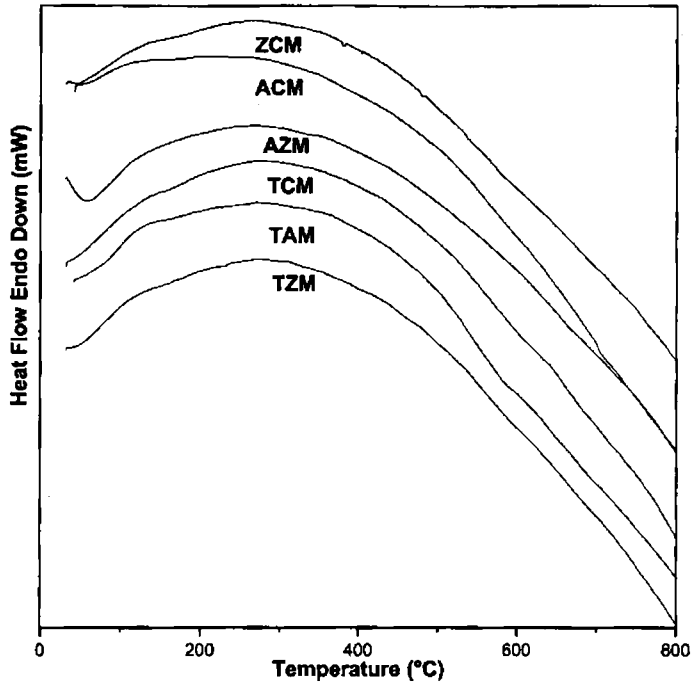

Figure 3.9.4 DTA curves of mixed PILCs

3.10 SCANNING ELECTRON MICROSCOPIC (SEM) ANALYSIS

The layer structure of clays is evident from SEM pictures. The retention of this structure in PILCs suggests that the basic clay layer is unaffected upon pillaring. The SEM pictures are shown in Figures 3.10.1 and 3.10.2.

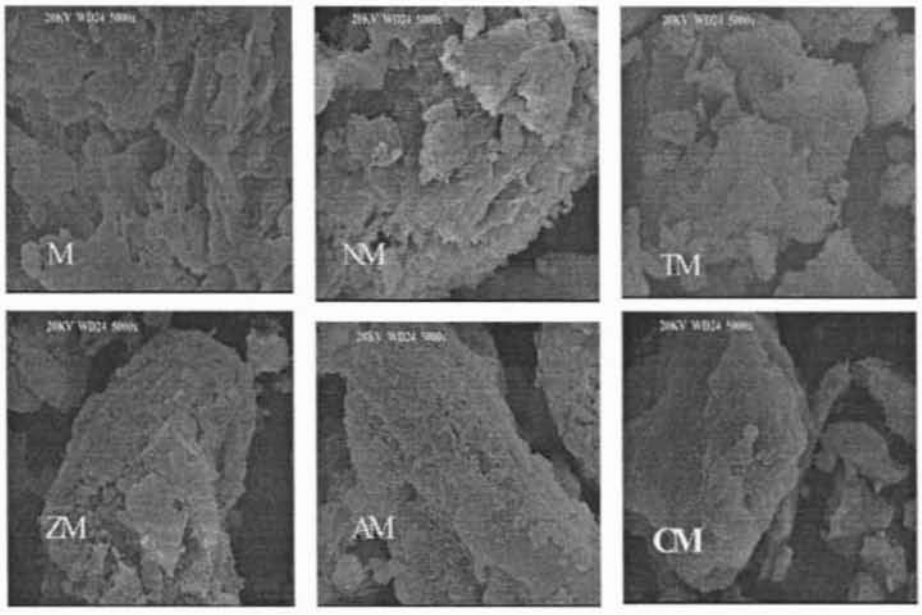

Figure 3.10.1 SEM pictures of M, NM and single PILCs.

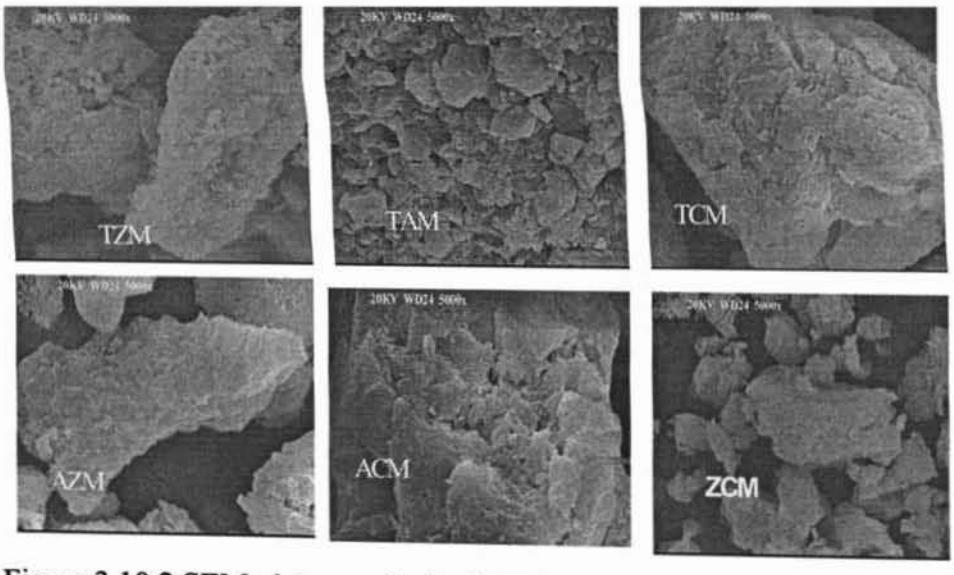

Figure 3.10.2 SEM pictures of mixed PILCs

3.11 MEASUREMENT OF ACIDITY

There are a large number of reactions which are catalyzed by acid sites, and their importance has surpassed the interest in the fundamental chemistry. It can be said that solid acids are the most important solid catalysts used today, considering both the total amount used and the final economical impact. Then, when a solid acid catalyst is to be designed and optimized in order to carry out a certain reaction, the following questions have to be necessarily answered: What type of acid sites are needed, either Brønsted or Lewis? What is the acid strength required to activate the reactant molecule, and finally, how are the number of the required acid sites in a given solid acid catalyst maximized? In order to answer these questions, different techniques have been developed to determine the surface acidity. The methods used and the results obtained in the present study will be briefly described in this section.

PILCs possess both Brønsted acid (proton donor) sites and Lewis acid (electron pair acceptor) sites[45,46]. To investigate the surface acidity on PILC samples, the most commonly used methods are the study of adsorbed ammonia or pyridine by infrared (IR) spectroscopy and temperature programmed desorption (TPD) of adsorbed ammonia[47]. By choosing adsorbed substrates with different basicity, both the number and strength of the acid sites can be determined.

Ming–Yuan showed that the same montmorillonite pillared by different metal oxides exhibit differences in acidity, with the highest acidity for Ti-PILC

and the lowest for Ni-PILC[48]. The acidity shown in this study is mainly attributed to Lewis acidity.

In the present work acidity is determined and compared using two independent techniques and is discussed in the following sections. A qualitative picture is obtained from pyridine IR of the clay samples.

3.11.1 TEMPERATURE PROGRAMMED DESORPTION (TPD) OF AMMONIA

The use of PILCs as acid catalysts could benefits from knowledge of the number, strength and nature of the acid sites involved. Clays, in general have both Brønsted and Lewis type acidity. Brønsted acidity essentially results from the dissociation of absorbed H_2O molecules. This dissociation is induced by the electric field of the exchangeable cations to which they are associated. The presence of surface silanol groups (≡ Si-OH), resulting from broken ≡ Si-O-Si≡ bonds in the tetrahedral, sheet, either via treatment with acids or by extended contact with water by the clay[49] also contributes to Brønsted acidity. In contrast, Lewis acidity results not only from low-coordinated Al and/or Mg on the crystal edges, but also, and most importantly, from the isomorphous substitution of Si^{4+} by Al^{3+} and of Al^{3+} by Mg^{2+}. These substitutions create Lewis base sites in clays, particularly in smectites, and Lewis acid sites in the interlayer.

Previously, acidity in pillared materials was thought to be of the Lewis-acid type and resulting mainly from dehydroxylation of the hydrated large interlayer cations. However, when heated, these polyoxycations form oxide clusters and protons, which are retained as charge compensating cations[50] and possibly enhance the Brønsted acidity. On the other hand, these protons can migrate to octahedral holes, thereby becoming inaccessible and finally resulting in the degradation of the octahedral sheet[51]. Recent reports[52] suggest that the host-guest interactions between clays and intercalated compounds enhance reactivity and modify the physico-chemical properties of the intercalation compounds. Thus, intercalation significantly increases the acid properties of the incorporated cations[53], inducing hydroxyl groups to be easily dissociated, and creating Brønsted acidity.

It is reported that[48] the acidity varies with the type of hydroxycation (Ti>Zr>Al>Fe), and acidity increases with the number of pillars. Pillars and clay layers show synergetic effects, involving both acidity and reactivity of the PILC. Thus the surface acidity determination plays an important role in catalyst characterization.

In the present work, the pillar metals used are Ti, Zr, Al and Cr. Mixed pillaring that contains 2 metals are also done. From the acidity values obtain from TPD of NH_3 shown in table 3.11.1 we get an idea about the influence of various pillar metals on the acidity of montmorillonite. After high temperature (500°C) calcination, the structure of montmorillonite KSF gets collapsed making the acidic sites in accessible. Ion exchange exposes some of the acidic

sites as a result of partial delamination. The increased acidity of NM may also be due to dealumination that occurs during ion exchange.

During the pillaring process the desegregation of the clay layer helps in exposing more number of acidic sites. The expansion in the layer structure in PILC also increases the accessibility of the interlayer protons which otherwise remain obscure to the reactant molecules in the parent clay due to smaller interlayer dimensions. In addition, the metal oxide pillars formed in the interlayer can contribute to the overall acidity of the PILC materials. Pillaring causes a drastic increase in acidity; in the weak, medium and strong acidic region.

Table 3.11.1 Acidity values calculated from TPD of NH_3

Clay	Weak (mmol/g)	Medium (mmol/g)	Strong (mmol/g)	Total (mmol/g)	Total $x10^{-2}$ ($mmol/m^{2)}$
M	0.0711	0.0508	0.0406	0.1625	2.0911
NM	0.4795	0.1653	0.1107	0.7561	1.4642
TM	0.6033	0.5057	0.2266	1.3356	1.0010
ZM	0.4831	0.3692	0.1500	1.0023	0.7604
AM	0.424	0.1357	0.2036	0.7633	0.6369
CM	0.2630	0.1188	0.0528	0.4356	0.3709
TZM	0.8318	0.5837	0.5275	1.943	1.1988
TAM	0.6924	0.577	0.5049	1.7743	1.4529
TCM	0.4773	0.1825	0.0561	0.7159	0.5224

AZM	0.6088	0.2327	0.1432	0.9847	0.7213
ACM	0.3020	0.1243	0.0178	0.4441	0.3654
ZCM	0.4886	0.1056	0.0528	0.6480	0.5167

Thus pillaring enhances both Brønsted as well as Lewis sites that may cause increased activity in acid catalyzed reactions. The values are greater than NM except in the case of Cr-containing PILCs. It is reported that Cr pillared systems possess lower acidity values. In PILCs the acidity in the weak + medium strength region is from Brønsted acid sites and coordinatively bound NH_3 on strong Lewis site can be desorbed only at high temperatures; thus acidity in strong region can be correlated to the amount of Lewis sites. The major acidity of the present clay systems lies in the weak + medium strength region. The acidity of single PILCs varies in the order TM> ZM> AM>CM and is in agreement with literature. Mixed pillaring results further increase in acidity values. Presence of Cr decreases the acidity of Ti, Al and Zr containing systems upon mixed pillaring, but the values are greater than single Cr-PILC (CM). Both Ti and Zr containing systems shows good Lewis acidity as clear from their comparatively high acidity values in the strong acid region. In addition, these systems show very high Brønsted acidity as evident from the high values in the weak and medium strength region. The acidity per unit area of the catalysts is also tabulated.

According to Sychev, the increased acidity upon Ti pillaring could be due to the occurrence of dealumination during the synthesis of Ti – PILCs[54]. Acidity is also due to the weak acidic character of the Ti species acting as

pillars and to the significant increase in micropore area after the pillaring process. The acidity of samples increased with increase in micropore volume. Present Ti containing systems follows this trend except in the case of TCM that contains Cr, and is interpreted as a result of the presence of Cr. As discussed by Farfan-Torres et al.[55], the Zr-PILCs when calcined at moderate temperatures can contain hydrated ZrO_2 pillars which are positively charged and contribute to the Brønsted acidity of the material by virtue of the following equilibrium:

$$ZrO_2 \cdot xH_2O \rightarrow ZrO_2(x-y)H_2O \cdot yH^+ + yOH^-$$

Similar will be the case of all metal oxide pillars.

3.11.2 FTIR OF PYRIDINE ADSORBED SAMPLES

Pyridine IR is commonly used to get an idea about the nature of the acid site present. Both qualitative and quantitative picture of the acidic site of a solid can be studied. In the present work, we had taken FTIR of pyridine adsorbed clay samples in order to know about the nature of the acid sites present. The characteristic bands of pyridine protonated by Brønsted acid sites (pyridinium ions) appear at 1540 and 1640 cm^{-1}, while the bands from pyridine coordinated to Lewis acid sites appear at 1450 and 1620 cm^{-1}.

From figure 3.11.1, it is clear that the peak at 1450 cm^{-1} is comparatively weaker than that at around 1550 cm^{-1}. The band at 1550 cm^{-1} is broad due to the physically adsorbed pyridine present on the clay systems (peak present around 1630 cm^{-1}). The parent clay posses peak mainly at 1636

cm^{-1} due to physisorbed pyridine present on this sample, where peak of Brønsted acid site is weak.

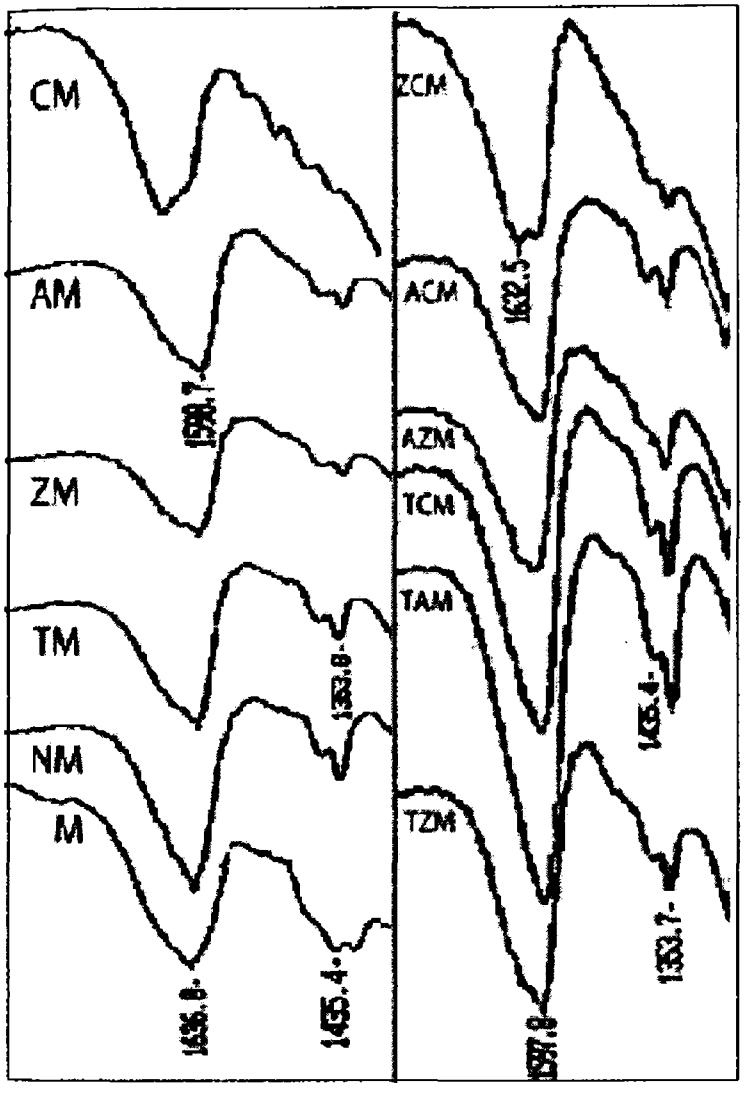

Figure 3.11.1 FTIR of pyridine adsorbed clay samples

In M peaks originating from both the sites are of equal strength. Upon ion exchange, i.e. NM shows increased strength to the peak around 15550 cm^{-1} indicating increased Brønsted acidity. PILCs shows improved strength of both peaks as a result of enhanced acidity, where peak from Brønsted site is of high intensity. But since the peak is merged with the peak of physisorbed pyridine, adsorbed water and Lewis site, as evident from the spectra, we did not try to measure the intensity of peaks to get the quantitative picture of each site present.

3.11.3 TEST REACTIONS FOR ACID - BASE PROPERTIES

In order to get an idea about the relative acidity of various clay systems we have carried out test reactions where acid sites are playing a major role. There are reactions that involve both the acidic sites (Brønsted and Lewis sites) leading to different products. Thus the yield of each product will give a comparative evaluation of each type of acid site present. Some other reactions are catalyzed by acid sites where only one product is formed over the acidic site whether it is Brønsted or Lewis. This will give an idea about the total amount of acid sites present independent of its nature or strength. We have selected two test reactions for acidity measurements and are discussed in detail.

3.11.3.1 CUMENE CRACKING REACTIONS

The desired properties of an efficient cracking catalyst are accessible acid sites, high surface area, and high thermal and hydrothermal stabilities. Cracking catalysts which are zeolite based possess pore sizes less than about 10 Å, which makes them inefficient for the cracking of larger hydrocarbons, for e.g. those in heavy oils[56]. The search for alternative materials with high cracking activities comparable to zeolites, but with larger pores, has motivated different research groups to investigate various metal oxide PILCs in recent years. These research activities have been directed towards understanding the process of pillaring, developing new pillaring species, and finding the role of clay sheet reactivity[57,58].

Cumene cracking reaction is performed to know the catalytic activity and acid site distribution. These types of catalytic cracking reactions are of primary interest in petroleum processing due to the large demand for aromatic petrochemicals of low molecular weight i.e., gasoline and paraffinic molecules for diesel fuel[59]. As bulk crude oil is not generally rich in these molecular types, their formation is very important. The reactions, which are required to produce the desired hydrocarbon fractions, are brought about through the use of acidic solids that activate the hydrocarbons through the formation of carbocations. Now the porous clays have recently received a great deal of attention for these types of reactions.

Cumene is a convenient model compound for such catalytic studies, because it undergoes different reactions over different types of active sites. The cracking of cumene, producing benzene and propene, is generally attributed to the action of Brønsted acid sites, following a carbonium ion mechanism and it is commonly used as a model reaction for characterizing the presence of this type of site on catalyst surface.

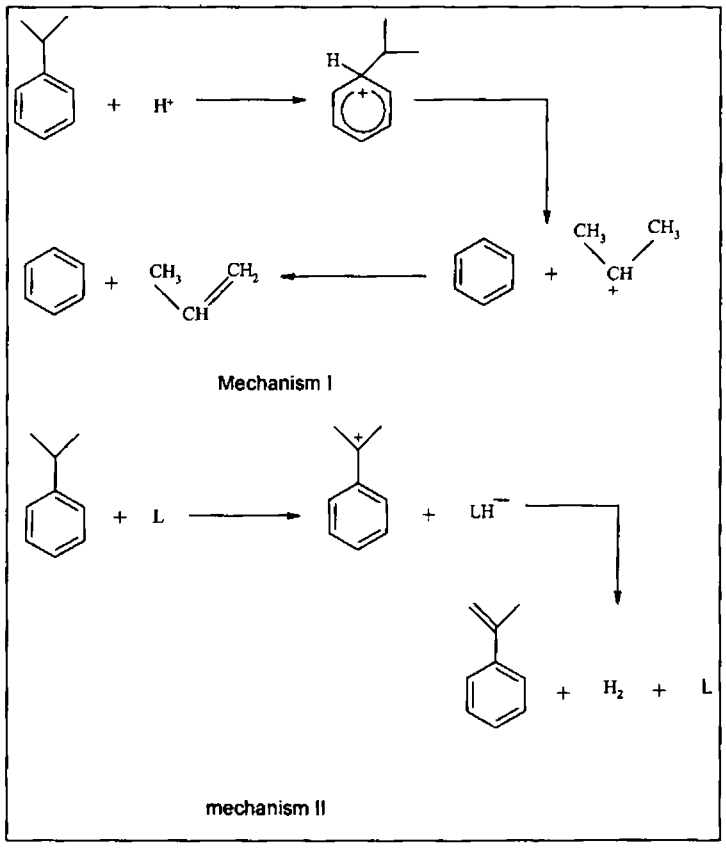

Scheme 3.11.1 Mechanism for cumene conversion over acidic sites

The formation of α-methyl styrene during cumene cracking, due to dehydrogenation, has been ascribed to Lewis acidity (mechanism is shown in scheme 3.11.1)[60,61]. Thus present study allows comparison of the distribution of both Brønsted as well as Lewis acid sites of the prepared catalysts.

Cumene cracking reaction gives a picture of the catalytic activity of different systems. Cracking results benzene whereas dehydrogenation leads to α-methyl styrene. A comparison of the relative amounts of these two products over the different systems provide some information about the relative effectiveness of the cracking and dehydrogenation sites i.e. Brønsted and Lewis acid sites on the catalysts respectively[62-64]. The formation of other products, like ethyl benzene, toluene and styrene is minimal. Dealkylation and side chain cracking results in the formation of ethyl benzene and toluene while dehydrogenation of ethyl benzene gives styrene[65] (scheme 3.11.2).

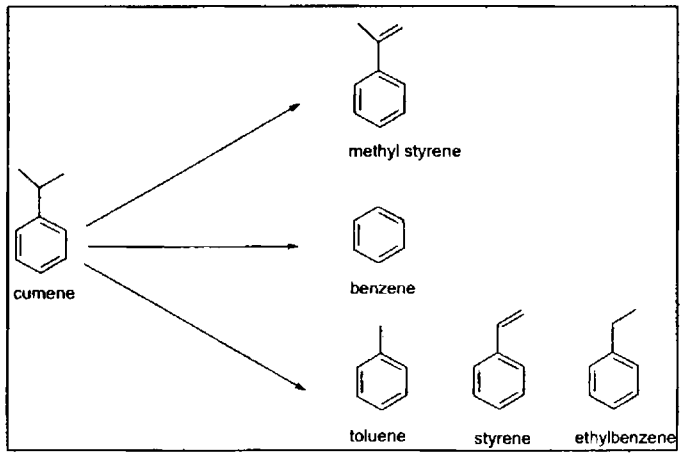

Scheme 3.11.2 various steps during cumene conversion over acid catalysts

3. 11.3.1.1 EFFECT OF REACTION VARIABLES

The percentage conversion and selectivity to the products are greatly influenced by the contact time and reaction temperature. In order to study the effect of contact time, cumene cracking reactions are performed under different weight hourly space velocities (WHSV). The reactions are done at different temperatures also to get the optimum conditions for good catalytic activity. ZM is selected for optimization studies.

3.11.3.1.1.1 Effect of WHSV

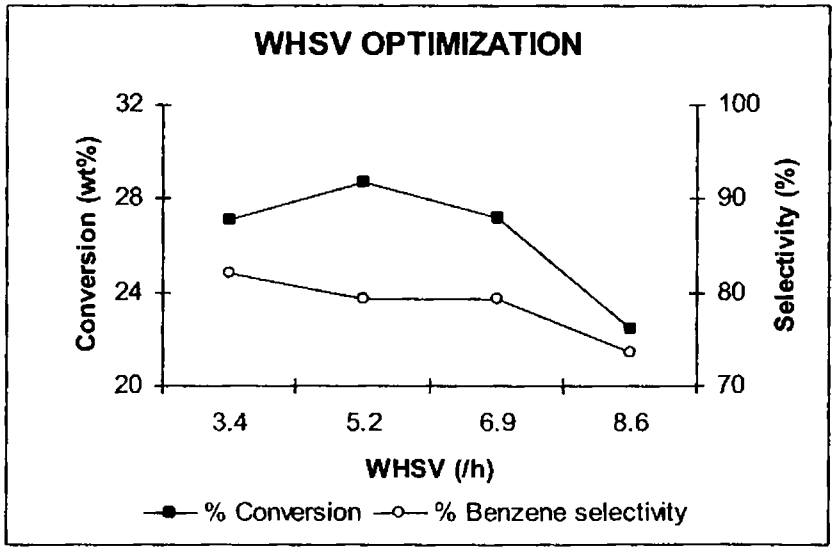

Figure 3.11.2 Influence of WHSV on catalytic activity at a temperature of 450°C, Time on stream 2 h and catalyst weight 0.5g

From the plot of WHSV versus cumene conversion and benzene selectivity in figure 3.2.2, it is clear that maximum conversion is at a WHSV of 5.2 h^{-1}. Benzene selectivity is also found to be good, around 80% in this condition and is thus selected as the optimum condition.

3.11.3.1.1.2 Effect of temperature

Increase in the reaction temperature increases both conversion as well as benzene selectivity. Thus it is concluded that cracking efficiency increases with temperature. At low temperatures of 300°C and 350°C conversion is found to be less than 10%, which increases with further increase in temperature. Present catalyst systems are calcined at a temperature of 500°C and thus we tried a high temperature only up to 450°C and it is selected for further studies (figure 3.11.3).

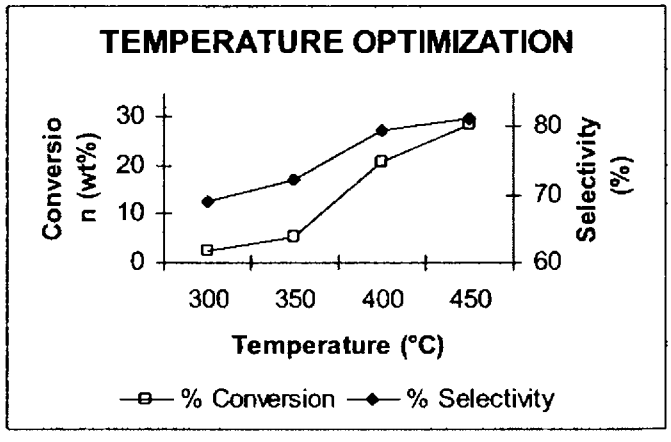

Figure 3.11.3 Effect of temperature on catalytic cumene conversion reaction at a WHSV of 5.2 h^{-1}, Time on stream 2 h and catalyst weight 0.5g

3.11.3.1.2 COMPARISON OF ACTIVITY OF DIFFERENT CLAYS

Pillaring as well as ion exchange is found to increase the catalytic activity of montmorillonite clays in cumene cracking reactions and thus is efficient to enhance clay acidity. This is in agreement with the increased acidity measured from TPD of NH_3. Parent montmorillonite, M shows very low activity. Benzene and α-methyl styrene selectivity is also found to be very low. Benzene is produced on the acid sites associated with tetrahedrally coordinated Al^{IV} and it is thought that octahedrally coordinated Al^{VI} is not effective[66]. M, as evident from its ^{27}Al NMR spectra, possesses very low amount of tetrahedral Al^{IV}. The major products over M are a result of side chain cracking. This may also be due to the low porosity resulted from the structural collapse occurred at high temperature calcinations. Ion exchange increases benzene selectivity and conversion. The increased Brønsted acidity may be due to the process of dealumination that occurred during ion exchange. ^{27}Al NMR spectra show increased amount of tetrahedral Al in NM which further increases upon pillaring. NM shows high α-methyl styrene formation than M. this is a result of exposure of the layer structure arising from partial delamination occurred during ion exchange. The results of cumene cracking over different catalysts are shown in table 3.11.2.

Pillaring process shows increase in both conversion and selectivity. Among the single pillared systems conversion is high over TM and ZM. Mixed pillaring increases conversion and selectivity except in the case of Cr containing systems. The increased benzene and α-methyl styrene selectivity is

a result of exposed and additionally introduced acidic sites. Highest conversion is obtained over TZM with very high benzene selectivity. Thus the assumption that pillaring process exposes and adds acidic sites is confirmed, since among the different PILCs maximum surface area, pore volume, amount of pillar metal etc are of TZM.

Table 3.11.2 Comparison of catalytic activity over different clays

Catalyst	Cumene conversion (wt %)	Selectivity (%)		
		Benzene	α-Methyl Styrene	Others
M	6.7	12.8	0.3	86.9
NM	21.1	62.8	4.9	32.3
TM	28.7	75.7	7.3	17.0
ZM	28.7	79.5	6.6	13.9
AM	22.3	77.2	3.0	19.8
CM	18.8	67.1	2.9	30.1
TZM	31.6	82.6	5.5	11.9
TAM	29.7	78.0	5.9	16.2
TCM	20.6	74.2	3.2	22.7
AZM	26.4	83.2	5.0	11.8
ACM	15.9	70.3	2.6	27.1
ZCM	17.8	67.4	7.22	25.3

Temperature 450°C, Time on stream 2 h, WHSV 5.2 h-1 and Catalyst weight 0.5 g

3.11.3.1.3 PERCENTAGE DISTRIBUTION OF ACID SITES

Table 3.11.3 Percentage distribution of acidic sites calculated from cracked and dehydrogenated products yield

Catalyst	Cumene Conversion (wt %)	Cracked Product (wt %)	Dehydrogenated Product (wt %)	% Brønsted Acidity	% Lewis Acidity
M	6.72	6.62	0.10	20.95	0.32
NM	21.09	19.47	1.62	63.55	5.12
TM	28.74	26.29	2.45	83.20	7.74
ZM	28.69	25.84	2.85	81.77	9.02
AM	22.34	21.43	0.91	67.82	2.88
CM	18.83	17.96	0.87	56.84	2.75
TZM	31.60	28.16	3.44	89.11	10.89
TAM	29.72	27.00	2.72	85.44	8.61
TCM	20.55	19.50	1.05	61.71	3.32
AZM	26.38	25.01	1.37	79.15	4.34
ACM	15.85	14.99	0.86	47.44	2.72
ZCM	17.84	16.40	1.44	51.90	4.56

Temperature 450°C, Time on stream 2 h, WHSV 5.2 h-1 and Catalyst weight 0.5 g

From the conversion and selectivity of cracked and dehydrogenated products formed over various clay systems, we tried to calculate the percentage Brønsted and Lewis acid sites distribution and are tabulated (table 3.11.3). We tried to correlate the acidity obtained using various techniques. Total acidity

obtained from TPD of NH_3 is correlated with cumene conversion over different clays. Figure 3.11.4 shows very good correlation suggesting that both methods provide similar results. Then we tried to correlate percentage Brønsted acid sites distribution calculated from the yield of cracked cumene product with the

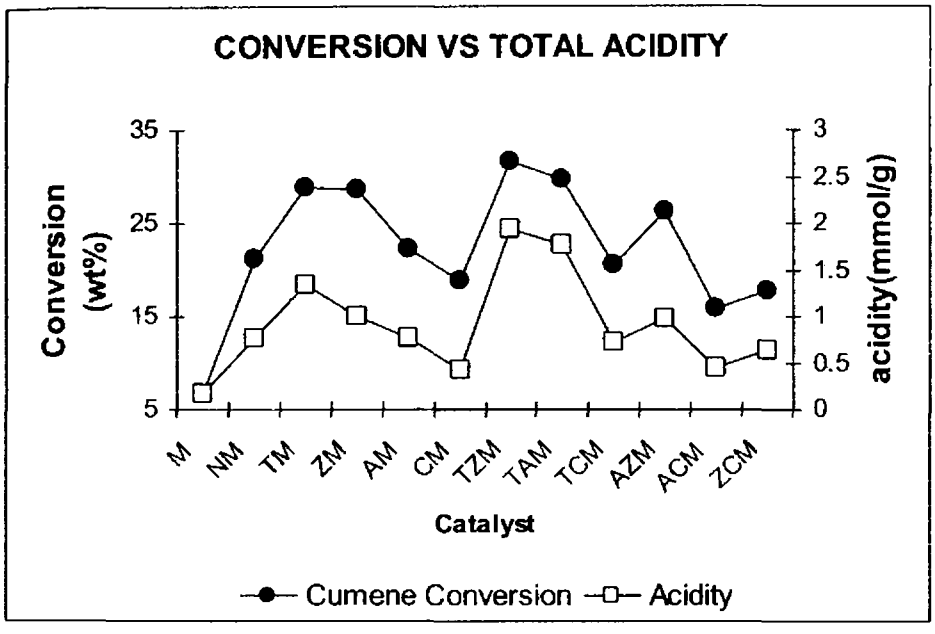

Figure 3.11.4 Correlation diagram for cumene conversion versus total acidity calculated from TPD of NH_3

acidity calculated from weak + medium acid strength region from TPD of NH_3 (figure 3.11.5). The relationship between percent Lewis acid sites distributions calculated from the yield of dehydrogenated products in cumene cracking reactions with the amount of strong acid sites in TPD of NH_3 is also studied (figure 3.11.6).

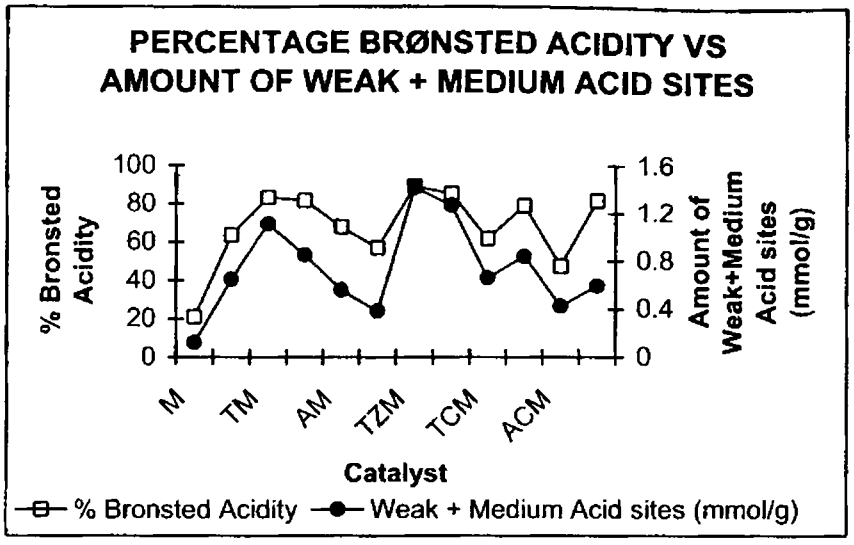

Figure 3.11.5 Plot of %Brønsted acidity obtained from cumene cracking reaction with the amount of weak + medium acid sites in TPD of NH_3

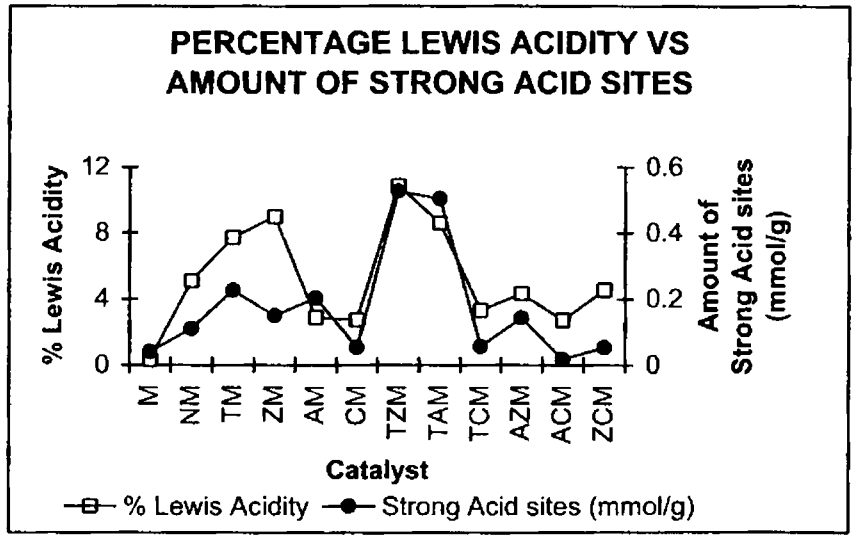

Figure 3.11.6 Plot of %Lewis acidity obtained from cumene dehydrogenation with the amount of strong acid site in TPD of NH_3

3.11.3.2 CYCLOHEXANOL DECOMPOSITION REACTIONS

Cyclohexanol undergoes dehydrogenation on acidic + basic sites to form cyclohexanone while dehydration step is favored on Brønsted acid sites leading to the formation of cyclohexene[67,68]. Scheme 3.11.3 shows various products of cyclohexanol decomposition reaction.

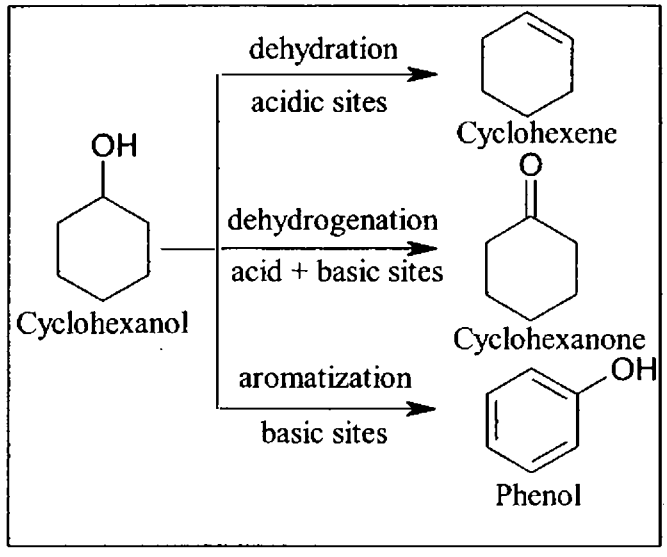

Scheme 3.11.3 various products of cyclohexanol conversion over solid acid catalysts

The formation of cyclohexene on PILC catalysts is thus consistent with acidic nature of these materials. Scheme 3.11.4 shows the role of acidic sites in the formation of cyclohexene and a combination of acidic and basic sites for cyclohexanone formation. The Brønsted acidity of clay samples is also found

to increase in the same order as that of the activity. Therefore, the catalytic activity of PILCs can directly be correlated with increased acidity due to pillaring.

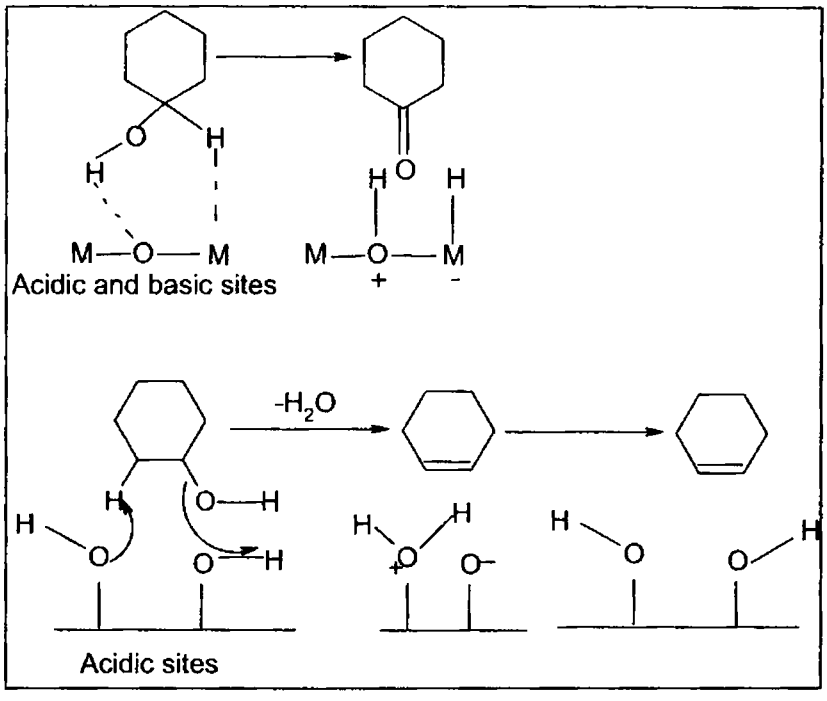

Scheme 3.11.4 Mechanism of gas phase cyclohexanol decomposition

3.11.3.2.1 Effect of reaction parameters

In order for getting good catalytic activity, we studied the influence of reaction parameters on conversion and selectivity of the products. ZM is selected to test the effect of temperature and WHSV on the catalytic activity.

3.11.3.2.1.1 Effect of temperature

Cyclohexanol transformation reaction has been performed on PILC samples in the temperature range of 200–350°C. Figure 3.11.7 summarizes the influence of temperature on catalytic activity over the PILC material. Under the reaction conditions, cyclohexene is obtained as the major product for all the catalysts (selectivity ≈80%) along with negligible amount of other products.

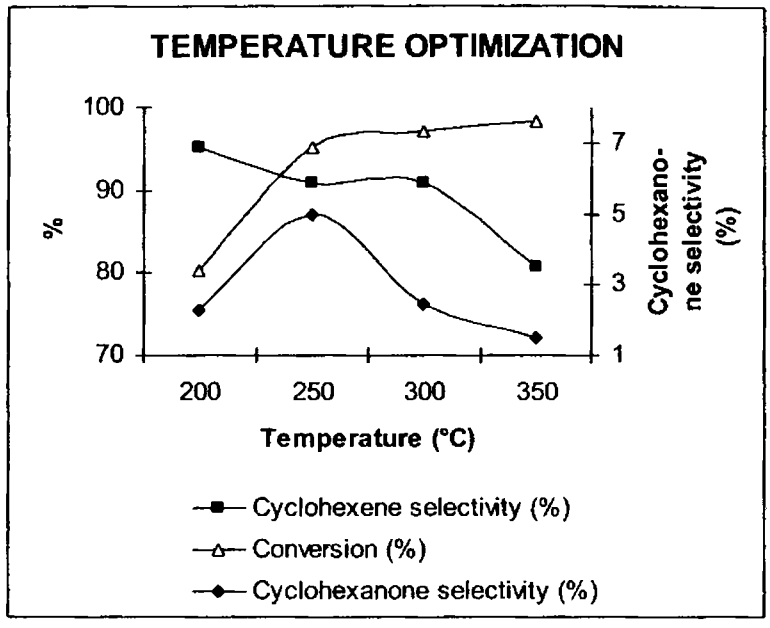

Figure 3.11.7 Effect of temperature on catalytic activity (wt% conversion) in the range of 200–350°C at WHSV 7.7 h^{-1}, Time on stream 2 h and Catalyst weight 0.5 g

The conversion increases with temperature. An increase in temperature from 200°C - 250°C shows a drastic increase in conversion as evident from the figure. Conversion reaches more than 97% when the temperature is greater than 250°C. Thus for the comparative evaluation of different catalysts (of conversion and acidity) we selected a temperature of 250°C.

3.11.3.2.1.2 Influence of WHSV

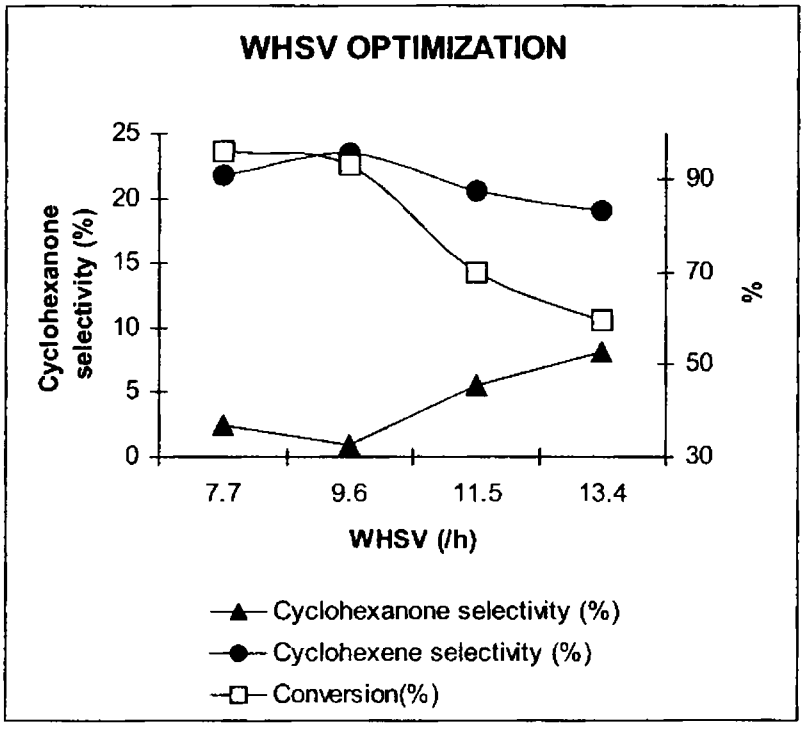

Figure 3.11.8 influence of WHSV on catalytic activity at a temperature of 250°C, Time on stream 2 h and Catalyst weight 0.5g

In order to study the effect of WHSV on the catalytic activity, cyclohexanol dehydration has been performed at 250°C on the catalyst. The catalytic activity shows a decreasing trend with increasing WHSV as shown in figure 3.11.8. Cyclohexene selectivity also decreases whereas cyclohexanone selectivity slightly increases with WHSV and we selected a WHSV of 7.7 as the optimum one. It is reported that a decrease in the conversion is observed at higher WHSV due to lesser contact time where the kinetics get affected[69].

3.11.3.2 COMPARISON OF DIFFERENT SYSTEMS

The comparison of activity over different clays gives an idea about the relative acidities. The presence of basic sites is proved from the formation of cyclohexanone. The catalytic activity of all systems is tested in the optimized conditions and is shown in Table 3.11.4. Among the various clays M is least active and the conversion increases upon modifications. Cyclohexanone selectivity is also very low over M. Cyclohexene is formed as the major product in all cases. Over NM, formation of other products is more when compared to cyclohexanone. All modified clays shows appreciable amount of cyclohexanone which is a result of exposure of the layer structure that makes basic sites accessible. This reveals the dual nature of montmorillonite clays which can be used for a number of organic transformations. All modified systems shows very good conversion and thus are efficient catalysts for cyclohexanol decomposition. Comparison of conversion and cyclohexene selectivity shows TZM as the best among different types of the modified

montmorillonites. The enhanced textural properties lead to highest catalytic activity for TZM.

Table 3.11.4 Comparison of catalytic activity in cyclohexanol decomposition reaction

Catalyst	Conversion (wt %)	Selectivity (%)		
		Cyclohexene	Cyclohexanone	Others
M	49.2	97.0	0.01	2.99
NM	96.6	79.8	7.4	12.8
TM	97.5	91.1	0.5	8.4
ZM	97.3	79.5	6.4	14.1
AM	96.8	91.3	5.3	3.4
CM	92.9	91.1	3.8	5.1
TZM	98.1	95.0	2.0	3.0
TAM	97.7	69.6	10.0	20.4
TCM	96.4	82.8	5.9	11.3
AZM	97.1	84.5	8.5	7.0
ACM	93.1	85.4	4.9	9.7
ZCM	96.2	90.9	6.7	2.4

Temperature 250°C, WHSV 7.7 h-1, Time on stream 2 h and Catalyst weight 0.5 g

Figure 3.11.9 compares the cyclohexanol conversion with the total acidity calculated from TPD of NH_3. The perfect correlation obtained shows the efficiency of both methods to give a comparative evaluation of acidity in clays (conversion of M is not shown to protect clarity of the picture).

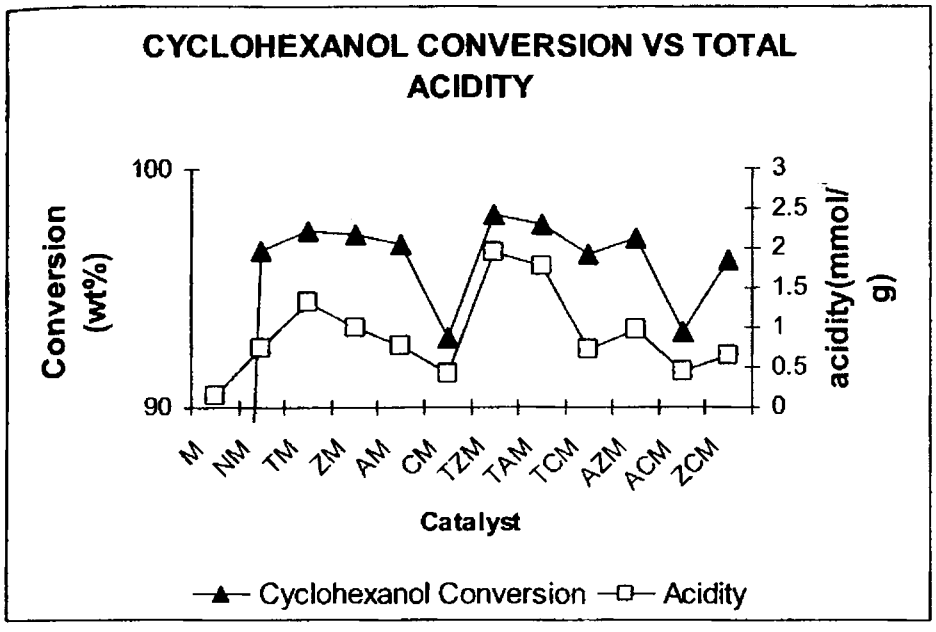

Figure 3.11.9 plot of conversion versus total acidity

3.12 CONCLUSIONS

The major conclusions at which we reach from the characterization of present clay catalysts are listed below.

- Pillaring is done to improve the structural as well as textural properties of montmorillonite.

- Ti, Zr, Al, Cr single and mixed pillared montmorillonite clays are prepared and characterized.

- Reduced CEC tells about the replacement of exchangeable cations which is a result of pillar metal polyoxocation insertion.

- Elemental analysis results say about the amount of pillar metal incorporated.

- Surface area- pore volume is increased drastically upon pillaring that again increases with mixed pillaring.

- XRD analysis is used as a proof for pillaring which provided the increased interlamellar distance.

- FTIR and SEM analysis of different systems show the retention of layer structure.

- ^{29}Si and ^{27}Al NMR results confirm pillaring; leaching of Al is also proved.

- High thermal stability is imparted to clays upon pillaring and is clear from thermal analysis.

- The increase in acidity of the parent montmorillonite as well as single PILC on mixed pillaring is clearly understood from TPD of NH_3, and test reactions for acidity measurements which offers the present systems as efficient catalysts for organic transformations.

- From the results obtained using various characterization methods the efficiency of pillaring that improve clay properties which show further enhancement upon mixed pillaring, with the retention of layer structure is revealed.

REFERENCES:

1. D.T.B. Tennakoon, W. Jones, J.M. Thomas, Solid State Ionics. 24 (1987) 205.
2. M.L. Occelli, J.A. Bertrand, S.A.C. Gould, J.M. Dominguez, Microporous Mater. 34 (2000) 195.
3. K. Norrish, Disc. Faraday Soc. 18 (1954) 120.
4. P. Falaras, F. Lezou, G. Seiragakis, D. Petrakis, Clays Clay Miner. 48 (2000) 549.
5. K. Bahranowski, E.M. Serwicka, Colloid Surf. A 72 (1993) 153.
6. B.G. Mishra, G.R. Rao, Microporous Mater. 70 (2004) 43.
7. J.L. Valverde, P. Sanchez, F. Dorado, I. Asencio, A. Romero, Clays Clay miner. 51 (2003) 41.
8. M. Kurian, S. Sugunan, Indian J. of Chem. 42A (2003) 2480.
9. S. Yamanaka, K. Makita, J. Porous Mater. 1 (1995) 29.
10. M.L. Occelli, J.V. Senders, J. Lynch, J. Catal. 107 (1987) 557.
11. L.S. Cheng, R.T. Yang, Microporous Mater. 8 (1997) 177.
12. A. Gil, A. Massinon, P. Grange, Microporous Mater. 4 (1995) 369.
13. A. Gil, M. Montes, J. Mater. Chem. 4 (1994) 1491.
14. J.T. Kloprogge, J. Porous Mater. 5 (1998) 5.

15. A. Gil, L.M. Gandia, M.A. Vicente, Catal. Rev. Sci. Eng. 42 (2000) 145.
16. J. Sterte, in Preparation of Catalysts V, G. Poncelet, P.A. Jacobs, P. Grange, B. Delmon (eds), Elsevier Science, Amsterdam, 1991), p. 301.
17. E. Booij, J.T. Kloprogge, J.A.R. v. Veen, Appl. Clay Sci. 11 (1996) 155.
18. E. Booij, J.T. Kloprogge, J.A.R.v. Veen, Clays Clay Miner. 44 (1996) 744.
19. J.H. Choy, J.H. Park, J.B. Yoon, J. Phys. Chem. B 102 (1998) 5991.
20. Y.S. Han, S. Yamanaka, J.H. Choy, Appl. Catal. A 174 (1998) 83.
21. Y.S. Han, H. Matsumoto, S. Yamanaka, Chem. Mater. 9 (1997) 2013.
22. M.L. Occelli, J.V. Senders, J. Lynch, J. Catal. 107 (1987) 557.
23. Z. Ding, H.Y. Zhu, G.Q. Lu, P.F. Greenfield, J. Colloid & Interface Sci. 209 (1999) 193.
24. J.M. de Boer, B.C. Lippens, B.G. Linsen, J.C.P. Broekhoff, A. Van der Heuvel, Th. Osinga, J. Colloid Interf. Sci. 21 (1966) 405.
25. S. Bodoardo, F. Figueras, E. Garrone, J. Catal. 147 (1994) 223.
26. S. Bodoardo, R.Chiappetta, B. Onida, F. Figueras, E. Garrone, Microporous. Mater. 20 (1998) 187.
27. L. Poppl, E. Toth, I. Paszli, V. Izvekov, M. Gabor, J. Thermal Anal. 53 (1998) 585.
28. D.E.W. Vaughan, R.J. Lussier, L.V. Rees (ed.), in: Proceeding of the 5th International Conference on Zeolites, Heyden, London,1980, p. 94.
29. M.L. Occelli, B. Drake, S. Gould, J. Catal. 142 (1993) 337.

30. D. Plee, F. Borg, L. Gatineau, J.J. Fripiat, J. Am. Chem. Soc. 107 (1985) 2362.
31. D.T.B. Tennakoon, W. Jones, J.M. Thomas, J. Chem. Soc., Faraday Trans. 182 (1986) 3081.
32. J.F. Lambert, S. Chevalier, R. Frank, H. Suquet, D. Barthomeof, J. Chem. Soc., Faraday Trans. 190 (1994) 67.
33. M.L. Occelli, A. Auroux, G.J. Ray, Microporous Mater. 39 (2000) 43.
34. B.M. Weckhuysen, R.A. Schoonheydt, Catal. Today 49 (1999) 441.
35. R.K. Rana, B. Viswanathan, Catal. Lett. 52 (1998) 25.
36. K.A. Carrado, S.L. Suib, N.D. Skoularikis, R.W. Coughlin, Inorg. Chem. 25 (1986) 4217.
37. S.W. Karickhoff, G.W. Bailey, Clays Clay Miner. 21 (1973) 59.
38. G. Ranga Rao, B.G. Mishra, React. Kinet. Catal. Letts. 75 (2002) 251.
39. G. Ranga Rao, B. Gopal Mishra, Materials Chemistry and Physics 89 (2005) 110.
40. A. Navio, M.C. Hidalgo, G. Colon, S.G. Botta, M.I. Litter, Langmuir 17 (2001) 202.
41. J.J. Fripat, Catal. Today 2 (1988) 281.
42. A. Gil, M. Montes, J. Mater. Chem. 4 (1994)1491.
43. M.J. Avena, R. Cabrol, C.P. De Pauli, Clays Clay Miner 38 (1990) 356.
44. D.Y. Zhao, Synthesis and Charactarization of Pillarad Clays Containing Mixed-Metal Complexes, Ph.D. thesis, Jilin University, P.R. ChangChun, China.
45. S. Chevalier, R. Franck, H. Suquet, J.F. Lambert, D. Barthomeuf, J.

Chem. Soc. Faraday Trans. 90 (1994) 667.

46. H. Auer, H. Hofmann, Appl. Catal. A 97 (1993) 23.
47. S.A. Zubkov, L.M. Kustov, V.B. Kazansky, G. Fetter, D. Tichit, F. Figueras, Clays Clay Miner. 42 (1994) 421.
48. H. Ming-Yuan, L. Zhonghui, M. Enze, Catal. Today 2 (1988) 321.
49. R.M. Barrer, Philadelphia Trans. Royal Soc. Lon. 311 (1984) 331.
50. M.L. Occelli, J. Mol. Cat. 35 (1986) 377.
51. D.E.W. Vaugham, R.J. Lussier, J.S. Magee, U.S. Patent 4248739.
52. S. Bodoardo, F. Figueras, E. Garrone, J. Catal. 147 (1994) 223.
53. K. Hashimoto, Y. Hanada, Y. Minami, Y. Kera, Appl. Catal. A. 141 (1996) 57.
54. M. Sychev, in: Proceedings of the Symposium "Characterization and Properties of Zeolitic Meterials" of the Polish-German Zeolite Colloquium, M. Rozwadowski (ed), Torun Poland, 1992, p. 63.
55. E.M. Farfan-Torres, E. Sham, P. Grange, Catal. Today 15 (1992) 515.
56. F. Figueras, Catal. Rev. Sci. Eng. 30 (1988) 457.
57. D.E.W. Vaughan, in W.H. Flank, T.E. Whyte Jr. (eds), Perspectives in Molecular Sieve Science, ACS Symposium Series, Vol. 368, American Chemical Society, Washington, DC, 1988, Ch. 19, p. 308.
58. D. Plee, L. Gatineau, J.J. Fripiat, Clays Clay Miner. 35 (1987) 81.
59. R.J. Lussier, J.S. Magee, D.E.W. Vaughan, Canadian Symp. Catal. 1980, p. 112.
60. J.T. Richardson, J. Catal. 9 (1967) 182.

61. E.T. Shao, E. MC Innich, J. Catal. 4 (1965) 586.
62. T. Mishra, K. Parida, Appl. Catal. A Gen. 174 (1988) 91.
63. T. Mishra, K. Parida, Appl. Catal. A Gen. 166 (1998) 123.
64. A. Gil, L.M. Gandia, M.A. Vicente, Catal. Rev. Sci. Engg. 42 (2000) 145.
65. S.M. Bradely, R.A. Kydd, J. Catal. 141 (1993) 239.
66. J.C. Davidtz, J. Catal., 43 (1976) 260.
67. D. Duprez, D. Martin, J. Mol. Catal. A: Chem. 118 (1997) 113.
68. B.G. Mishra, G. R. Rao, Bull. Mater. Sci. 25 (2002) 155.
69. R.M. Koros, E.J. Novak, Chem. Eng. Sci. 22 (1967) 470.

★★★★★★★★★★★★★★★★

Chapter 4

FRIEDEL-CRAFTS ALKYLATION REACTIONS: WHY HETEROGENEOUS CATALYSIS? A GREEN ROUTE IN CHEMICAL SYNTHESIS

In this now universal contamination of the environment, chemicals are the sinister and little recognized partners of radiation in changing the very nature of the world -the very nature of its life. Green chemistry provides the technical alternatives that the economists need. If the cost of disposal of wastes, treatment, liability compliance and poor public image are taken into consideration, environmentally benign processes can compete with traditional approaches. A related ambition is the minimization of the use of materials, energy in production, the increased use of recycled materials and renewable resources. Heterogeneous catalysis is widely regarded as one of the most important ways to reduce the environmental footprint of chemical processes. In this context, Friedel - Crafts alkylation, the important tool for introducing alkyl groups into the aromatic ring system is introduced in this chapter giving details of conventional catalysts used which reminds the need for heterogeneous catalysts for the protection of Green Chemistry.

4.0 INTRODUCTION

Substituted aromatic compounds have found wide applications in the chemical industry and, therefore, their synthesis is of great importance. For instance ethylbenzene is used to make styrene, from which polystyrene plastics are made. Inexpensive detergents, the alkylbenzenesulfonates, are prepared industrially from benzene and alkene[1].

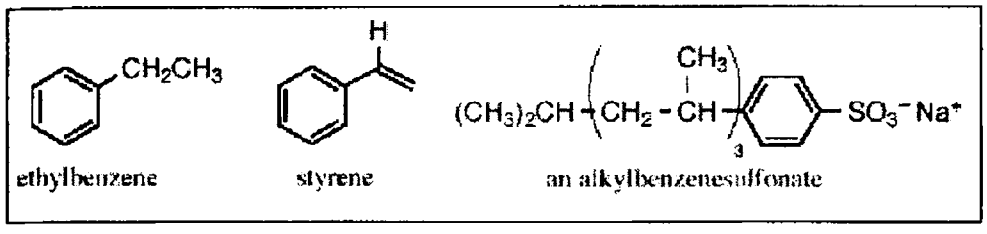

The simple aromatic hydrocarbons used as starting materials for the complex molecules used by today's society are readily available either from coal tar or petroleum. Examples include benzene, toluene, naphthalene, phenanthrene, xylenes, and anthracene.

Although simple alkyl benzenes such as toluene and xylene are isolated from coal and petroleum, more complex arenes must be synthesized by chemists by reacting the aromatic ring with other compounds. The single most important class of reactions of the benzene ring is electrophilic aromatic substitution reactions, as illustrated in the above generalized reaction:

4.1 FRIEDEL-CRAFTS REACTIONS

Electrophilic aromatic substitution reactions are characterized by a two step process in which the first step is the attack of an electrophile, E^+, by the π-electrons of the aromatic ring, yielding a carbocation intermediate. The second step is the loss of a proton on the ring to re-form the neutral aromatic π-system. Examples of electrophilic aromatic substitution reactions are nitration, sulfonation, halogenation, alkylation, and acylation. The current lab experiment will focus on alkylation and acylation of arenes. These reactions, in which the electrophile is a carbocation, are called Friedel-Crafts reactions, named for the two men who first reported the method in 1877.

These reactions form a large part of the more general problem of electrophilic reactions. C.C. Price, in the Encyclopedia Britannica gives definition to Friedel-Crafts reaction. "The Friedel-Crafts reaction is commonly considered as a process of uniting two or more organic molecules through the formation of carbon to carbon bonds under the influence of certain strongly acidic metal halide catalysts such as aluminium chloride, boron trifluoride, ferric chloride, zinc chloride, etc". There are a number of reactions bearing the general name of "Friedel-Crafts" and a large number of reactions related to this type. In a general sense, we consider Friedel-Crafts type reactions to be any substitution, isomerization, elimination, cracking, polymerization or addition reactions taking place under the catalytic effect of Lewis acid type acid halides (with or without co-catalyst) or proton acids. One of the original characteristics of the reaction, namely that hydrogen halide should be evolved in the course of

the reaction is by no means a limiting condition any more. It is felt to be appropriate to maintain the name "Friedel-Crafts" for these reactions in honor of the achievement of the original inventors of the aluminium chloride reaction and at the same time to use the term in a more general sense, pointing out that reactions related to the "Friedel-Crafts reactions" are to be included.

It is also unnecessary to limit the scope of the Friedel-Crafts reaction to the formation of carbon-oxygen, carbon-nitrogen, carbon-sulfur, carbon-halogen, carbon-phosphorous; carbon-deuterium, carbon-boron and many other types of bonds all conform to the general Friedel-Crafts Principle.

Although Friedel and Crafts made their original observation on a reaction involving replacement of hydrogen in an aliphatic compound, i.e. amyl chloride, the main emphasis of the reaction was concerned first of all with aromatic compounds. The preparation of aliphatic compounds involving Friedel-Crafts methods was of minor importance until World War II, when isomerization of paraffins and cyclo paraffins and the polymerization of alkenes achieved considerable importance. The development of aliphatic chemistry of Friedel-Crafts reactions stems largely from advances made in the production of relatively pure aliphatic hydrocarbons and their utilization for motor fuels (Patieff and co workers) and the increasing importance of polyalkenes. Ethylbenzene, needed for the manufacture of styrene, detergent alkylates and related products helped to push aromatic Friedel-Crafts reactions into large scale production[2].

4.1.1 Composition of reaction systems

In the absence of any complications or side reactions, a Friedel-Crafts reaction mixture involves the following components:

1. The substance to be substituted.
2. A reagent that supplies the substituent. This may be an alkene, alkyl halide, alcohol, acid halide or anhydride, etc.
3. A catalyst, which may be a Lewis acid type acidic halide or a proton acid in the Bronsted-Lowry sense.
4. A solvent; the function of which is sometimes taken over by excess of the substrate or reagent. Solvents are generally of the non-ionizing type, e.g., CS_2, CCl_4, etc, although solvents with high dielectric constants are also employed, e.g., nitrobenzene, nitromethane etc.
5. The substituted product formed in the reaction (alkylated, acylated product, etc.).
6. The by-product conjugate acid HX, where X originates from the catalyst.

Of the possible combinations of these constituents, many give rise to complexes that play an important role in governing the results of a given reaction.

4.1.2 Friedel-Crafts Alkylation reactions

Alkyl groups can be introduced into aromatic, aliphatic or cycloaliphatic compounds using various methods. The reactants may be of

varied natures, as may also the substrates undergoing substitution, the catalyst needed to achieve the condensation, as well as the solvents and the conditions of the reaction.

4.1.3 Alkylation of Aromatic compounds

4.1.3.1 Alkylating Agents and Catalysts

In aromatics alkylation a hydrogen atom (or other substituent group) of an aromatic nucleus is replaced by an alkyl group through the interaction of an alkylating agent in the presence of a Friedel-Crafts catalyst. Alkyl halides, alkenes and alcohols are the common alkylating agents, although aldehydes, ketones and various other reagents have also been used (table 4.1.1).

Table 4.1.1 Most frequently used alkylating agent in aromatic alkylation reactions

Alkyl halides	Ethers
Alkenes	Aldehydes and ketones
Alkynes	Paraffins and cycloparaffins
Alcohols	Mercaptans
Esters (of	Sulfides
carboxylic and	Thiocyanates
inorganic acids)	

$AlCl_3$, $FeCl_3$, BCl_3, $SbCl_5$, $ZnCl_2$, $TiCl_4$ etc are the Lewis acid type catalysts used for aromatic alkylation and Bronsted acid type are HF, H_2SO_4, H_3PO_4 etc.

The reactions involved using common alkylating agents in the presence of aluminium chloride may be written

$$Ar\text{-}H + RX \xrightarrow{AlCl_3} Ar\text{-}R + HX$$

$$Ar\text{-}H + R\text{-}OH \xrightarrow{AlCl_3} Ar\text{-}R + H_2O$$

$$Ar\text{-}H + R\text{-}CH{=}CH_2 \xrightarrow{AlCl_3} R\text{-}CH(Ar)\text{-}CH_3$$

In the case of alcohols as alkylating agents, it reacts with $AlCl_3$.

$$R\text{-}OH + \xrightarrow{AlCl_3} R\text{-}OH.AlCl_3 \longrightarrow$$

$$RO\text{-}AlCl_2 + HCl \longrightarrow R\text{-}Cl + AOCl$$

It is not necessary for the alcohol-aluminium chloride reaction to go to completion with the formation of the alkyl chloride, as the intermediate Lewis acid complex itself contains a sufficiently polarized alkyl group to enter the reaction. However, the reaction depends very much on the conditions used. Only catalytic quantities of $AlCl_3$ are necessary for the reaction of alkyl halide and alkenes in Friedel-Crafts alkylations, considerably larger quantities of the catalysts are necessary when alcohols are used as alkylating agents.

4.1.3.2 Activity of Catalysts

The general order of alkylation activity of metal halide catalysts is reported to be: $AlCl_3$> $SbCl_5$> $FeCl_3$> $TiCl_2$, $SnCl_4$> $TiCl_4$> $TeCl_4$> $BiCl_3$> $ZnCl_2$[3,4]. The general order of activity of proton acid catalyst is HF> H_2SO_4> H_3PO_4. Activity depends on nature of alkylating agent in addition to the nature of catalyst and other conditions. For e.g. H_2SO_4 and H_3PO_4 are most effective catalysts in alkylation with alkenes and alcohols than with alkyl halides. BBr_3 and BCl_3 are more effective in alkylation with alkyl fluorides than BF_3. BBr_3 and BCl_3 cannot be applied in alkylations with alcohols owing to the fact that they react to give the corresponding borates. The boron halides generally fail to catalyze alkyl chlorides and bromides, but BF_3 shows some activity if a proton donor co-catalyst is present. The choice of a particular Friedel-Crafts alkylation catalyst depends upon the activities of the substrate to be alkylated and the alkylating agent, as well as the solvent, the reaction temperature and several other conditions.

4.1.3.3 Reactivity of aromatics

Electron donor ortho para directing substituents generally facilitate the alkylation of aromatic rings whereas electron withdrawing meta directing substituents usually inhibit Friedel-Crafts alkylations by deactivation of the nucleus. This deactivation can be upset by the simultaneous presence of powerful ortho-para directing groups. A characteristic feature of Friedel-Crafts alkylation is a general tendency to form di- and polyalkylated products, besides

the desired monoalkylates. This is particularly the case when simple alkyl groups such as methyl and ethyl are introduced.

4.1.4 Alkylating agents in Aromatic alkylations

4.1.4.1 Alkyl halides

Alkyl fluoride is the most reactive alkyl halides in alkylation reactions. $AlCl_3$ and related catalysts and BF_3 were found to be the suitable catalysts for alkylation of alkyl halides. In case where alkyl halide is used, the catalyst is required only in minute amounts.

A simple, uncluttered mechanism for the electrophilic substitution reaction between an arene for e.g., benzene and an alkyl halide, say chloromethane in the presence of an aluminium chloride catalyst are described here. Any other chloroalkane would work similarly.

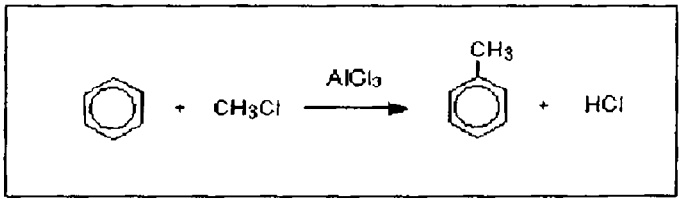

As discussed above, alkylation means substituting an alkyl group into something - in this case into a benzene ring. A group like methyl or ethyl and so on replaces hydrogen on the ring. Substituting a methyl group gives toluene.

The electrophile is CH_3^+. It is formed by reaction between the chloromethane and the aluminium chloride catalyst.

$$CH_3Cl + AlCl_3 \longrightarrow CH_3^+ + AlCl_4^-$$

The electrophilic substitution mechanism involves two stages

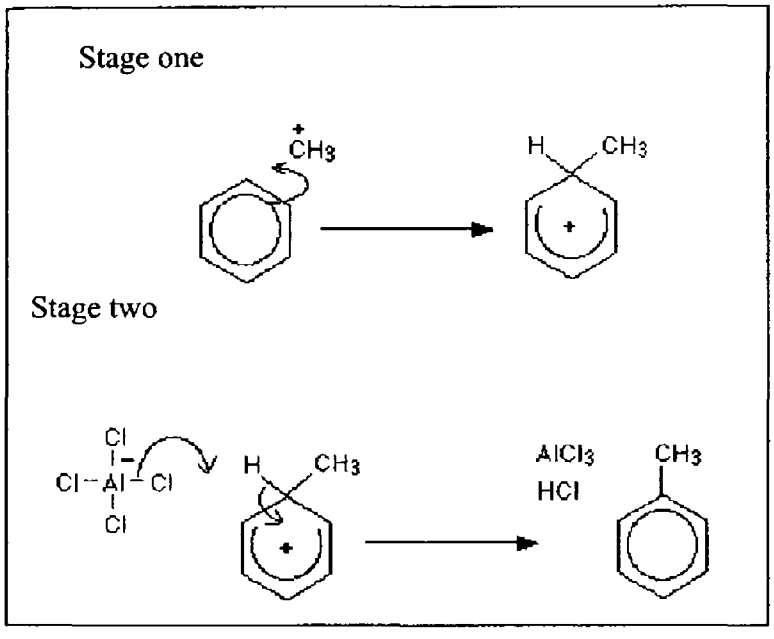

The hydrogen is removed by the $AlCl_4^-$ ion, which was formed at the same time as the CH_3^+ electrophile. The aluminium chloride catalyst is regenerated in this second stage. The methylbenzene formed is more reactive than the original benzene, and so the reaction doesn't stop there. We may get further methyl groups substituted around the ring.

4.1.4.2 Alkenes

Alkenes are industrially the most frequently used alkylating agents because of their cheapness and availability. The alkenes most frequently employed are ethylene, propylene, butylenes, amylene etc. Tri, tetra and pentamers of propylene such as dodecylene, have been frequently used in alkylations in recent years to prepare alkylates (dodecyl benzene) as starting materials for detergents. The alkenes employed are easily and inexpensively available directly form petroleum cracking. As alkenes tend to polymerize in the presence of acid catalysts they are often employed with excess of aromatics to suppress polymerization. Most Lewis and Brønsted acids are active as catalysts in alkylation with alkenes. Catalysts are needed only in small amounts in alkene alkylation.

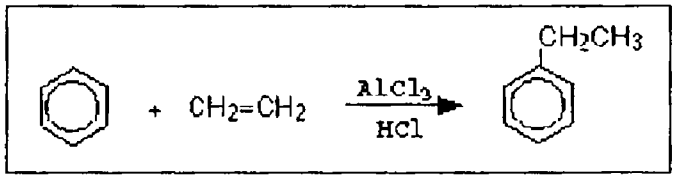

To put an ethyl group on the ring (to make ethylbenzene), benzene is treated with a mixture of ethene, HCl and $AlCl_3$.

The electrophile is $CH_3CH_2^+$. It is formed by reaction between the ethene and the HCl - exactly as if you were beginning to add the HCl to the ethene.

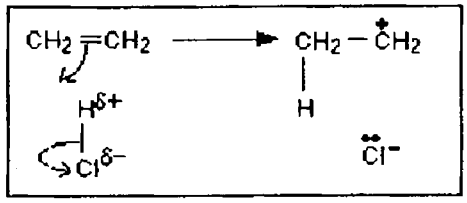

The chloride ion is immediately picked up by the $AlCl_3$ to form an $AlCl_4^-$ ion. That prevents the chloride ion from reacting with the $CH_3CH_2^+$ ion to form chloroethane.

It wouldn't matter if it did react, because chloroethane will react with benzene using a simple Friedel-Crafts alkylation reaction to give the product.

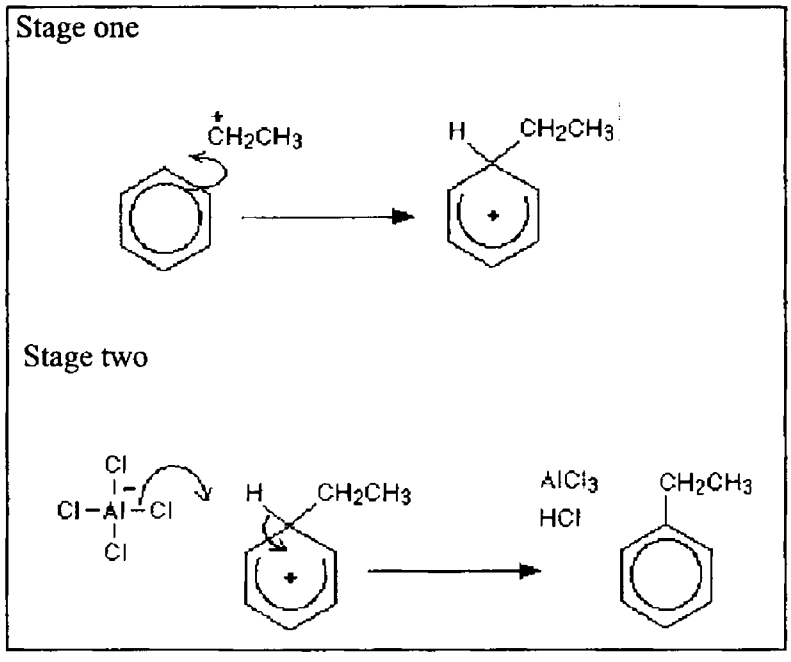

4.1.4.3 Alcohols

Primary, secondary as well as tertiary alcohols use the same catalysts as that of alkyl halides and alkenes. Alcohols are more reactive than alkyl halides. When we use alcohols as the alkylating agents, it reacts with $AlCl_3$ and thus stoichiometric amount of the catalyst is required. Although it is not necessary that the interaction of Lewis acid catalyst with the alcohol should continue until the formation of the alkyl halide, an equimolar quantity of catalyst is required to form the primary complex. BF_3 forms only addition compounds and is very effective alkylating agent for alcohols. Thus the alkyl halide formation is not a necessary step for alkylation. In H_2SO_4 catalyzed reaction, alcohol is first esterified and the corresponding alkyl sulfate then reacts with the aromatic compound.

Esters, ethers, alkynes, aldehydes, ketones, lactones, sulfides, mercaptants, aryl halides etc are the other alkylating agents used.

4.2 DEMERITS OF CONVENTIONAL HOMOGENEOUS CATALYSTS

The use of traditional Lewis as well as Brønsted acid homogeneous catalysts are laden with several problems like difficulty in separation and recovery of products, disposal of spent catalyst, corrosion, high toxicity etc. These catalysts also catalyze other undesirable reactions like alkyl isomerizations, trans alkylation reactions and polyalkylation reactions[5]. In order to reduce isomerization and disproportionation in aromatic alkylation

catalyzed by $AlCl_3$, the reactions are generally carried out at low temperature (below −10°C) and in solvents like carbon disulphide and nitromethane, which present hazards. Moreover these catalysts are moisture sensitive and hence demand moisture free solvent and reactants, anhydrous catalysts and dry atmosphere for their handling[6]. Most of the catalysts have to be added in stoichiometric amounts, there by adding to the cost of the desired product. The work-up procedure for reactions using the traditional homogeneous, Brønsted as well as Lewis acid catalysts involves a water quench which prevents the acid from being reused and on subsequent neutralization leads to an aqueous salt waste stream. Hence worldwide efforts have been made to replace the present environmentally malignant catalysts.

Our environment, which is endowed by nature, need to be protected from ever increasing chemical pollution associated with contemporary lifestyles and emerging technologies. Developments in water treatment, waste disposal methods, agricultural pesticides and fungicides, polymers, material science, detergents, petroleum additives and so forth have all contributed in improvement in our quality life. But all these advantages come with a price tag – of pollution. Cleaner production has been identified as a key method for reconciling environment and economic development. The basic idea of cleaner production is to increase production efficiency while at the same time eliminate or at least minimize wastes and emissions at their source rather than treat them at the end of pipe after they have been generated.

The sustainable development, which means the "development that meets the needs of the present without compromising the ability of future generations to meet their own needs", is a must in protection of environment. Sustainable development[7-9] demands change, requires doing more with lesser resource input and less waste generation. Instead of end-of-pipe technology, it requires pollution prevention philosophy, which is: "First and foremost, reduce waste at the origin- through improved housekeeping and maintenance, and modification in product design, processing and raw material selection. Finally, if there is no prevention option possible, treat and safely dispose off the waste".

4.3 GREEN CHEMISTRY

Green chemistry is considered as an essential piece of a comprehensive program to protect human health and the environment. In its essence green chemistry[10-15] is a science based non-regulatory and economically driven approach to achieving the goals of environmental protection and sustainable development.

In order to be eco-friendly, or green, organic synsthesis[16-19] must meet, if not all, at least some of the following requirements: avoid waste, be atom efficient, avoid use and production of toxic and dangerous chemicals, produce compounds which perform better or equal to the existing ones and are bio-degradable, avoid auxiliary substances, reduce energy requirements, use renewable materials, use catalysts rather than stoichiometric reagents. These requirements can be easily met by the concept of green chemistry. In a broad

sense, green chemistry includes any chemical process or technology that improves the environment and thus our quality life.

Green strategies include the replacement of organic solvent by water, altogether elimination of a solvent, the substitution of environmentally benign substances to replace toxic heavy metals, development of solid support reagents and catalysts for synthesis, launching of eco-friendly methods of organic synthesis, designing of products, which can be recycled or safely disposable, use of dry media reactions and many other important aspects. The overall strategy is to virtually eliminate toxic persistent substances from the environment by allowing no further release or by collecting and destroying the existing deposits. Harmful synthetic products either should be replaced by green products or should be synthesized by environment friendly techniques.

4.3.1 Principles of Green Chemistry

The twelve principles of green chemistry proposed by Paul Anastas and John Warner encompass all aspects on the product and the production level from prevention to the design of more efficient synthesis, from the design of less hazardous substances to the use of renewable feedstocks.

1. It is better to prevent waste than to treat or clean up waste after it is formed.
2. Synthetic methods should be designed to maximize the incorporation of all materials used in the process into the final product.

3. Whenever practicable synthetic methodologies should be designed to use and generate substances that possess little or no toxicity to human health and the environment.

4. Chemical products should be designed to preserve efficiency of function while reducing toxicity.

5. The use of auxiliary substances (solvents, separation agents etc) should be made unnecessary whenever possible and when used, innocuous.

6. Energy requirements should be recognized for their environmental and economic impacts and should be minimized. Synthetic methods should be conducted at ambient temperature and pressure.

7. A raw material or feedstock should be renewable rather than depleting whenever technically and economically practical.

8. Unnecessary derivatization (blocking group, protection/deprotection, temporary modification of physical/chemical processes) should be avoided whenever possible.

9. Catalytic reagents (as selective as possible) are superior to stoichiometric reagents.

10. Chemical products should be designed so that at the end of their function they do not persist in the environment and instead break down into innocuous degradation products.

11. Analytical methodologies need to be further developed to allow for real time in-process monitoring and control prior to the formation of hazardous substances.

12. Substances and the form of a substance used in a chemical process should be chosen so as to minimize the potential for chemical accidents, including releases, explosions and fires.

4.4 ATOM ECONOMY

In order to achieve high selectivity in industries, the practice has been to use stoichiometric quantities of inefficient reagents that intrinsically create a significant amount of wastes[20,21]. In this context, waste is defined as everything except the intended product. In view of these trends, Trost[22] came up with a new set of criteria upon which chemical processes can be evaluated for efficiency. These criteria fall under the category of selectivity and atom economy. Selectivity includes chemoselectivity, regioselectivity, diasteroselectivity and enantioselectivity. Atom economy considers how much of the reactants end up in the final product. An ideal synthesis is that in which all of the atoms in the reactants are incorporated into the final product. Roger A. Sheldon[23,24], has quantified the concept of atom economy.

$$\% \text{ Atom Utilization} = \frac{\text{MW of the desired product} \times 100}{\text{MW of (desired product + waste by products)}}$$

Catalysis using $AlCl_3$ some times needs in stoichiometric amounts, which generates large amounts of aluminium trichloride hydrate as waste byproduct, which is generally land filled. But green synthesis uses many catalysts that is recovered and reused repeatedly.

The key to achieving the goal of reducing the generation of environmentally unfriendly waste and the use of toxic solvents and regents is the widespread substitution of "stoichiometric" technologies by greener, catalytic alternatives. The first two involve 100% atom efficiency while the latter is slightly less than perfect owing to the co-production of molecular water. The longer trend is towards the use of the simplest raw materials –H_2, O_2, H_2O, NH_3, CO, CO_2 – in catalytic low salt processes. For many years catalysis prouted life and led to evolution. The widespread substitution of classical mineral and Lewis acids by recyclable solid acids, such as zeolites and acidic clays, and the introduction of recyclable solid bases, such as hydrotalcites will result in a dramatic reduction of inorganic waste.

Because of the deleterious effects that many organic solvents have on the environment and/or health, media such as halogenated hydrocarbons (e.g., $CHCl_3$, CH_2Cl_2) are being phased out of use and benign replacements are being developed. A possible alternative for the use of organic solvents is the extensive utilization of water as a solvent. Traditionally, water is not a popular reaction medium for organic reactions due to the limited solubility of many substrates and also to the fact that a variety of functional groups are reactive towards water. But recently there had been a revival of interest in water as a solvent[25,26] and chemistry in aqueous medium, as it offers many advantages for a clean green chemistry. The addition of surfactants can strongly modify the attitude of water to solubilize organic molecules.

An important incentive for the use of supercritical fluids (SCFs)[27] in synthetic chemistry comes form this increasing demand for environmentally and toxicologically benign processes for the production of high value chemicals. Promoting a reaction photochemically rather than thermally is greener, since light is the green reagent par excellence. Biocatalysis[28], in contrast involves aqueous environments.

Present study adopts heterogeneous catalysts, for some Friedel-Crafts alkylation reactions of aromatics that maintain the concepts of green chemistry.

4.5 HETEROGENEOUS CATALYSIS

As we know catalysts have the remarkable property of facilitating a chemical reaction repeatedly without being consumed. In principle, a catalyst can function as long as reactants are available. Catalysis is astonishing. Very small quantities of the most active catalysts can convert thousands or millions of times their own weight of chemicals. Equally astonishing is just how selective they can be. A catalyst may increase the rate of only one reaction out of many competing reactions. Catalysts bring reactants together in a way that makes reaction more likely.

Catalysts can be divided into two main types - heterogeneous and homogeneous. In a heterogeneous reaction, the catalyst is in a different phase from the reactants. In a homogeneous reaction, the catalyst is in the same phase as the reactants. In a mixture, if there is a boundary between two of the

components, those substances are in different phases. A mixture containing a solid and a liquid consists of two phases. A mixture of various chemicals in a single solution consists of only one phase, because we can't see any boundary between them.

4.5.1 Working of Heterogeneous Catalysts

Most examples of heterogeneous catalysis go through the same stages:

One or more of the reactants are adsorbed on to the surface of the catalyst at active sites. Adsorption is where something sticks to a surface. It isn't the same as absorption where one substance is taken up within the structure of another. An active site is a part of the surface, which is particularly good at adsorbing things and helping them to react. There is some sort of interaction between the surface of the catalyst and the reactant molecules, which makes them more reactive.

This might involve an actual reaction with the surface, or some weakening of the bonds in the attached molecules. When reaction occurs, both of the reactant molecules might be attached to the surface, or one might be attached and hit by the other one moving freely in the gas or liquid. The product molecules are desorbed. Desorption simply means that the product molecules break away. This leaves the active site available for a new set of molecules to attach to and react. A good catalyst needs to adsorb the reactant molecules strongly enough for them to react, but not so strongly that the product molecules stick more or less permanently to the surface. Silver, for example, isn't a good catalyst because it doesn't form strong enough

attachments with reactant molecules. Tungsten, on the other hand, isn't a good catalyst because it adsorbs too strongly. Metals like platinum and nickel make good catalysts because they adsorb strongly enough to hold and activate the reactants, but not so strongly that the products can't break away.

A reaction catalyzed by a heterogeneous catalyst can be represented by a flow chart.

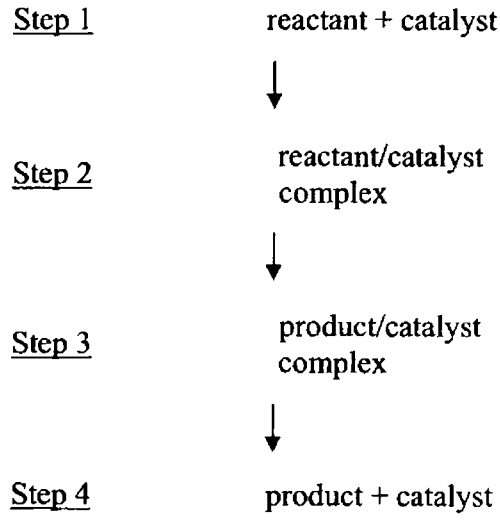

Running a reaction under heterogeneous catalytic conditions has several advantages compared to homogeneous catalytic processes:

- Avoids formation of inorganic salts
- Regenerable
- Non-toxic
- Easy to handle
- Safe to store, long life time

- Easy and inexpensive removal from reaction mixture by filtration or centrifugation
- Tolerates a wide range of temperatures and pressures
- Easy and safe disposal

From the above discussions, the importance of Friedel-Crafts alkylation reactions, need for the replacement of homogeneous catalysts and organic solvents, for the development of eco-friendly nature following the principles of green chemistry is well understood. We selected some industrially important Friedel-Crafts alkylation reactions that use pillared montmorillonite clays as the shape selective solid acid catalyst. In the present study, we are conducting all the reactions in gas phase, which allows continuous run of the reaction and regeneration of the catalysts within the reactor itself. This method eliminates toxic organic solvents. The arene and alkylating agents are taken in such a molar ratio to get good conversion with efficient selectivity.

Alkylation of benzene and toluene with some lower alcohols and benzene alkylation with higher alkenes for LAB synthesis with high % of atom utilization are presented in the following 5 chapters

4.6 CONCLUSIONS

The major conclusions at which we reach from the above discussions are

- Friedel-Crafts reactions invented in 1877 is still used as an important tool in industry.

- The eco-friendly society demands the replacement of the conventional homogeneous Friedel-Crafts catalysts.
- Heterogeneous catalysis offers solid acids as efficient alternatives.

REFERENCES:

1. C. Perego, P. Ingallina, Green Chem. 6 (2004) 274.
2. Friedel-Crafts and Related Reactions, George A. Olah, vol1. Interscience Publishers, John Wiley and Sons, New York, 1963, p.28.
3. W. Ploeg, Rec. Trav. Chim, 45 (1926) 342.
4. C.C. Price, Org. Reactions, 3 (1946) 1, John Wiley and Sons, New York.
5. C.C. Price, Chem. Rev. 29 (1941) 37.
6. V.R. Choudhary, S.K. Jana, B.P. Kiran, J. Catal. 192 (2000) 257.
7. B. Fischhoff, S. Lichtenstein, P. Slavic, D. Keeney, Acceptable Risk, Cambidge University Press, Cambridge, 1981.
8. Colin Baird, Environmental Chemistry, W.H. Freeman and Company New York, 1998.
9. D.J. Amy, The politics of Environmental mediation, Columbia University Press New York 1987.
10. M.C. Cannon, M.E. Connelly, Real World Green Chemistry, American Chemical Society, Washington DC, 2000.
11. M.D. Bagley, C.A. Kroll, C. Clark, Aesthetics in Environmental Planning, Environmental Protection Agency, Washington DC, 1973.

12. N. Lee, Applied Geography. 3 (1993) 27.
13. N. Khoshoo, Environmental Concerns and strategies, Ashish Publishing House, New Delhi, 1998.
14. P.T. Anastas, P.C. Williamson, Green Chemistry: Challenging Perspectives, Oxford University Press Oxford, 1988.
15. P. Tundo, P.T. Anastas, Green Chemistry: Frontiers in Chemical Synthesis and Process, Oxford University Press Oxford, 2000.
16. R. Sanghi, Curr. Sci. 79 (2000) 1662.
17. R. Ryal Dupont, L.Theodore, K. Ganesan, Pollution Prevention, Lewis Publishers, New York, 2000.
18. S.A. Abbasi, D.S. Arya, Environmental Impact Assessment, Discovery Publishing House, New Delhi, 2000.
19. S. Stein, D. Chavew, Environmental Management. 19 (1995) 189.
20. R.A. Sheldon, Chemtech. 39 March 1994.
21. J.H. Clark (editor) Chemistry of Waste Minimization, Blackie, Cambridge, 1995.
22. B.M. Trost, Sci. 254 (1991) 1471.
23. R.A. Sheldon, in Industrial Environmental Chemistry, M.P.C. Weijnen, A.A.H. Drinkenburg (eds) Kluwer Amsterdam, 1993.
24. R.A. Sheldon, in Industrial Environmental Chemistry, D.T. Sawyer, A.E. Martel (eds) Plenum Press, New York, 1992.
25. G.J. Brink, I.E. Arends, R.A. Sheldon, Sci. 287 (2000) 1636.
26. P.A. Grieco, Organic Synthesis in Water, Blackie, London, 1988.
27. P.G. Jessop, W. Leitner (eds), Chemical Synthesis in Supercritical Fluids, Wiley-VCH Weinheim.

28. P. Lozano, T. de Diego, D. Carrie, M. Vaultier, J.L. Iborra, Chem. Commun. 692 (2002) 2002.

★★★★★★★★★★★★★★★★★★

Chapter 5

CUMENE PREPARATION

Friedel-Crafts reactions have long been considered, together with the Grignard reactions as one of the most versatile tool of organic chemistry. One of its serious limitations is the lack of selectivity in addition to the challenges it creates for green chemistry. Introduction of heterogeneous catalysts is proved to be a fruitful area of research in solving these problems. Because of the occurrence of reactions in the interlamellar region, which can be considered a bidimensional reactor, satisfactory reaction rates can be reasonably expected, especially after suitable modulation of the interlayer distance of clays by pillaring. The strong demand in chemical industry for phenolic compounds makes shape selective cumene preparation very important which is efficient over pillared clays and is described in this chapter.

5.0 INTRODUCTION

Cumene, the important petrochemical commodity is still used as the chief starting material for the co-production of phenol and acetone and thus the propylation of benzene to yield cumene is an industrially important reaction. The demand for cumene is expected to grow at a rate of 3.5% a year over the next few years mainly because of the increased demand for the products which are obtained by the processing of phenol with other chemicals to produce various resins, plastics and other value added products such as bisphenol A, hydroquinol, resorcinol, catechol etc[1]. Today, more that 90% of phenol production is met by cumene only. Conversion of cumene to α-methyl styrene adds the value of cumene. Until recently, solid phosphoric acid and Friedel Craft's catalysts like $AlCl_3$ and BF_3 were used for its commercial production. The disadvantages of solid phosphoric acid process lies in its lower activity, catalyst non-regenerability, unloading of spent catalyst from the reactor, relatively high selectivity to hexyl benzenes and significant yields of diisopropyl benzenes and other heavier products[2]. The $AlCl_3$ route requires special materials and coatings to prevent corrosion of equipment, and additional washing step for catalyst removal. Disposal of spent catalyst also creates great environmental hazard. Hence alternative routes employing environmentally benign molecular sieve catalysts are favoured over conventional ones.

Use of propene, as alkylating agent, is associated with coke formation due to its oligomerization, which results in deactivation of catalyst and loss of

propene. Therefore, the use of isopropanol (IPA) as alkylating agent is attracting a lot of attention. The relatively low cost, ease of operation, low coke formation and its extensive use in industry[3,4] makes IPA as the alkylating agent in the present study. IPA is supposedly helpful in reduction of coke formation and is dehydrated into propylene and it is the olefin, which is the alkylating agent.

Almost all zeolites give best conversions at temperatures above 327°C. Such energy intensive operating conditions constitute a major portion of the operating costs and need to be cut down to ensure sustenance of any industrial operation in today's competitive world. Sasidharan et al.[5] evaluated the suitability of NCL-1, a large pore zeolites, to achieve 95% IPAconversion with 70.5% selectivity towards cumene at 230°C at a WHSV of 7 h^{-1}. A 100% conversion of IPA with 82% selectivity at 225°C at 3.5 h^{-1} is reported by utilizing a unique shape and structural selective modified β-zeolites[6]. Other catalysts such as USY[7], H-ZSM-5[7], MCM-41/γ Al_2O_3[8] and silicon substituted aluminophosphate (SAPO)[9] were found to give low conversions. In all these processes, use of high temperature resulted into coke formation and catalyst deactivation.

Thus, there still exists scope to develop better catalysts which would catalyze the isopropylation of benzene to cumene with excellent conversion and selectivity at comparatively low temperatures, a practical value of time – on – stream, ease of preparation, reusability and reactivation of the catalysts.

The isopropylation of benzene with IPA is a multistep and sequential reaction network. The main reaction scheme involved may be represented as in scheme 5.0.1.

The alkylation with IPA is a complex reaction network. The major reaction involves alkylation of benzene with propene formed by dehydration of IPA, to produce cumene. But this reaction is always associated with several side reactions such as transalkylation, disproportionation, dealkylation etc which produces a range of products. The alkylation of benzene to cumene is often accompanied by the formation of n-propylbenzene. Formation of n-propylbenzene in the product stream is detrimental to the cumene synthesis process mainly because of difficulty in separating from cumene by distillation due to their similar physical properties. This is formed either from isomerization of cumene on the catalyst surface or due to the formation of a primary C_3 cation before it alkylate benzene to give cumene. Kaeding and Holland[10] found considerable amount of n-propylbenzene at reaction temperatures above 250°C. According to them, the isomerization of cumene to n-propylbenzene is not a favourable reaction at low temperature due to the wide variation in thermodynamic equilibrium ratios. Other workers also made the same observations and interferences[11].

In the present work, we monitor on a cumene preparation process using PILCs that operates at low temperature with IPA as the alkylating agent.

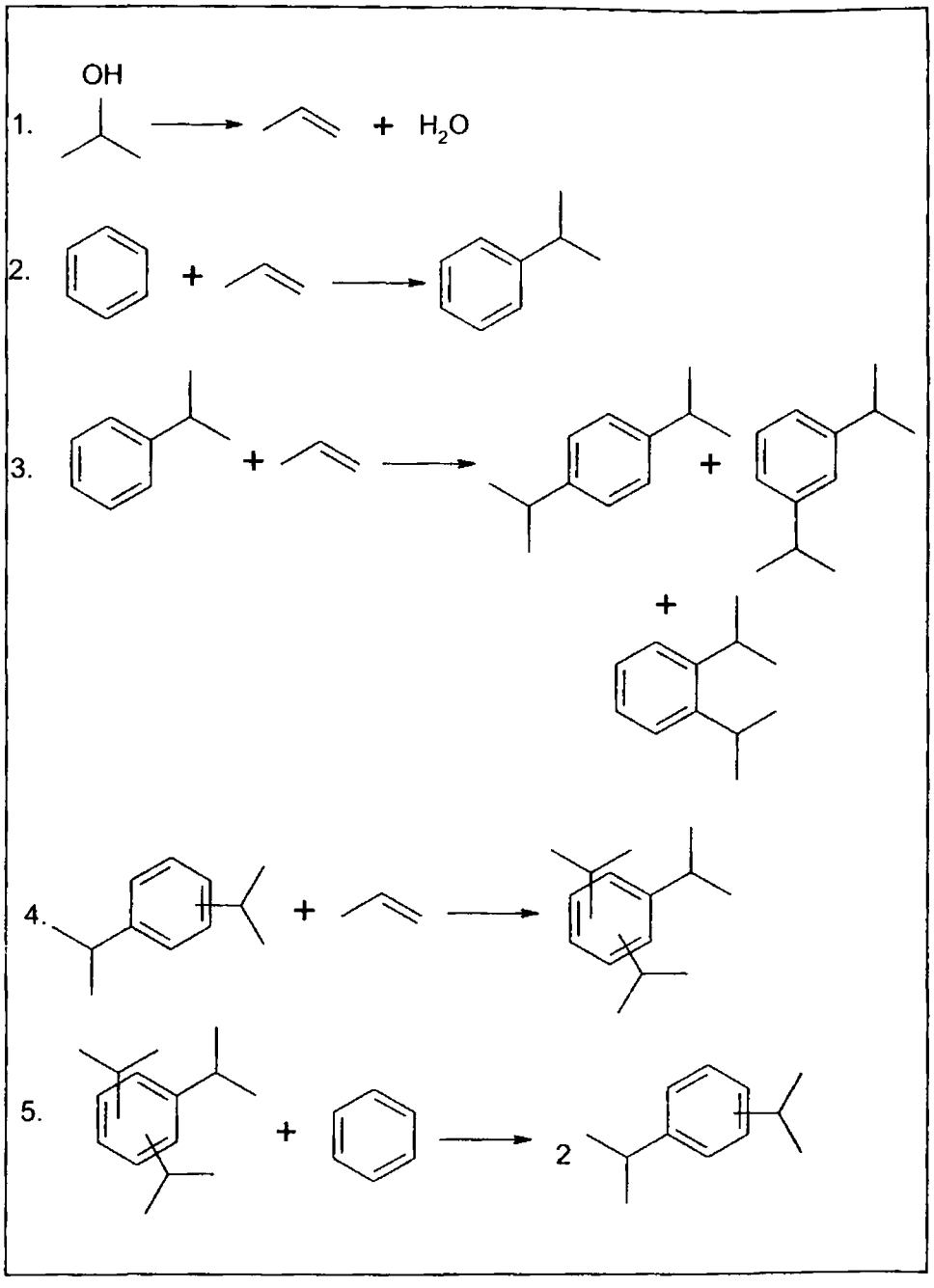
OH
1.
+ H_2O
2.
+
3.
+
+
4.
+
5.
+
2

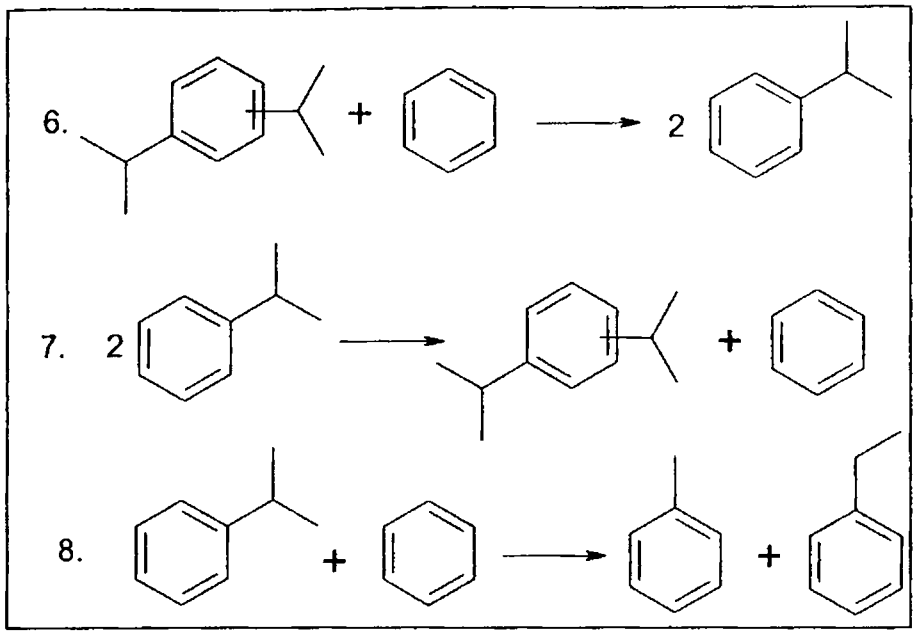

Scheme 5.0.1 Major reactions occurring during benzene isopropylation

5.1 CUMENE FROM BENZENE – INDUSTRIAL PRODUCTION

The manufacture of cumene as a blending agent for high octane gasoline was carried out during the Second World War on very large scale. The alkylation catalysts used was H_2SO_4. The problems related to the use of free mineral acids were later overcome by using supported phosphoric acid on Kieselguhr. This catalyst is still largely used for the production of cumene. However, due to the release of the acid, corrosion problems frequently arise. Besides, because of the decay also due to the formation of organic residues on the catalyst surface, at the end life circle this catalyst cannot be regenerated.

The research efforts for the evolution of the heterogeneous catalytic systems for cumene production took longer time to reach an industrial application. The reason lies in increased cumene isomerization to n-propylbenzene at high temperature of the reaction. Besides, a quite rapid decay was observed to the Mobil-Badger ethylbenzene ZSM-5 due to the higher tendency of propylene to oligomerise.

Based on Zeolites (zeolite Y, mordenite, ZSM-12, zeolite Omega, zeolite Beta and MCM-22) new commercial processes or industrial test runs were announced in the 1990s by Dow-Kellogg, Mobil-Raytheon, CDTech, EniChem and Uop. According to Degnan et al. in 2001, 14 cumene units in the world were already operating with zeolite catalysts[12].

The alkylation of benzene with IPAhas been extensively studied: in one of the most studies it has been shown that a catalyst based on zeolite Beta is highly adequate for the reaction, producing results comparable to those performed in an industrial plant using propylene[13].

5.2 EFFECT OF REACTION VARIABLES

The reaction is done over a wide temperature range, molar ratio and WHSV at a time on stream (TOS) of 2 h in order to study the effect of various parameters on the conversion and selectivity to know the condition for getting maximum catalytic properties. ZM is the selected catalyst to check effect of reaction parameters.

5.2.1 Effect of temperature on conversion and selectivity

Temperature has a paramount influence in the conversion as well as product distribution for isopropylation of benzene. The results in figure 5.2.1 show that selectivity varies markedly with temperature. At a temperature of 100°C, no conversion occurs at all. Maximum cumene selectivity with good conversion is obtained at a temperature of 150°C, but both di- and tri-substitution also occurs. Conversion is maximum at 250°C at the expense of selectivity.

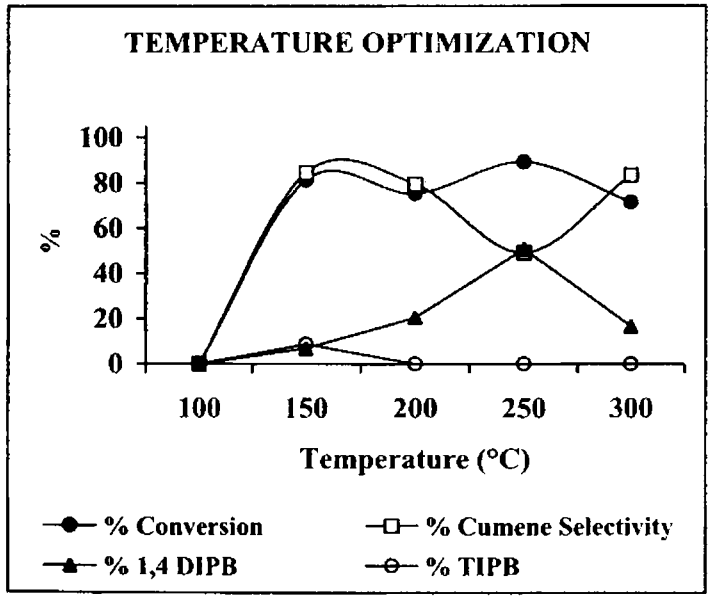

Figure 5.2.1 Effect of temperature on conversion and selectivity at a WHSV of 6.9 h^{-1}, benzene/IPA molar ratio 7:1, Time on stream 2 h and Catalyst weight 0.5g

Thus a temperature of 150°C is selected as the optimum one as clear from the figure 5.2.1. Further increase in temperature results in cumene and di-substituted product. This could be due to the trans alkylation of 1,3,5-triisopropylbenzene (TIPB) to form cumene as well as diisopropylbenzene (DIPB)[5].

Das et al.[14] reported the formation of TIPB at temperatures below 165°C. The selectivity of cumene + DIPB is 100% at and above 200°C in the present study. Among the di- substituted products we are getting only 1,4 DIPB. This may be due to the restricted porosity developed as a result of pillaring which leads to the less sterically hindered product. With temperature, the selectivity towards DIPB increases, reaches a maximum and then decreases. This is probably due to the fact that initially at lower temperatures, the alkylation of cumene competes favorably with the trans alkylation of DIPB with benzene to cumene. However, at higher temperatures the trans alkylation of DIPB with benzene predominates over the alkylation of cumene.

5.2.2 Influence of Benzene/IPAmolar ratio

Benzene to IPA molar ratio in the feed plays important role in the conversion as well as selectivity. During the reaction number of moles of IPA/h/g of catalyst was kept constant. The amount of benzene is changed. Both conversion as well as selectivity increases with increase in the benzene: IPA molar ratio. At low molar ratio of 4, DIPB and TIPB selectivity is higher due to the increased alkylation of cumene to DIPB and DIPB to TIPB. With

increase in the ratio the selectivity of higher alkylated product decreased. The decrease in selectivity of di- and tri- isopropyl benzenes is due to the fact that trans-alkylation of these products is more favored with increased benzene: IPA molar ratio. At and above a molar ratio of 10, present systems give cumene as the only product as seen from figure 5.2.2.

The isopropylation proceeds after the dehydration of IPA to propene. In an earlier work Siffert et al.[15] reported that propene is more strongly adsorbed than benzene on β-zeolite surface. Therefore increase in benzene: propene (in the present case produced form dehydration of IPA) ratio increases the possibility of interaction of benzene with catalyst surface resulting higher selectivity of alkylated product compared to cracking/disproportionation etc. which is thus absent over the present catalyst systems. Present study assumes to have a similar process. The higher benzene: IPA molar ratio favours trans-alkylation of benzene with DIPB and TIPB to produce cumene. At a high molar ratio of benzene the chance for higher substitution is also minimized, increasing the cumene selectivity.

The conversion is found to increase with molar ratio. At a ratio of 10 and 14, conversion remains almost constant and at a molar ratio of 20 all systems shows 100% conversion as well as selectivity. Thus to get a comparative evaluation on the efficiency of different clay systems for acid catalyzed alkylation reactions a molar ratio of 10 is selected.

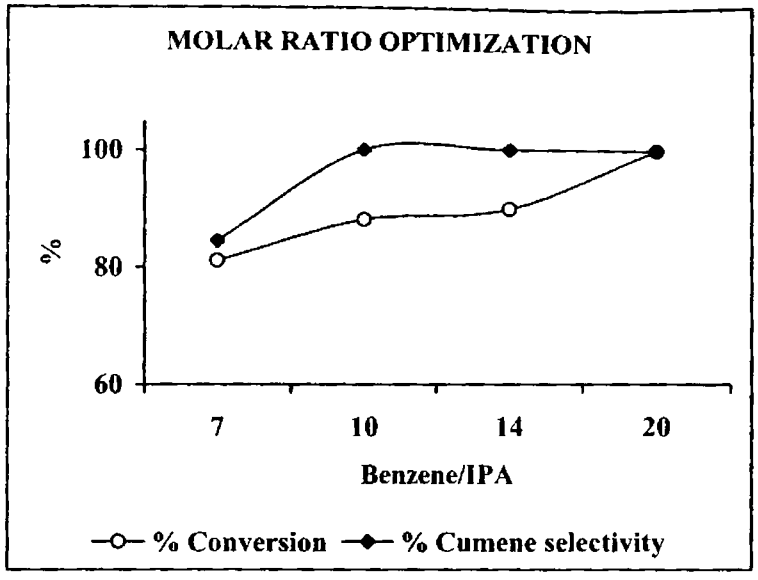

Figure 5.2.2 Optimization of molar ratio at a temperature of 150°C, WHSV of 6.9 h^{-1}, Time on stream 2 h, and Catalyst weight 0.5 g

5.2.3 Influence of WHSV

The effect of WHSV on the product distribution is presented in table 5.1.1. Cumene selectivity is found to decrease with WHSV but at a higher WHSV of 12.1 h^{-1} we are getting only cumene as the product with very low conversion. This may be due to the very low contact time. At a WHSV of 8.7 h^{-1} we are getting cumene and DIPB as products. Further increase in WHSV results in decreased cumene selectivity. WHSV of 10.4 h^{-1} gives TIPB as one product. Increase in WHSV to 12.1 h^{-1} as already mentioned drops down the

conversion below 50% but gives 100% cumene selectivity. At a WHSV of 10.4 h^{-1}, DIPB further alkylates to form TIPB.

Table 5.2.1 Catalytic activity and selectivity at various WHSV

WHSV (h^{-1})	Conversion (Wt %)	Selectivity (%)		
		Cumene	DIPB	TIPB
6.9	75.3	79.5	20.5	-
8.7	75.0	62.0	38.0	-
10.4	78.2	21.3	45.8	32.9
12.1	44.6	100.0	-	-

Benzene/IPA molar ratio 7:1, Time on stream 2 h, Temperature 200°C and Catalyst weight 0.5 g

With higher contact times, i.e. at low WHSV, the DIPBs, which are the primary alkylated products with cumene, got trans-alkylated leading to higher cumene selectivity. Decreased contact time (of 8.7 & 10.4 h^{-1}) diminishes the possibility of trans alkylation of di- and tri- substituted products that resulted decrease in cumene selectivity.

5.3 MECHANISM OF THE REACTION

The reaction of propene with benzene takes place over Brønsted acid sites[16]. First step is the dehydration of 2-propanol to propene. Proton abstraction from Brønsted acid sites results in the formation of carbocation,

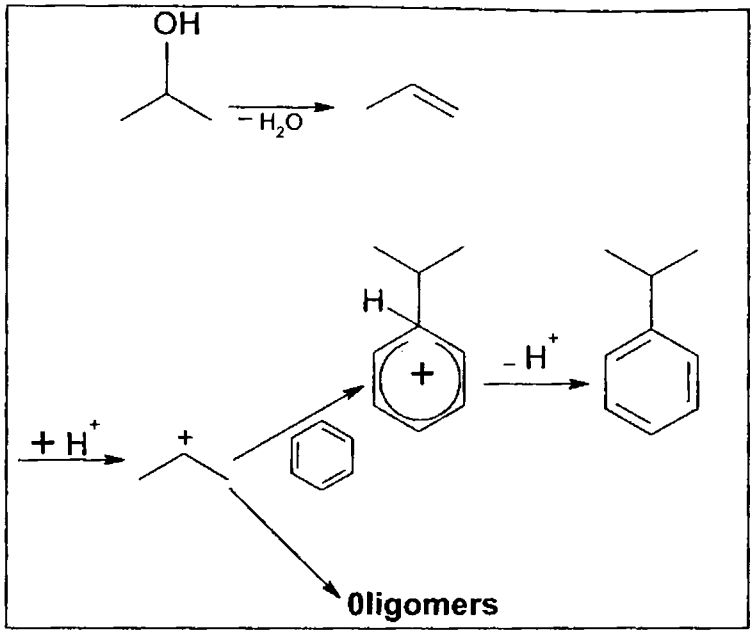

Scheme 5.3.1 A plausible mechanism for benzene isopropylation over Brønsted acid sites

which alkylates benzene to form the isopropyl benzene after removal of H^+ back to the catalyst. The mechanism is shown in scheme 5.3.1. According to classical concepts[17], applied later to zeolites[18], alkylation occurs via olefin protonation, formation of carbonium ion intermediate and subsequent electrophilic attack on the aromatic π-system to form a benzenium cation which can re-aromatize by proton loss. The formation of carbonium ion is believed to be the rate limiting step. A concerted mechanism including subsequent formation and decomposition of surface alkoxy groups is also proposed[19,20]. Since the transition state in this mechanism has a cationic character it obeys all rules of carbonium ion formalism.

5.4 COMPARISON OF DIFFERENT SYSTEMS

The conversion over parent montmorillonite is very low with poor cumene selectivity. n-propylbenzene (20%) and DIPB are the other products. Dealkylation to toluene and ethylbenzene, and TIPB formation is found to be absent in the parent system. Na^+-exchange increases the conversion and selectivity. Pillaring improves both conversions as well as selectivity to a great extent. The enhanced porosity that allows shape selective catalysis within the pores may be the reason for increased selectivity whereas the increased activity may be attributed to the introduction as well as exposure of more acids sites upon pillaring. Among the different pillared systems, AZM gives maximum conversion. Titania containing system, TZM shows side chain cracking. Toluene and ethylbenzene is formed. TM and TAM give cumene, DIPB and TIPB, where TCM gives cumene as the only product. From elemental analysis data (chapter 3, table 3.2.1) it is clear that cumene selectivity increases with decrease in titanium content and is seen from the activity data shown in table 5.4.1. Thus Ti may be the active site for side chain cracking. Alumina containing systems show good conversion, except TAM other Al containing systems shows 100% cumene selectivity. The conversion is found to be comparatively low in chromia pillared systems which may be due to their low acidity values.

It was found[21] that very strong acid sites catalyze the isomerization of isopropylbenzene to n-propylbenzene, particularly at relatively higher temperatures. Relatively low strong acid sites concentration and the low

temperature operation avoid the formation of n-propylbenzene over present clay systems.

Table 5.4.1 Activities of the catalysts for benzene isopropylation at 150°C

Catalyst	isopropanol Conversion (wt %)	Selectivity (%)		
		Cumene	DIPB/TIPB	Toluene/ Ethylbenzene
M	39.3	10.0	70.0	-
NM	68.3	100.0	-	-
TM	90.0	31.6	68.4	-
ZM	94.3	100.0	-	
AM	90.3	100.0	-	
CM	70.0	100.0	-	-
TZM	97.0	79.7	-	20.3
TAM	91.1	71.2	28.8	-
TCM	89.1	100	-	-
AZM	100.0	100.0	-	-
ACM	88.1	100.0	-	-
ZCM	70.7	57.7	42.3	-

Benzene/IPA molar ratio 10:1, Time on stream 2 h, WHSV 6.9 h-1 and Catalyst weight 0.5 g

5.5 ACTIVITY – ACIDITY RELATIONSHIPS

From the mechanism suggested, it is evident that benzene isopropylation occurs over Brønsted acid sites and we attempted to correlate

the catalytic activity with the Brønsted site distribution calculated from cumene cracking studies. Figure 5.5.1 shows a perfect correlation of IPA conversion over the Brønsted acid sites.

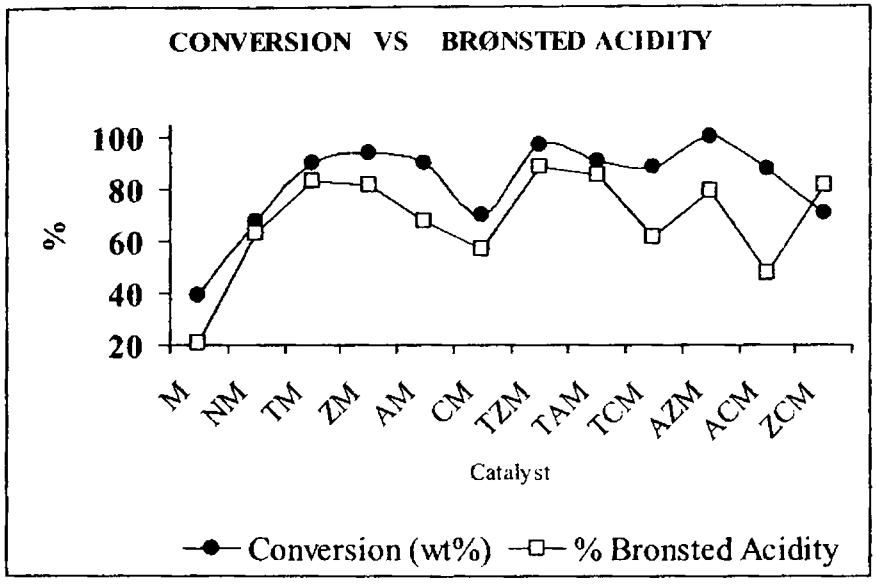

Figure 5.5.1 Dependence of activity over Brønsted acid site distribution

An attempt to correlate the activity in the benzene isopropylation with the acid properties of various clay catalysts is made by plotting the IPAconversion versus the amount of Brønsted acid sites obtained from TPD of NH_3 (weak + medium strength acid sites). Figure 5.5.2 shows a good correlation between conversion with acid sites responsible for alkylation.

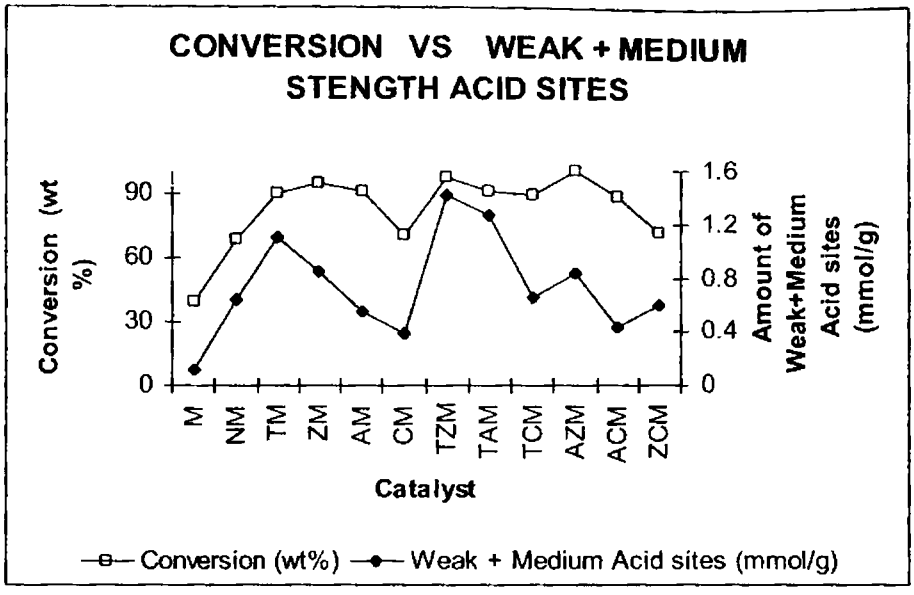

Figure 5.5.2 Dependence of activity versus amount of weak + medium acid sites obtained from TPD of NH_3

5.6 DEACTIVATION OF CATALYSTS

One of the main advantages of heterogeneous catalysts over homogeneous ones lies in its reusability. Unlike liquid phase reactions, reactions carried out in gas phase offers the introduction of more and more fresh reagents into the catalyst system without any work up. Thus the effect of time on steam on conversion says the ability of a heterogeneous catalyst. A catalyst's efficiency is found to be high when deactivation on continuous run is low. Figure shows the deactivation of some selected catalysts in benzene isopropylation in a continuous run of 8 h. There is a decrease in conversion due

to blocking of active sites by coke where selectivity remains constant. M gets completely deactivated after 4th hour, where NM retains 30% of the initial activity after 8 h of continuous run. Single pillared systems, AM and CM loses only 20% of initial activity where mixed pillared AZM and ACM retain 95% of its activity even after 8 h. The results above indicate the efficiency of pillaring on clays and say mixed pillaring as more efficient one in catalysis. Deactivation pattern of different systems are shown in figure 5.6.1. The increased activity and decreased deactivation of single as well as mixed pillared clays (PILCs) are clearly understood form the deactivation pattern.

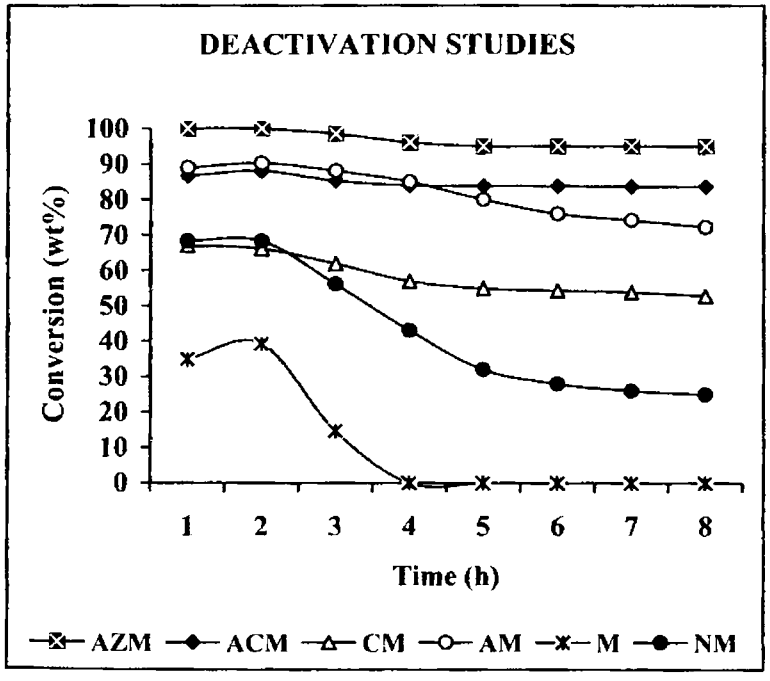

Figure 5.6.1 Deactivation of the given systems in the optimized conditions in continuous run

5.7 CATALYST REGENERATION

The regenerability of the catalyst within the reactor system is another attraction of gas phase heterogeneous catalysis. Regeneration of the deactivated catalysts is done by burning off the coked formed by heating in air at 500°C for 10 h. The initial activity is regained in all pillared systems whereas M becomes catalytically inactive towards benzene isopropylation, which may be due to the structural collapse occurring at continuous high temperature treatment. NM also is non-regenerable, where it becomes catalytically inactive from the 5^{th} hour of continuous run in the second cycle. The regenerated pillared systems shows same trend towards deactivation on continuous run and is found to be regenerable up to four repeated cycles.

5.8 CONCLUSIONS

From the above discussions we reach in the following promising conclusions.

- Present PILCs are found to be efficient catalysts for benzene isopropylation reactions.

- Replacement of environmentally hazardous homogeneous acids and introduction of green chemistry becomes possible.

- Here we offer a low temperature method for selective cumene formation when compared to the existing zeolite, mesoporous or mixed oxide catalytic methods.

- The critical role of reaction parameters such as temperature, space velocity and molar ratio is well established.

- The participation of Brønsted sites of catalysts in reaction is proved from the perfect correlation of activity with Brønsted acid site distribution.

- Deactivation is found to be very low over PILCs, especially over mixed pillared montmorillonite when compared to parent or ion-exchanged montmorillonite.

- The regenerability and high thermal stability offered to montmorillonite clays upon pillaring is evident from the preceding discussions.

REFERENCES:

1. T.C. Tsa, S.B. Liu, I. Wang, Appl. Catal. A: Gen. 181 (1999) 355.
2. U. Sridevi, N.C. Pradhan, B.K.B. Rao, C.V. Satyanarayana, B.S. Rao, Catal. lett. 79 (2002) 1.
3. J. Panming, W. Qiuying, Z. Chao, X. Yanhe, Appl. Catal. A: Gen. 91

(1992) 125.

4. 10. K.S.N. Reddy, B.S. Rao, V.P. Shiralkar, Appl. Catal. A: Gen. 95 (1993) 53.
5. M. Sasidharan, K.R. Reddy, R. Kumar, J. Catal. 154 (1995) 216.
6. B. Halgery, J. Das, Appl. Catal. A. 181 (1999) 347.
7. G. Bellussi, G. Pazzuconi, C. Perego, G. Girotti, G. Terzoni, J. Catal. 157 (1995) 227.
8. J.M. Valtierraa, O. Zaldivara, J.A. Montoyab, J. Navarreteb, J.A. De Los Reyesc, M.A. Sancheza, Appl. Catal. A. 166 (1998) 387.
9. U. Sridevi, V.V. Bokadea, C.V.V. Sathyanarayana, B.S. Rao, C. Pradhan, B.K.B. Rao, J. Mol. Catal. A. 181 (2002) 257.
10. W.W. Kaeding, R.E. Holland, J. Catal. 109 (1988) 212.
11. J. Panming, W. Qiuying, Z. Chao, X. Yanhe, Appl. Catal. A: Gen. 91 (1992) 125.
12. T.F. Degnan, C.M. Smith, C.R. Venkat, Appl. Catal. A: Gen. 221 (2001) 283.
13. G. Girotti, F. Rivetti, S. Ramello, L. Carnelli, J. Mol. Catal. A: Chem. 204-205 (2003) 571.
14. D. Das, H.K. Mishra, A.K. Dalai, K.M. Parida, Catal. Lett. 93 (2004) 185.
15. S. Siffert, L. Gaillard, B.L. Su, J. Mol, Catal. 183 (2000) 267.
16. A. Corma, V.M. Soria, E. Schnoeveld, J. Catal. 192 (2000) 163.
17. G.A. Olah (ed), Friedel-Crafts and Related reactions, Vol. 2, Wiley, New York, 1964.
18. P.B. Venuto, P.S. Landis, Adv. Catal. 18 (1968) 259.

19. J.F. Haw, B.R. Richardson, I.S. Oshiro, N.D. Lazo, J.A. Speed, J. Am. Chem. Soc. 111 (1989) 2052.

20. V.B. Kazansky, Sov. Chem. Rev. 1 (1988) 1109.

★★★★★★★★★★★★★★★★

Chapter 6

SHAPE SELECTIVE P-CYMENE PREPARATION OVER PILLARED CLAYS

The development of new green catalysts is a challenging area in organic synthesis. A number of such catalysts have been reported, which exhibits much higher catalytic efficiency and more eco-friendliness. Among the green catalysts, clays possess its own place in organic synthesis due to its tunable acidity and high level tolerance towards experimental conditions & functional groups upon modifications. This chapter deals with toluene isopropylation for selective p-cymene synthesis due to its crucial role as an intermediate in pharmaceutical industries in addition to many industrial applications. Higher substitution, the major problem associated with all types of catalysts is minimized to large extent in the present study.

6.0 INTRODUCTION

Catalyst reforming process produces toluene as a major product and is much abundant and of low cost, thus the conversion of toluene to valuable products is of current interest[1]. Isopropylation of toluene produces p-cymene, which is an important intermediate used in pharmaceutical industries and for the production of fungicides, pesticides, as flavoring agent and as a heat transfer medium[2]. In many petrochemical plants, p-cymene is produced by alkylation of toluene with propene or 2-propanol over the Friedel – Craft's catalysts such as HCl containing $AlCl_3$, BF_3 or H_2SO_4. However the use of these homogeneous acids gives rise to many problems regarding handling, safety, corrosion and treatment of the disposed catalyst. In addition, because the reagents are mixed with acids, separation of the products from the catalyst is often a difficult and energy consuming process. Solid acid catalysts solve this problem and are considered to be candidates for the alkylation catalysts[3-5]. The common heterogeneous catalysts used for p-cymene preparation are zeolites, mesoporous molecular sieves and mixed metal oxides.

Shape selective conversions of benzene and toluene by alkylation over zeolites catalysts have been extensively studied[6,7]. Medium pore zeolites (pore diameter 3.5 – 5.6 Å) such as ZSM-5 and ZSM-35 have already been studied in a number of these processes due to the advantage that they present[8,9]. Nevertheless there are a few studies concerning the selective conversions on mesoporous materials and pillared clays (PILCs). Catalytic alkylation of toluene is also used as a good probe reaction for selectivity studies[10]. This

reaction is taken as a model with the aim to identify potential solid acid catalysts for alkylation reactions of industrial interest.

Possible alkylation products from toluene and isopropanol are mainly isopropyltoluenes (para, meta and ortho) and diisopropyltoluenes (DIPT). Regarding para isopropyltoluene (p-IPT) it has a smaller kinetic diameter. Thus this isomer is expected to be selectively formed into the channels of some shape selective zeolites such as ZSM-5[10].p-IPT is formed as the primary product of isopropylation which do not easily isomerizes to the m-IPT.

Some researchers reported that in the gas phase alkylation of toluene with 2-propanol using different large pore zeolites such as mordenite and Y (T = 250°C), para selectivity (46.0 %) is higher in mordenite than in Y (37.6 %) zeolite. An increased selectivity of cymene in the gas phase alkylation of toluene with 2-propanol was reported using different large zeolites at a lower temperature (180°C)[11].

Perego et al.[12] and Cejka et al.[13] have used rich Al contents of MCM-41, and obtained 85 % and 90 – 97 % selectivity of cymenes prepared using propene and toluene in the low temperature range of 180°C - 250°C under liquid reaction conditions. However, the percentage of p-cymene in the cymene mixture was only 37 - 47 %[13] and 38%[12]. Selvaraj et al.[14,15] have used low Al content and a combination of low Al and Zn using 2-propanol and toluene in the temperature range of 225 - 275°C under vapour - phase reaction conditions over mesoporous materials.

Owing to its low cost and extensive use in industry present study had chosen 2-propanol as the alkylating agent instead of propene. The reaction is shown in scheme 6.0.1

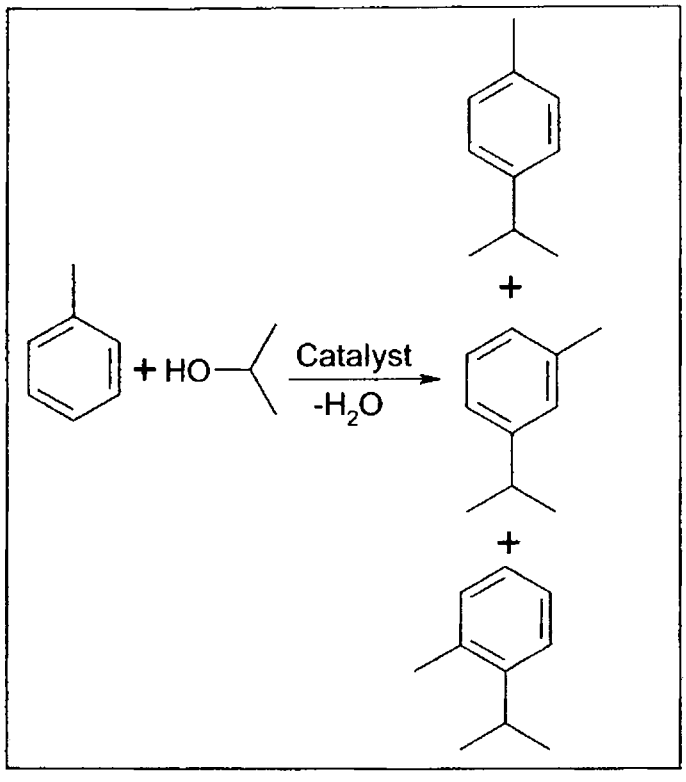

Scheme 6.0.1 Toluene isopropylation reaction over acid catalysts giving ortho, para and meta- substituted products

6.1 EFFECT OF REACTION VARIABLES

The effect of reaction parameters such as temperature, WHSV and toluene/2-propanol molar ratio on the conversion and p-cymene selectivity is

investigated. The variation of catalytic activity with reaction parameters is studied using CM as the reference catalyst.

6.1.1 Variation with reaction temperature

Figure 6.1.1 clearly shows the variation of conversion and p-cymene selectivity with temperature. Maximum conversion and selectivity is obtained at 200°C.

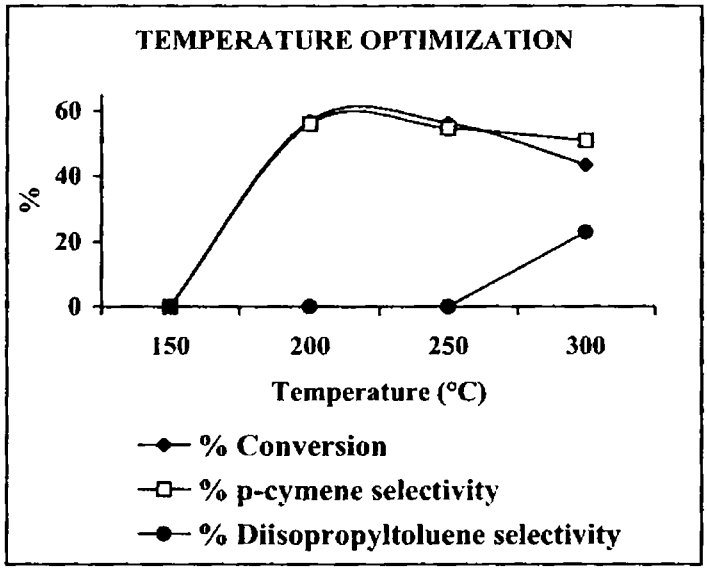

Figure 6.1.1 Variation of temperature at Toluene/isopropanol molar ratio 3:1, Time on stream 2 h, WHSV 6.8 h^{-1} and Catalyst weight 0.5 g

At higher reaction temperature, both the conversion and selectivity are found to decrease. This may be due to de-isopropylation and formation of

propene by dehydration over Brønsted acid sites[14]. At a low temperature of 150°C no conversion occurs at all. Only at a temperature of 300°C diisopropyltoluene formation occurs. Side reactions such as toluene disproportionation and cracking are found to be absent over the present catalyst at all temperature used.

6.1.2 Variation with WHSV

Isopropylation of toluene is carried out at WHSV of 6.8 h^{-1} – 11.9 h^{-1} and a temperature of 200°C. The results of the variation of percentage conversion of isopropanol and p-cymene selectivity with different WHSV values are shown in figure. The best WHSV value for this reaction is 6.8 h^{-1}.

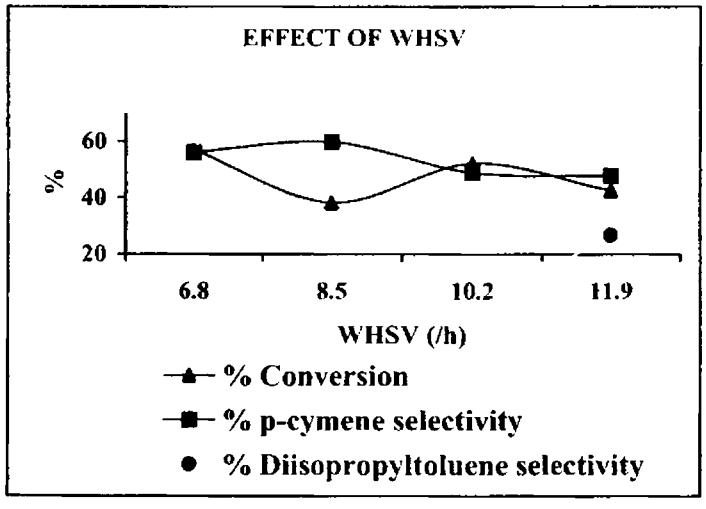

Figure 6.1.2 Optimization of WHSV at a temperature of 200°C, Toluene/isopropanol molar ratio 3:1, Time on stream 2 h and Catalyst weight 0.5 g

As the WHSV value is further increased, the percentage conversion decreases and at a WHSV of 11.9 h^{-1} disubstituted product formation occurs. The low conversion with increase in WHSV may be due to the deactivation of catalyst by coke formation[16]. It may be assumed that at higher WHSV, because of the less effective diffusion of the toluene molecule into the interior surface of the catalyst, reaction occurs outside the pores, thus no shape selective catalysis occurs which leads to disubstituted product.

6.1.3 Variation with toluene/2-propanol molar ratio

Isopropylation of toluene is carried out over various toluene/2-propanol molar ratios, where we get cymenes as the major products.

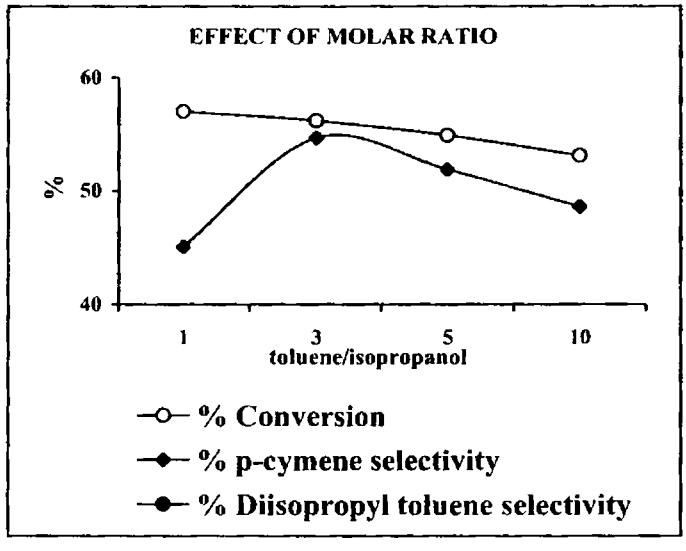

Figure 6.1.3 Optimization of molar ratio at a temperature of 250°C, WHSV 6.8 h^{-1}, Time on stream 2 h and Catalyst weight 0.5 g

At a molar ratio of 1:1, we are getting diisopropyl toluene as one of the products. Increase in molar ratio results formation of ortho and para cymenes as the only products. Maximum p-cymene selectivity is obtained at a toluene/2-propanol ratio of 3 as seen in figure 6.1.3. Eventhough we are getting maximum conversion at a molar ratio of 1, the p-cymene selectivity is found to be very poor. Increase in molar ratio from 3 decreases both conversion as well as selectivity and at a molar ratio of 10, we are getting ortho cymene as the major one. The decreasing conversion may be attributed to increase in coke formation. Hence the optimal molar ratio of toluene: isopropanol is 3:1 at a reaction temperature of 250°C.

6.2 MECHANISM OF THE REACTION

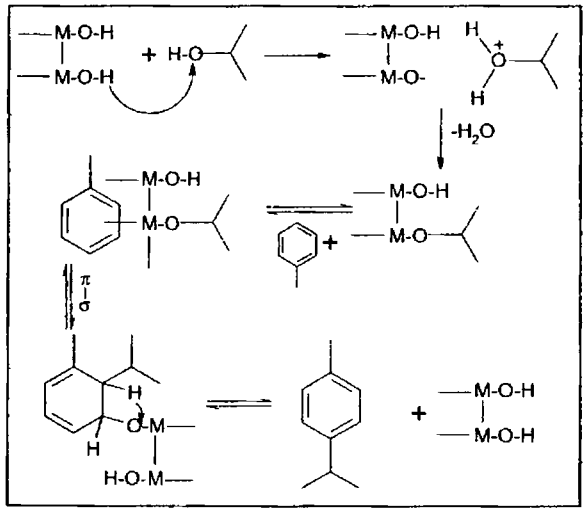

Scheme 6.2.1 Electrophilic aromatic substitution of 2-propanol on toluene in the presence of a solid acid catalyst

The isopropylation of toluene with 2-propanol is an electrophilic substitution reaction on the aromatic ring. Isopropylation reactions catalyzed by acids or solid acids are generally considered to proceed via carbonium ion mechanism as shown in scheme 6.2.1.

6.3 COMPARISON OF DIFFERENT SYSTEMS

In the optimized reaction conditions the catalytic activities of various systems are tested which gives an idea about the performance of different clay systems in catalytic shape selective alkylation reactions. All PILCs except AM gives conversion above 50%. Sabu et al.[17] suggested that the isopropylation of toluene (aromatic alkylation) requires sites of high acid strength where as the dehydration of 2-propanol takes place even on weak acid sites.

Table 6.3.1 Activities of the catalysts for toluene isopropylation at 200°C

Catalyst	isopropanol Conversion (wt %)	Selectivity (%)		
		p-Cymene	0-Cymene	Di/Tri Substitution
M	36.5	33.6	7.9	53.7
NM	46.2	14.0	11.6	74.3
TM	66.6	57.9	42.1	-
ZM	55.1	58.9	41.1	-
AM	48.1	59.1	40.9	-
CM	56.9	56.0	44.0	-

TZM	78.5	47.0	27.7	25.3
TAM	53.0	58.8	41.2	-
TCM	62.0	57.1	29.9	13.0
AZM	58.9	61.7	38.3	-
ACM	67.5	63.5	36.5	-
ZCM	68.1	33.8	32.5	33.7

Toluene/isopropanol molar ratio 3:1, Time on stream 2 h, WHSV 6.8 h^{-1} and Catalyst weight 0.5 g

Both M and NM shows higher substitution and low conversion. Conversion of parent montmorillonite increases on Na^{+} ion exchange at the expense of cymene selectivity which gives diisopropyltoluene as the major products. M results in ortho, para and meta (4.8%) cymenes as the products. m-cymene formation is found to be absent over all other catalyst systems. Also disproportionation as well as cracking is found to be absent over the present clay catalyst systems. Pillaring allows shape selective catalysis within the pores to get p-cymene as the major product. Higher substitution occurs only over TZM, TCM and ZCM. In the present conditions all other PILCs shows 100% cymene selectivity. Table 6.3.1 shows the catalytic activity as well as selectivity of each system. Manivarnan et al[18] reported formation of isobutyl benzene as major product in their study and is found to be absent over the present catalyst systems.

6.4 ACTIVITY – ACIDITY RELATIONSHIPS

We attempted to correlate the conversion with total acidity obtained from ammonia TPD measurements and got a very good correlation between activity and acidity showing the occurrence of toluene isopropylation of toluene over acidic sites supporting the suggested mechanism. Figure 6.4.1 shows the correlation of isopropanol conversion with the total amount of acid sites in mmol/g obtained from TPD of ammonia.

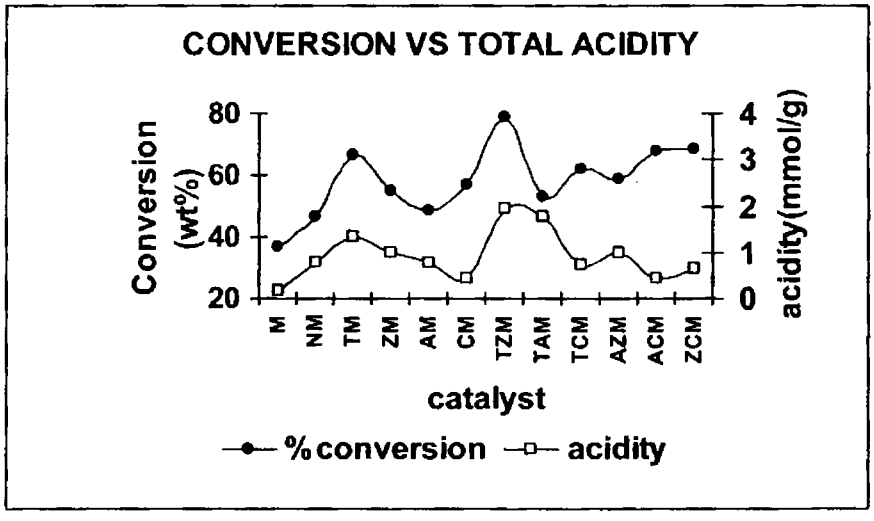

Figure 6.4.1 Correlation diagram of conversion with total acidity

We also tried to correlate conversion with strong acid sites as Sabu et al.[17] suggested that the isopropylation of toluene (aromatic alkylation) requires sites of high acid strength (Figure 6.4.2).

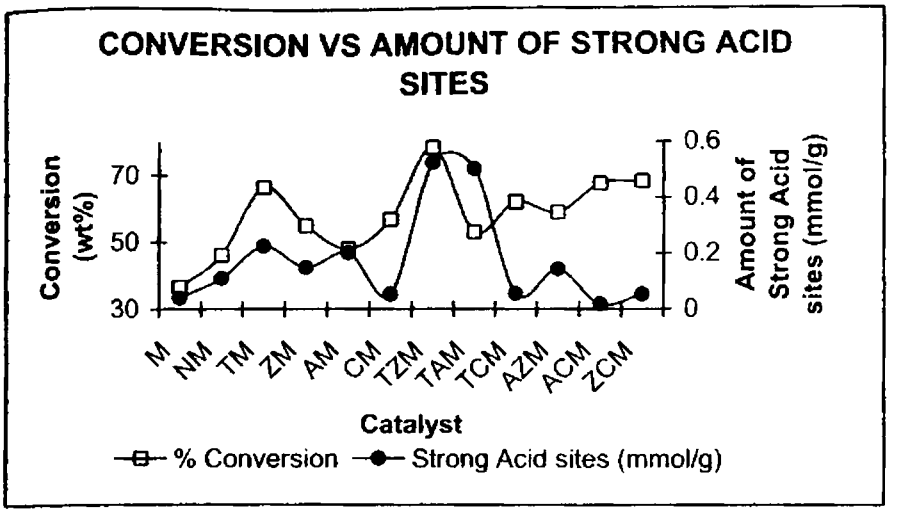

Figure 6.4.2 Correlation diagram of conversion with amount of strong acid sites

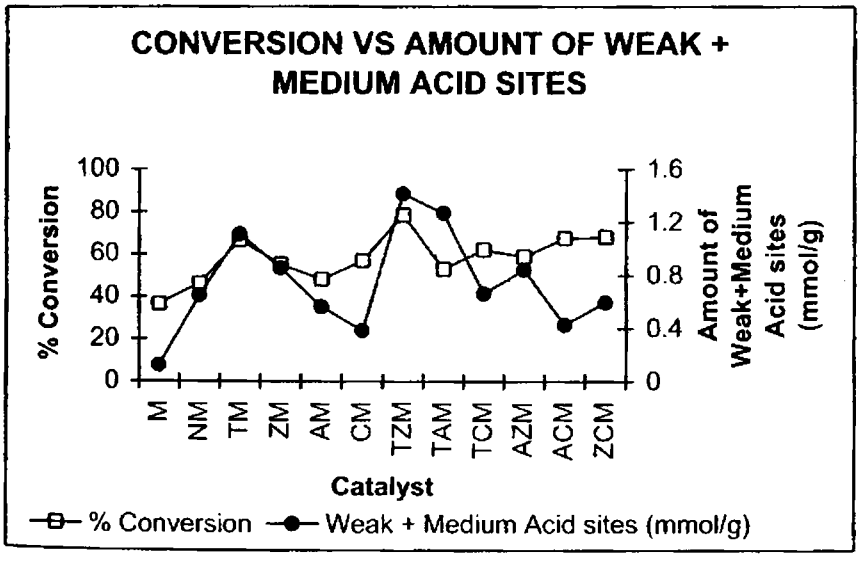

Figure 6.4.3 Correlation diagram of conversion with amount of weak + medium acid sites

The correlation diagram in figure 6.4.3 suggests that weak + medium acidic sites may also contribute to the reaction. Here also we are getting good correlation.

6.5 DEACTIVATION STUDIES

The activity of the catalyst systems are tested at various time intervals at 8 hours of continuous run in order to check whether the catalysts get deactivated or not. Due to the high amount of coke formed and structural instability, both M and NM becomes completely deactivated from 5^{th} h onwards.

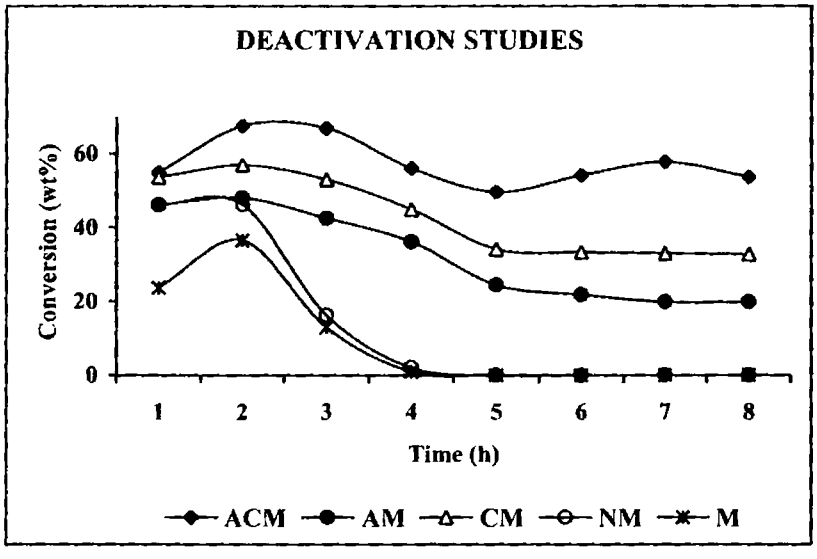

Figure 6.5.1 Deactivation of the given systems in the optimized conditions in continuous run

The pillared systems selected for deactivation studies retain the activity even after 8 h as seen from fig. 6.5.1. The selectivity remains constant in all the cases. There is initial sharp decrease in activity up to 5th h and then conversion remains almost constant. This implies that the coke formed during the reaction is not sufficient to block all the catalytically active sites. The retention of initial activity is greater in mixed pillared system when compared to single pillared systems which supports that mixed pillaring is most efficient when compared to single pillaring. The retained activity is 41.3%, 57.4% and 79.4% for AM, CM and ACM respectively.

6.6 REGENERABILITY OF THE CATALYSTS

The Regenerability of the deactivated catalysts are done by burning off the coke formed by heating in air at 500°C for 10 h and is again used for continuous run. Both M and NM are found to be non-regenerable even after the complete coke removal at 500°C which may be due to the low thermal stability that leads to structural collapse during prolonged high temperature treatment. A similar pattern as in the 1st cycle is obtained for PILCs in continuous run of 8 hours. It has been found that even after 4 regeneration cycles the activity, i.e. both conversion as well as selectivity remains same as in the initial cycle, showing the efficiency of pillaring in the retention of layer structure at a high temperature of 500°C.

6.7 CONCLUSIONS

From the preceding discussions we arrive at the following conclusions.

- PILCs are found to be good catalysts for p-cymene preparation where higher substitution is found to be minimal or even absent.

- The reaction parameters that influence both conversion and selectivity can be optimized in such a way to get maximum catalytic efficiency.
- Running the reaction in gas phase avoids toxic solvents present in liquid phase reactions and permits continuous use.

- Present systems show good conversion and selectivity when compared to the reported catalyst systems.

- The decreased deactivation upon pillaring improves the reusability of montmorillonite in continuous run.

- The regenerability upon pillaring and improvement upon mixed pillaring is proved.

REFERENCES:

1. 1. L.F. Hatch, S. Mater, Hydrocarbon process. 58 (1979) 189.

2. B.S. Flockhart, K.Y. Liew, R.C. Pink, J. Catal. 72 (1981) 314.
3. P. A. Parikh, N, Subrahmanyam, Y.S. Bhat, A.B. Halgeri, Appl. Catal. A. Gen. 90 (1992) 1.
4. K.S. Reddy, B.S. Rao, V.P. Shiralkar, Appl. Catal. A. Gen. 121 (1995) 191.
5. J. Cejka, G.A. Kapustin, B. Wichtetlova, Appl. Catal. A. Gen. 108 (1995) 187.
6. S.G.T. Bhat, J. Catal. 75 (1982) 196.
7. W.W. Kaeding, J. Catal. 120 (1989) 409.
8. S.M. Csicsery, Zeolites. 4 (1984) 202.
9. S.J. Rane, C.V.V. Satyanarayana, D.K. Chakrabarty, Appl. Catal. 69 (1991) 77.
10. J.M. Valtierra, M.A. Sanchez, J.A. Montoya, J. Navarrete, J.A. de los Reyes, Appl. Catal. A. Gen. 158 (1997) L1.
11. K.S. Reddy, B.S. Rao, V.P. Shiralkar, Appl. Catal. A. Gen. 121 (1995) 191.
12. C. Perego, S. Amarilli, A. Carati, C. Flego, G. Pazzuconi, C. Rizzo, G. Bellussi, Microporous Mater. 27 (1999) 345.
13. J. Cejka, G.A. Kapustin, B. Wichtetlova, Appl. Catal. A. Gen. 108 (1995) 187.
14. M. Selvaraj, A. Pandurangan, K.S. Seshadri, P.K. Sinha, V. Krishnasamy, K.B. Lal, J. Mol. Catal. A. Chem. 186 (2002) 173.
15. M. Selvaraj, A. Pandurangan, K.S. Seshadri, P.K. Sinha, K.B. Lal, Appl. Catal. A. Gen. 242 (2003) 347.
16. M. Selvaraj, A. Pandurangan, P.K. Sinha, Ind. Eng. Chem. Res. 43

(2004) 2399.

17. K.R. sabu, K.V.C. Rao, C.G.R. Nair, Bull. Chem. Soc. Jpn 63 (1990) 3632.

18. R. Manivannan, A. Pandurangan, Catal. Lett. 81 (2002) 119.

★★★★★★★★★★★★★★★★★

Chapter 7

ETHYLBENZENE FROM ETHANOL AND BENZENE

The petroleum industry is presently faced with increasingly stringent requirement regarding transportation fuels' specifications, and since the last few years, great effort is being made to decrease the concentration of sulfur and nitrogen compounds in gasoline and diesels. However among the toxic and pollutant compounds of gasoline, benzene is considered as a powerful cancer producing agent and its content in the reformulate gasoline must be reduced. In the gasoline, benzene mainly comes from the catalytic reformate, and therefore, the reduction of benzene production could be obtained by minimizing its formation during the reforming process, or by eliminating the benzene- rich light reformate stream by extraction or conversion. Taking into account economical and practical considerations as hydrogen production, octane number of the resulting gasoline, market of petrochemical products etc., the transformation of this toxic compound by alkylation appears to be the best alternative. This chapter deals with the shape selective conversion of benzene to ethylbenzene using PILCs as the efficient alternative to homogeneous catalysts.

7.0 INTRODUCTION

Ethylbenzene (EB) is an important raw material in the petrochemical industry for the manufacture of styrene, which is one of the most important industrial monomers world wide capacity of EB production is about 23 million metric tons/year[1]. EB is primarily produced by benzene alkylation with ethylene, and in commercial process the reaction has conventionally been catalyzed by mineral acids such as $AlCl_3$ or phosphoric acid[2]. However, handling, safety, corrosion and waste disposal problems commonly associated with the conventional Friedel-Crafts catalysts have prompted the development of new technologies in which solid acids such as zeolite based catalysts are used to catalyze the direct alkylation of benzene with ethylene[3]. In this way, several commercial processes have been developed in the past few years for the production of EB based on zeolite catalysts[4-7]. In the production of EB, the $AlCl_3$-based processes are progressively substituted with zeolite-based processes. The most recently reported process makes use of MCM-22or SSZ 25 as alkylating agents[8-13]. Although EB has been largely studied over zeolites, studies with molecular sieves and pillared clays (PILCs) are scarce. Lenarda et al. reported aluminium and aluminium–gallium pillared bentonites for benzene alkylation with ethylene[14].

Ethylation of benzene is carried out over PILCs (scheme 7.0.1). Considering the availability and easiness for handling instead of ethylene we use ethanol as the alkylating agent. Here the dehydration [ethanol to ethylene] and alkylation steps are combined in to a one stage operation. NCL Pune, India developed a

process called Albene technology that uses ethanol instead of ethylene in one step EB process based on a stabilized Enclilite catalyst[15]. As the ethylation of benzene with ethanol requires prior formation of ethyl cation, the reaction requires the presence of Bronsted acid sites on the catalyst surface (Scheme 7.0.1)[16].

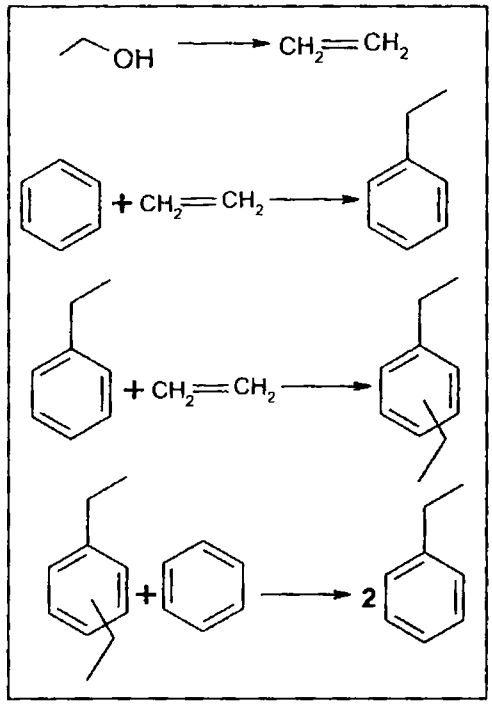

Scheme 7.0.1 Benzene ethylation reaction over acid catalysts

7.1 ETHYLBENZENE PRODUCTION INDUSTRY

From the point of view of production volume, the acid catalyzed alkylations are by far the most important. In 2002 the world overall demand for

benzene was around 33 million tons. Alkylbenzene derivatives account for about 75% of the total benzene production. Transalkylation is often combined with alkylation in order to convert low valued by-products such as polyalkylobenzene in to their monosubstituted homologues, globally improving the efficiency of the process.

In the traditional process, developed since the 1930s, the alkylation is performed by reacting benzene and ethylene in the presence of Friedel-Crafts catalysts ($AlCl_3$-HCl) under mild conditions. The highly toxic and corrosive nature, danger in handling and transport, the separation difficulty and the environmental problems replaces these Friedel-Crafts catalysts by heterogeneous solid acid catalysts.

Starting from the mid-1960s different zeolite-based catalysts were extensively evaluated in the alkylation. In spite of the big effort, it still took 10 years to accomplish the first industrial alkylation process based on a zeolite catalyst, which in fact occurred in 1976. Since 1976, the medium pore zeolite-ZSM-5 has been used in the Mobil-Badger process for the vapour phase alkylation of benzene with ethylene[17-19].

Starting from 1980, the Mobil-Badger process has been extensively applied in the alkylation units. Recently a new process was developed by UOP/ Lmmus/ Monsanto/ Unocal/ Chemical Research-Licensing[20]. The catalyst is based on Y-type zeolite and it operates at much lower temperatures and higher pressure at which the feedstock is in liquid phase. Later improvements were

obtained by introducing the liquid phase alkylation and a separate step of transalkylation. The development of the liquid phase process by UOP/Lummus/Unocal[21], was first commercialized in Japan in 1990, with a catalysts based on zeolite Y. Chevron (USA) and EniChem (Europe)[20] have claimed more recently the use of zeolite MCM-22 and is also introduced as efficient and selective catalyst. Some processes that are used in EB industry are EBMax[sm],EBOne, CDTECH etc[22,23].

Of around 70 EB units operating in the world, 24% are still based on $AlCl_3$-HCl. The rest are based on zeolite catalysts: 40% in the gas phase and 36% in the liquid phase[24].

7.2 EFFECT OF REACTION VARIABLES

The influence of reaction parameters over ethanol conversion and EB selectivity is studied using TM as the reference catalyst to know the optimum conditions of the reaction.

7.2.1 Effect of Temperature

There is a linear response of conversion with increase in temperature, but the conversion remains almost constant at 350°C and 400°C as seen from figure 7.2.1. Reaction at a high temperature of 450°C produces toluene as major product due to cracking over PILC. Kato et al.[25] reported toluene and xylene formation as a result of cracking and isomerization at high temperatures

during alkylation of benzene with ethane over platinum- loaded zeolite catalysts.

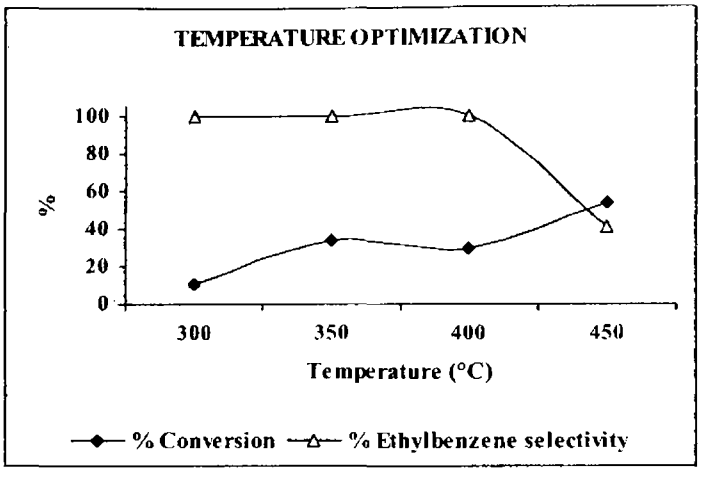

Figure.7.2.1 Effect of temperature on conversion and selectivity at a WHSV of 6.9 h^{-1}, benzene/ethanol molar ratio 4:1, Time on stream 2 h and Catalyst weight 0.5 g

Over the PILC, poly alkylation is not observed which may be due to the rapid diffusion of the products. Thus considering conversion with high EB selectivity we selected a temperature of 350°C as optimum one for further studies.

7.2.2 Effect of WHSV

Figure.7.2.2 illustrates the influence of WHSV on conversion as well as selectivity. The conversion first increases and then decreases with WHSV.

Over the pillared system, at a WHSV 6.9 h^{-1}, in the given temperature and molar ratio, we are getting maximum conversion. Change in WHSV decreases conversion and thus we selected 6.9 h^{-1} as the suitable WHSV for the further studies. At all WHSV selected for the present study EB is selectively formed without any higher substitution, cracking etc.

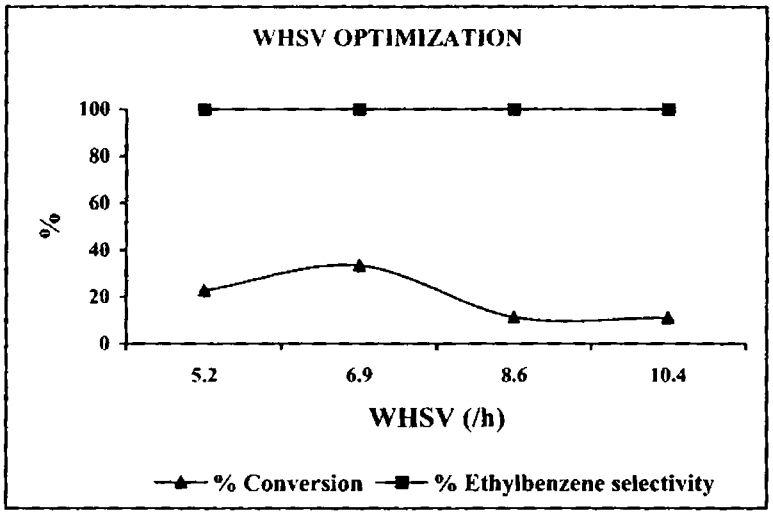

Figure.7.2.2 Effect of WHSV at a temperature of 350°C, benzene/ethanol molar ratio 4:1, Time on stream 2 h, and Catalyst weight 0.5 g

7.2.3 Effect of molar ratio

The influence of molar ratio on conversion is studied at 350°C. From figure.7.2.3 it is clear that the selectivity of EB at a molar ratio of 1:1 is very less due to the formation of polyalkylated products. The polyalkylated product formed is PDEB (p-diethylbenzene), there is no formation of MDEB or ODEB

due to steric hindrance. Polyalkylation is due to the increased amount of ethanol and is absent with increase in the amount of benzene (to a molar ratio of 2:1 and higher). We are getting good conversion with 100% EB selectivity at a molar ratio of 4:1.

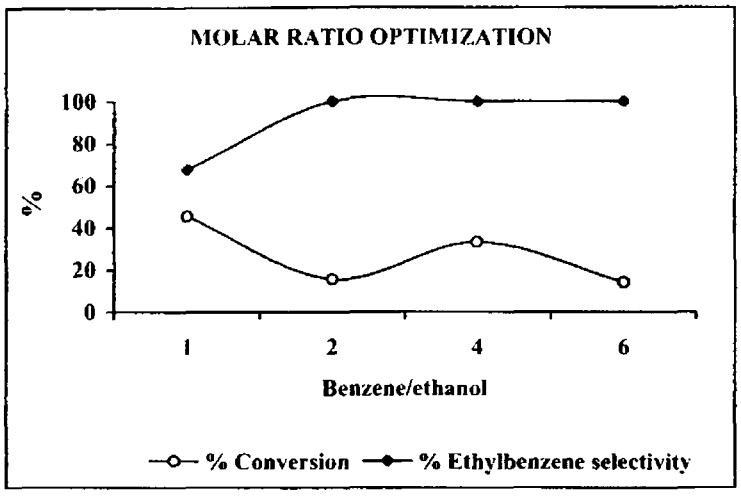

Figure.7.2.3 Effect of molar ratio at a temperature of 350°C, WHSV of 6.9 h^{-1}, Time on stream 2 h and Catalyst weight 0.5 g

7.3 MECHANISM OF THE REACTION

It is well known that the Friedel-Crafts alkylation of benzene with ethylene over acidic zeolites take place via the generally accepted carbonium ion mechanism[14] illustrated in scheme 7.3.1. On the basis of this mechanism, the ethanol is first dehydrated to ethylene; the ethylene molecule is protonated by the Brønsted acid site to a carbonium ion that generates, by electrophilic

attack an aromatic π-electron, a mono- or poly- alkyl benzenium ion. Desorption of the latter and the loss of proton gives the alkylated aromatic and restores the Brønsted acid site.

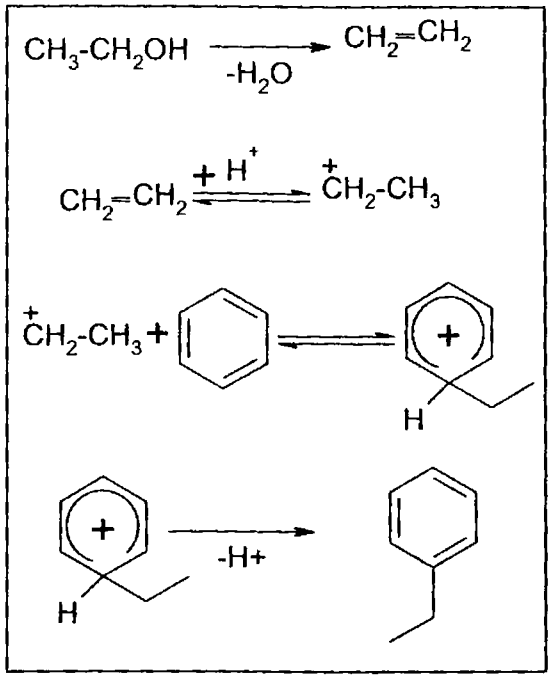

Scheme 7.3.1 A plausible mechanism for benzene ethylation over Brønsted acid sites

Elucidation of the reaction mechanism of benzene alkylation on heterogeneous catalysts is of great interest from an industry point of view, understanding the alkylation mechanism could help in optimizing the reaction conditions and designing a new catalyst for a more efficient process. However, the reaction mechanism of alkylation of aromatics with short chain olefins on zeolite type catalysts is not yet clearly understood. Venuto et al.[26] and

Weitkamp[27] suggested that the alkylation of benzene with ethylene over acidic faujasite and ZSM-5 zeolites takes place by Eley-Rideal mechanism. Corma et al.[11] reported the Eley-Rideal mechanism for alkylation of benzene with propene over MCM-22. While the Langmuir-Hinshelwood mechanism of alkylation of benzene with short chain alkenes has also been reported[28,29]. Recently Panagiotis and Ruckenstein[30] suggested that the size of the pores of the zeolites in combination with the size of the aromatics and the alkylating agents could regulate the alkylation mechanism. In the case where the size of the aromatic molecule is comparable to the pores of the zeolite, the alkylation proceeds via the Langmuir- Hinshelwood mechanism. For large pore zeolites such as faujasite and beta zeolites, the alkylation occurs via the Eley-Rideal mechanism.

Lenarda et al.[14] assumed the ethylation of benzene over aluminum and aluminium- gallium PILCs proceeds according to the Langmuir-Hinshelwood mechanism. We, having comparable interlayer spacing assume the same mechanism, the rate determining step being the reaction between benzene molecules adsorbed on aprotic sites probably better coordinate the benzene molecules allowing an easier reaction with the ethylene adsorbed on the protic sites.

7.4 COMPARISION OF DIFFERENT SYSTEMS

Vijayaraghavan and Raj[16] had reported ethylation of benzene with ethanol over aluminophoshate based molecular sieves. The various products

formed include para and meta diethylbenzene and polyalkylated benzenes in addition to EB. Lenarda et al.[14] reported ethylation of benzene with PILCs. Here alkylating agent selected is ethylene. Selectivity of EB is found to be up to 86%. Platinum loaded zeolites reported by Kato et al.[25] showed toluene, xylene, styrene and cumene as the side products. Thus the development of a catalyst with 100% EB selectivity is challenging.

The activity and selectivity to EB over various systems are shown in table 7.4.1. The present catalyst systems are highly shape selective and we are getting EB as the only product except in the unpillared systems M, the parent montmorillonite as well as pillared TAM and AZM where diethylbenzene is also formed. M results in all possible disubstituted products while pillared systems gave only para diethylbenzene. Thus the development of uniform porous structure upon pillaring is well established in addition to the characterization techniques used. ZM gives maximum conversion. Ti and Zr containing systems show good conversion that decreases with decrease in the metal content.

Table 7.4.1 Activities of the catalysts in Benzene ethylation reaction at 350°C

Catalyst	Conversion (wt%)	EB selectivity (%)
M	12.4	43.0
NM	17.5	100.0
TM	30.1	100.0

ZM	63.0	100.0
AM	20.8	100.0
CM	18.8	100.0
TZM	47.4	100.0
TAM	18.5	58.0
TCM	19.5	100.0
AZM	88.6	48.2
ACM	14.07	100.0
ZCM	37.66	100.0

Benzene/ethanol molar ratio 4:1, Time on stream 2 h, WHSV 6.9 h^{-1} and Catalyst weight 0.5 g

Activities of Cr single as well as mixed pillared systems are found to be low except that of ZCM. The increased conversion over ZCM may be due to the presence of very low amount of Cr and high percentage of Zr as clear from the elemental analysis data (chapter 3, table 3.2.1). The low conversion over alumina single pillared system increases upon mixed pillaring except in ACM. These observations clearly show the efficiency of Zr and Ti in benzene ethylation reaction.

The high selectivity of EB and the absence of polyalkylbenzene over PILCs in the optimized conditions may be due to the rapid diffusion of the product and the increased layer distance which allows intercalation of more and more reactants within the layers where shape selective constraints leads to EB as the only product. The conversion over PILCs is comparable with earlier reports for the ethylation of benzene with ethylene over aluminium gallium mixed pillared bentonites[14], but with increased selectivity.

7.5 ACTIVITY – ACIDITY RELATIONSHIPS

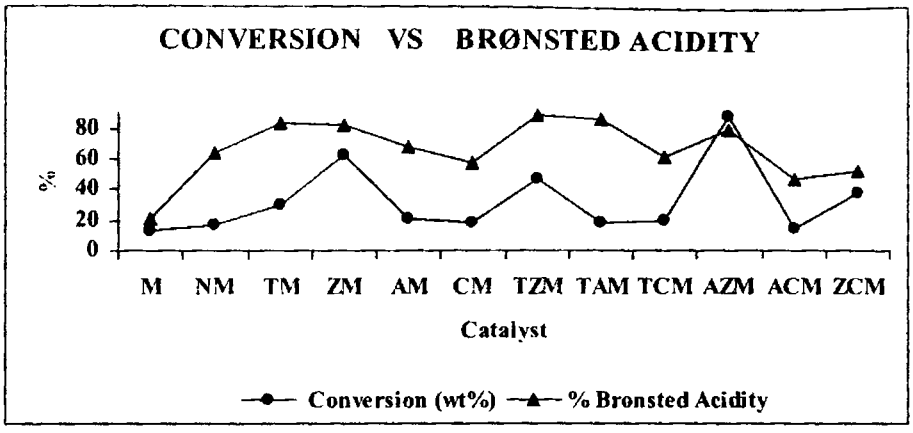

Figure 7.5.1 Correlation diagram for Brønsted acidity and ethanol conversion

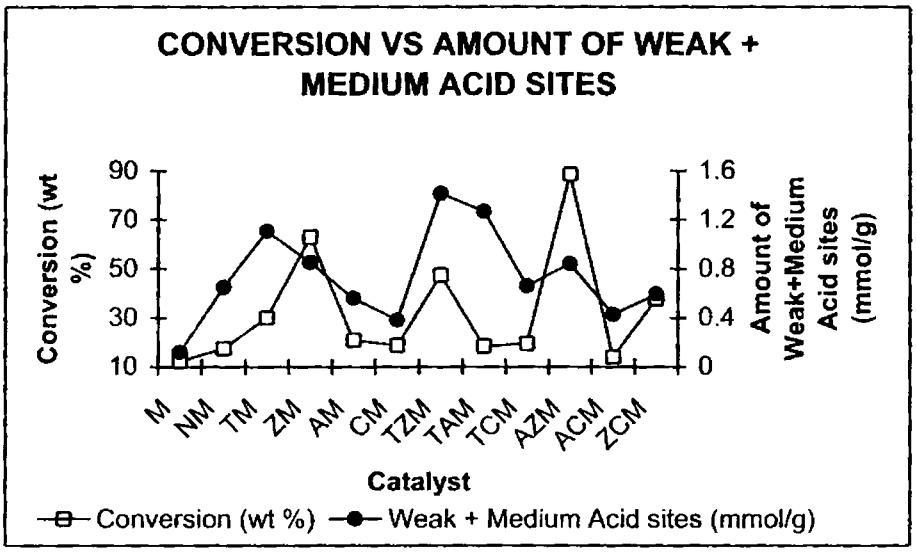

Figure 7.5.2 Correlation diagram of conversion with amount of weak + medium strength acid sites obtained from TPD of NH_3

The ethanol conversion is correlated with the Brønsted acidity obtained from cumene cracking reactions and TPD of NH_3, where we get good correlation as evident from figures 7.5.1 and 7.5.2.

7.6 EFFECT OF TIME ON STREAM; DEACTIVATION STUDIES

As expected, there is a decrease in conversion with increase in time on stream due to blocking of active sites by coke.

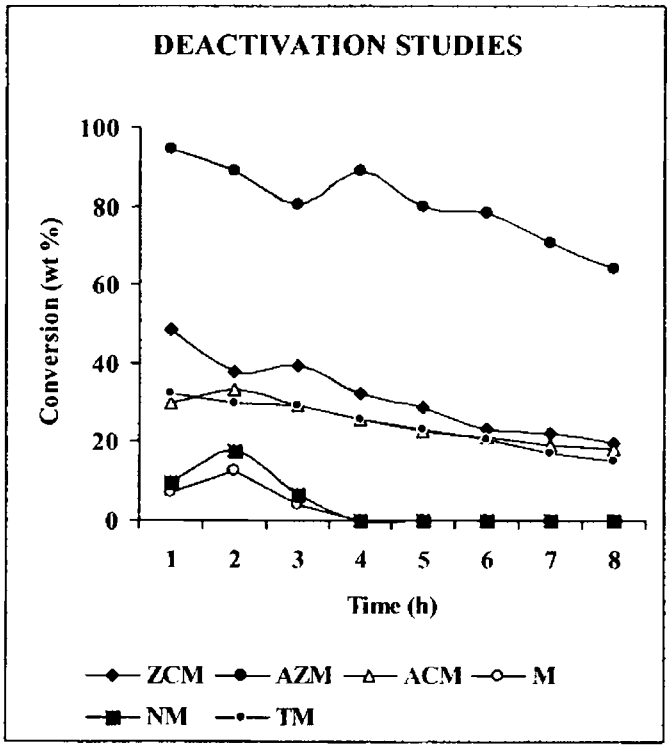

Figure 7.6.1 Deactivation of the clay catalysts in the optimized conditions in continuous run

Rapid decrease in activity of the catalysts with time might be due to the microporous nature that offers much diffusional constraint for the primary product facilitating formation of coke. The activity decreases sharply but even after 8 h retains around 50% activity over PILCs showing that the coke formed is not so effective to block all the catalytically active sites present (Figure 7.6.1). The selectivity remains unaffected with time. From the percentage retention of initial activity, among the pillared systems, Cr containing systems shows more deactivation which may be due to heavy coke formation. Both M and NM shows high amount of coke formation and becomes catalytically inactive from 4^{th} h onwards. The retained activities (%) after 8 h are 52.0, 79.7, 54.9 and 50.0 for ZCM, AZM, ACM and TM respectively. Thus the deactivation is found to be low over mixed pillared systems.

7.7 REGENERATION STUDIES

Regenerability is an important property which is non attainable with homogeneous catalysts where the catalyst becomes deactivated after the reaction. The separation of the catalysts from the reaction mixture is very difficult and the use of costly catalysts is restricted. Introduction of heterogeneous catalysts solves this problem. In addition to the possibility of continuous run, the solid catalysts can be regenerated when it is deactivated. The regenerability of the catalysts is done by burning of the coke formed in air at 500°C. Pillaring process improves catalytic activity and selectivity, decreases deactivation and provides regenerability for montmorillonite clays in benzene ethylation reaction. M and NM becomes non regenerable which may

be due to structural collapse by continuous high temperature treatment. Pillaring gives thermally stable porous structure to clays which retains the initial activity after regeneration. From figure 7.7.1 it is seen that the pillared systems are showing complete regeneration of catalytic activity even up to four repeated cycles.

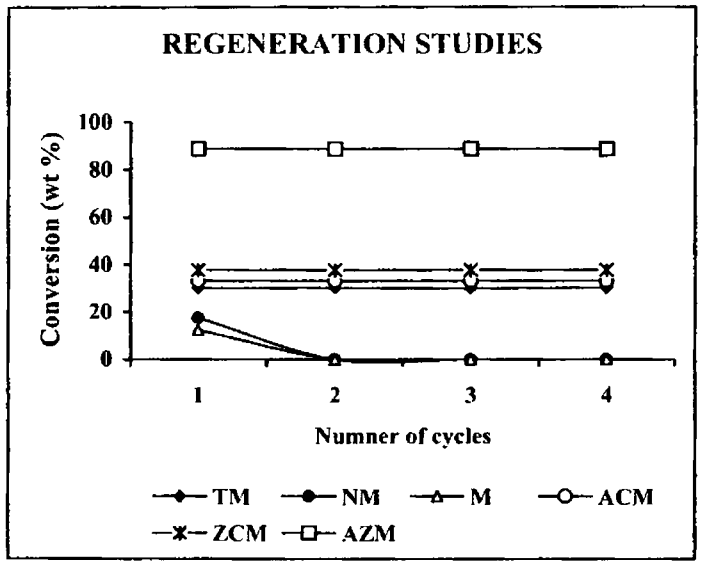

Figure 7.7.1 Activity of different regenerated systems in repeated cycles

7.8 CONCLUSIONS

The major conclusions from the above discussion are

- PILCs are found to be better catalysts over montmorillonite for benzene ethylation reaction.

- We use the alkylating agent ethanol instead of ethylene considering the availability and easiness for handling.

- The successful use of solid acid catalyst instead of environmentally hazardous homogeneous catalysts is well established.

- We introduce PILCs as efficient alternative to the commonly used zeolite catalysts because PILCs can be prepared under moderate conditions with much simple procedures compared to zeolite synthesis.

- The role of reaction parameters to get increased catalytic activity is proved.

- The 100% EB selectivity is the main attraction when compared to literature.

- Deactivation is found to be low over PILCs.

- One important property imparted to montmorillonite clays upon pillaring is regenerability.

REFERENCES:

1. T.F. Degnan Jr, C.M. Smith, C.R. Venkat, Appl. Catal. A Gen. 221 (2001) 283.
2. M.F. Bentham, G.J. Gajda, R.H. Jensen, H.A. Zinnen, Erdöl Erdgas Kohle 113 (1997) 84.
3. A. Corma, Chem. Rev. 95 (1995) 559.
4. J. Chen, in: Proceedings of the Worldwide Solid Acid Process Conference, Session 3, Catalyst Consultant Inc., Houston, TX, 14–16 November 1993.
5. G.R. Meima, M.J.M. Vander Aalst, M.S.V. Samson, N.J. Vossenbeerg, R.J. Adiansens, J.M. Garces, J.G. Lee, in: Proceedings of the Worldwide Solid Acid Process Conference, Session 3, Catalyst Consultant Inc., Houston, TX, 14–16 November 1993.
6. Chem. Eng. News 12 (18 December 1995); Hydrocarbon Process. 40, october 1996.
7. B. Coughlan, M. William, Carroll, J. Nunan, J. Chem. Soc., Faraday Trans. I 79 (1983) 311.
8. C.T. Kresge, Q.N. Le, W.J. Roth, R.T. Thompson, US Patent 5,259,565, 1993.
9. P. Chu, M.E. Landis, Q.N. Le, US Patent 5,334,795, 1994.
10. D.L. Holtermann, R. Innes, US Patent 5,149,894, 1992.
11. A. Corma, V. Martinez-Soria, E. Schnoeveld, J. Catal. 192 (2000) 163.

12. R.A. Innes, S.I. Zones, G.J. Nacamuli, US Patent 4,891,458, 1990.
13. G. Bellussi, G. Pazzuconi, C. Perego, G. Girotti, G. Terzoni, J. Catal. 157 (1995) 227.
14. M. Lenarda, Loretta Storaro, G. Pellegrini, L. Piovesan, R. Ganzerla, J. Mol Catal A: Chem. 145 (1999) 237.
15. B.Viswanathan, S.Sivasanker, A.V.Ramaswamy (eds.), Catalysis - Principles and Application, Narosa Publishing House, New Delhi, 2002, p. 248.
16. V.R. Vijayaraghavan K. J. Antony Raj, J. Mol Catal A: Chem. 207 (2004) 41.
17. N.Y. Chen, W.E. Garwood, Catal. Rev. Sci. Eng. 28 (1986) 185.
18. H. Itoh, A. Miyamoto, Y. Murakami, J. Catal. 64 (1980) 284.
19. H. Itoh, T. Hattori, K. Suzuki, Y. Murakami, J. Catal. 79 (1983) 21.
20. PEP Report 33C, SRI International, March 1993.
21. C. G. Wight, U. S. Pat. 4,169,111 to Union Oil Company of California, 1979.
22. B. Maerz, S. S. Chen, C. R. Venkat, D. Mazzone, 1996 Dewitt Petrochemical Review, Houston, TX, March 19–21, 1996, A-1;
23. S. Cho, Wei. Zhu, ERTC Petrochemical Conference, Paris, France, March 3–5, 2003.
24. C. Perego, P. Ingallina, Catal. Today. 73 (2002) 3.
25. S. Kato, K. Nakagawa, N. Ikenaga, T. Suzuki, Catal. Lett. 73 (2001) 175.
26. P.B. Venuto, L.A. Hamilton, P.S.Landis, J. Catal. 5 (1966) 484.

27. J. Weitkamp, Acta Phys. Chem. (1985) 217.

28. Y. Morita, H. Matsumoto, T. Kimura, F.Kato, M. Takayasu, Bull. Jpn. Pet. Inst 15 (1973) 37.

29. K.A. Becker, H.G. Karge, W.D. Streubel, J.Catal. 28 (1973) 403.

30. G.S. Panagiotis, E. Ruckenstein, Ind. Eng. Chem. Res. 43 (1995) 1517.

★★★★★★★★★★★★★★★★

Chapter 8

TOLUENE METHYLATION: AN ALTERNATIVE ROUTE TO XYLENE PREPARATION

The most important role of a catalyst is to provide selectivity to direct a chemical reaction along a very specific, desired path. If almost all of the catalytic sites are confined within the pore, the fate of a reactant molecule and the probability of a specific molecule being produced are affected by their molecular dimension and configuration. Only a molecule whose dimension is smaller than the pore size can enter the pore, having access to internal catalytic sites and react there. Furthermore, only a molecule that can leave the pore can appear in the final product. The concept in selectivity due to such a steric effect, which is called as shape selectivity is obtained by pillaring of montmorillonite clays, whereas pillars prop open the clay layers. This increases the accessibility of reactant molecules to the interlamellar catalytic sites, resulting in a high catalytic activity. This chapter deals with the shape selective toluene methylation where the shape selective constraints limit higher substitution to get xylenes as the major product over pillared clays (PILCs).

8.0 INTRODUCTION

The Friedel-Crafts alkylation reaction is a very useful tool for the synthesis of alkylaromatic compounds both in the laboratory and on an industrial scale[1]. The reaction is generally carried out with alkylating reagents such as alkenes, alkyl chlorides and alcohols by using a stoichiometric amount of Lewis and Brønsted acids[2]. In recent years, the use of heterogeneous catalysts has greatly increased due to their advantages such as high activity and selectivity, reusability, ease of separation, no corrosion or disposal of effluent problems, regenerability, etc[3]. Various catalysts for the alkylation reaction of aromatic compounds with alkenes, alcohols or alkyl chlorides such as zeolite[4], nafion-H[5] and clays[6] have been used.

The reaction of methanol with aromatic molecules is a key reaction, as it has been claimed that methylbenzenes are the organic reaction centers in the MTO (methanol-to-olefin) process[7]. For this reason, the reaction of methanol with benzene and toluene can be seen as a model reaction for zeolite/solid acid catalyzed reactions.

Shape selective xylene preparation by alkylation of toluene with methanol (scheme 8.0.1) is an interesting way as an alternative route to the conventional adsorption separation of xylene isomers or toluene disproportionation. Since p-xylene serves as a raw material for the production of monomers for the polymer industry, the attention has in particular been focused on the selective formation of p-xylene. The methylation of toluene

with methane over zeolite catalysts is shown to be complicated by extensive disproportionation, hydrodealkylation and hydrocracking reaction[8].

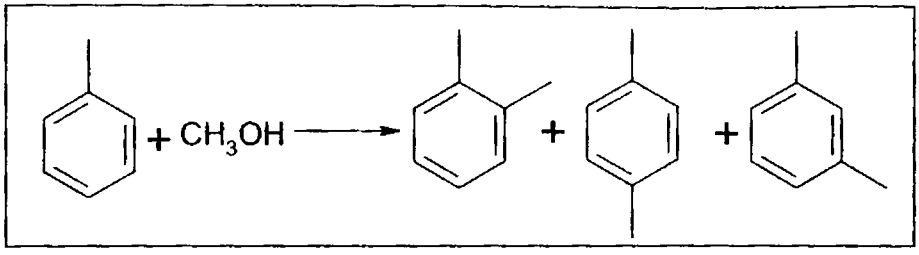

Scheme 8.0.1 Toluene methylation reaction over acid catalysts giving ortho, para and meta- xylenes

Zhirong-zhu et al.[9] reported toluene methylation over a number of zeolite type catalysts which includes toluene disproportionation to produce benzene as a side product. In general, alkylation of toluene with methanol, i.e. methylation of toluene, is carried out over acidic zeolites, such as ZSM-5, Mordenite, Y-Zeolite and SAPO-11, etc[10-12].

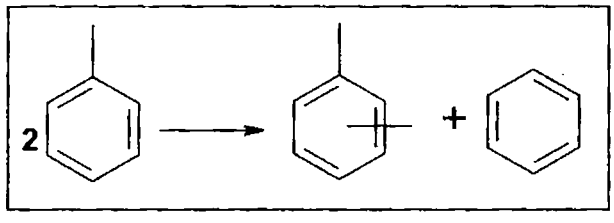

Scheme 8.0.2 Toluene disproportionation reaction over acid catalysts giving benzene

Toluene disproportionation to benzene and xylene, as a main side reaction (scheme 8.0.2), may also take place over acidic zeolites, which is directly related to acidity of zeolites. New catalysts are needed for toluene methylation that avoids disproportionation to enhance selectivity.

8.1 EFFECT OF REACTION VARIABLES

Toluene methylation is done using the prepared catalysts. ZCM is selected for finding out the optimized conditions for the reaction in such a way to get xylene without higher substitution and disproportionation. Reaction was studied at different temperature, molar ratio and WHSV in order to find suitable conditions for maximum selectivity and conversion.

8.1.1 Effect of temperature

Figure 8.1.1 shows a linear response of conversion with increase in temperature up to 350°C and shows a small decrease at 400°C which then increases at 450°C. We are getting 100% xylene selectivity at and above a temperature of 400°C. Temperature has a profound influence on conversion and no conversion occurs up to 300°C. Polyalkylbenzene is formed at a temperature of 350°C and is found to be absent at higher temperatures. The lower selectivity for polyalkylbenzene compared to xylenes at higher temperatures may be due to rapid diffusion of the products. 100% xylene selectivity and maximum conversion is obtained at 450°C and is selected as the optimum temperature for further studies.

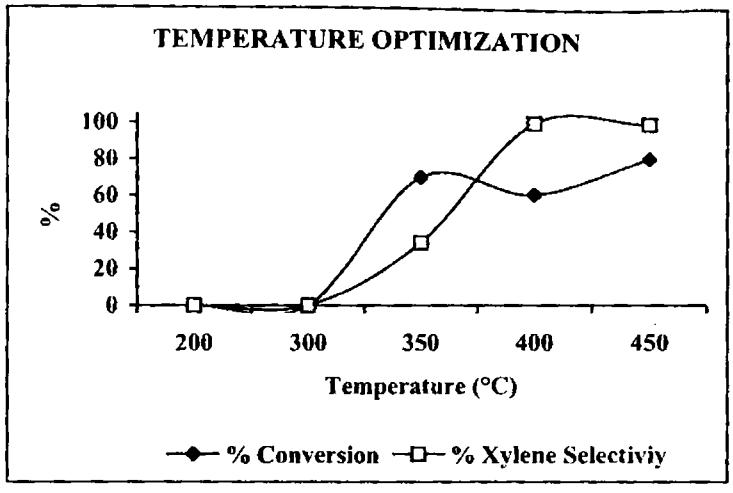

Figure 8.1.1 Temperature optimization at a WHSV of 7.2 h^{-1}, Toluene/methanol molar ratio 3:1, Time on stream 2 h and Catalyst weight 0.5g

8.1.2 Influence of Toluene/Methanol molar ratio

The influence of molar ratio on conversion is studied at 450°C and at a WHSV of 7.2 $h^{-1}$with toluene to methanol molar ratios 1:1, 1:2, 1:3 and 1:4. The results are presented in Figure 8.1.2. A nonlinear response is obtained over the selected catalyst, first the conversion increases, then show a slight decrease at 3:1 which again increases at 4:1. A nonlinear variation in disproportionation to form benzene is also seen from the plot and only at a molar ratio of 3:1 it is found to be absent. Considering the absence of disproportionation, to enhance selectivity, we adopted 3:1 as the optimum molar ratio.

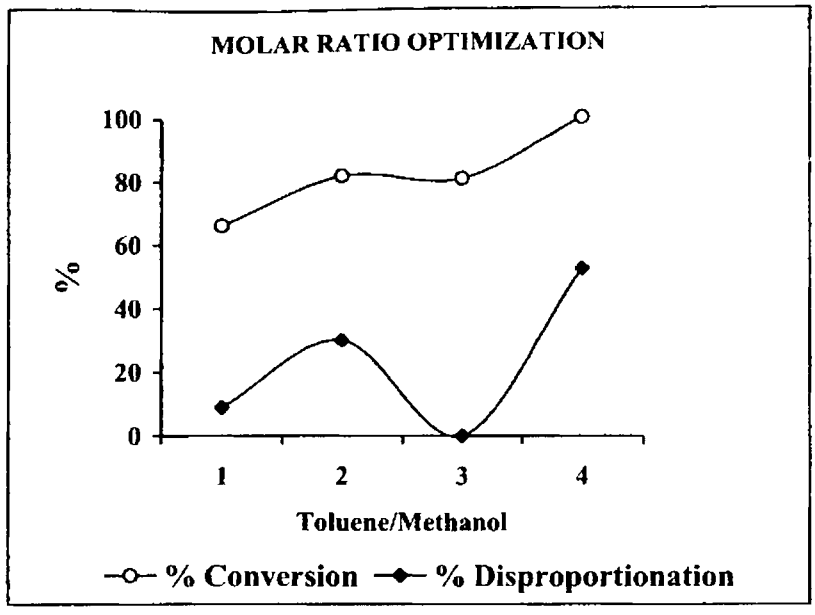

Figure 8.1.2 Optimization of molar ratio at a temperature of 450°C, WHSV of 7.2 h^{-1}, Time on stream 2 h, and Catalyst weight 0.5g

8.1.3 Influence of WHSV

Figure 8.1.3 illustrates the influence of WHSV on conversion and higher substitution selectivity. Conversion first increases which then shows a steady decrease with increase in WHSV. At a WHSV of 7.2 h^{-1}, higher substitution is found to be absent whose formation occurs at higher WHSV. Thus we considered xylene selectivity and a WHSV of 7.2 h^{-1}.

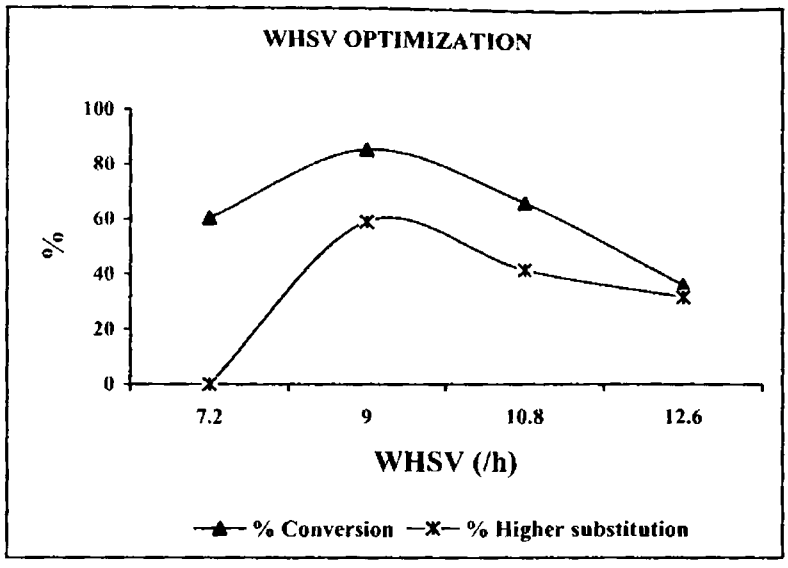

Figure 8.1.3 Optimization of WHSV at a temperature of 450°C, Toluene/methanol molar ratio 3:1, Time on stream 2 h and Catalyst weight 0.5 g

8.2 MECHANISM OF THE REACTION

In general, a reaction catalyzed by a solid acid proceeds via minimum three distinct steps:

(1) Migration of the reactants to and adsorption on the active site,

(2) Catalytic reaction and

(3) Desorption of products.

An enormous amount of experimental research has been done on electrophilic aromatic substitution (EAS) reactions as catalyzed by solid acids; the mechanism is still not fully unraveled. Experiments on the methylation of benzene and toluene with methanol are usually explained by assuming an Eley – Rideal type mechanism. We assume the same mechanism which is adopted over zeolite catalysts. Methanol strongly adsorbs on the catalyst acidic site before it reacts with the aromatic species for which interaction with the solid acids are much weaker. In the past a methoxide was assumed to be the reactive species[13], but more recent in-situ studies indicate that methanol and the aromatic co-adsorb on the acid sites, with methanol in the end-on adsorption mode and the aromatic system in interaction with this methanol molecule[14].

During the reaction, toluene and methanol are adsorbed on the Brønsted acid bridging hydroxyl. The reaction starts when the acid proton of the clay moves towards the oxygen atom of methanol. Then the CH_3 group becomes chemisorbed to the oxygen of the hydroxyl group. The dehydration of methanol to water and a methoxide has been studied by several authors[15-17]. The reaction was found to proceed in one step: the acid proton migrates from oxygen of the solid acid site to the oxygen of methanol and simultaneously the methyl group moves to oxygen of the acid site going through only one transition state. The methyl group of methanol attaches on toluene which forms π-complex with the layer metals. After π-σ conversion, a proton of toluene is given back to clay to form a new bridging hydroxyl group. After reaction, xylene and water are adsorbed on the clay, which is then desorbed. Scheme

8.2.1 shows the suggested mechanism, where M is the layer metal (Al, Si, Mg, Fe etc) and in the hydroxyl group H is acidic one.

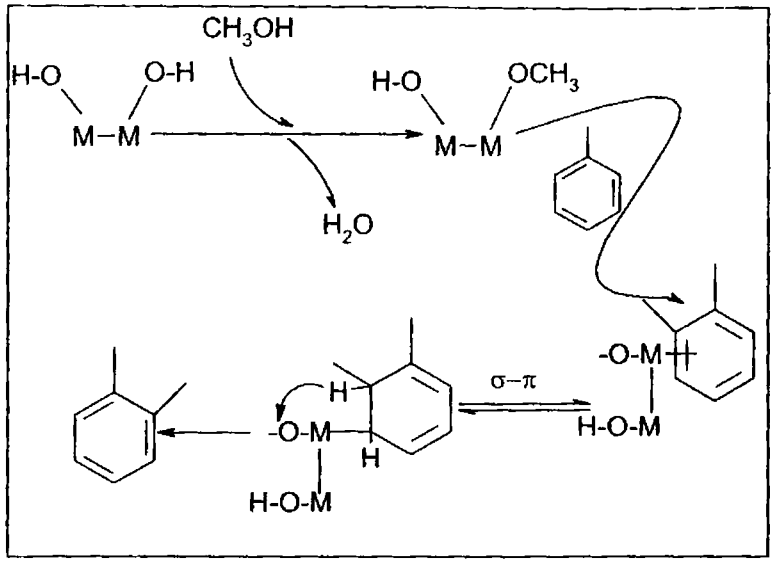

Scheme 8.2.1 Suggested mechanism of toluene methylation over clays

8.3 COMPARISON OF DIFFERENT SYSTEMS

Formation of xylene with high selectivity over present catalysts might be due to its free diffusion without steric hindrance through the pores. The lower selectivity towards polyalkylated products might be due to steric hindrance to diffusion facilitating their disproportionation with toluene to xylenes. A comparison of catalytic activity and selectivity over various catalyst systems are shown in table 8.3.1.

The catalytic activity as well as p-xylene selectivity is very poor over montmorillonite KSF. This may be due to the non-availability of pores for shape selective catalysis and the partial structural collapse that occurred during high temperature calcination. As already mentioned, the process of pillaring exposes and adds acidic sites (chapter 3, section 3.11.3.1.2) which increases conversion, whereas enhanced layer distance and porosity allows shape selective catalysis where higher substitution is found to be least. The increased activity of NM may be due to the increased acidity obtained as a result of dealumination. The process of delamination resulted in increased porosity which is responsible for xylene selectivity. The delamination and dealumination is a result of Na^{+}-ion exchange. But these changes are not as effective as that of pillaring.

Table 8.3.1 Activities of the catalysts for toluene methylation at 450°C

Catalyst	Methanol Conversion (wt %)	Selectivity (%)		
		P-xylene	Di/Tri substitution	Disproportionation
M	34.0	9.9	51.2	-
NM	82.1	26.1	43.0	-
TM	89.6	37.5	35.7	7.2
ZM	94.3	100.0		
AM	83.1	59.6	-	-
CM	74.8	50.7	-	-
TZM	100.0	56.7	-	-

TAM	92.8	52.6	8.5	3.3
TCM	80.6	44.8	-	20.7
AZM	83.7	51.1	-	-
ACM	80.0	59.6	-	-
ZCM	80.8	57.1	-	-

Toluene/methanol molar ratio 3:1, Time on stream 2 h, WHSV 7.2hr-1 and Catalyst weight 0.5 g

In agreement with the acidity, both Ti and Zr containing systems show very high conversion and is slightly lower in Al and Cr containing systems. Anyway it is clear that all PILC systems show very good activity towards toluene methylation reaction.

The major side reaction during toluene methylation reaction is disproportionation to give benzene and is found to be present only over 3 – Ti containing PILC systems. This may be the property of the Ti-pillar. Except Ti –containing systems, over all PILC catalysts xylene is the only product where p-xylene is the major one. Presence of Zr may be the reason for the absence of disproportionation and higher substitution over TZM. This assumption is supported by the very high conversion and 100% p-xylene selectivity over ZM. It is reported that the acidic sites, needed for catalyzing alkylation of toluene with methanol are relatively weaker than that for catalyzing toluene disproportionation[9]. This assumption is found to be correct over present PILC systems. The acidity in the strongly acidic region (obtained form TPD of NH_3, data is shown in Chapter 3, Table 3.11.1) is greater for Ti-containing systems. The high p-xylene selectivity over PILCs is based on the faster diffusion of the

para isomer, with respect to o- and m- xylenes, which enriches the product in the most desired p-xylene.

8.4 ACTIVITY – ACIDITY RELATIONSHIPS

We tried to correlate the activity with Brønsted acidity obtained from benzene selectivity in cumene cracking reactions. From figure 8.4.1 a perfect correlation is obtained which supports the role of Brønsted acid sites in the suggested mechanism. In the case of PILCs, acidity from weak and medium strength region obtained from TPD of NH_3 represents Brønsted acidity. The clear correlation obtained in the present study as evident from figure 8.4.2 supports the above assumption.

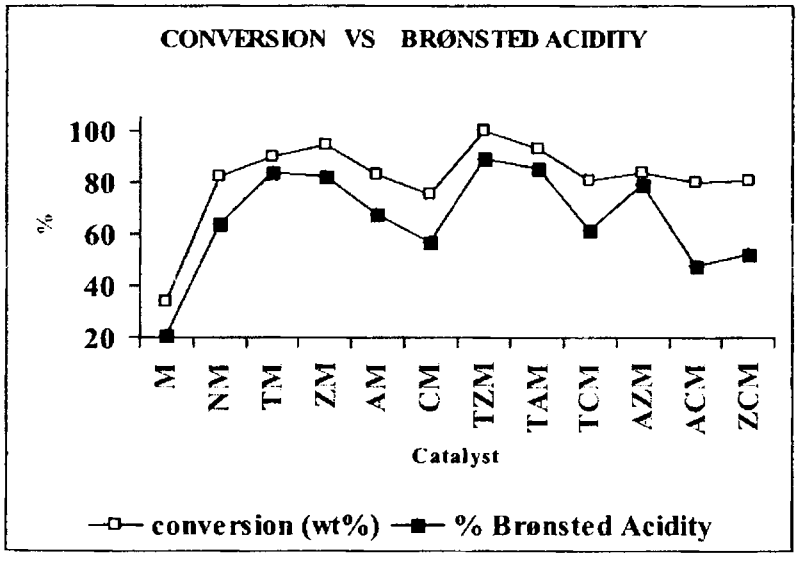

Figure 8.4.1 Correlation diagram for Brønsted acidity and methanol conversion

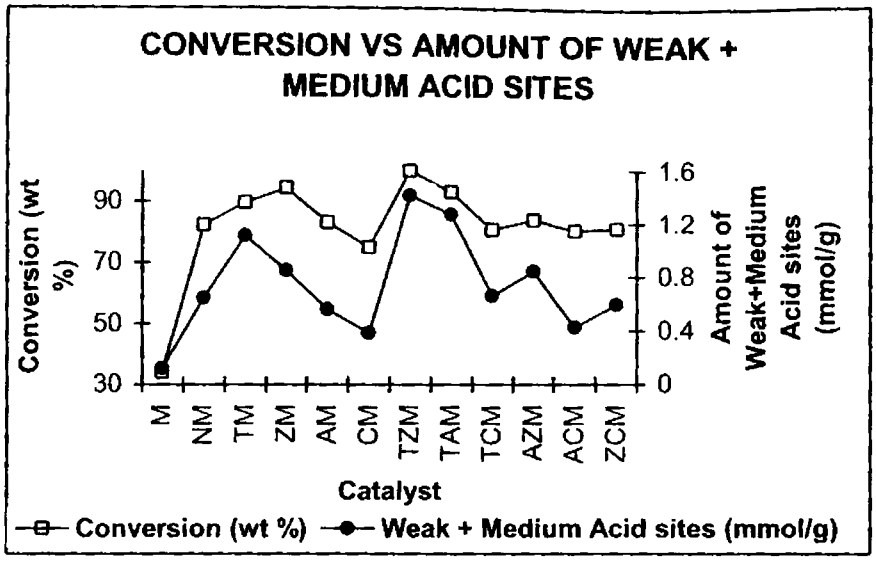

Figure 8.4.2 Correlation diagram of conversion with amount of weak + medium acid sites obtained from TPD of NH_3

8.5 DEACTIVATION OF CATALYSTS

Figure 8.5.1 illustrates the effect of time-on-stream on the conversion over various systems. There is a decrease in conversion with increase in stream due to blocking of the active sites by coke. Thus the catalysts get deactivated with stream. The rapid decrease in activity is due to the microporous nature which offers much diffusional constraint for the primary products facilitating formation of multialkylated products with the precursors of coke.

The selectivity did not vary much with time. The absence of polyalkylated products even after deactivation may be due to a partial decrease

in the pore size due to coke deposition. The activity remains almost constant from 5th h onwards after the initial sharp decrease up to 4th h. Thus the coke formed during the reaction is not so large as to block all catalytically active sites present.

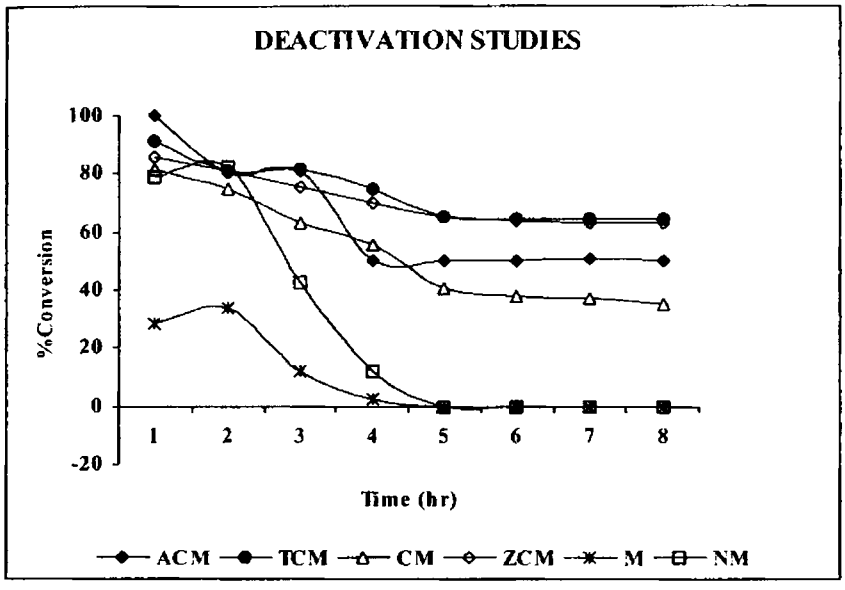

Figure 8.5.1 Deactivation of the given systems in the optimized conditions in continuous run

Parent montmorillonite and NM becomes completely deactivated by 4 h of continuous run. The decrease in porosity and blocking of the pore present may be the reason for complete deactivation. Among the pillared systems studied CM shows 48% of the initial activity after 8 h where as mixed pillaring shows further decrease in the deactivation. TCM shows 80% retention and from 5th hour onwards disproportionation is absent. Here the coke formed may

block the active sites responsible for disproportionation. ZCM shows 78% of the initial activity, where ACM retains 63%. Initial activity is taken as the conversion at 2nd hour, since in the 1st hour, attainment of a steady state for the reaction over the catalysts may not be possible and also temperature fluctuations may occur. It is evident that mixed pillaring shows a marked effect in the catalytic properties of single pillared montmorillonite.

8.6 CATALYST REGENERATION

Regenerability of the catalysts is tested by burning off the coked formed by heating in air at 500°C for 12 h. The initial activity is regained in all pillared systems whereas M and NM becomes catalytically inactive towards toluene methylation, which may be due to the structural collapse occurring at high temperature. The regenerated systems show same trend towards deactivation on continuous run and is found to be regenerable up to four repeated cycles. This observation confirms the thermal stability of PILCs.

8.7 CONCLUSIONS

From the above discussions we reach in the following conclusions.

- Present catalytic systems are proved to be good catalysts for toluene methylation reaction with appreciable conversion.

- Eventhough ion-exchange of montmorillonite increases the conversion; it fails to provide shape-selectivity to montmorillonite.

- The main advantage of majority of present PILC catalysts is the absence of disproportionation.

- The reaction parameters can introduce drastic changes in catalytic activity and selectivity.

- The role of Brønsted acid sites in catalytic activity is clear from the perfect correlation of activity with Brønsted acid site distribution.

- The problem of deactivation of parent or ion exchanged montmorillonite is solved upon pillaring, where mixed pillaring is found to be more efficient.

- The regenerability and high thermal stability offered to montmorillonite clays upon pillaring makes it promising green catalyst instead of homogeneous catalysts.

REFERENCES:

1. Kirk-Othmer, Encyclopedia of Chemical Technology, 3rd edn. 2 (1978) 50.
2. G.A. Olah, (ed), Friedel-Crafts and Related Reactions, John Wiley, New York, 1964.
3. G. Bellussi, G. Pazzuconi, C. Prego, G. Girotti, G. Terzoni, J. Catal. 157 (1995) 227.
4. A.P.Bolton, in: J.A. Rabo (ed), Zeolite Chemistry and Catalysis, Am. Chem. Soc. Washington DC, 1976, p. 762.
5. I.I. Ivanona, D. Brunel, J.B. Nagy, E.G. Derouance, J. Mol. Catal. 95 (1995) 243.
6. G.A. Olah, G.K.S. Prakash, J. Sommer, in: Superacidsw, Wiley, New York, 1985, Ch.5, p. 243.
7. S. Song, J.B. Nicholas, J.F. Haw, J. Am. Chem. Soc. 122 (2000) 10726.
8. M.O. Adebajo, R.F. Howe, M.A. Long, Energy & Fuels. 15 (2001) 671.
9. Z. Zhu, Q. Chen, W. Zhu, D. Kong, C. Li, Catal. Today. 93-95 (2004) 321.
10. A.M. Vos, X. Rozanska, R.A. Schoonheydt, R.A.V. Santen, F. Hutschka, J. Hafner, J. Am. Chem. Soc. 123 (2001) 2799.
11. P. Ratnasamy, R.N. Bhat, S.K. Pokhriyal, S.G. Hegde, R. Kumar, J. Catal. 119 (1989) 65.
12. I. Benito, A. Ded Riego, M. Martinea, Appl. Catal. A. 180 (1999) 175.

13. J. Rakoczy, T. Romotowski, Zeolites. 13 (1993) 256.
14. I.I. Ivanova, A. Corma, J. Phys. Chem. B. 101 (1997) 547.
15. S.R. Blaszkowski, R.A. Van santen, J. Phys. Chem. 99 (1995) 11728.
16. S.R. Blaszkowski, R.A. Van santen, J. Phys. Chem. B. 101 (1997) 2292.
17. P.E. Sinclair, C.R.A. Catlow, J. Chem. Soc., Faraday. Trans. 92 (1996) 2099.

★★★★★★★★★★★★★★★★

Chapter 9

LINEAR ALKYL BENZENE SYNTHESIS

The manufacture of fine and speciality chemicals has commonly been associated with the production of large quantities of toxic waste. Use of traditional reagents such as mineral acids, strong bases, stoichionetric oxidants and toxic metal reagents is widespread and has many drawbacks including handling difficulties, in organic contamination of the organic products, the formation of large volumes of toxic waste and poor reaction selectivity leading to unwanted isomers and side products. These problems can be largely overcome if genuinely catalytic, heterogeneous alternatives to environmentally unacceptable reagents can be developed. Recent developments in the design and application of solid acid catalysts offer considerable potential for clean synthesis. Present chapter deals with eco-friendly pillared clay catalyzed synthesis of LAB to get 2-phenyl isomer as the major product.

9.0 INTRODUCTION

For the past 25 years, linear alkyl benzene (LAB) is widely used in industry as an intermediate for the production of linear alkylbenzene sulphonate (LAS), the surfactant of choice throughout the world, because it is cost-effective and biodegradable. The increasing use of detergents by households discharges large quantities of alkyl benzene and its sulphonated derivatives into rivers. Rapid biodegradation of the disposed organic compounds is important to keep the pollution levels as low as possible. Surfactants owe their properties to their characteristic hydrophilic-hydrophobic structure, which enables them to aggregate at the surface of an aqueous solution and hence reduce its surface tension properties. Studies on the solubility, foam stability and surface-active properties of LAS have shown that the length of their alkyl chain and the position of the phenyl group on it are important factors in determining their performance characteristics[1]. Certain constant synergistic effects have also been observed for various combinations of phenyl alkanes[2] (the linear 1- aryl compound would be ideal, but is not formed due to the unstable nature of the primary carbocation which leads to its formation). In general, the 2-phenyl alkane isomer differs substantially from the other internal isomers in its performance characteristics, which makes the control of its amount in the product, a mater of considerable importance.

Commercially benzene alkylation to form LAB is done using HF or $AlCl_3$ catalysts. HF acid has been used as catalyst for LAB production since 1968. It has high efficiency, superior product and is of higher use relative to

the alternative $AlCl_3$ catalyst. These two Friedel-Crafts catalysts give different phenyl isomer distributions in the LABs produced. The $AlCl_3$ gives about 30% of the 2-phenyl isomer, 20% of the 3-phenyl isomer, decreasing to 15-16% of the 4-, 5- and 6-phenyl isomers. With HF, there is a more even isomer distribution with all the phenyl isomers present at approximately 17 to 20%. Alkylation using homogeneous catalysts such as H_2SO_4, HF and $AlCl_3$ has been investigated extensively by Alul[3] and Olson[4]. However the potential applications of a heterogeneous catalyst have long been recognized, principally because of the concern about handling concentrated HF and disposing of fluorinated neutralization products[5]. Thus as these homogenous catalysts are very corrosive and polluting, a great effort is made for their substitution by solid acid catalysts such as zeolites, clays etc that do not have these inconvenience[6,7].

Large pore zeolites have been demonstrated as active and selective catalysts for mono alkylation of benzene or toluene by linear alkenes[8,9]. Other solid acid catalysts reported for the alkylation of benzene with alkenes include heteropolyacids[10], clays[11], ZSM-12[12], HY[13], metal oxides[14] etc. To ensure environmental protection, the detergent industry must develop a clean LAB production process capable of not only replacing the conventional homogeneous catalysts but also having a high selectivity for the 2-phenyl LAB isomer.

9.1 RECENT ADVANCES IN THE INDUSTRIAL LAB PRODUCTION

LAB global demand is about 2.7 million metric tonnes per year. Traditional processes[15] for LAB production include an alkylation unit with liquid catalysts, which depending on the process may imply the following.

1. Alkylation of benzene with alkenes $C_{10}-C_{14}$ in the presence of HF.
2. Alkylation of benzene with chloroparaffins C_{10}–C_{14}, in the presence of $AlCl_3$.
3. Alkylation of benzene with alkenes $C_{10} - C_{14}$ in the presence of $AlCl_3$.

Nowadays, most of the LAB is produced from linear internal alkenes and the majority of commercial applications worldwide are based on HF catalysts. The main reaction is usually accompanied by benzene and alkene side reactions, with co-production of undesired compounds.

Polyalkyl benzenes, indanes and tetralines are the typical compounds produced by benzene side reactions, while branched alkyl benzenes and oligomers, which are precursors of tars and coke, are usually produced by alkene side reactions. Polyalkylation and oligomerization reactions are depressed by increasing the benzene to alkene ratio in the feed, which in commercial processes is set at 8. In addition, as a general feature, the processes are designed, by controlling the reaction temperature, to minimize skeletal

isomerization of the alkenes, since high linearity is necessary to yield a product that biodegrades at high rates.

As already mentioned now various solid acid catalysts are used for LAB synthesis. However most of them give results, which have not industrially exploited so far. An important breakthrough was achieved by UOP in 1992, which jointly with CEPSA developed the new Detal™ process, based on a fixed bed of acidic, non-corrosive catalyst to replace the liquid HF acid used in the UOP former process[16]. According to the published literature, the catalyst, a fluorinated silica-alumina was discovered and patented by UOP[17,18]. The researchers found that selectivity of the fluorinated silica-alumina increases with increasing silica content. However, the best overall performance comes from those catalysts with silica to alumina ratio from 65/35 to 85/15. The catalyst is prepared by impregnating the silica-alumina with HF and the finished catalyst contains 1-6% fluorine. The Detal™ process proved to yield a superior product compared to that from HF technology, the product linearity is higher and tetralins are lower. Table 9.1.1 lists LAB linearity and tetralin weight percentage of some commercial catalysts.

As far as the stability is concerned, the Detal™ catalyst is satisfactorily active with periodic mild rejuvenation: it was demonstrated that during the commercial test, in 14 months of operation, the catalyst temperature was within 5°C of the start of run temperature[19]. As a proof of the improvement achieved with the use of solid acid catalyst, the process economics[20] turned to be favorable. The estimated erected cost for Detal™ process is about 7% lower

than HF process. The difference is due to the lower cost of Detal™ unit, which does not require costly materials or equipment for safety and effluent treating. Another additional saving in operating costs is expected because Detal™ process does not require scrubbing and inorganic salts waste disposal.

Table 9.1.1 LAB linearity and tetralin weight percentage of some commercial catalysts

	Alkylation with chloroparaffins	Alkene/$AlCl_3$	UOP/HF alkylation	UOP/Detal™ process
Catalyst	$AlCl_3$	$AlCl_3$	HF	fluorinated silica-alumina
Lab linearity (n-alkyl benzene wt%)	<90	98	92-94	95
Tetraline (wt%)	3-4	<1.0	<0.3	<0.5

The Detal™ catalyst and process was successfully demonstrated at Petresa's demonstration unit in Spain in 1992, and today three LAB complexes use this technology[21].

The various possible steps during alkylation of an arene with alkene as the alkylating agent are shown in scheme 9.1.1.

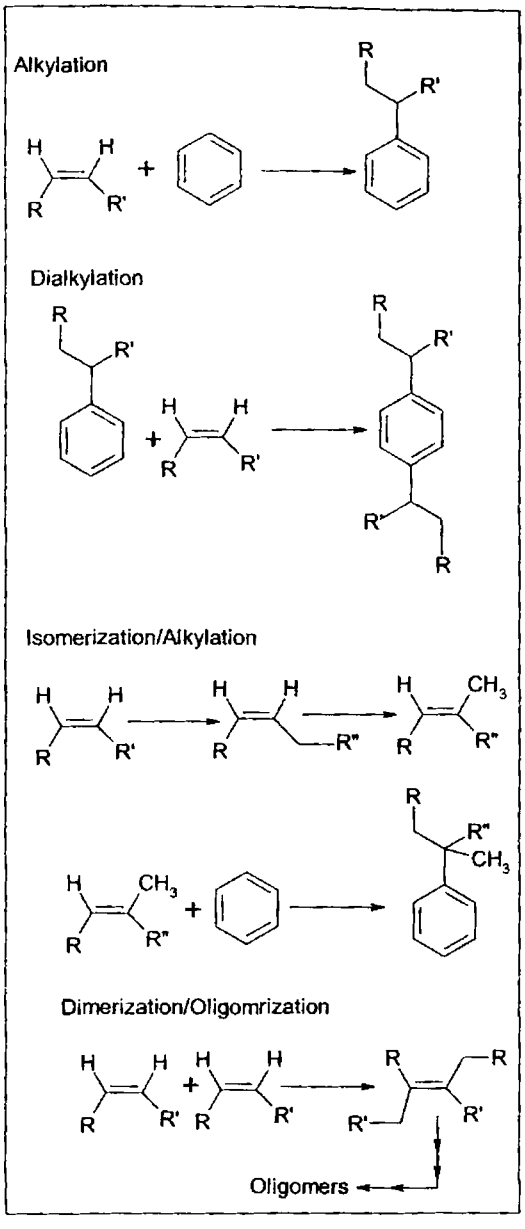

Scheme 9.1.1 Various possible reactions during benzene alkylation with higher alkenes

9.2 MECHANISM OF THE REACTION

The alkylation of benzene with alkenes goes through a carbonium ion mechanism (scheme 9.2.1).

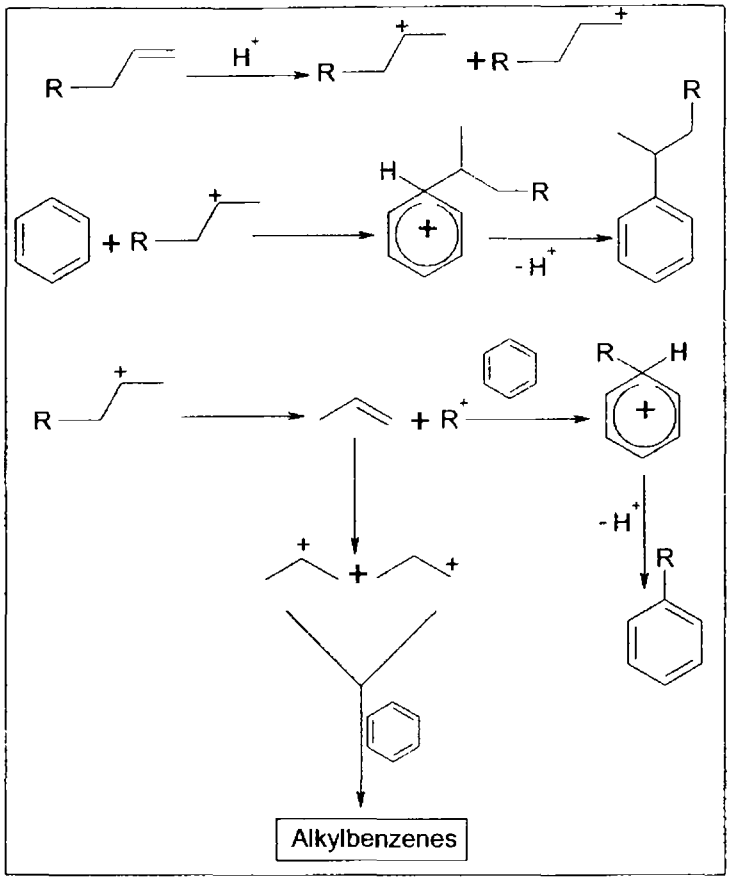

Scheme 9.2.1 Mechanism of benzene alkylation with alkenes

In the case of octene, decene and dodecene, 4, 5 and 6 carbonium ions are respectively possible. The relative stabilities of carbonium ions increase as

the C-number increases, for e.g. the least stable being the primary ion (1-position). In fact, due to its very low stability, the 1-phenyl isomer is not detected in the product. On the basis of the relative stabilities of the other carbonium ions (all secondary), it is expected that the isomer content will increase with the carbon number (towards the centre of the chain). This is found to be so in the case of HF, in which thermodynamic equilibrium is probably reached. However, in the cases of solid acid catalysts, the content 2-phenyl isomer is greater, suggesting the non-attainment of thermodynamic equilibrium.

9.3 ALKYLATION OF BENZENE WITH 1-OCTENE

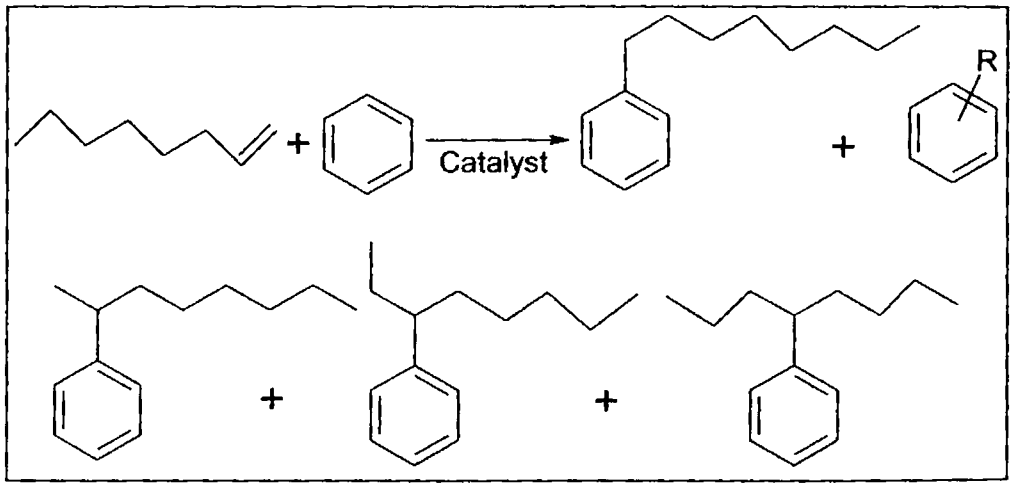

Scheme 9.3.1 Benzene alkylation with 1-octene

The development of new catalysts to replace HF is crucial for a clean petrochemical process of detergent production. Here we are alkylating benzene

with 1-octene over PILC catalysts. Benzene alkylation with 1-octene is generally carried out as a model reaction in LAB synthesis. As per the above suggested mechanism in scheme 9.2.1, four isomers are possible among which 2-phenyloctane is the desired/major product. The non-attainment of thermodynamic equilibrium is the reason for the high 2-phenyl LAB selectivity. We are getting high selectivity to 2-phenyl LAB over clay catalysts. The reaction conditions are optimized in order for getting the highly biodegradable product as the major one and also to decrease higher substitution as well as cracking. Schematic representation of benzene alkylation with 1-octene is shown below (scheme 9.3.1).

9.3.1 EFFECT OF REACTION VARIABLES

The influence of reactants/catalyst contact time (WHSV), Benzene/1-octene molar ratio and reaction temperature is studied in detail to get good percentage Atom Utilization, protecting the principles of Green Chemistry. AZM is selected for optimization studies.

9.3.1.1 Effect of WHSV

The catalysts/reactant contact time is varied from a space velocity of 6.9 h^{-1} to 12.1 h^{-1} in order to study its influence in 1-octene conversion and 2-phenyl LAB selectivity. Increase in 2-phenyloctane selectivity with WHSV is due to the lower chance for the isomerization of the 2° carbocation towards the center (hydride shift) since the contact time over catalyst is the decreased. The

conversion drops sharply with WHSV, whereas the selectivity increase is only to a low extent (figure 9.3.1). Thus we selected a WHSV of 6.9 h^{-1} for further studies.

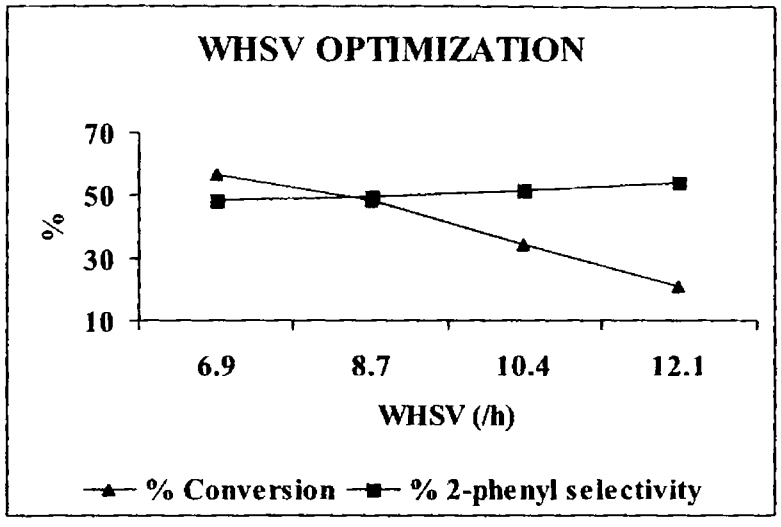

Figure 9.3.1 Optimization of WHSV at a temperature of 350°C, Benzene/1-octene molar ratio 20:1, Time on stream 2 h and Catalyst weight 0.5 g

9.3.1.2 Effect of molar ratio

The ratio of arene/alkylating agent is a critical parameter in LAB synthesis. On the one hand, to ensure the total conversion of alkene and to decrease the by-product from the polymerization of alkene, a high arene/alkylating agent is needed; i.e., a high arene/alkylating agent will cause a large amount of benzene to be separated from the product and recycled.

Therefore, the optimal molar ratio on the reaction conversion should be determined.

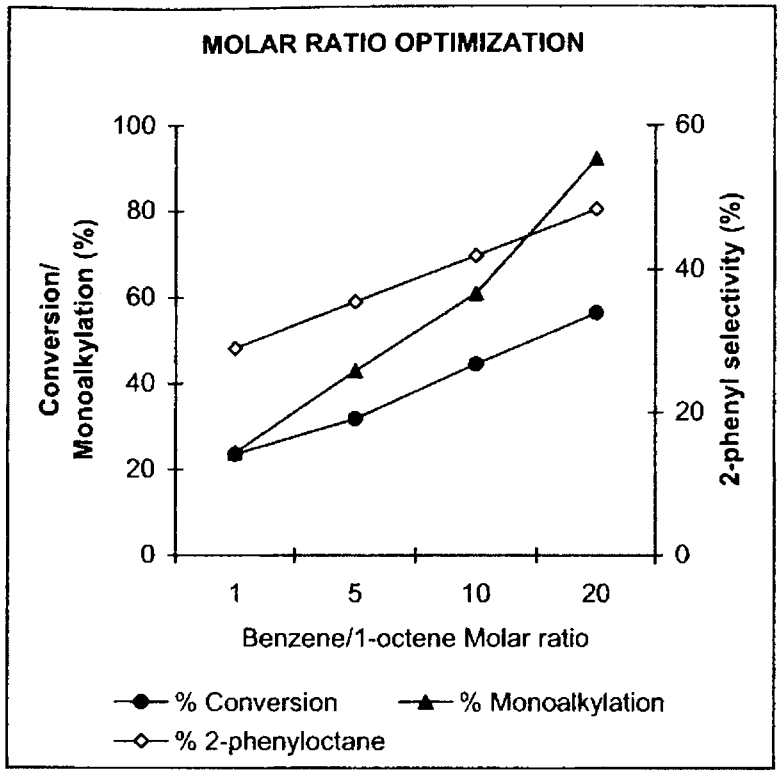

Figure 9.3.2 Effect of benzene/1-octene molar ratio on conversion and selectivity at a WHSV of 6.9 h^{-1}, temperature of 350°C, Time on stream 2 h and Catalyst weight 0.5g

Benzene to 1-octene molar ratio is varied from 1:1 to 20:1 in order to get good conversion and 2-phenyloctane selectivity. Increase in arene/alkylating agent molar ratio decreases polyalkylation. 2-phenyl LAB selectivity also increases with increase in molar ratio. This is due to the

solvation effect of benzene. The solvation of the carbocations by benzene molecules reduces the differences in their stabilities. This reduces the isomerization of the 2° carbocation towards the center which results in greater formation of 2-phenyloctane. This effect is pronounced in excess benzene and is absent at a molar ratio of 1:1. However, a high mole ratio of benzene to alkenes will cause large amount of benzene to be separated from the product and recycled. For this reason, a low molar ratio of benzene/alkene is desirable and thus we did not study the influence of benzene/alkene molar ratio higher than 20 which is selected as the optimum one. Figure 9.3.2 shows the 1-octene conversion as well as 2-phenyl LAB selectivity with molar ratio.

9.3.1.3 Effect of temperature

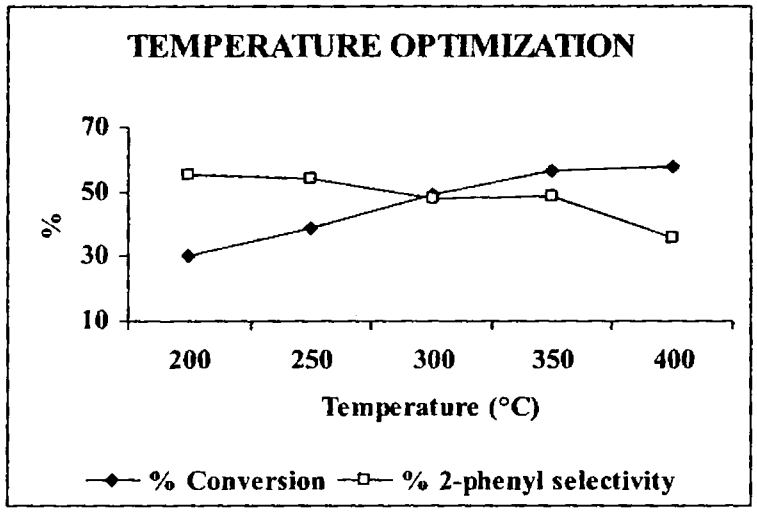

Figure 9.3.3 Effect of temperature on conversion and selectivity at a WHSV of 6.9 h^{-1}, benzene/1-octene molar ratio of 20:1, Time on stream 2 h and Catalyst weight 0.5 g

Reaction temperature is varied from 200°C-400°C and its influence in conversion and selectivity is noted. From figure 9.3.3 it is clear that 2-phenyl selectivity is low at a temperature of 400°C whereas the conversion is found to be high. The decreased selectivity with temperature is due to a series of fast hydride shifts of the carbocation to produce the isomer ions. Conversion increases with temperature at the expense of selectivity due to the increased amount of cracking, cation isomerization and higher substitution. The increase in conversion is sharp with temperature. Eventhough there is decrease in selectivity; it is not sharp up to a temperature of 350°C. Thus a temperature of 350°C is selected as the optimum one.

9.3.2 COMPARISON OF DIFFERENT SYSTEMS

Table 9.3.1 gives the conversion and product distribution of benzene alkylation with 1-octene over various clay catalysts. The alkene conversion is found to be low over parent montmorillonite. The monoalkyl and 2-phenyl selectivity is found to be comparatively low over M. Cracking is found to be a notable side reaction in this case. The high amount of cracking is due to the less porous structure after calcination of M that resulted in its structural collapse. NM also shows high amount of cracked products but is better than M which may be due to its comparatively high porous structure. PILCs show better conversion and monoalkyl/2-phenyl selectivity. The possible side reactions such as alkene polymerization, alkene isomerization to produce tertiary alkyl benzenes and tri alkylation is found to be very low or practically absent over the present clay catalysts and is evident from GC-MS analysis.

Table 9.3.1 Catalytic activity of benzene alkylation with 1-octene over clay catalysts at 350°C

Catalyst	Conversion (wt %)	Selectivity (%)			
		Monoalkylation	2-phenyloctane	Higher substitution	Cracking
M	18.6	62.2	20.1	10.0	27.8
NM	34.1	74.7	24.8	10.6	14.7
TM	55.7	86.6	37.9	4.4	9.0
ZM	46.6	89.5	44.9	3.2	7.3
AM	38.1	88.7	39.1	2.5	8.8
CM	37.5	77.6	30.5	7.6	14.8
TZM	56.9	90.5	47.0	2.3	7.2
TAM	53.5	89.1	42.5	3.0	7.9
TCM	51.4	85.8	33.1	4.2	10.0
AZM	56.5	92.3	48.3	2.2	5.5
ACM	38.1	85.1	34.9	5.7	9.2
ZCM	53.0	83. 7	33.73	5.1	11.2

Benzene/1-octene molar ratio 20:1, Time on stream 2 h, WHSV 6.9 h-1 and Catalyst weight 0.5 g

Among the PILCs, Ti and Zr containing systems shows good catalytic activity and selectivity. The high conversion/selectivity over AZM, TZM and TAM are in agreement with their high surface area and pore volume. Cracking is found to be very low over these systems, supporting their highly porous structure. Dialkylated products are also formed over various systems in a low amount

and tri substitution is practically absent over present clay catalysts which may be due to the bulkiness of that product.

9.3.3 DEACTIVATION STUDIES

The shape selective catalysis benefits product distribution, but the bulkier molecules will block the pores of the catalysts and deactivate them. The reaction conversion decreases quickly with increase of the reaction time due to the large amount of coke formed on the catalysts.

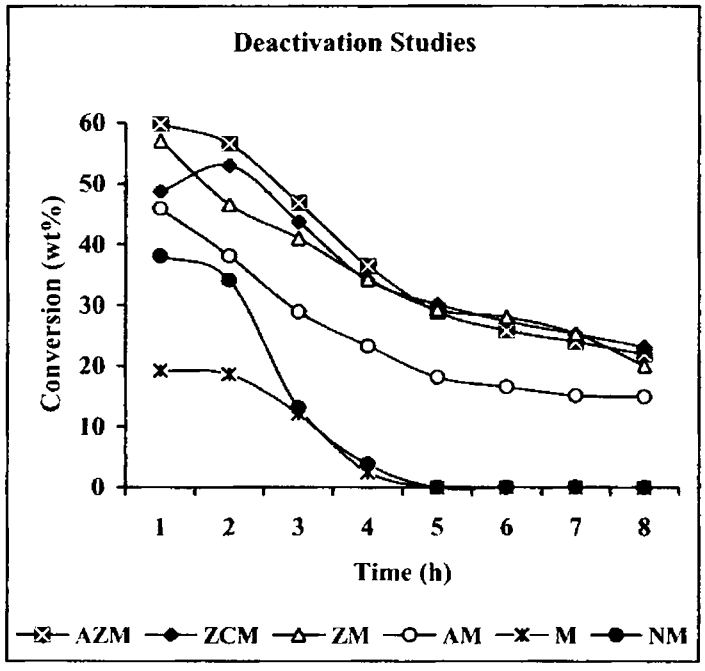

Figure 9.3.4 Activity of pillared, ion exchanged and parent Montmorillonite in continuous run

For the deactivated catalyst, the deposited compounds are more complicated than those from undeactivated catalyst, it is reported that[22] some new species, such as naphthalene, 1-methyl-3-nonyl-indan, 1,4-dibutyl-1,2,3,4-tetrahydro-naphthalene and 5-hexyl-2,3-dihydro-1H-indene are also formed. Steric hindrances of these compounds are more significant than those of the reactants, so the deactivation of catalyst may be due to channel blocking by these bulkier molecules.

The deactivation profiles of some selected catalysts are shown in figure 9.3.4. Fast deactivation is seen over all the catalysts which is very fast over M and NM. The unpillared systems drop their activity from 5th hour onwards. PILCs retain more than 50% of the initial activity even after 8 h of continuous run.

9.3.4 REGENERATION OF THE CATALYSTS

Because of the fast deactivation, catalyst regeneration is inevitable and very important for the industrial application of the catalysts. The deactivated catalysts are regenerated by burning off the coke formed in air at 500°C for 10 hours. Activity of the deactivated catalysts recovers almost 100% even after four repeated cycles showing the regenerability of the PILC catalysts. Both M and NM are to be non-regenarable even after coke removal suggesting complete structural collapse during the continuous high temperature treatment. Thus the deactivation study supports the attainment of thermal stability of clays upon pillaring.

9.3.5 ACTIVITY - BRØNSTED ACIDITY RELATIONSHIP

The mechanism discussed in section 9.2 suggested that alkylation occurs over Brønsted acidic sites of the clay catalysts. Figure 9.3.5 correlates 1-octene conversion with % Brønsted acidity (calculated from the yield of benzene in cumene cracking reactions).

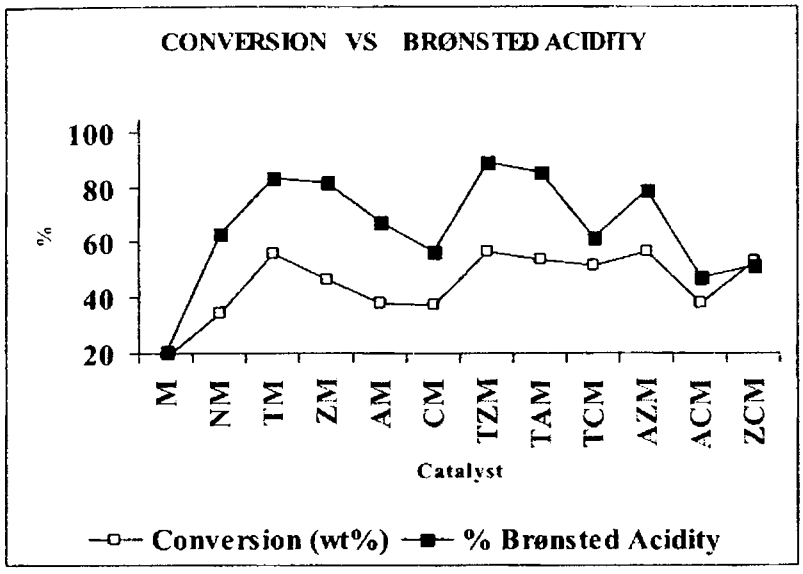

Figure 9.3.5 correlation diagram of 1-octene conversion with % Brønsted acidity

We are getting a perfect correlation diagram in accordance with the suggested mechanism. In the case of PILCs, the acidity in the weak + medium strength region (from TPD of NH_3) corresponds to Brønsted acidity. Thus the correlation diagram shown in figure 9.3.6 is in agreement with our expectation.

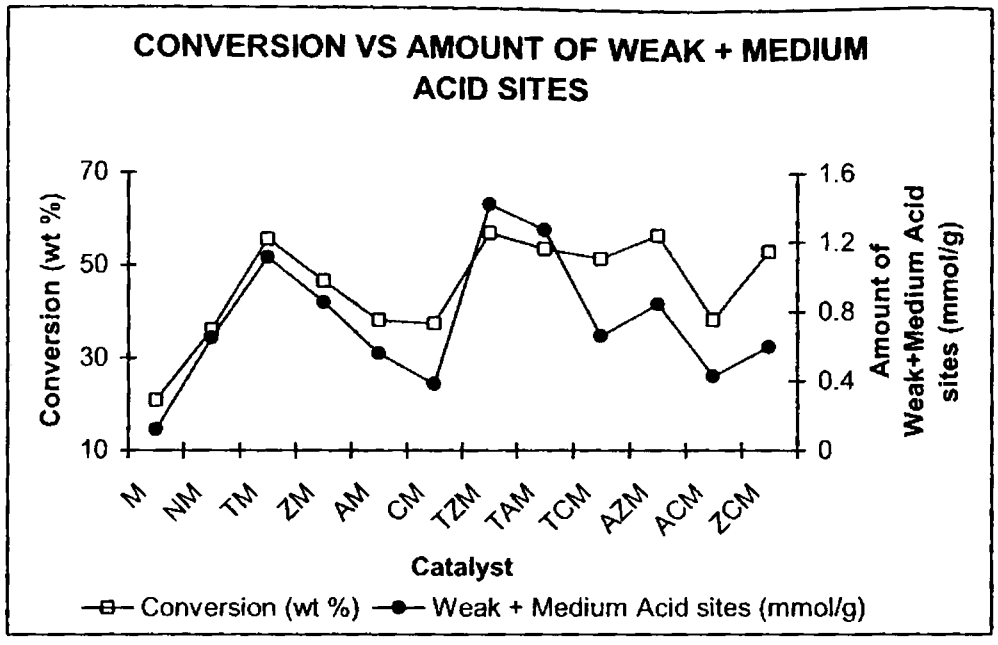

Figure 9.3.6 Dependence of conversion with the amount of weak + medium acidic sites

9.4 ALKYLATION OF BENZENE WITH 1-DECENE

Benzene alkylation with 1-decene produces 5-monoalkylated benzene isomers. The mechanism suggested in scheme 9.2.2 rule out the possibility for the formation of 1-phenyldecane due to highly unstable nature of the primary carbocation. Alkylation of benzene with higher 1-alkenes, typically C_{10}-C_{13}, is performed industrially for the manufacture of the LABs, an intermediate used in the production of biodegradable surfactants; Linear Alkylbenzene Sulphonates (LAS).

9.4.1 EFFECT OF REACTION CONDITIONS

The interaction of benzene with a straight-chain alkene affords all the possible secondary phenyl alkanes. The isomerization of the alkylating agent and, under certain conditions, of the product alkylbenzene is well established[23]. The extent of these two types of isomerization, which determines the final isomer distribution of the product, has been found to depend on the reaction conditions. The influence of reaction conditions are studied to get high conversion with good 2-phenyl LAB selectivity. TZM is used as the reference catalyst for optimization studies.

9.4.1.1 Effect of WHSV

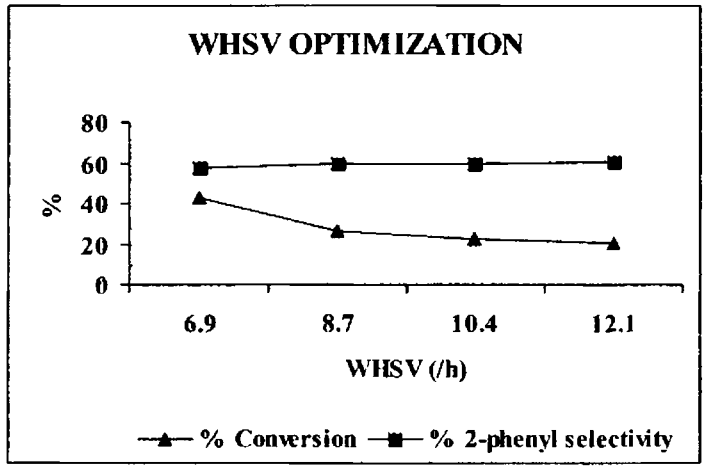

Figure 9.4.1 Effect of WHSV of 1-decene conversion at a temperature of 200°C, Benzene/1-decene molar ratio 20:1, Time on stream 2 h and Catalyst weight 0.5 g

Figure 9.4.1 shows the influence of contact time of the reactant with the catalyst. As expected there is a decrease in conversion with WHSV. The possibility of higher substitution also decreases with space velocity. As in the case of alkylation with 1-octene decrease in contact time decreases hydride shift and thus increases the 2-phenyldecane selectivity. Here the rate of alkylation competes over isomerization to get high 2-phenyl alkane selectivity. There is a sharp drop in conversion when WHSV is increased from 6.9 h^{-1} to 8.7 h^{-1}, but the increase in selectivity is only to a small extent and thus we selected 6.9 h^{-1} as the optimum one.

9.4.1.2 Effect of molar ratio

Solvent effect of benzene increases the 2-phenyl LAB selectivity with increase in molar ratio. At molar ratio of 1:1 this effect is found to be practically absent. Increase in the molar ratio of arene/alkylating agent is again favored due to the decreased amount of higher substitution. The formation of highly substituted product is decreased due to the low availability of decene at a high benzene/decene molar ratio. Figure 9.4.2 shows the influence of molar ratio on conversion and selectivity. Both increases with molar ratio, the increased selectivity is due to the solvation of the reaction intermediates by benzene molecules that reduces the differences in their stabilities. This decreases the possibility of hydride shifts of the 2° carbocation towards the centre that leads to the formation of 3-, 4-and 5-phenyldecane (scheme 9.4.1). The solvation effect is already reported in certain aromatic substitution reactions[24,25].

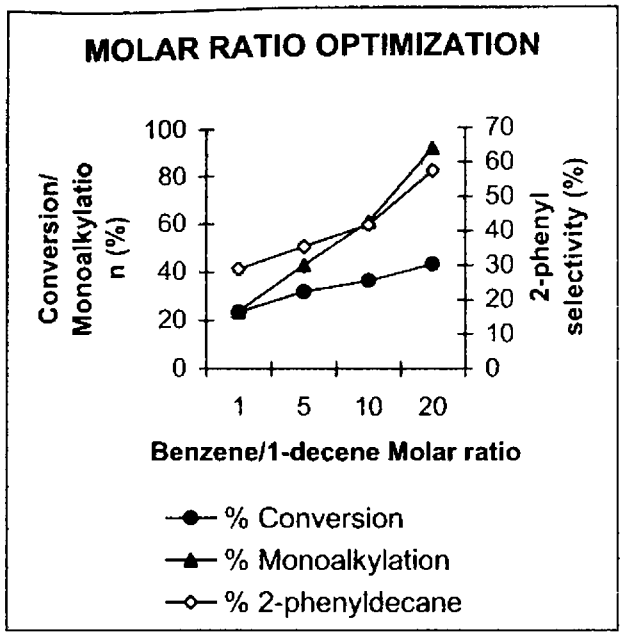

Figure 9.4.2 Effect of benzene/1-decene molar ratio on conversion and selectivity at a temperature of 200°C, WHSV of 6.9 h^{-1}, Time on stream 2 h and Catalyst weight 0.5g

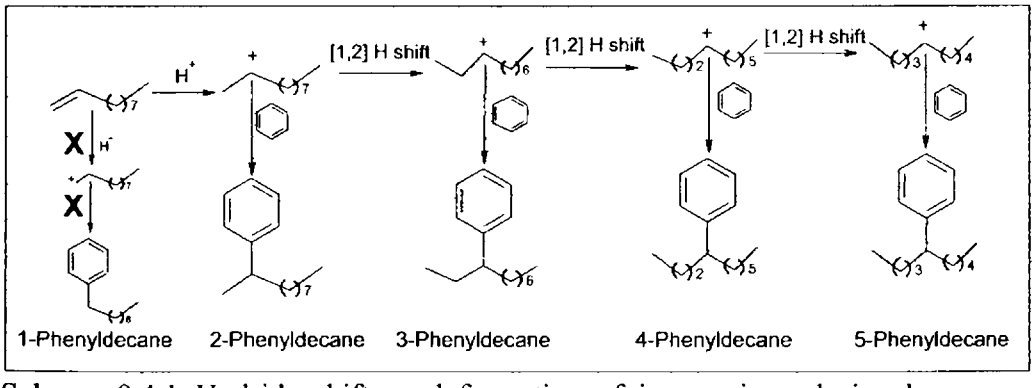

Scheme 9.4.1 Hydride shifts and formation of isomer ions during benzene decylation

9.4.1.3 Effect of temperature

Conversion increases at the expense of selectivity with increase in temperature from 200-400°C at a temperature interval of 50°C.

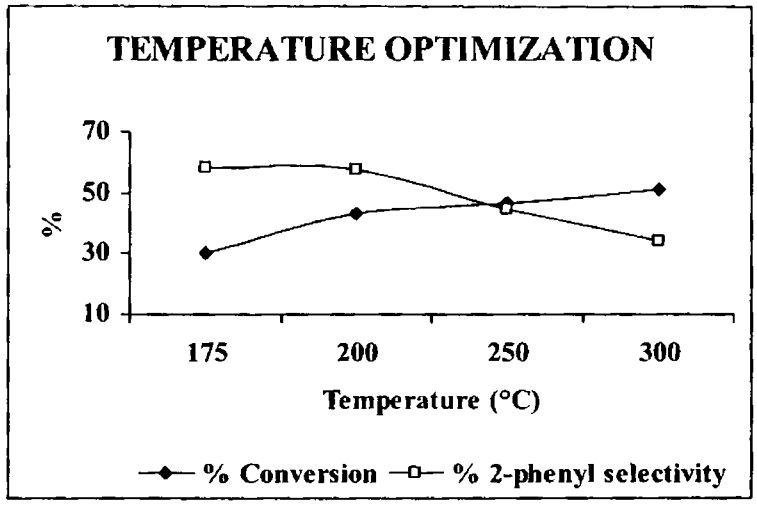

Figure 9.4.3 Effect of temperature on conversion and selectivity at a WHSV of 6.9 h^{-1}, benzene/1-decene molar ratio of 20:1, Time on stream 2 h and Catalyst weight 0.5 g

The decreased selectivity as evident from figure 9.4.3 may be due to the fast hydride shifts of the carbonium ion intermediate to produce the isomer ions[6]. This increases the probability of formation of other phenyl isomers 3-, 4- and 5-phenyldecane. The total conversion increase and decrease of selectivity may also be due to cracking and higher substitution. Thus to get good 2-phenyldecane selectivity we selected a temperature of 200°C for further studies.

9.4.2 COMPARISON OF CATALYTIC EFFICIENCY OVER DIFFERENT SYSTEMS

Table 9.4.1 Conversion and selectivity values of benzene alkylation with 1-decene at 200°C

Catalyst	Conversion (wt %)	Selectivity (%)			
		Monoalkylation	2-phenyl decane	Higher substitution	Cracking
M	14.8	94.7	27.7	1.3	4.0
NM	20.5	61.0	38.3	18.2	20.8
TM	35.9	100.0	65.2	-	-
ZM	35.8	79.5	45.3	12.5	8.0
AM	29.4	100.0	48.5	-	-
CM	26.3	79.9	49.5	8.0	12.1
TZM	43.4	91.6	57.5	5.3	3.1
TAM	42.0	100.0	50.6	-	-
TCM	39.4	94.1	36.1	4.7	1.2
AZM	41.5	96.9	55.2	2.0	1.1
ACM	18.1	100.0	64.0	-	-
ZCM	24.6	100.0	66.8	-	-

Benzene/1-decene molar ratio 20:1, Time on stream 2 h, WHSV 6.9 h-1 and Catalyst weight 0.5 g

The conversion is found to be very low over M and NM. Over NM, cracking as well as higher substitution is found to be the major side reactions. PILCs decrease these side reactions with increased monoalkylated product

formation. From the table 9.4.1, it is clear that many systems show 100% monoalkylated product. 2-phenyldecane selectivity is very good when compared to the conventional homogeneous acid catalysts. Among the different phenyl LABs, over the PILC catalysts formation of 5-phenyl isomer is practically absent.

9.4.3 DEACTIVATION STUDIES

Alkylation with 1-decene, over clay catalysts in a continuous run shows very fast deactivation as in the case with 1-octene. Both M and NM become completely deactivated from 4th hour onwards (figure 9.4.4).

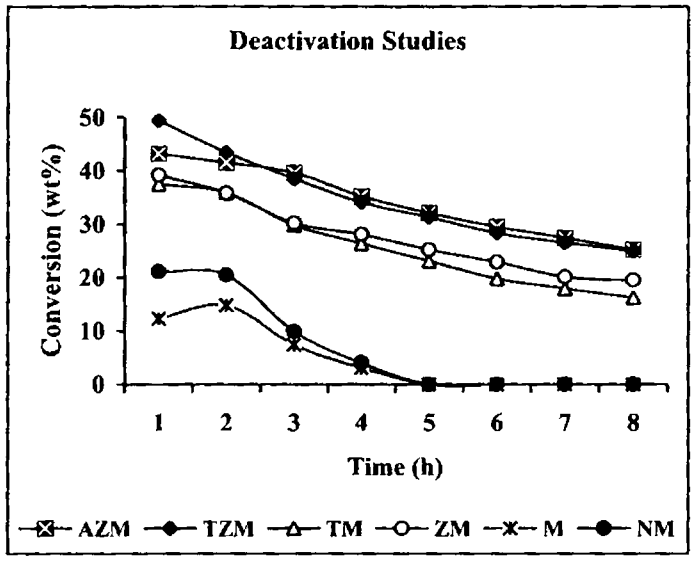

Figure 9.4.4 Deactivation profile of pillared, ion exchanged and parent Montmorillonite in continuous run

The percentage retention of the initial activity is found to be high over the mixed pillared systems (60.7% - AZM & 57.3% - TZM) than single pillared systems (45.1% - TM & 54.5% - ZM). Good retention in the initial activity implies that coke formed during the reaction is not so bulky to block all the catalytically active sites (pores) of the PILCs.

9.4.4 REGENERATION OF THE CATALYSTS

Because of the low reaction temperature, the carbonaceous compounds formed in the pores from polymerized products (alkene polymerization and polyalkylation of benzene) may be considered as liquid coke. It may diffuse out of the pores under high temperatures, regenerating the catalyst's porous network. Regenerability of the deactivated PILC catalysts is found be 100% up to four repeated cycles where the unpillared systems are nonregenerable.

9.4.5 ACTIVITY -ACIDITY RELATIONSHIP

The activity of benzene alkylation with 1- decene shows a similar trend with Brønsted acidity like that with 1-octene. Figures 9.4.5 and 9.4.6 compares conversion with Brønsted acidity obtained from cumene cracking as well as TPD of NH_3. The positive effect of increased acidic strength on the alkylation activity when compared to the side reaction is highly demanding over solid acid catalysts. The alkylation is more demanding than cis–trans isomerization of the alkenes and/or the double bond migration[26]. Therefore, the selectivity

towards the 2-phenyldecane isomer should vary with the ability of the site to promote alkylation versus isomerization.

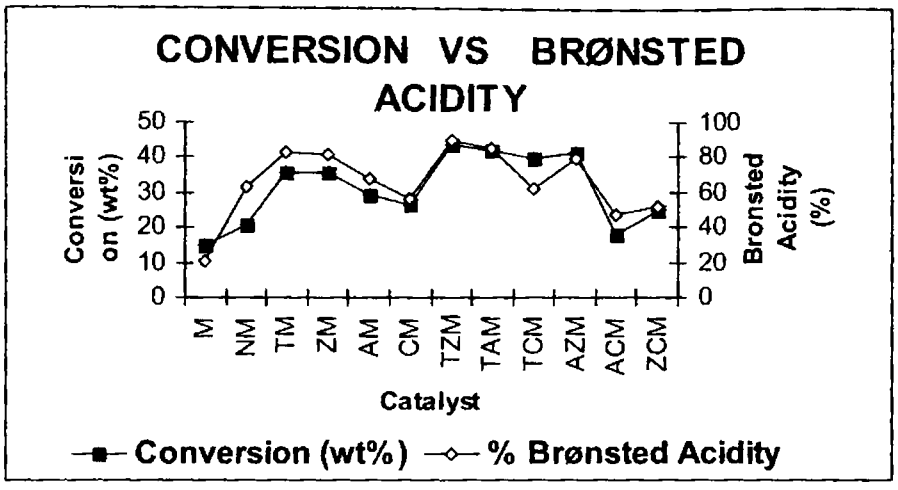

Figure 9.4.5 correlation diagram of conversion with % Brønsted acidity

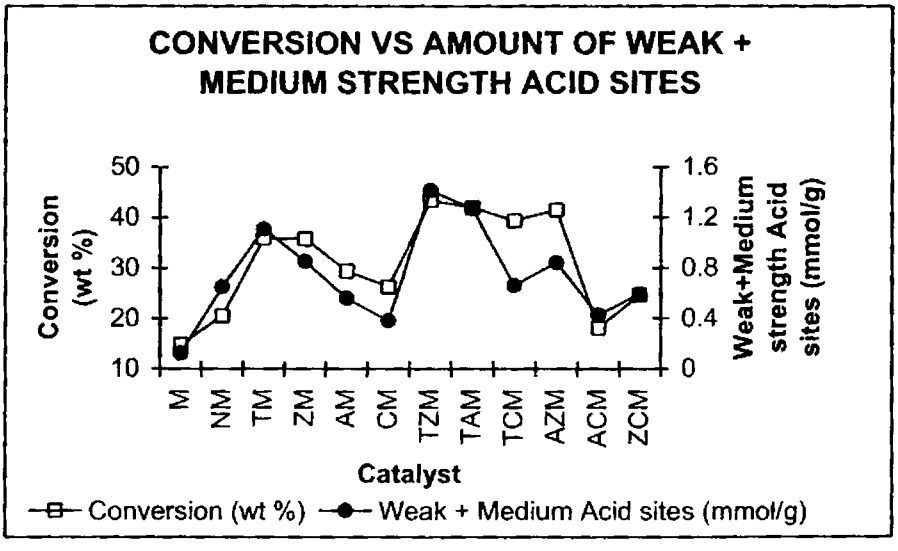

Figure 9.4.6 Dependence of conversion with the amount of weak + medium acidic sites

Thus selectivities towards the 2-phenyl isomer should increase with acid strength. Figure 9.4.7 shows the variation of the selectivity in 2-phenyl isomer as a function of total acidity. The curves clearly indicates that the higher the acid strength, the higher the selectivity to 2-phenyldecane. Cr containing pillared systems shows high selectivity eventhough they have low total acidity values, which may be due to their comparatively lower d-spacing that offer high steric constraints for the formation of bulkier isomers.

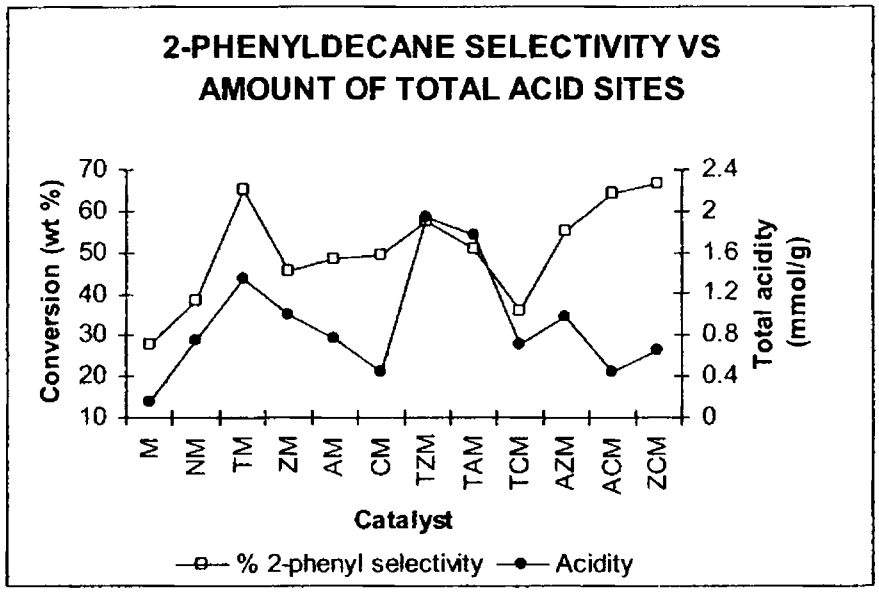

Figure 9.4.7 Plot of 2-phenyl isomer selectivity versus total acidity

9.5 ALKYLATION WITH 1-DODECENE

Alkylation with 1-dodecene is very important in LAB synthesis due to the wide application of 2-phenyldodecane sulphonicacid in detergent industry.

The reaction is done over various systems in the same conditions as that with 1-decene.

9.5.1 COMPARISON OF DIFFERENT CATALYSTS

The 1- phenyl isomer is not formed over the present catalysts due to the much lower stability of the primary carbocation compared to the secondary carbocation. The formation of internal isomers is also expected as a result of the hydride shifts of the initially formed secondary carbocation towards the centre to form isomer ions. Hydride shifts enhance the stability of the initially formed carbocation. At a high molar ratio of benzene, solvation of these carbocation occur which decreases the difference in their stabilities. This decreases the possibility of hydride shifts that leads to the formation of isomer ions, when compared to the rate of alkylation. This increases the 2-phenyl alkane selectivity at a benzene /1-dodecene molar ratio of 20:1. The catalytic activity results are shown in Table 9.5.1

Table 9.5.1 Results of benzene alkylation with dodecene over various clays at 200°C

Catalyst	Conversion (wt %)	Selectivity (%)			
		Monoalkylation	2-phenyl dodecane	Higher substitution	Cracking
M	6.64	76.2	36.5	3.3	20.5

NM	19.8	69.8	45.3	18.2	12.0
TM	38.1	86.8	46.4	5.6	7.6
ZM	38.3	79.5	55.9	12.5	8.0
AM	40.7	89.0	51.2	5.2	5.8
CM	28.0	89.1	53.5	4.8	6.1
TZM	47.0	90.4	58.9	6.3	3.3
TAM	44.8	76.8	49.8	-	-
TCM	40.4	75.9	45.7	4.7	18.5
AZM	46.8	90.1	56.9	4.8	5.1
ACM	27.5	74.0	46.2	4.6	21.4
ZCM	32.4	84.9	46.3	5.1	20.0

Benzene/1-dodecene molar ratio 20:1, Time on stream 2 h, WHSV 6.9 h-1 and Catalyst weight 0.5 g

Parent montmorillonite shows very low conversion showing its inability in benzene alkylation with 1-dodecene. Eventhough M shows 76.2% monoalkylation selectivity, the 2-phenyl isomer selectivity is not in comparison with PILCs. The reason may be the fast hydride shifts of carbocation when compared to the rate of alkylation. The higher substitution is also found to be low over M where cracking is the major side reaction. Over NM higher substitution is also present to a notable extent. The conversion is high compared to M. All pillared clay systems show very good monoalkylation and 2- phenyldodecane selectivity. The side reactions are found to be minimal over pillared clays showing the efficiency of pillaring in shape selective catalysis of montmorillonite clays.

9.5.2 PRODUCT DISTRIBUTION: COMPARISON WITH CONVENTIONAL CATALYSTS

The product distribution of alkyl benzene will influence the detergent property enormously. Table 9.5.2 shows the comparison of the phenyl alkane isomer distribution for different processes in which different catalysts are used. Obviously, these processes exhibit a great difference in the selectivity of 2-phenyl isomers. The possible monoalkylated products are shown in scheme 9.5.1.

Table 9.5.2 Product distribution of various monoalkylated products

Catalyst	Selectivity (%)				
	2-phenyl dodecane	3-phenyl dodecane	4-phenyl dodecane	5-phenyl dodecane	6-phenyl dodecane
HF	20	17	16	23	24
$AlCl_3$	32	22	16	15	15
H_2SO_4	41	20	13	13	13
M	37	25	15	12	11
NM	45	25	13	10	8
TM	46	35	19	-	-
ZM	56	30	12	-	-
AM	51	31	18	-	-
CM	54	28	18	-	-
TZM	59	26	15	-	-

TAM	50	29	21	-	-
TCM	46	32	22	-	-
AZM	57	36	7	-	-
ACM	46	30	24	-	-
ZCM	46	35	19	-	-

Formation of 5- and 6-phenyl isomers over M & NM is due to the occurrence of reaction out side the pores due to the collapsed structure (as a result of high temperature calcinations that lead to low porosity) just like that in homogeneous catalytic systems.

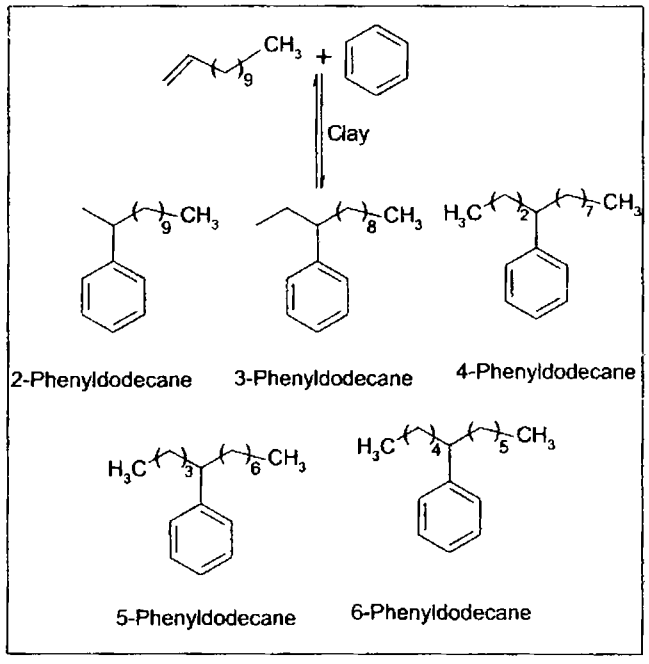

Scheme 9.5.1 Possible monoalkylated products formed during benzene dodecylation

As expected, 1-phenyl isomer formation is found to be absent over the studied catalysts. However, as with other solid catalysts, clays are easily deactivated. To industrialize a PILC process, one must study the deactivation systematically, and a convenient regeneration method is needed.

9.5.3 DEACTIVATION STUDIES

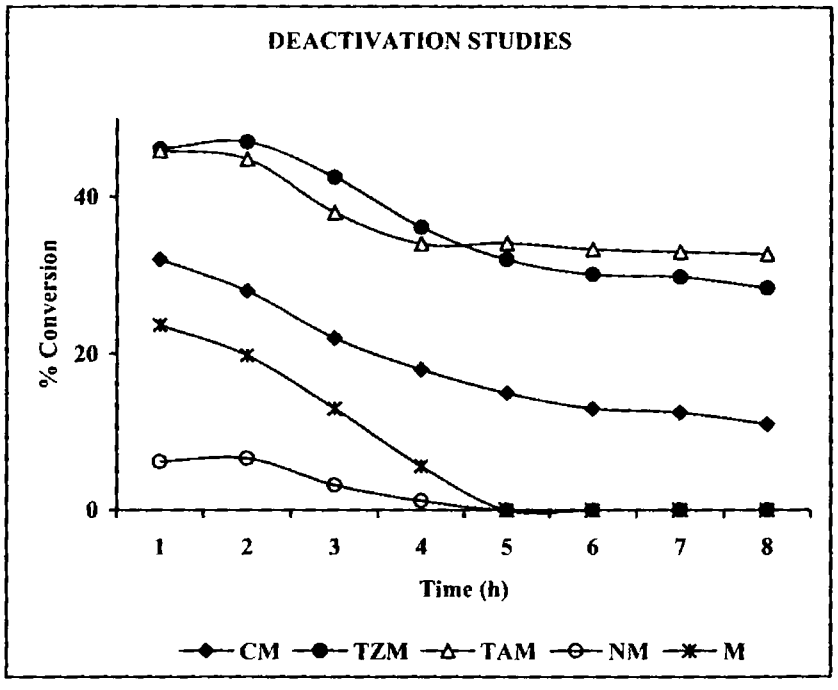

Figure 9.5.1 Deactivation profile of benzene dodecylation

During the reaction bulkier molecules blocks the channels and decrease the conversion of alkene remarkably, and the deposition of the bulkier molecules in the pores increases with increase in the reaction time. The

deactivation profiles of some selected catalysts in a continuous run of 8 hours are shown in figure 9.5.1. In addition, the sizes of alkyl benzene are bigger than those of the reactants, especially 5- and 6- isomers, which will slow down the diffusion of compounds in catalysts channels. During the reaction, the 5- and 6- isomers accumulate gradually, so the activity of the catalyst will decrease slowly until the catalysts are finally deactivated. This may be the reason for complete deactivation of M and NM from 4^{th} hour onwards. Over PILCs these isomers are not formed and the catalysts shows notable conversion even after 8 hours of continuous run, showing that the coke formed is not so bulky to block all the catalytically active sites.

9.5.4 CATALYST REGENERATION

For industrial application, the catalyst must be regenerated repeatedly. The regenerability of the deactivated clays is tested by burning off the coke formed in air at 500°C for 10 hours. All the PILC systems show complete regeneration up to 4 repeated cycles, where N and NM are found to be non-regenerable. The reason for the inactivity of M and NM even after complete coke removal may be due to the structural collapse occurring to the clay layers during continuous high temperature treatment. The metal oxide pillars, propping apart the clay layers, avoids the dehydration steps of the clay layers, preventing structural collapse.

9.5.5 ACIDITY-ACTIVITY RELATIONSHIP

The role of Brønsted acidity on the activity of various catalysts is investigated. Conversion is in perfect correlation with the Brønsted acidity obtained from two independent techniques. Figures 9.5.2 and 9.5.3 clearly shows the dependence of catalytic activity on the Brønsted acid sites.

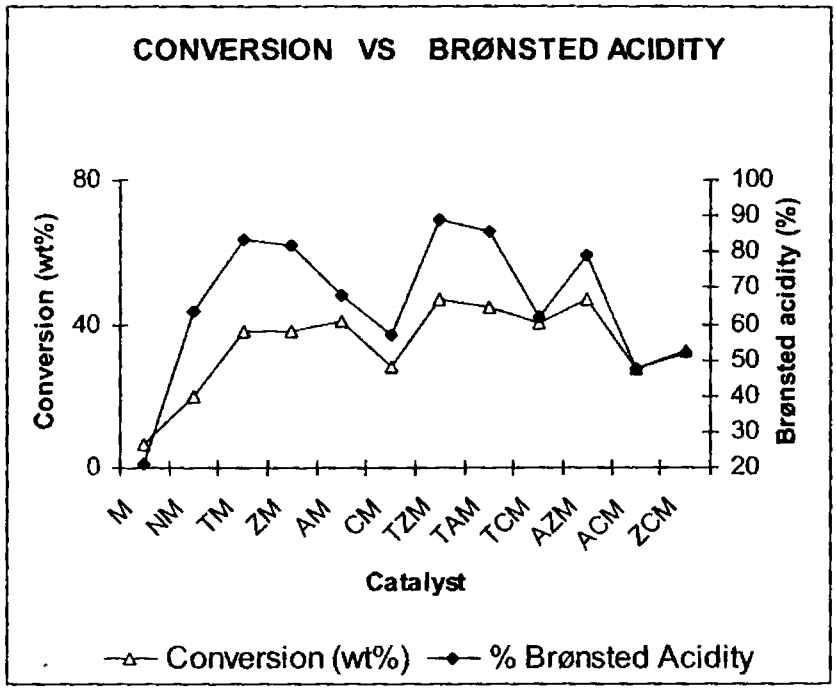

Figures 9.5.2 Correlation diagram of activity versus % Brønsted acidity

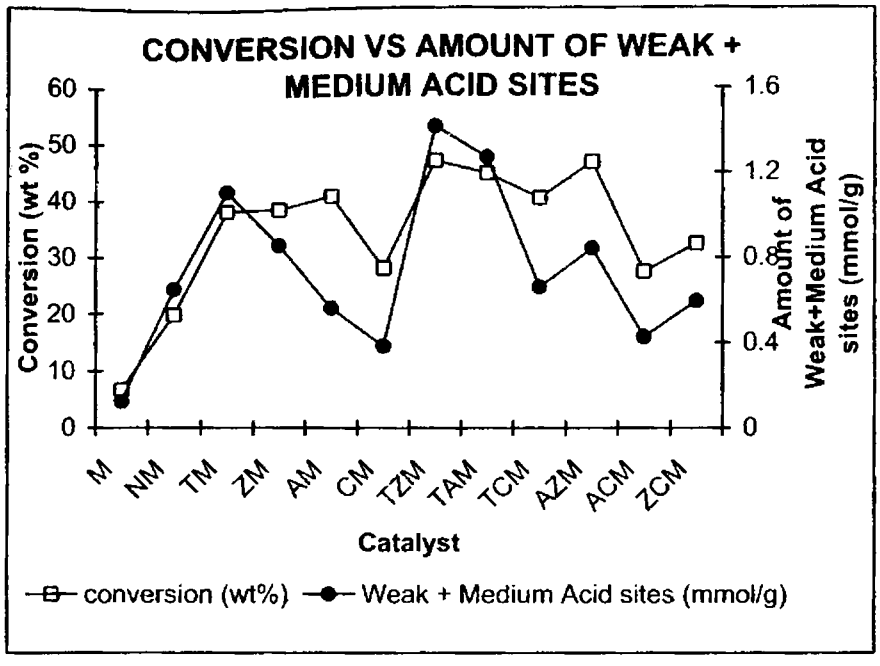

Figures 9.5.3 Influence of conversion with the amount of weak + medium acidic sites

9.6 EFFECT OF ALKYLATING AGENT IN LAB SYNTHESIS

We have adopted same conditions for the alkylation using 1-decene and 1- dodecene. From the comparison of conversions over various catalysts from table 9.4.1 and 9.5.1, it is observed that the 1-dodecene conversion is always greater than the 1- decene conversion. The effect of alkylating agent on the rate of Friedel-Crafts alkylation reactions is well documented. Conversion generally increases with chain length. For e.g. isopropylation occurs about 1460 times faster than ethylation[27].

9.7 CONCLUSIONS

- The montmorillonite clays show very good conversion in LAB synthesis upon pillaring.
- PILCs exhibit both product and transition state type shape selectivity favoring the formation the less bulky 2-phenyl isomer.
- Effect of reaction variables in catalytic efficiency is studied.
- The side reactions are found to be minimal over PILC catalysts.
- The comparison of product distribution with the conventional homogeneous catalysts reveals the promising nature of present PILCS.
- The role of Brønsted acidity on alkene conversion is well established.
- The increased conversion with length of the alkyl chain is found over PILCs.

REFERENCES:

1. R.M. Anstett, P.A. Munger, J. Rubinfeld, J. Am. Oil Chemists' Soc. 43

(1966) 25.

2. W.A. Sweeny, A.C. Olson, J. Am. Oil Chemists' Soc. 41 (1964) 815.
3. H.R. Alul, Ind. Eng. Chem. Prod. Res. Dev. 1 (1968) 7.
4. A.C. Olson, Ind. Eng. Chem. 52 (1960) 833.
5. B. Vora, P. Pujado, T. Imai, T. Fritsch, Chemistry and Industry. 19 (1990) 187.
6. B.V. Vora, R.P. Pugado, T. Imai, Chem. Ind. 19 (1990) 187.
7. S. Sivasanker, A. Thangaraj, R.A. Abulla, P. Ratnasami, Stud. Surf. Sci. Catal. 75 (1993) 397.
8. A. Mourran, P. Magnoux, M. Guisnet, J. Chim. Phys. 92 (1995) 1394.
9. L.B. Zinner, K. Zinner, M. Ishige, A.S. Araujo, j. Alloys Compounds. 193 (1993) 65.
10. R.T. Sebulsky, A.M. Henke, Ind. Eng. Chem. Process, Res. Dev. 10 (1971) 272.
11. J.L. Berna Tejero, A.M. Danvila, US Patent, 5146026, 1992
12. P. Meriaudeau, Y.B. Taarit, A. Thangaraj, J.L.G. Almeida, C. Naccache, Catal. Today. 38 (1997) 243.
13. S. Sivasanker, A. Thangaraj, J. Catal. 138 (1992) 386.
14. J.H.Clark, G.L. Monks, D.J. Nightingale, P.M. Price, J.F. White, J. Catal. !93 (2000) 348.
15. J.L.G. De Almedia, M. Dufaux, Y. Ben Tarrit, C. Naccache, JAOCS 71 (1994) 675.
16. A. Banerji, T.R. Fritsch, P.R. Pujado, Dewitt Petrochemical Review, Houston, TX, 19-21 March 1991.
17. T. Imai, J.A. Kocal, B.V. Vora, in: Y. Izumi, H. Arai, M. Iwamoto

(eds.), science and Technology in Catalysis 1994, Kodansha Ltd., Tokyo, 1995.

18. J.A. Kocal, US Patent 5, 196,574 to UOP, 1993.
19. M.F.Bentham, G.J. Gajda, R.H. Jensen, H.A. Zinnen, in: J. Weitkamp, B. Lucke (eds.), Proceedings of the DGMK Conference on Catalysis on Solid Acids and Bases, Berlin, Germany, 14-15 March 1996, p. 155.
20. J.L. Berna, A. Moreno, A. Banerji, T.R. Fritsch, B.V. Vora, in: Proceedings of the World Surfactant Congress, Montreaux, CH, September 1993,
21. Hydrocarbon Processing, March 1999, p. 91.
22. M. Han, Z. Cui, C. Xu, W. Chen, Y. Jin, Appl. Catal. A: Gen. 238 (2003) 99.
23. R.D. Swisher, E.F. Kaelble, S.K. Liu, J. Org. Chem. 26 (1961) 1066.
24. L.M. Stock, H.C. Brown, Advn. Phys. Org. Chem. 1 (1963) 49.
25. H.C. Brown, C.J. Kim, E.C. Scheppele, J. Am. Chem. Soc. 89 (1967) 376.
26. J.L. Goncalves de Almeida, M. Dufaux, Y.B. Taarit, C, Naccache, Appl. Catal. A: Gen. 114 (1994) 141.
27. J.E. Szulejko, T.B. Macmahon, J. Am. Chem. Soc. 81 (1993) 7839.

★★★★★★★★★★★★★★★★

Chapter 10

CONDUCTING POLYANILINE AND ITS NANOCOMPOSITES: INTRODUCTION, MATERIALS AND METHODS

Polymer systems with special properties are a field of increasing scientific and technical interest, offering the opportunity to polymer and synthetic organic chemists to synthesize a broad variety of promising new material, with a wide range of electrical and magnetic properties. Technological uses depend crucially in the reproducible control of the molecular and supramolecular architecture of the macromolecule via a simple methodology. Polyaniline is one such polymer whose synthesis does not require any special equipment or precaution. The formation of Polyaniline/montmorillonite nanocomposites with outstanding physical properties has considerable research attention due to its wide applications. In this chapter a general introduction to polyaniline and its clay nanocomposites are given revealing their importance in industry. The preparation conditions and various characterization techniques adopted for polyaniline/montmorillonite nanocomposites are also described.

10.0 INTRODUCTION

Polyaniline (PANI) is the typical phenylene based polymer having a chemically flexible -NH- group in the polymer chain flanked either side by a phenylene ring. The protonation, deprotonation and various other physico-chemical properties of PANI is due to the presence of the -NH- group[1]. It is the oxidative polymeric product of aniline under acidic conditions and has been known since 1862 as aniline black. At the beginning of the 20th century organic chemists began investigating the constitution of aniline black and its intermediate products. Willstatter et al.[2,3] in 1907 and 1909 regarded aniline black as an eight nuclei chain compound having an indamine structure.

During those periods it did not occur to anyone to investigate its electrical and magnetic properties for the obvious reason that organic compounds are insulators though in 1911 Mecoy and Moore suggested electrical conduction in organic solids[4]. Almost 50 years later Survile et al[5] in 1968 reported proton exchange and redox properties with the influence of water on the conductivity of PANI. It was reported in 1973 that conductivity of inorganic polymer poly sulphur nitride $(SN)_x$ is of the order of 10^3 Scm^{-1} to be comparable with $6x10^5$ Scm^{-1} for Cu and 10^{-14} Scm^{-1} for polyethylene. However, interest in PANI was generated only after the fundamental discovery in 1977 that iodine doped polyacetylene has a metallic conductivity[6], which triggered research interest in new organic materials in the hope that these would provide new and improved electrical, magnetic, optical material or devices. The hope was based on electronic structure and the combination of the

metal like or semiconducting conductivity with the processability and flexibility of classical polymers and above all, the ease with structural modification can be carried out via synthetic organic chemical methodologies.

A significant breakthrough occurred in 1979 by the discovery that poly(para-phenylene) could be doped to conducting levels quite comparable to those in polyacetylene[7-9]. This polymer is the first example of a non-acetylenic hydrocarbon polymer that can be doped with electron acceptors or electron donors to give polymers with metallic properties. This lead to the development of a new family of polymers, which with appropriate structural modifications can display conductivity from poor semiconductors comparable with that of copper.

The basic requirements of an organic material to become electrically conductive[10] are that the component molecules or basic repeat units must be arranged in close proximity with overlapping orbitals with large extension perpendicular to the plane of the molecule. They must possess electron withdrawing substituents or highly polarizable side groups attached to the chain. The arranged units must be in crystallographically similar environments. This condition implies that the location of electrons is forestalled. Most general feature for efficient charge transport in organic systems is the existence of equally spaced atoms or groups not all in the same oxidation state. Migrations of positive charges occur from one end of the molecule to the other. Such a system will be metallic if it were infinitely long.

There are two types of electrical conductors, ionic and electronic. Ionic conduction in polymers is associated with polyelectrolyte, whereas electronic conduction is associated with π-conjugated polymers and is a relatively new phenomenon.

10.1CONDUCTION MECHANISM IN CONJUGATED POLYMER

The reduction or oxidation process consists of adding or removing one electron to or from polymer chain, which causes the injection of states from the top of the valence band and bottom of the conduction band into the energy gap. This electronic excitation in polymeric material is accompanied by a distortion or relaxation of the lattice around the excitation, which minimizes the local lattice strain energy. The combined structural and electronic excitation will now look like a defect on the chain. From a chemical viewpoint, this defect is interpreted as a radical cation or radical anion, whereas physicists refer to it as a polaron which carriers both spin (1/2) and unit charge.

Removal or addition of a second electron from or to a polaron results in the formation of a bipolaron. A bipolaron is thus identified as a dication or dianion associated with a strong lattice site distortion, i.e. a bipolaron consists of two coupled polarons with charge equal to $2e^-$ and zero spin. The energy increase due to the coulombic repulsion (in the formation of a bipolaron) is compensated by the energy gained when the two charges share the same lattice distortion. Quantum chemical calculations indicate that the formation of bipolaron requires 0.4 eV less energy than the formation of two polarons.

Bipolarons must be formed by the coupling of pre existing polarons or possibly by the addition of charge to pre-existing polaron.

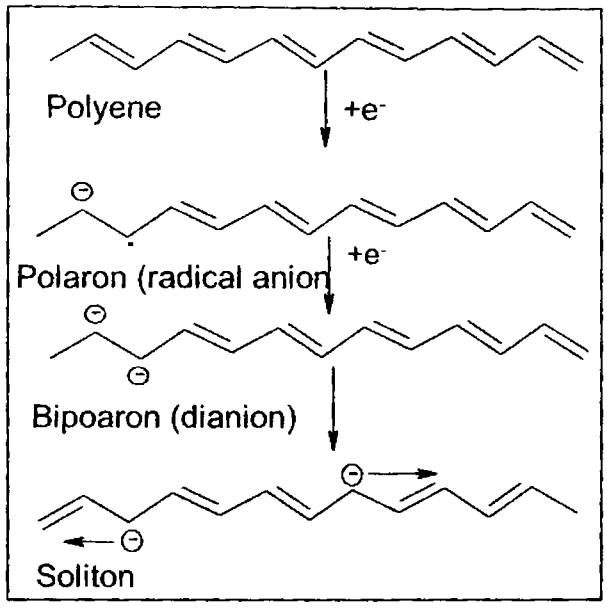

Scheme 10.1.1 Formation of charge carriers in conjugated polymer

In the case of polymers with degenerate ground state as in the case of polyacetylene, the charges can migrate apart to form solitons, i.e. two energetically equal structures at a point where they couple give a surface effect known as kink or a soliton. Soliton means 'solitary wave', implying a non-linear phenomenon involving non-dispersive transport of energy in a dispersive medium i.e. soliton has a movement. In a conjugated system soliton may be neutral, positively or negatively charged according to the number of electrons in the π-orbital. The separation of the charges is possible because a polyene

segment of equivalent energy is formed between the charges as they separate. The formation of polaron, bipolaron and soliton is represented in scheme 10.1.1.

10.2 POLYANILINE (PANI)

The interesting variety of electronic structures that distinguishes PANI from other common conducting polymers was known from an early study by Green and Woodhead[11]. Among all conducting polymers PANI has a special representation due to its easy synthesis, environmental stability, simple non-redox doping by protonic acids etc.

PANIs can be considered as being derived from a polymer, the base form of which has the generalized composition

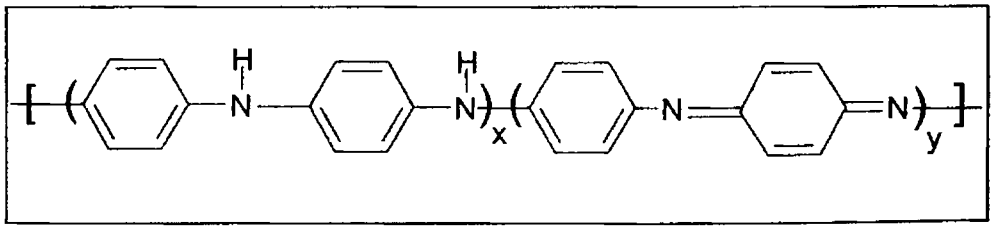

As seen from the above structure it consists of reduced and oxidized repeating units. The average oxidation state (1-y) can be varied continuously from zero, the completely reduced leucoemeraldine

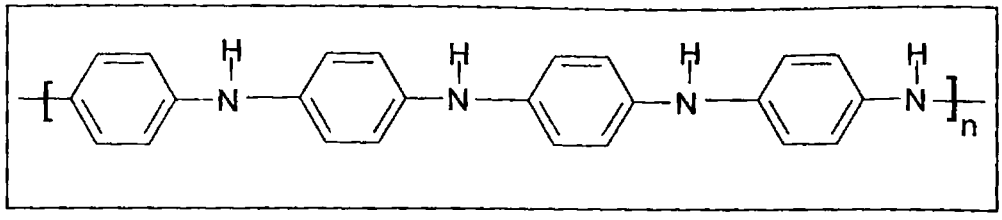

To half, the 'half oxidized' polymer emeraldine

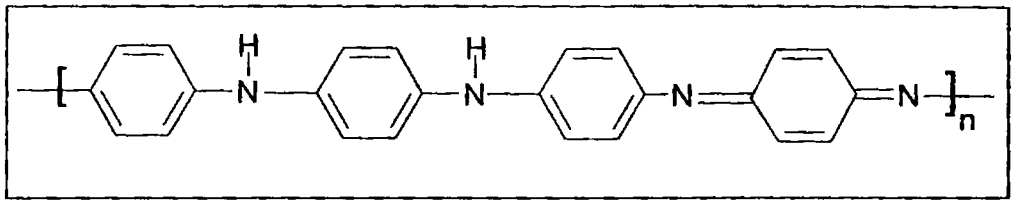

to one, the completely oxidized polymer pernigraniline.

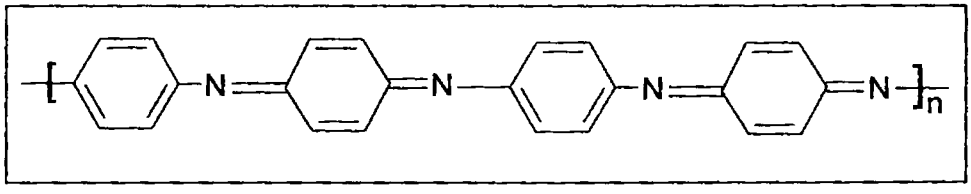

MacDiarmid et al.[12] described five oxidation states and colours of PANI as: fully reduced or leucoemeraldine, protoemeraldine, emeraldine, nigraniline and pernigraniline. Protoemeraldine and emeraldine are conducting forms in the protonated state.

10.3 SYNTHESIS OF PANI

Chemical methods[13] (figure 10.3.1) are widely employed for the synthesis of soluble and processable conducting polymers, electrochemical pathways are also used in several cases, and photochemical method is also known.

The simple polymerization process can be represented as

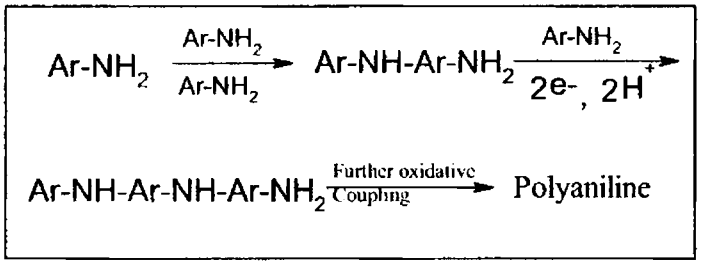

The most preferred method for synthesis is to use either HCl or H_2SO_4 with $(NH_4)_2S_2O_8$ as an oxidant[14-17]. Oxidative polymerization is a two electron change reaction and hence, the persulphate requirement is one mole per mole of a monomer. However, the smaller quantity of oxidant is used to avoid oxidative degradation of the polymer formed.

Several reports are there on the electrochemical synthesis of PANI[18]. Electrochemical polymerization is carried out by dissolving 0.1 mole of aniline in 1 mole protonic acid in distilled water at the platinum electrode by

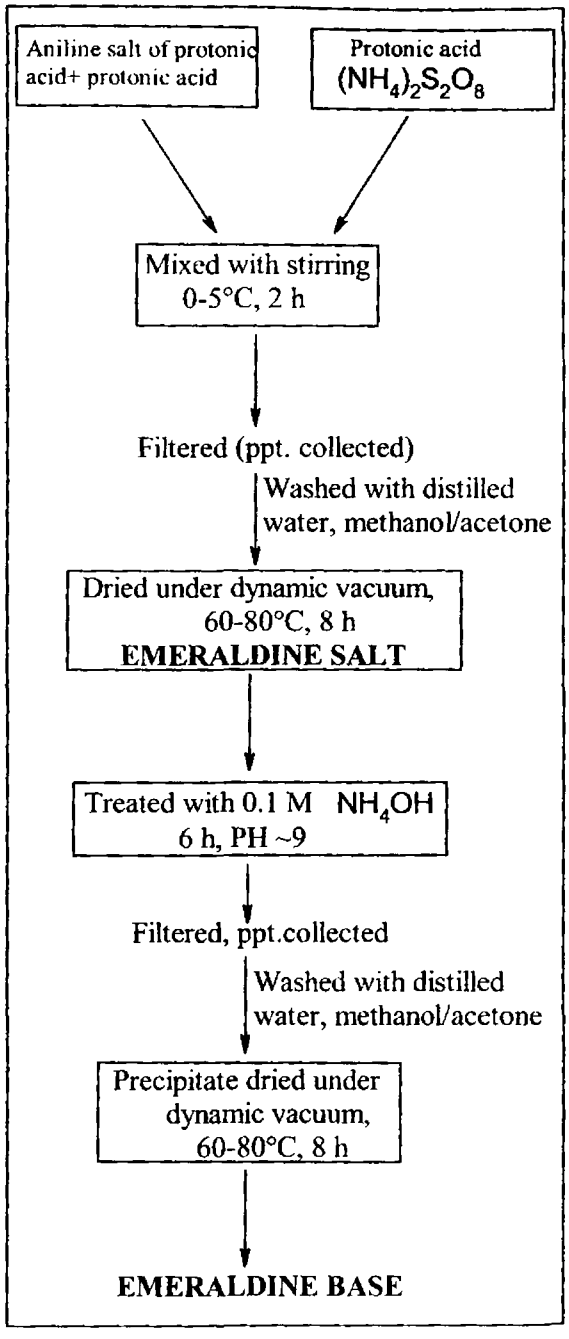

Figure 10.3.1 Flowchart for chemical synthesis of PANI

galvanostatic, potentiostatic or potentiodynamic methods as adopting the following conditions. Mechanism of PANI formation is shown in scheme 10.3.1.

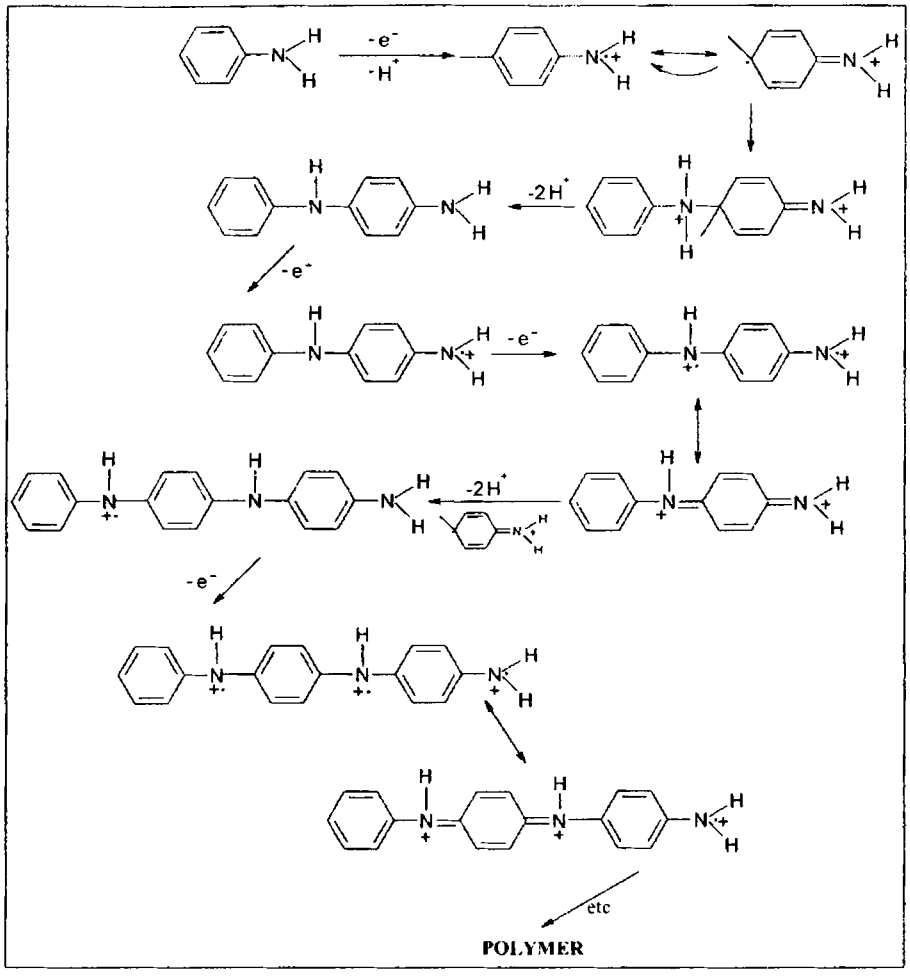

Scheme 10.3.1 Mechanism of electrochemical polymerization of aniline

1. Galvanostatic ⟶ constant current – Cd 1-10 mA during electrolysis
2. Potentiostatic ⟶ Keeping potential constant
3. Sweeping the potential ⟶ Between two potential limits - 0.2 to +1.0 vs SC

Electro polymerization appears to be a very straight-forward synthesis, but for a proper understanding of the phenomenon attention should be paid to the metal electrode/solution interface. Electrode materials normally used are transition and noble metals, whose electronic properties are governed by stronger localization of the d and f atomic orbitals, and the electronic work function of a metal plays an important role.

10.4 DOPING

The concept of doping is the unique, central, underlying and unifying themes, which distinguishes conducting polymers from all other types of polymers[19]. The controlled addition of known, usually small (≤ 10%) non stoichiometric quantities of chemical species results in dramatic changes in the electronic, electrical, magnetic, optical and structural properties of the polymer. Doping is reversible to produce the original polymer with little or no degradation of the polymer backbone[20,21].

Table 10.4.1 Conductivity of electronic polymers

		Conductivity (Scm^{-1})		Conductivity (Scm^{-1})
Metals	Ag, Cu	10^{8}	Doped trans	10^{5}
	Mg	10^{4}	$(CH)_x$	10^{3}
			Doped PANI	
Semi-conductors	Ge	10^{-2}	Trans $(-CH-)_x$	10^{-3}
	Si	10^{-4}		
Insulators	Nylon	10^{-10}	PANI	10^{-10}
	Quartz	10^{-16}		

Conductivity increases with doping as seen from table 10.4.1. By controllably adjusting the doping level, conductivity anywhere that of the non-doped and that of the fully doped form of the polymer can be easily obtained. Conducting blends of a (doped) conducting polymer with a conventional polymer (insulator), whose conductivity can be adjusted by varying the relative properties of each polymer, can be made. This permits the optimization of the best properties of each type of polymer. PANI provides the prototypical example of a chemically distinct doping mechanism[22].

Protonation by acid-base chemistry leads to an internal redox reaction and the conversion from semiconductor (emeraldine base) to metal (the emeraldine salt) (scheme 10.4.1). The chemical structure of the semiconductor

emeraldine base form of PANI is that of an alternating copolymer. Upon protonation of the emeraldine base to the emeraldine salt, the proton induced spin-unpairing mechanism leads to a structural change with one unpaired spin per repeating unit, but with no change in the number of electrons.

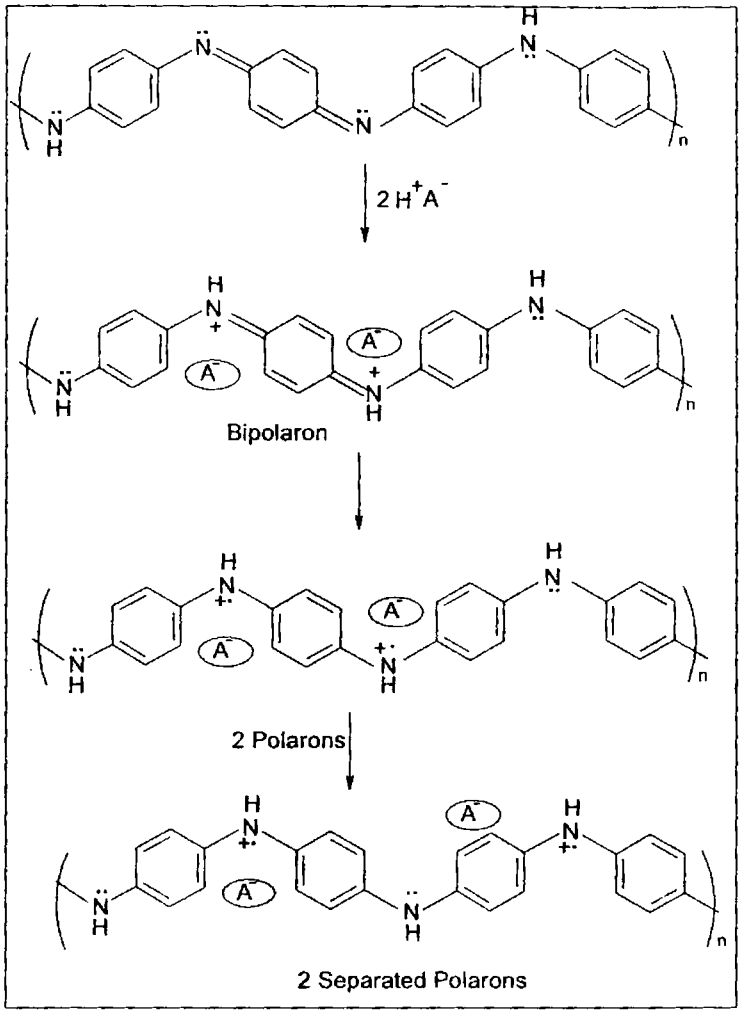

Scheme 10.4.1 Internal redox reactions leading to the formation of polaron and bipolaron as a function of dopant

The result is a half filled band and potentially, a metallic state where there is a positive charge in each repeating unit (from protonation) and an associated counter ion such as Cl^-, HSO_4^-, dodecyl benzene sulfonate etc.

PANI on doping to emeraldine salt form, undergoes an insulator to metal transition with a concomitant conformational change in the polymer back bone to accommodate this electronic transition. Zheng et al[23] have suggested that this conformational change from compact coil to expanded coil is initiated by a proton doping mechanism, which generates (without loss of electrons) charge carriers along the backbone. The columbic repulsion of these polarons forces the polymer chain to adopt a more planar conformation. The result of this conformational change is a reduction of structural defects along the PANI chain, which increases the π-orbital overlap between the phenyl π-electron and nitrogen p-electrons. This, in turn increases both conjugation of the chain backbone and the polaron delocalization length. However, due to this conformational change, and greater polarity of the ionomeric form, the solubility of salt form is markedly reduced in dimethyl sulfoxide (DMSO) and N-methyl pyrrolidone (NMP) solvents compared to PANI base. This has resulted in PANI being often categorized as an intractable polymer. Recently, several methods has been reported to dissolve and process PANI in NMP, selected amines, conc.H_2SO_4 and other strong organic acids.

The melt and solution processability of PANI can be increased by protonation of PANI with a functionalized protonic acid. A functionalized protonic acid is generally denoted as $H^+(M^-R)$, where H^+M^- is the protonic

acid group which may be sulphonic acid, carboxylic acid, phosphonic acid, sulphate or phosphate etc and R is an organic group. The proton of the protonic acid reacts with imine nitrogens of PANI and convert the base form to the conducting salt form; the (M^--R) group which serves as the counter ion. The R functional group is chosen to be compatible with non-polar or weakly polar organic solvents (e.g. dodecyl benzene sulphonic acid and camphor sulphonic acid). The organic substituted groups lead to solubility in common solvents such as toluene, xylene, chloroform etc and to compatibility with bulk polymers with similar molecular structure. The functionalized counter ions act as surfactants that enable intimate mixing of PANI in a variety of bulk polymers. PANI can be made soluble by substituting one or more hydrogens by alkyl, alkoxy, aryl, hydroxyl, amino or halogen groups in an aniline nucleus.

10.5 PANI – MONTMORILLONITE NANOCOMPOSITES

With the advent of newer and newer technologies, the demand for materials possessing a combination of a wide range of desirable properties is increasing day by day. One of the techniques to develop such materials is the formulation of composites from compatible materials individually possessing the desirable properties. In view of light weight, low cost, low temperature fabrication as well as mechanical strength and environmental stability, electrically conducting polymer, PANI with inorganic materials to form composites are important. Thus conducting polymers such as PANI have

attracted great attention from researchers engaged in the research and development of new materials for various areas of modern engineering[24].

The introduction of an organic guest into an inorganic host material by the intercalation technique has resulted in the fabrication of nanocomposite materials with high potential for advanced applications[25]. These nanocomposites consist of multilayered sandwich – like elements in which polymer chains are sandwiched between ultrathin sheets of an inorganic particle[26]. Such confinement of polymer molecule is expected to lead to a high degree of polymer ordering and enhanced thermal and oxidative stability which is hard to find in pristine polymers.

It is important to note that many fundamental applications have become possible due to the use of nanoscale structural models for conducting polymers. Nanocomposites based on conducting polymer[27] and different inorganic compounds are the representatives of the further development of ideas about nanostructuring, because such nanocomposites display novel and frequently important mechanical, electronic, magnetic, optical and catalytic properties inaccessible to both individual components of the nanocomposites and their micro analogues[28,29]. The applications of polymer and inorganic materials includes as flame retardant, selective gas permeability[30,31] and other synergistic properties that cannot be attained from individual materials[32,33].

Bein et al.[34,35] demonstrated that encapsulation of PANI in a three dimensional host lattice (i.e. zeolites) and also reported the preparation of

conducting PANI filaments in a channel of mesoporous host MCM-41. This represents an important step towards the design and understanding of well defined conducting structures for nanometer scale electronic devices. Of the many possible organic guest/inorganic host combination available for study, the intercalation of PANI into layered compounds has received a great deal of attention and interest in the past decade. Many hybrid composites such as PANI/$VOPO_4.2H_2O$[36], PANI/FeOCl[37], PANI/MoO_3[38], PANI/V_2O_5[39], PANI/graphite oxide[40], PANI/clay[41-46]etc have been synthesized and studied. The combination of conducting polymer with host materials having different characteristics leads to new hybrid materials with novel properties and different conformation of polymer chains in the interlayer space may enable to further characterize the polymer structure.

Nano silicate layers leads to nanocomposites with important tensile strength and modulus, reduced gas permeability and decreased thermal expansion coefficient when compared with micro and macro composites counterparts and pure polymer matrix because of the high aspect ratio (width to thickness, 100~1000) of silicate layers and large surface area available for contact with the matrix polymer.

Clays among other hosts are natural, abundant and inexpensive mineral that have unique layered structure, high mechanical strength as well as high chemical resistance. Adoption of montmorillonite clay to the field of nanocomposites lies in its small particle size (<10 μm), ease of intercalation, easy hydration and capability to contain various organic/inorganic materials[47].

Their lamellar elements display high in-plane-strength, stiffness as well as high aspect ratio[48]. Montmorillonite is the most abundant naturally occurring clay mineral.

Present study includes the preparation of PANI/montmorillonite composites and its characterization to know the nanocomposite structure. The confined, enhanced and non-expandable pillared clay (PILC) layers offer high polymer ordering within the matrix. The catalytic environment of montmorillonite allows efficient polymerization that allows high degree of polymer order and the restricted PILC matrix allows the formation of PANI nanofibers within the matrix.

The experimental procedure and characterization techniques used are discussed below. Next chapter discusses the results of nanocomposite fibers prepared over PILCs.

10.6 PREPARATION OF PANI/PILC NANOCOMPOSITES

The study of conducting polymers has become a major part of modern material science and in many institutes and commercial establishments involves multidisciplinary research into chemical synthesis, polymer preparation, electronics, physics and applied physics. The combination of metal-like or semiconducting conductivity and processability of classical polymers has created opportunities for scientists and technologies to investigate possible technological applications.

The most important characteristic of monomer molecules for the formation of conducting polymer is the requirement for the conversion of a closed shell system to a corresponding cation or anion radical and the stability of the product to form during the process. PANI is generally prepared by either chemical or electrochemical oxidation of aniline under acidic conditions. The control of the morphology of conducting polymers is a very stimulating challenge. The confined media polymerization of these conducting polymers is a very pertinent way to give them controlled shape and dimension.

PANI nanocomposites are prepared using PILCs as the inorganic host material.

Materials	Suppliers
Aniline	Merck
Ammonium peroxodisulfate	Qualigens
Hydrochloric acid	Qualigens
Ethanol	s.d.Fine chemicals
Acetone	s.d.Fine chemicals
Montmorillonite, KSF	Aldrich
Na+-Exchanged Montmorillonite	
PILCs	

All materials are of high purity and used as it received

The nanocomposite is prepared by in-situ intercalative polymerization of aniline. The PILC is added to 1 M HCl aqueous solution and is stirred for 1

h. Aniline monomer is then added to this colloidal suspension of clay in a ratio of 50 mmol aniline/g clay, stirred for the intercalation of aniline into the silicate layers and is kept at 0°C. Ammonium persulfate, $(NH_4)_2S_2O_8$, dissolved in 1M HCl is added slowly to solution containing aniline and PILC at an aniline/oxidant molar ratio of 1:1.25, then stirred for 8 h and is kept overnight. The nanocomposite is separated by filtration and washing with acetone, methanol and distilled water. This is done to remove oligomers, excess oxidant and residual aniline monomer. The dark green PANI/Montmorillonite composite thus obtained is dried at 50°C. The washing for the removal of excess monomer and oligomers formed are done by extraction in a soxhlet apparatus.

The composites obtained are designated as PM, PNM, PXM and PXYM respectively when the clays are M, NM, XM (single PILCs) and XYM (mixed PILCs).

10.7 CHARACTERIZATION OF PANI/MONTMORILLONITE NANOCOMPOSITES

A thorough characterization of the composites are needed to know the extent of hybrid formation, structure of PANI within the layers, the polymer order, morphology, nature of charge carriers and stability of the polymer backbone within the layer. Here the different characterization techniques used and the results available are discussed. All instruments for the characterization studies are the same which is used in clay characterization.

10.7.1 FTIR ANALYSIS

PANI as described in 10.2 possess various structures among which emeraldine form is commonly found and promising with emeraldine salt possessing high conductivity. FTIR analysis reveals the chemical structure because the amount of energy (IR radiation) adsorbed is a function of the number of molecule present and provides both qualitative and quantitative information. In addition it gives an idea about the extent of oxidation and degree of protonation in the polymer chain. Infrared spectroscopy is a powerful tool to determine the structural changes that occur during doping. Various groups have reported FTIR results of PANI[50-56]. Generally, spectra of the composite show characteristic vibrations of both clay as well as the polymer. The peaks due to the benzenoid ring of PANI are present at around 1500 cm^{-1}, 1512 cm^{-1}, 1484 cm^{-1}, 1289 cm^{-1}, and 824 cm^{-1}. Peaks at around 1581 cm^{-1}, 1172 cm^{-1}, and 800 cm^{-1} correspond to quinoid ring. The Si-O-Si stretching frequency of the clay matrix (~1050cm^{-1}) present in the composite confirms the retention of basic clay structure[57].

10.7.2 UV-VIS DRS ANALYSIS

The possible electronic transitions give an idea about the type charge carriers present in the PANI/montmorillonite nanocomposites. The diffuse reflectance spectra of PANI/montmorillonite shows peaks due to π- π^* (325-360 nm), polaron - π^* (400-430 nm) and π - polaron (780-826 nm) when PANI is in the doped state[58,59].

10.7.3 XRD PATTERNS

XRD patterns of the PANI/Montmorillonite composites gives 2 types of observations. First one is the information about whether PANI is intercalated between the clay layers or not. In the case of montmorillonite as well as ion exchanged montmorillonite there is layer expansion as a result of polymer intercalation. This is found from the shift in 2θ value of ~8.9° in montmorillonite corresponds to the periodicity in the direction of (100) plane of the clay sample. Intercalation of PANI between the clay layers is evident from the shift of the peak towards left from Bragg equation. It is not possible in PILCs where appreciable layer expansion is already present but, the retention of the expanded layer structure may indicate that PANI polymers formed within the layers are in the order of nanometer range (<23 Å).

The second information available from the XRD is about the crystallinity and thus the polymer order in the nanocomposite. High order leads to improved properties.

10.7.4 SEM ANALYSIS

The nanocomposite formation and the morphology of PANI within the matrix of clay layers are clearly seen from SEM pictures. Knowing the morphology allows the tuning of the composite to the required application.

10.7.5 TG/DTG ANALYSIS

The composite shows a four step weight loss in thermogravimetric analysis. The first weight loss just below 100°C is attributed to the loss of water from PANI as well as from the interlayer galleries of clay. The second weight loss ranging from 200 - 300°C is due to the elimination of dopant HCl present[60]. The third weight loss is assigned to the thermal decomposition of PANI backbone chains[61]. The weight loss around 620°C is attributed to the dehydroxylation of silicate structure. The polymer backbone breakage for pure PANI is at 530.6°C[62]. In composite this is shifted to high temperature which may be due to the additional stability inside the matrix due to the restricted motion.

10.7.6 CONDUCTIVITY MEASUREMENTS

Conductivity is the reciprocal of specific resistance or resistivity, ρ. It can be designed as the conductance of $1cm^3$ of a material.

Conductivity = (t/a) x (1/R) Scm^{-1}, where

t = thickness of the conductor

a = cross sectional area

R = resistance of the conductor

To determine the value of an electrical resistance of PANI composite, the dried samples were palletized and placed in between two electrodes which

were connected to a voltmeter. By applying a known current the resistance of the pellet was measured directly from the voltmeter.

$R = V/I$

R - Resistance

V - voltage drop across the resistance due to current 'I' passing through the resistance.

Conductivity of pure emeraldine salt with HCl dopant lies in the order of 10^{2}-10^{3}. Composite formation with insulator clay will decrease the conductivity which lies in the order of 10^{-1}-10^{-2}. Anyway the conductivity can be tuned to a great extent to required level by varying the dopant concentration[63]. The dc conductivity of PANI/clay composites at room temperature are measured through a linear four-probe Keithley resistivity set up.

10.8 CONCLUSIONS

- PANI is found to be one of the most important conducting polymers.

- Conductivity is due to the presence of conjugated double bonds, where delocalization is possible.

  Composite formation is a widely used method for improving the properties and processability of polymers.

- Clays, having a unique layer structure are important inorganic host material for the hybrid nanocomposite formation.

- PANI/montmorillonite nanocomposites are prepared by using $(NH_4)_2S_2O_8$ as the initiator oxidant following the in-situ intercalation of the monomers within the layers and subsequent oxidative polymerization.

- FTIR shows the structure of PANI inside the layers and the basic clay layer retention.

- UV–Vis DRS Analysis shows the possible electronic transition over the PANI chain.

- XRD patterns show the intercalation and the crystallinity of PANI within the layers.

- The morphology of the nanocomposite formed is studied from SEM photographs.

- TG/DTG shows the temperature of PANI backbone breakage in composites.

REFERENCES:

1. Handbook of organic conductive molecules and polymers, H.S. Nalwa, (ed) John Wiley & Sons, Vol.1-4, 1997.
2. Wilstatter, Moore, Ber. 40 (1907) 2669.
3. Wilstatter, Dorogi, Ber. 42 (1909) 2147.
4. H.N. Mecoy, W.C. Moorer, J. Am. Chem. Soc. 33 (1911) 273.
5. R. Surville, N. Jose Fowicz, L.T. Yu, J. Perichon, R. Buvet, Electrochin. Acta. 13 (1968) 1451.
6. H. Shirakawa, E.J. Louis, A.G. MacDiarmid, C.K. Chiang, A.J. Heeger, J. Chem. Soc. Chem. Commun. (1977) 578.
7. L.W. Shacklette, R.R. Change, D.M. Jvory, G.G. Miller, R.H. Banghman, Synth. Met. 1 (1979) 307.
8. D.M. Jvory, G.G. Miller, J.M. Sawa, L.W. Shacklette, R.R. Change, R.H. Banghman, J. Chem.. Phys. 71 (1979) 1506.
9. B.C. Trivedi, J. Chem. Soc., Chem. Commun. (1989) 544.
10. C.K. Chiang, C.R. fincher, Y.W. Park, A.J. Heeger, H. Shirakawa, E.J. Louis, Phys. Rev. Lett. 39 (1977) 1098.
11. R.K. Paul, Ph.D thesis, Kerala University, Kerala, India, 2000.
12. M.E. Jozefowicz, R. Laversamme, H.H.S. Javadi, A.J. Epsteim, J.P. Pouget, X. Tang, A.G. MacDiarmid, Phys. Rev. B. 39 (1989) 12958.
13. A.G. MacDiarmid, H. Shirakawa, A.J. Heeger, Angew. Chem. 40 (2001) 2574.
14. J.C. Chiang, A.G. MacDiamid, Synth. Met. 13 (1986) 193.

15. S.P. Armes, J.F. Miller, Synth. Met. 22 (1988) 385.
16. J.E. Asturias, A.G. MacDiamid, A.G. Epstein, Synth. Met. 29 (1989) E157.
17. Y. Cao, A. Andreatta, A.J. Heeger, P. Smith, Polym. 30 (1989) 2305.
18. D. Kobayashi, H. Yoneyama, H. Tamura, J. Elctroanal. Chem. 177 (1984) 281.
19. N. Thoshima, H.Yan, Y. Gotoh, M. Ishiwatari, Chem. Lett. (1994) 2229.
20. C.K. Chiang, S.C. Gau, C.R. Fincher Jr, Y.W. Park, A.G. MacDiarmid, Appl. Phys. Lett. 37 (1978) 18.
21. A.J. Heeger, S. Kivelson, J.R. Schrieffer, W.P. Su, Rev. Mod. Phys. 60 (1988) 781.
22 P.J. Nigrey, A.G. Mac Diarmid, A.J. Heeger, J. Chem. Soc. Chem. Commun. (1979) 594.
23. W.Y. Zheng, K. Lenon, J. Laakso, J.E. Osterholm, Macromol. 27 (1995) 7754.
24. J.K. Scott, Sci. 280 (1998) 1141.
25. T.L. Porter, M.E. Hagerman, M.P. Eastman, Recent Res. Dev. Polym. Sci. 1 (1997) 1.
26. A. Akelah, A. Moet, J. Appl. Polym. Sci. 55 (1994) 153.
27. B. Wessling, in: H.S. Nalwa (ed) Handbook of Nanostructured Meterials amd Nanotechnology, vol. 5, Academic Press, San Diego, 2000.
28. C. Oriakhi, J. Chem. Ed. 77 (2000) 1138.
29. R. Gangopadhyay, A. De, Chem. Mater. 12 (2000) 608.
30. A. Blurmstein, Bull. Chem. Soc. (1961) 899.
31. B.K.G. Theng, Formation and Properties of Clay-Polimer Complexes,

Elsevier, New York, 1979.

32. A. Riede, J. Helmstedt, V. Riede, J. Zemek, J. Stejskal, Langmuir, 16 (2000) 6240.
33. M.I. Goller, C. Barthet, G.P. Mc Carthy, R. Corradi, B.P. Newby, S.A. Wilson, S.P. Armes, S.Y. Luk, Colloid polym. Sci. 276 (1998) 1010.
34. P. Enzel, T. Bein, J. Phys. Chem. 93 (1989) 6270.
35. T. Bein, P. Enzel, Angew. Chem. Int. ed. Engl. 28 (1989) 1962.
36. N. Kinomura, T. Toyama, N. Kumada, Solid State Ionics. 78 (1995) 281.
37. C.G. Wu, B.C. DeGroot, H.O. Marcy, J.N. Schindler, C.R. Kannewurf, T. Bakas, V. Papaefthymiou, W. Hirpo, J.P. Yesinowski, Y.J. Liu, M.G. Kanatzidis, J. Am. Chem. Soc. 117 (1995) 229.
38. T.A. Kerr, H. Wu, L.F. Nazar, Chem. Mater. 8 (1996) 2005.
39. C.G. Wu, Y.C. Liu, S.S. Hsu, C. Li, Synth. Met. 102 (1999) 1268.
40. P. Xiao, M. Xiao, P. Liu, K. Hong, Carbon 38 (2000) 623.
41. V. Mehrotra, E.P. Giannelis, Solid State Commum. 77 (1991) 155.
42. Q. Wu, Z. Xue, Z. Qi, F. Wang, Polym. 41 (2000) 2029.
43. M. Viswas, S.S. Ray, J.Appl. Polym. Sci. 77 (2000) 2948.
44. B.H. Kim, J.H .Jung, J.W. Kim, H.J. Choi, J. Joo, Synth. Met. 117 (2001) 115.
45. B.H. Kim, J.H. Jung, J.W. Kim, H.J. Choi, J. Joo, Synth. Met. 121 (2001) 1311.
46. H.J. Choi, J.W. Kim, J. Joo, B.H. Kim, Synth. Met. 121 (2001) 1325.
47. M.S. Whittingham, A.J. Jacobson (eds), Intercalation Chemistry, Academic Press, New York, 1982.
48. T.J. Pinnavaia, Sci. 220 (1983) 365.

49. H.R. Allcock, Sci. *255* (1992) 1106.
50. H. Kuzmany, N.S. Sariciftci, H. Neugebauer, A. Neckel, Phys. Rev. Lett. 60 (1988) 212.
51. L.W. Schacklette, J.F. Wolf, S. Gould, R.H. Baughman, J. Chem. Phys. 88 (1988) 3955.
52. D. Bloor, A. Monkman, Synth. Met. 21 (1987) 175.
53. A.J. Epstein, A.G. MacDiarmid, Mol. Cryst. Liq. Cryst. 160 (1988) 165.
54. J. Pang, X. Jing, B. Wang, F. Wang, Synth. Met. 24 (1988) 231.
55. I. Hazda, Y. Furukawa, F. Ueda, Synth. Met. 29 (1989) 303.
56. S. Li, H. Dong, Y. Cao, Synth. Met. 29 (1989) E329.
57. N.I.E. Shewring, T.G.J. Jones, G. Maitland, J. Yarwood, J. Colloid Interface Sci. 176 (1995) 306.
58. F.L. Lu, F. Wudll, M. Nowak, A.J. Heeger, J. Am. Chem. Soc. 108 (1986) 8311.
59. S. Stafstrom, J.L. Breadas, A.J. Epstein, H.S. Woo, D.B. Tenner, W.S. Huang, A.G. MacDiarmid, Phys. Rev. Lett. 59 (1987) 1464.
60. K.G. Neoh, E.T. Kang, K.L. Tan, Thermochim Acta. 171 (1990) 279.
61. H.S.O. Chan, M.T.B. Teo, E. Khor, C.N. Lim, J. Thermal Ana. 35 (1989) 765.
62. S. Moreau, V. Balek, F. Beguin, Mater. Re. Bull., 34 (1999) 503.
63. A.G. MacDiarmid, Angew. Chem. Int. Ed. 40 (2001) 2581.

★★★★★★★★★★★★★★★

Chapter 11

POLYANILINE/PILLARED CLAY NANOFIBERS

Materials and material development are fundamental to our very culture. The nanoscale, and the associated excitement surrounding nanoscience and technology, affords unique opportunity to create revolutionary material combination. Polymeric nanocomposites have been an area of intense industrial and academic research for the past 20 years. Its importance comes from providing value - added properties not present in the neat polymer without sacrificing the polymer's inherent processability and mechanical properties. Clay/polymer nanocomposites offer tremendous improvement in a wide range of physical and engineering properties. This technology can be applied commercially and has received great attention in recent years. The production of polyaniline molecular wires and tubules in nanometric scale dimension are a very stimulating challenge. The confined polymerization within clay layers is a very pertinent way to give them controlled shape and dimension. These layered conducting materials are very well suited for electrochemical applications. This chapter discusses the results of Polyaniline/PILC nanofiber formation using various analytical methods.

11.0 INTRODUCTION

Conducting polyanilines have increasing scientific and technical interest to synthesize a broad variety of promising new materials due to its unique electrical, optical and optoelectrical properties as well as its ease of preparation and environmental stability[1,2]. The formation of polyaniline (PANI) composites with inorganic materials provides new synergistic properties that cannot be attained from individual materials[3,4]. The ability to have a tunable conductivity by doping make PANI an ideal material for the applications in batteries[5], microelectronics[6], displays[7], antistatic coatings[8], electromagnetic shielding materials[9], sensors and actuators[10]. From the industrial point of view the fabrication of a thermally processable conducting polymer would be preferable. Composite formation improves the thermal stability, mechanical strength[11]; gas barrier[12], fire retardant properties[13], processability etc of PANI and the electrical conductivity can be tailored for a given application. They have attractive mechanical and other properties of the inorganic material.

Clay/polymer nanocomposites offer tremendous improvement in a wide range of physical and engineering properties for polymers and this technology can now be applied commercially and has received great attention in recent years[14]. The montmorillonite clay whose lamella is constructed from an octahedral alumina sheet sandwiched between two tetrahedral silica sheets, exhibits a net negative charge on the surface layers, mainly due to substitution of some Al^{3+} by Mg^{2+}. Cations such as Na^{+} or Ca^{2+} are present between layers

to compensate the net negative charge[15]. Nowadays, one - dimensional conducting polymer nanostructures has been synthesized both chemically and electrochemically through polymerization of the monomer with the aid of an external template (e.g. anodized alumina or track-etched polycarbonate)[16,17], or a self assembly process[18-20]. In addition, the multifunctionalized PANI nanotubes or nanowires have also been synthesized either by doping with a functional dopant[21,22] or by blending with inorganic, electrical, optic, and magnetic nanoparticles to form composite nanostructures[23].

Clays, due to many attractive properties (section 10.5) are adapted to the field of inorganic material for the hybrid formation. PANI is prepared either chemically or electrochemically by oxidation of aniline under acidic conditions and some photochemical methods are also used. Although many papers on PANI/clay nanocomposites have been published in the literature[24-29], no paper dealing with PANI/montmorillonite composite nanofiber has been published yet. Here the successful synthesis of PANI/montmorillonite composite nanofibers with pillared clays (PILCs) is well established using various characterization techniques. The role of confined matrix and catalytic environment in the polymer formation is investigated.

11.1 RESULTS AND DISCUSSION

Smectites are hydrophobic, arising from the hydration of the interlayer alkali metal and alkaline earth cations. Thus they are incompatible with many polymer systems. One common solution for this is ion exchange reactions with

cationic surfactants, such as organic ammonium and phosphonium ions, render the layered silicate organophilic. Pillaring results in a decrease in the interlayer hydrated cations present within the layer and thus decreasing the hydrophobic nature. This results in enhanced intercalation. Additionally, PILCs have increased interlayer distance and porosity allowing the intercalation of more and more monomers for efficient polymerization within the matrix.

Two idealized polymer–layered silicate morphologies are conventionally discussed, intercalated and exfoliated. Intercalated structures results from polymer penetration into the interlayer and subsequent expansion to a thermodynamically defined equilibrium spacing[30,31]. The expansion of the interlayer is finite (<10 Å), and is nominally associated with incorporation of individual polymer chains (scheme 11.1.1). In contrast, idealized exfoliated morphologies consist of individual nanometer-thick silicate layers suspended in a polymer matrix, and result from extensive penetration of the polymer within and delamination of the crystallites. The greatest property enhancements are observed in exfoliated structure. These two structures are thought to be thermodynamically stable and have been predicted by many field[30] and self consistent field models[31]. The formation of one dimensional PANI nanostructures is most important and nanofibre/nanowire/nanotube preparation is a challenge.

We have synthesized PANI nanocomposite fibers through in-situ polymerization of aniline[32-37] inside the matrix of pillared montmorillonite. To the best of our knowledge no papers dealing with PANI/montmorillonite

composite nanofibers have been published yet. This may be due to a low amount of exfoliation occurring to silicate layers. Eventhough there is intercalation, the Van der Waals force binding the clay layers is weak and in aqueous solution, the layers swells and some silicate layers may become exfoliated. This prevents one-dimensional structural formation since the confined matrix is relaxed.

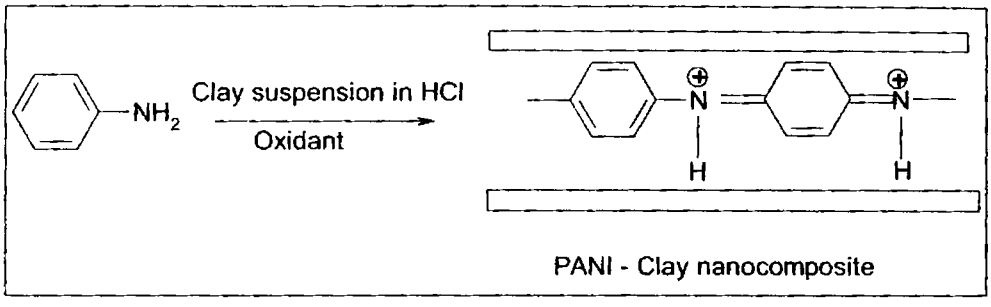

Scheme 11.1.1 In-situ intercalative polymerization of aniline inside the clay layers

As already mentioned, pillaring of montmorillonite results in enhanced interlamellar distance and the force acting between the clay layers become covalent upon pillaring[38]. Since in PILCs the further layer expansion in polar medium is absent (swelling properties are lost[39]) which is found in montmorillonite, there is no chance of exfoliation. This may result in increased intercalation of aniline into the matrix and polymerization occurs in the confined environment and as a result, polymer with high crystallinity and polymer order are expected. This explains the nanofiber formation. Scheme

11.1.2 shows a representation of well ordered PANI/PILC nanocomposites. This assumption is proved from the various characterization methods used and are discussed below.

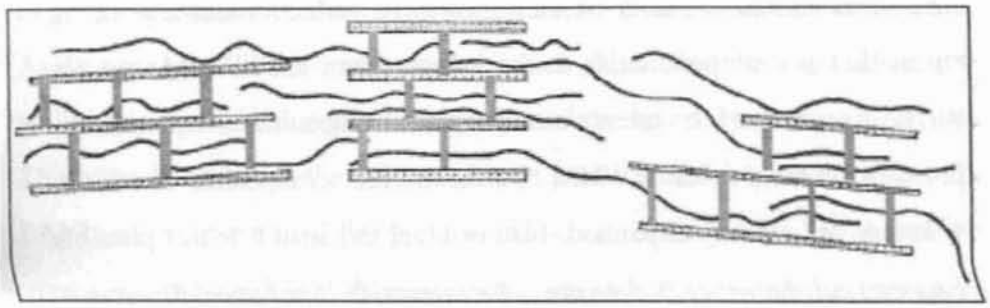

Scheme 11.1.2 Pictorial representation of the relative arrangement of Polymer-Intercalated particles in the pillared clay (PILC) matrix

11.1.1 XRD ANALYSIS

Microscopy is a useful tool to provide real-space information on the special distribution of the phases and defect structures. However it is not always feasible to use microscopy as a rapid characterization tool. In contrast, diffraction and scattering rapidly provide globally averaged information, potentially over six or more orders of magnitude, and with the potential for in situ, real-time studies. Traditionally, powder diffraction is used to characterize the structure of polymer-layered silicate nanocomposites. The extensive use of powder diffraction for these nanocomposites is largely based on the established

procedure developed for identification and structural characterization of layered silicate minerals.

Powder diffraction is used to monitor the position, full width at half maximum (FWHM) and intensity of the (100) basal reflection corresponding to the repeat distance perpendicular to the layers. From the FWHM, we can calculate the dimension of the intercalated polymer using scherrer equation ($L_z = 0.9\lambda/\beta \cos\theta$), where β is the FWHM. But in the nanocomposites of PILCs, since the layers are already expanded, further layer expansion is not possible and we cannot find the exact dimension. The intercalated polymer dimension will always be less than the interlayer space.

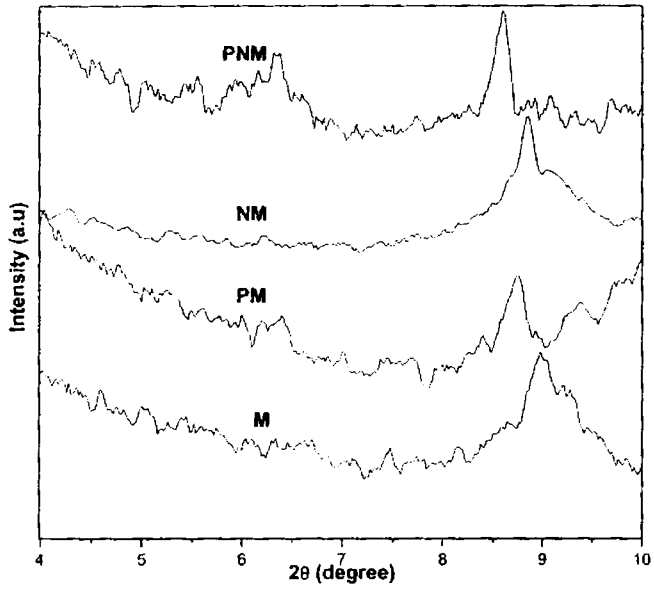

Figure 11.1.1 XRD patterns of the composites with M and NM

Figure 11.1.1 represent the X-ray diffraction pattern of parent as well as ion exchanged clay and their composites. It is clear that layer expansion is found to be almost absent in M where NM upon composite formation shows a peak at a 2θ value of 6.46°. This is an indication of layer expansion as a result of PANI intercalation. Thus the inserted PANI is in the nanometer range (<15 Å). But the peak at 8.9° still remains which shows that the ion exchange with anilinium ions is not complete and most of the layers remain un-intercalated. Thus over M and NM, the polymerization is not effective as in the case of bulk PANI and is clear from XRD patterns. This may be due to the high temperature treatment of M and NM during calcination at 500°C in the present work. At this temperature the layer collapse of un-PILCs starts. This process limits the intercalation of aniline and effective polymerization. This factor is again proved from the large amount of monomer and oligomers separated during soxhlet extraction.

We can not prove polymer intercalation from the diffraction of (100) plane due to the reason that, in PILCs the layers are already expanded and further layer expansion is not possible as in the case of montmorillonite or organically modified montmorillonite. The force acting between the clay layers become covalent upon pillaring and this is the reason for the absence of layer expansion over PILC nanocomposites. In montmorillonite clays there is ionic attraction between layers and thus expansion occurs as a result of polymer intercalation. We propose intercalated polymer nanocomposite formation within the layers.

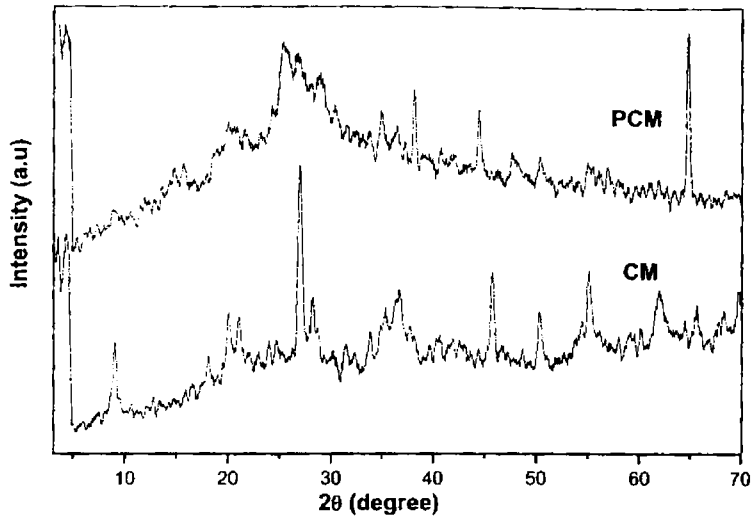

Figure 11.1.3 XRD patterns of PILC and nanocomposite

11.1.2 FTIR SPECTRA

The structure of the confined conducting polymer nanocomposites are understood from IR analysis. It is helpful in deciding the presence of benzenoid and quinoid rings present, the extent of oxidation, whether protonation had occurred or not etc. The FTIR of some representative nanocomposites are shown in figure 11.1.4.

In the nanocomposites characteristics peaks of doped PANI are observed at 1578, 1496, 1306, 1248 and 836 cm^{-1}, corresponding to δ_{N-H} (quinoid ring structure), δ_{N-H} (benzenoid ring structure), ν_{C-N}, $\nu_{C-N}{}^{+}$, δ_{C-H} (out of plane bending), respectively[43]. The peak at 1151 is due to the δ_{C-H} in plane

bending of the quinoid ring. Chracteristic peak of PILC is observed at 1053 cm^{-1} (ν_{Si-O})[44]. The peaks at 1248 cm^{-1} and 1306 cm^{-1} originate from the C-N stretching vibrations associated with the oxidation or protonation (doped) states in PANI[45]. FTIR of different PILCs are shown in chapter 3, figures 3.6.1 and 3.6.2.

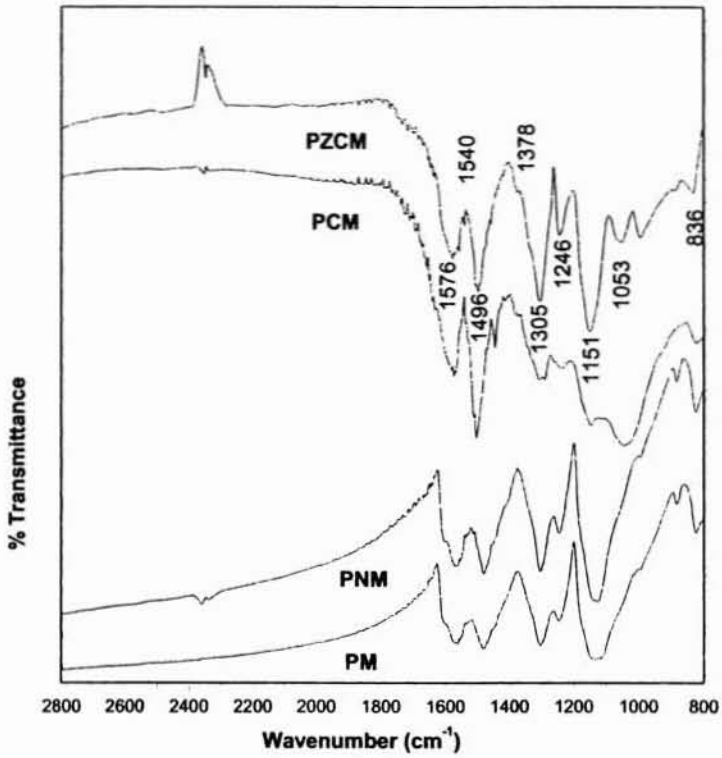

Figure 11.1.4 FTIR spectra of some selected PANI/PILC nanocomposites

11.1.3 UV-VIS DIFFUSE REFLECTANCE SPECTRA

The diffuse reflectance spectra of PANI/PILC (figures 11.1.5 and 11.1.6.) and PILC (figures 3.8.1 and 3.8.2) gives information about the extent of delocalization and the interaction of PANI within the clay matrix. PANI/PILC shows peaks due to π- π* (371 nm) and polaron- π* (458 nm).

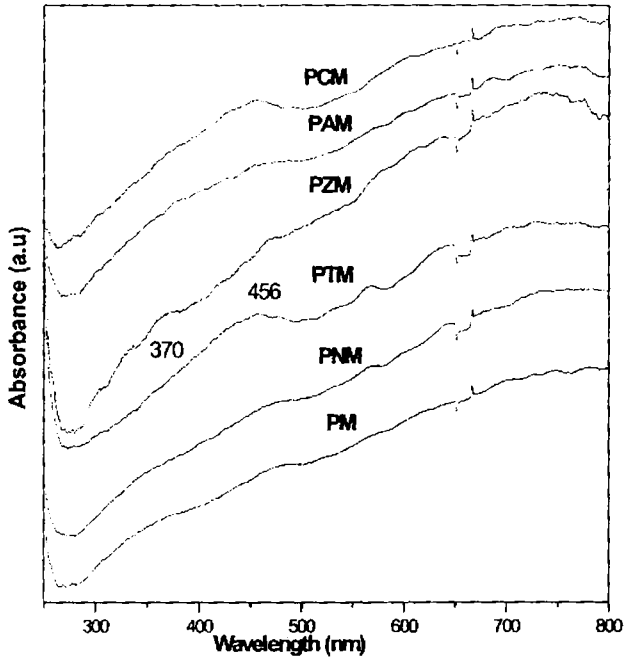

Figure 11.1.5 UV-VIS DRS of PANI/PILC composites

The results suggest that the prepared PANI is in the doped state[46,47].

On nanocomposite formation the UV absorption around 360 nm present in Cr containing PILCs are strengthened, which is due to the overlap of peaks of π- π^* transitions in PANI with the d-d transitions of chromium ions present in the clay. This result indicates that there is strong interaction between PANI and PILC.

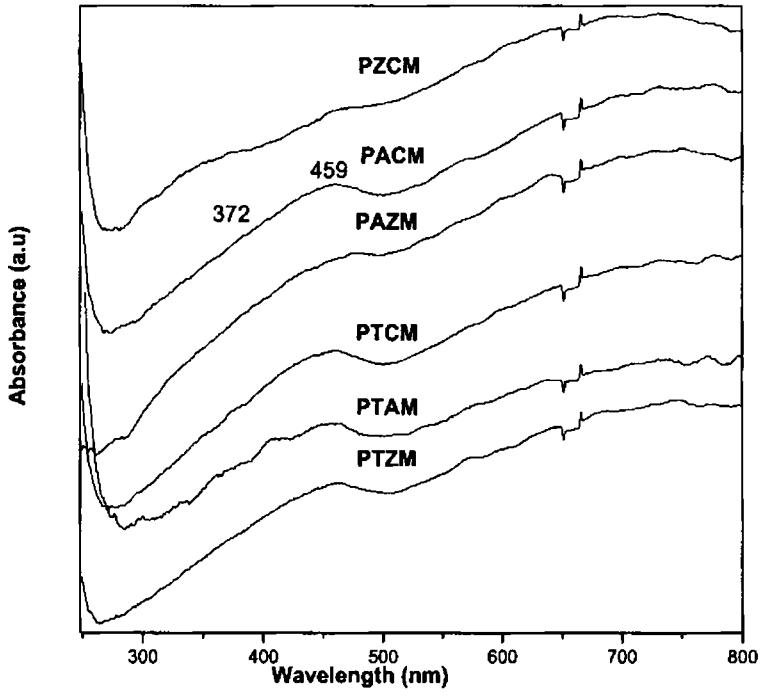

Figure 11.1.6 UV-DRS of PANI/PILC nanocomposites

In bulk PANI a strong absorption peak generally appears between 780-826 nm as a result of π-polaron transitions[46,47]. But in the hybrid nanocomposite this peak is not sharp and is broadened. The broad absorption

around 750 nm is a characteristic band of the polaron of PANI – emeraldine salt, formed by the head to tail coupling of the anilinium radical[48]. The broadening may be due to the shift of peak towards near IR region[49] (free-carrier tail[50], in the higher wavelength region). It is consistent with the delocalization of electrons in the polaron band promoted by an extended conformation of the polymer chains.

11.1.4 SEM ANALYSIS

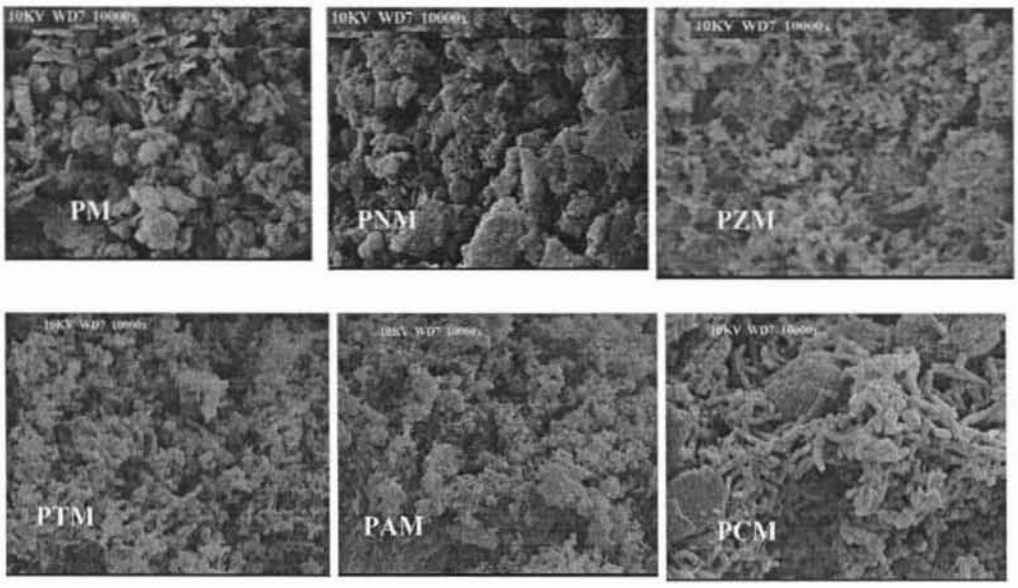

Figure 11.1.7 SEM photographs of PANI/montmorillonite, PANI/Na^+-montmorillonite and PANI-single PILC nanocomposites

Inside the clay layers which are apart in the nanometer scale, the interaction of different polymer chains are eliminated and the chain contraction is limited. This strengthens the interaction between the polarons, and the

polaron bands become more dispersed in energy. This explains the presence broad bands where polaron transitions are present[51].

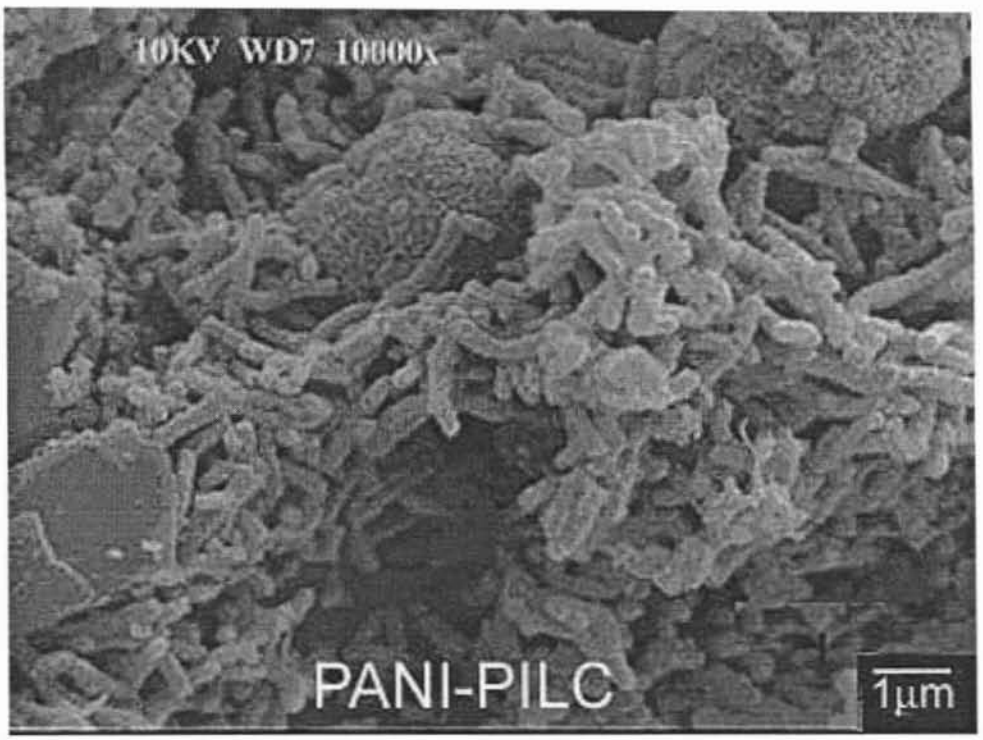

Figure 11.1.8 Enlarged SEM photograph showing nanofibers of PCM PILC composite

SEM photographs in figure. 11.1.7, 11.1.8, 11.1.9 and 11.1.10 show the nanofibrous morphology of PANI/PILC composites. The layered structure of the clay is evident from SEM pictures shown in chapter 3, figures 3.1.15 and 3.1.16. The enhanced layer distance and confined media results in polymer with high crystallinity and polymer order are expected. This explains the nanofiber formation as seen in the SEM pictures.

Note that traditional chemical polymerization in the presence/absence of any inorganic material using common mineral acids yields granular PANI[52,53]. Here the parent and Na^+-exchanged clay composites did not show any fibrous nature and is comparable with reports. Thus the nanofiber formation is a result of pillaring of clays is evident.

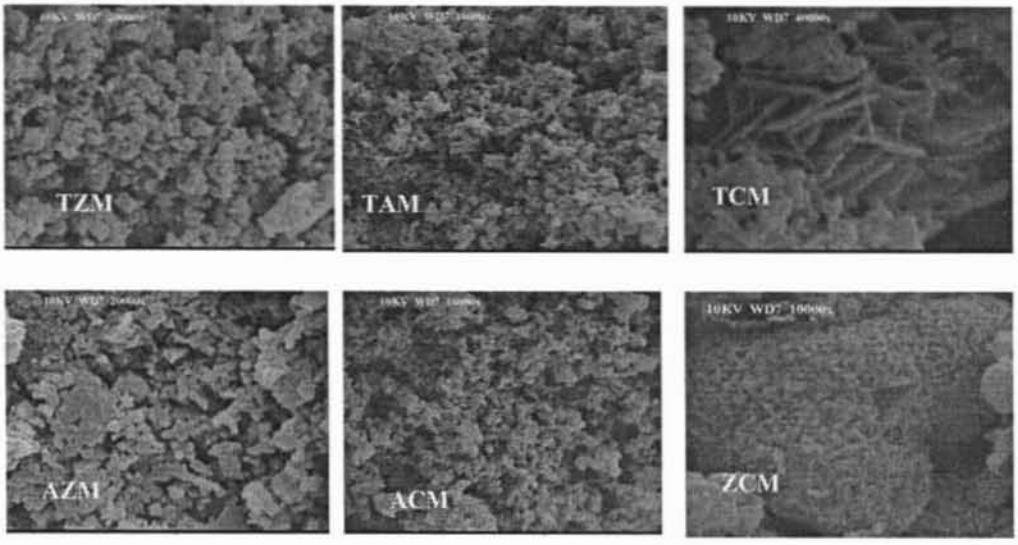

Figure 11.1.9 SEM photographs of PANI-Mixed PILC nanocomposites

The morphology of the composite seen from SEM photographs suggests polymer intercalation. The nanofiber formed within the clay layers may be molecule fiber of doped PANI. Molecular models and crystal structure studies of emeraldine.HCSA[54] synthesized by surfactant-assisted chemical oxidative polymerization of aniline in dilute aqueous organic acids shows that

the 'diameter' of a single chain (molecule fiber of doped PANI) is in the range 1.0 - 1.8 nm.

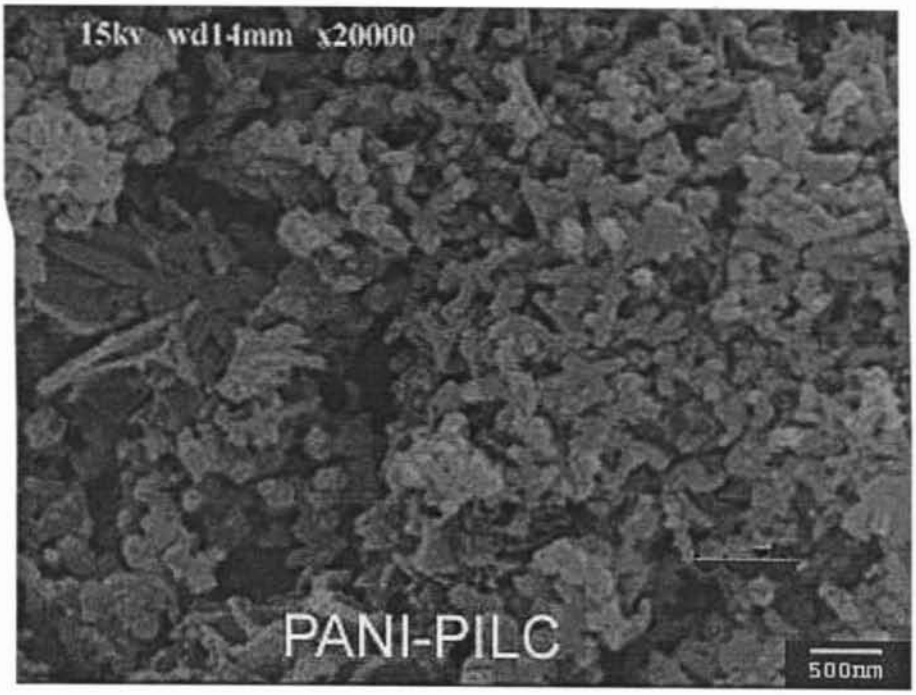

Figure 11.1.10 Enlarged SEM photograph showing nanofibers of PTAM composite

PANI nanofibers obtained in that study are chemically robust nanofibers having average fiber diameter in the range 30–50 nm and they deform readily under mechanical stress and fragment to smaller pieces (of fiber diameter 1.0–1.8 nm) under strong probe sonication.

SEM pictures in the present study show that diameter of the PANI fibers are between 100 nm - 300 nm. We suggest aggregation of the single PANI chains as it emerges out the clay layers. It is reported that one nanofiber contains lots of PANI chains. In HCl doped PANIs Cl^- ions have small size. Then the interchain separation may be small, resulting in an existence of strong coherence/coupling between the chains[55,56].

11.1.5 TG/DTG ANALYSIS

In order to clarify whether PANI is formed within the clay layers, TGA/DTG (Derivative Thermogravimetric curves are shown in fig. 11.1.11) analysis of the clay as well as composite is taken. In montmorillonite clays, the huge weight loss in the 50–150°C regions is due to the removal of the physically adsorbed water molecules present. However at higher temperature the weight loss is more gradual without any well-defined inflection point. These losses have been assigned to the removal of chemisorbed water. The weight loss corresponding to the dehydroxylation of the clay sheet is found to be occurring in temperature range of 425°C - 650°C. From the DTG of montmorillonite the weight loss around 620°C is clearly seen as a dip (minima) which is attributed to the dehydroxylation of silicate structure[26].

Figure 11.1.11 show the DTG curves for PANI/PILC nanocomposites of representative systems. The composites show a four step weight loss, as can be seen from the four minima in the DTG curve indicating the majority weight loss for respective steps.

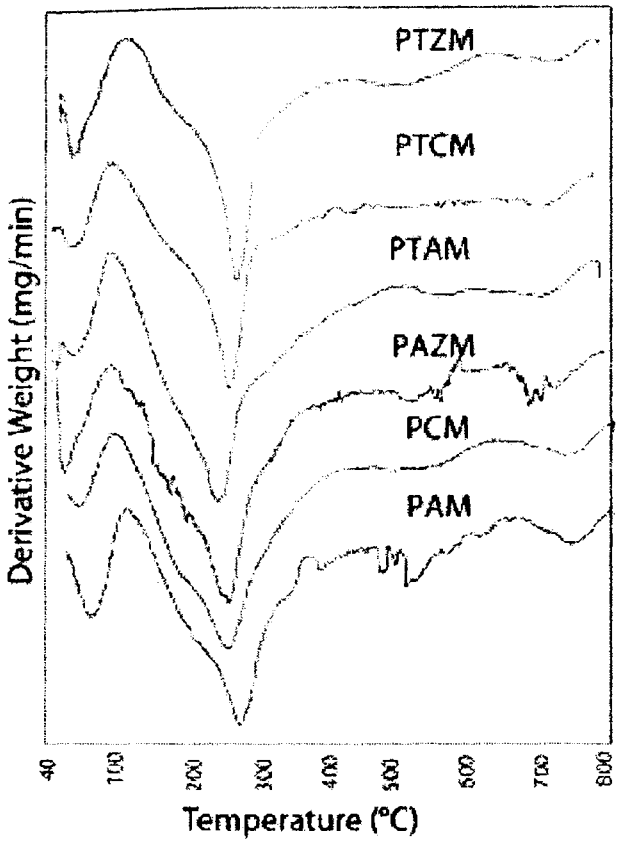

Figure 11.1.11 DTG plots of some representative PILC nanocomposite fibers

The first weight loss just below 100°C is attributed to the loss of water from PANI as well as from the interlayer galleries of clay. The second weight loss ranging from 200 - 300°C, centered at 275°C is due to the elimination of dopant HCl present[57,58]. The polymer backbone breakage for pure PANI (ES) is at 530.6°C[59]. In composite PCM this is shifted to 579.2°C, a higher temperature by about 48.6°C which may be due to the additional stability inside the matrix as a result of restricted motion. Similar shift is seen in all

PILC composites. The fourth weight loss in the composite occurs at 763.3°C which may be due to the silicate layer dehydroxylation.

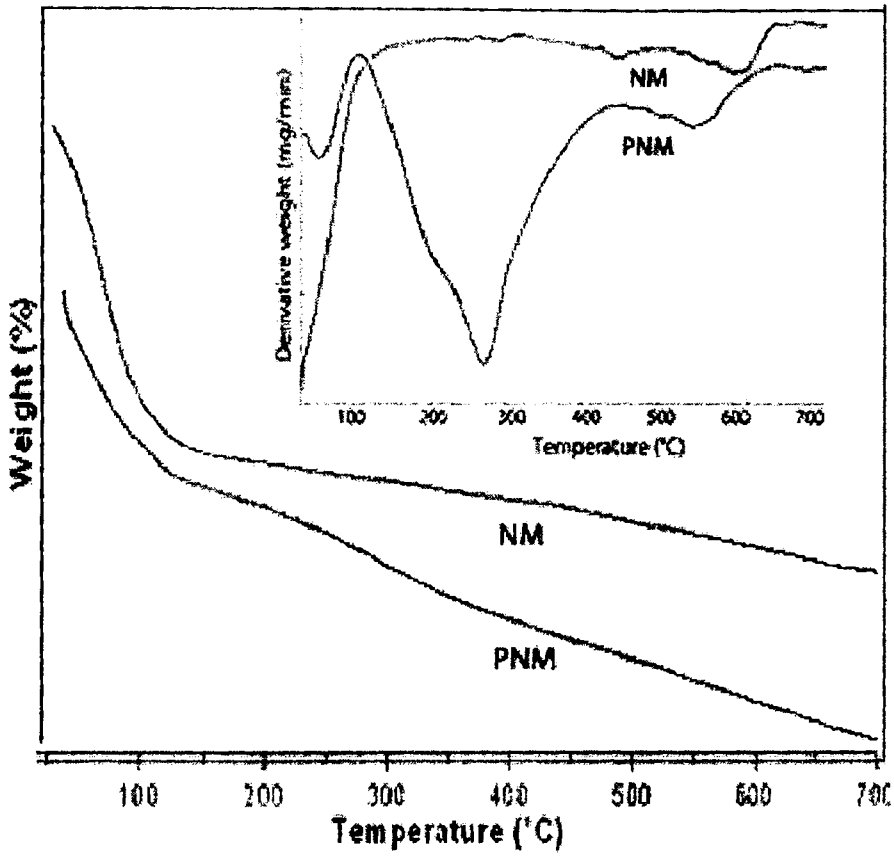

Figure 11.1.12 TG/DTG pattern of NM and PNM

These results suggests that the intercalated nanocomposite system is more thermally stable, i.e. upon nanohybrid formation the stability of organic as well as inorganic material is enhanced. A shift is also seen for both PM and PNM but is less when compared to PILCs this supports the additional stability

over PILCs. The weight loss around 750°C seen in the PILC DTG shown in figure 6 is attributed to the dehydroxylation of silicate structure, loss of water from the interlayer galleries results in a weight loss around 100°C.

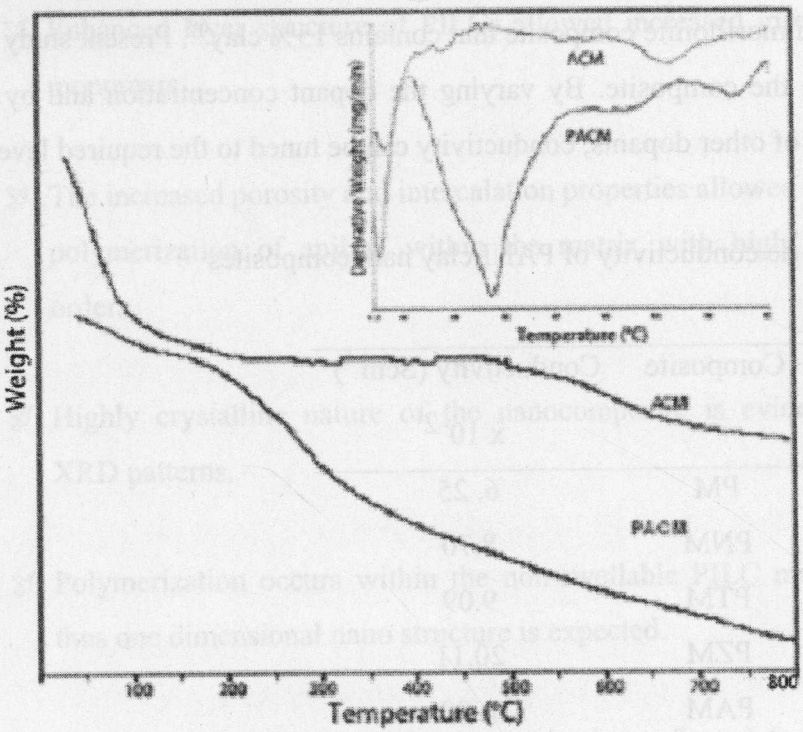

Figure 11.1.13 TG/DTG pattern of ACM and PACM

Figure 11.1.12 shows the TGA/DTG pattern of PNM where similar pattern with a shift of polymer backbone breakage temperature towards 21°C. Figure 11.1.13 shows the TG/DTG pattern of PACM and ACM. Here the shift is around 47°C.

11.1.6 CONDUCTIVITY MEASUREMENTS

The dc conductivity of PANI/clay composites show a high conductivity in the range 10^{-1} - 10^{-2} Scm^{-1}, which is found to be comparable with the PSSA-g-PANI/montmorillonite composite that contains 13% clay[60]. Present study has 19% clay in the composite. By varying the dopant concentration and by the introduction of other dopants, conductivity can be tuned to the required level.

Table 11.1.1 dc conductivity of PANI/clay nanocomposites

Composite	Conductivity (Scm^{-1}) x 10^{-2}
PM	6. 25
PNM	8.70
PTM	9.09
PZM	20.11
PAM	1. 90
PCM	3.72
PTZM	9.05
PTAM	2.32
PTCM	3.86
PAZM	12.05
PACM	2.02
PZCM	15. 32

11.2 CONCLUSIONS

From the above results and discussions we reach in the following conclusions.

- Enhanced layer structure of PILCs allowed increased insertion of monomers.

- The increased porosity and intercalation properties allowed efficient polymerization of aniline within the matrix with high polymer order.

- Highly crystalline nature of the nanocomposite is evident from XRD patterns.

- Polymerization occurs within the non-swellable PILC matrix and thus one dimensional nano structure is expected.

- Formation of PANI/clay nanocomposite is confirmed from FTIR, XRD, DRS, SEM and TG analysis.

- PANI formation inside pillared clay matrix leads to nanofiber formation, fibrous morphology is evident from SEM pictures.

- In composite polymer backbone breakage temperature is shifted which may be due to the additional stability inside the matrix due to restricted motion.

- FTIR and UV-DRS spectral analysis shows the strong interaction between PANI and PILC.

REFERENCES:

1. G. Gustafsson, Y. Cao, G.M. Treacy, F. Klavetter, N. Colaneri, A.J. Heeger, Nature. 357 (1992) 477.
2. M.J. Sailor, E.J. Ginsburg, C.B. Gorman, A. Kumar, R.H. Grubbs, N.S. Lewis, Sci. 249 (1990) 1146.
3. A. Riede, J. Helmstedt, V. Riede, J. Zemek, J. Stejskal, Langmuir, 16 (2000) 6240.
4. M.I. Goller, C. Barthet, G.P. Mc Carthy, R. corradi, B.P. Newby, S.A. Wilson, S.P. Armes, S.Y. Luk, Colloid polym. Sci. 276 (1998) 1010.
5. M. Kaneko, H. Nakamura, J. Chem. Soc. Chem. Commun. (1985) 346.
6. H. Sirringhaus, N. Tesser, R.H. Friend, Sci. 280 (1998) 1741.
7. H. Pages, P. Topart, D. Lemordant, Electrochim Acta, 46 (2001) 2137.
8. C.B. Duke, H.W. Gibson, Kirth – Othmer Encyclopedia of Chemical Technology, John Wiley, New York, 1982.
9. S. Koul, R. Chandra, S.K. Dhawan, Polymer, 41 (2000) 9305.
10. S.nSukeerthi, A.Q. Contractor, Anal. Chem. 71 (1999) 2231.
11. B.H. Kim, J.H. Jung, S.H. Hong, J. Joo, Macromol. 35 (2002) 1419.
12. T. Lan, P.D. Kaviratna, T.J. Pinnavaia, Chem. Mater. 6 (1994) 573.
13. J.W. Gliman, C.L. Jackson, A.B. Morgan, E.Jr. Hayyis, E. Manias, E.P. Giannelis, M. Wuthenow, D. Hilton, S.H. Philips, Chem. Mater.

12 (2000) 1866.

14. F. Gao, Mat. today 11 (2004) 50.
15. M.S. Whittingham, Intercalation Chemistry, Academic Press, New York, 1982.
16. C.G. Wu, T. Bein, Sci. 264 (1994) 1757.
17. C.R. Matin, Chem. Mater. 8 (1996) 1739.
18. J.C. Michaelson, A.J. McEvoy, Chem. Commun. (1994) 79.
19. Z. Wei, Z. Zhang, M. Wan, Langmuir. 18 (2002) 917.
20. L.M. Huang, Z.B. Wang, H.T. Wang, X.L. Cheng, A. MItra, X.Y. Yan, J. Mater. Chem. 12 (2002) 388.
21. Y. Yang, M. Wan, J. Mater. Chem. 12 (2002) 897.
22. K. Huang, M. Wan, Chem. Mater. 14 (2002) 3486.
23. Z. Zhang, M. Wan, Synth. Met. 132 (2003) 205.
24. K.H. Chen, S.M. Yang, Synth. Met. 135 (2003)151
25. Q. Wu, Z. Qi, F. Wang, Polym. 41(2000) 2029.
26. D. Lee, K. Char, Polym. Degrad. Stab. 75 (2002) 555.
27. D. Orata, F. Segor, React. Funct. Polym. 43(2000) 305.
28. Y.T. Lim, J.H. Park, O.O.J. Park, Colloid Interface Sci. 245 (2002) 198.
29. B.H. Kim, J.H. Jung, J.W. Kim, H.J. Choi, J. Joo, Synth. Met. 17(2001) 115.
30. R.A. Vaia, H. Ishii, E.P. Giannelis, Macromol. 30 (1997) 7990.
31. A.C. Balazs, C. Singh, E. Zhulina, Y. Lyatskaya, Acc. Chem. Res. 32 (1999) 651.
32. F.Leroux, G.Goward, W.P. Power, L.F. Nazar, J. Electrochem. Soc.

144 (1997) 3886.

33. T.A.Kerr, H. Wu, L.F. Nazar, Chem. Mater. 8 (1996) 2005.
34. Q. Wu, Z. Xue, Z. Qi, F. Wang, Polym. 41 (2000) 2029.
35. G.M. Nascimento, V.R.I. Constantino, M.L.A. Temperini, Macromol. 35 (2002) 7535.
36. H.R. Allcock, Sci.255 (1992) 1106.
37. E.P. Giannelis, Adv. Mater. 8 (1996) 29.
38. F. Figueras, Catal. Rev. Sci. Eng., 30 (1988) 457.
39. Pillared Clays, R. Burch, (ed.) Catal Today, Elsevier, New York, Vol. 2, 1988, p 289.
40. K. Tzou, R.V. Gregory, Synth. Met. 53 (1993) 365.
41. X. Sui, Y. Chu, S. Xing, C. Liu, Matter. Lett., 25 (2004) 1255.
42. J.P. Pouget, M.E. Jozefowicz, A.J. Epstein, X. Tang, A.G. MacDiarmid, Macromol. 24 (1991) 779.
43. Handbook of Conductive Molecules and Polymers: Conductive polymers. Synthesis and Electrical Properites, Nalwa, H. S. (ed) John Wiley & Sons Ltd, India, 1997; Vol 2, p. 506.
44. A. Geatti, M. Lenarda, L. Storaro, R. Ganzerla, M. Perissinotto, J. Mol. Catal. A: Chem. 121 (1997) 111.
45. S. Quillard, G. Louran, S. Lefrant, A.G. Mac Diarmid, Phys. Rev. B 50 (1994) 12496.
46. F.L. Lu, F. Wudll, M. Nowak, A.J. Heeger, J. Am. Chem. Soc., 108 (1986) 8311.
47. S. Stafstrom, J.L. Breadas, A.J. Epstein, H.S. Woo, D.B. Tenner, W.S. Huang, A.G. Macdiarmid, Phys. Rev. Lett.59 (1987) 1464.

48. A.G. Mac Diarmid, Huang, W. S. Polym. 34 (1993) 1833.
49. T. Hatano, A.H. Bae, M. Takeuchi, A. Ikeda, S. Shinkai, Bull. Chem. Soc. Jpn. 77 (2004) 1951.
50. G.M. Alan, J.E. Arthur, Synt. Met. 69 (1995) 85.
51. Q. Wu, Z. Xue, Z. Qi, F. Wang, Polym. (2000) 2029.
52. J.K. Avlyanov, J.Y. Josefowicz, A.G. MacDiarmid, Synth. Met., 73 (1995) 205.
53. P. Chandrasekhar, Conducting polymers, Fundamentals and Applications: A Practical Approach, Kluwer Academic Publishers, Boston 1999.
54. X. Zhang, S.K. Manohar, Chem Commun. (2004) 2360.
55. J. Li, K. Fang, H. Qiu, S.P. Li, W.M. Mao, Synth. Met., 142 (2004) 107.
56. J. Li, K. Fang, H. Qiu, S.P. Li, W.M. Mao, Q. Wu, Synth. Met. 145 (2004) 191.
57. H.S.O. Chan, M.T.B. Teo, E. Khor, C.N. Lim, J. Thermal Ana. 35 (1989) 765.
58. K.G. Neoh, E.T. Kang, K.L. Tan, Thermochim Acta. 171 (1990) 279.
59. S. Moreau, V. Balek, F. Beguin, Mater. Re. Bull. 34 (1999) 503.
60. W.J. Bae, K.H. Kim, W.H. Jo, Macromol. 37 (2004) 9850.

****

Chapter 12

SUMMARY AND CONCLUSIONS

Recent advances in the intercalation chemistry of smectite clays has rekindled interest in these material as catalysts, catalyst support inorganic-organic hybrid nanocomposites etc. Smectite intercalation compounds make use of robust cations as molecular props or pillars between the silicate layers that leads to the formation of porous networks analogous to zeolites. These pillared clays (PILCs) have pore size larger than those of zeolites that offer promising new means of facilitating the reactions of large molecules. By mediating the chemical and physical forces acting on interlayer reactants, one often can improve catalytic specificity. Present work deals some industrially important Friedel-Crafts alkylation reactions where shape selective constraints of PILCs leads to the desired product formation. The enhanced layer distance as a result of pillaring allowed increased intercalation of monomers for efficient polymerization within the matrix to form nanocomposites. The thesis describes preparation, characterization, shape selective solid acid catalysis and nanocomposites of PILCs and is discussed in the preceding chapters. This chapter summarizes the results and major conclusions of the present work.

12.0 SUMMARY

Highly porous solids that possess channels, cavities or cages with diameters in the range of micro/meso offer the best means for designing or modifying new inorganic materials with wide applications. In the present work, structural tuning of montmorillonite clays are done by the method of pillaring for improving its intercalating properties. This will provide additional properties such as thermal stability, enhancement in porosity, surface area, acidity etc with retention of basic layer structure. The pillar metals used are Ti, Zr, Al and Cr; mixed pillaring that contains two metals in a ratio of 1:1 are also prepared. A thorough characterization of the prepared PILCs is done using various available techniques. The three dimensional porous network of PILCs are applied for shape selective catalysis and organic-inorganic nanocomposite formation. The extracted essence of each chapter is presented below.

Chapter 1 A detailed description of clays is presented in this chapter. Literature of PILCs describes the available preparative methods and major characterization techniques used. An introduction to shape selective catalysis of PILCs and clay/polymer nanocomposites are also given.

Chapter 2 The materials and methods of PILC preparation, characterization and catalysis are displayed in this chapter giving the principles and experimental details of each technique employed. A novel method for Ti-PILC preparation is presented using titania sol from a cheap precursor titanyl sulphate. The surface acidity determination by different techniques including

the test reactions like cumene cracking and cyclohexanol decomposition is the additional feature of this chapter.

Chapter 3 The physico-chemical characterization of the PILC systems is discussed in this chapter. Pillaring and the improvement in clay properties are proved from various analytical results which include CEC measurements, elemental analysis (ICP-AES), XRD, BET surface area and pore volume measurements, FTIR Spectroscopy, UV-Vis Diffuse Reflectance Spectroscopy, TG/DTA analysis and SEM analysis. Acidity measurements are done using three independent methods such as TPD of NH_3, Pyridine IR and test reactions for acidity measurements. TPD of NH_3 and test reactions show the same trend in acidity of different clays. Cumene cracking reactions allowed the calculation of relative percentage Brønsted and Lewis acid site distribution of present catalysts. The dual nature of clays is understood from formation of cyclohexanone in cyclohexanol decomposition reaction.

Chapter 4 A detailed investigations on Friedel-Crafts Alkylation Reactions and the need for the introduction of heterogeneous catalysis for the protection of environment, following the principles of Green Chemistry is presented in this chapter.

Chapter 5 Shape selective preparation of cumene, which is the only intermediate for the co production of phenol and acetone, is presented in this chapter. The influence of reaction variables, temperature, arene/alkylating agent molar ratio and WHSV (weight hourly space velocity) is studied in

detail. In the selected optimum conditions, PILCs are found to be promising catalysts which operate at low temperature with low amount of coke formation and reduced operational costs.

Chapter 6 Isopropylation of toluene is carried out over the clay systems to get p-cymene as the major product with good conversion. The chapter deals with the effect of reaction parameters on the catalytic activity, and the comparison of the activity over various PILCs. The suggested mechanism reveals the role of acidic sites on isopropanol conversion.

Chapter 7 Ethylbenzene, which is widely used for styrene production, is prepared using benzene alkylation with ethanol as the alkylating agent. 100% ethylbenzene selectivity is the major attraction of the present PILC catalysts. The role of Brønsted acidity on the conversion is correlated.

Chapter 8 Toluene methylation is carried out over PILCs to get good p-xylene selectivity. Toluene disproportionation is minimized or even eliminated by optimizing the reaction conditions. Acidity – activity relationship is also investigated.

Chapter 9 Linear Alkyl Benzenes (LABs), which is used for the production of Linear Alkyl benzene Sulphonates (LAS), the largest volume synthetic surfactants, are synthesized over PILCs using 1-alkenes as the alkylating agents. Improved 2-phenyl alkane and monoalkylation selectivity is obtained in the optimized conditions when compared to the conventional homogeneous

catalysts. The mechanism suggested supports the perfect correlation obtained between Brønsted acidity and alkene conversion. The selected alkenes are 1-octene, 1-decene and 1-dodecene.

Chapter 10 Introduction and literature survey of Polyaniline (PANI) and PANI/clay nanocomposites are given in this chapter. The preparative method adopted and the characterization techniques employed are discussed in detail.

Chapter 11 Results and discussion of the PANI/PILC composite nanofibers obtained are explained in this chapter. The increased porosity and intercalation properties allowed efficient polymerization of aniline inside the PILC matrix with good conductivity. Formation of PANI/PILC nanocomposite is confirmed from FTIR, XRD, DRS, SEM and TG analysis. Aniline polymerization inside PILC layers leads to nanofiber formation.

Chapter 12 This chapter gives the summary and major conclusions of the work done. The future outlook is also presented.

12.1 CONCLUSIONS

The major conclusions that can be drawn from the present research work are the following.

- Pillaring is done to improve the structural as well as textural properties of montmorillonite.

- Ti, Zr, Al, Cr single and mixed pillared montmorillonite clays are prepared and characterized. A novel method for Ti-PILC preparation is presented.

- FTIR and SEM Analysis of different systems show the retention of layer structure.

- XRD and NMR results confirm pillaring.

- High thermal stability is imparted to clays upon pillaring as evident from thermal analysis and regenerability studies.

- The increase in acidity of the parent montmorillonite as well as single PILC on mixed pillaring is clearly understood from TPD of NH_3, Pyridine IR and test reactions for acidity which offers the present systems as efficient catalysts for organic transformations.

- Cumene preparation is done in gas phase at low temperature using isopropanol as the alkylating agent – reduced operational cost & coke formation with promising cumene selectivity is obtained.

- Cymene is efficiently prepared with the pillared systems.

- A good method for the benzene ethylation using ethanol is presented with 100% ethylbenzene selectivity.

- Good p-xylene selectivity is obtained in toluene methylation due to the restricted porous structure. Disproportionation is found to be minimal or even absent over PILC systems

- The high Brønsted acidity and efficiency in Friedel Crafts alkylation reactions premits LAB synthesis with the present catalyst systems.

- High 2-phenyl as well monoalkylation selectivity is obtained with the PILCs.

- The increased porosity and intercalation properties allowed efficient polymerization of aniline within the matrix with high polymer order.

- Formation of PANI/Montmorillonite nanocomposites is confirmed from FTIR, XRD, DRS, SEM and TG analysis.

- PANI formation inside confined PILC matrix leads to nanofiber formation.

12.2 FUTURE OUTLOOK

Clays, which are layered silicate minerals, continued to evoke interest for basic research because of their applications to such diverse and technologically important fields as catalysis, ion exchange, environmental issues, and organic-inorganic nanocomposites. This is especially true for the montmorillonite type clay minerals, where in a so-called 2:1 primary unit consisting of two tetrahedral silicate layers that sandwich a central alumina octahedral layer is separated from another via electrostatic interactions that arise from exchangeable cations in hydrated interlayers. The intercalation of montmorillonite clays by hydroxy-metal polycations results, after calcination at approximately 500°C, in the formation of so-called PILCs. When compared to parent non-pillared montmorillonites such PILCs have been demonstrated to possess improved thermal stability as well as increased surface area – porevolume, interlayer distance and surface acidity. The three dimensional porous structure developed as a result of pillaring allowed shape selective catalysis and increased intercalation properties.

In the 21st century we have a growing world population with ever increasing requirements for better health and living standards which will place greater demands on the chemical industry. The tarnished image of the industry can be attributed to the common belief among the general public that chemical manufacturing is responsible for many disasters and much of the pollution that plagues our planet. The concept of Green Chemistry is based on the acceptance that chemical manufacturing needs to be improved and seeks to promote

research into and encourage the application of more environmentally friendly chemical technologies and processes.

In recent years, solid acid catalysts such as montmorillonite clays have received considerable attention in different areas of organic synthesis because of their environmental compatibility, reusability, high selectivity, operational simplicity, non corrosiveness and low cost. Friedel-Crafts reactions remain a great challenge for Green Chemistry. In the present study, homogeneous environmentally hazardous Friedel-Crafts catalysts are replaced by PILC catalysts where the shape selective constraints lead to the formation of the desired product.

Solvent minimization can improve a process by reducing the problem of volatile organic compound emissions, and by reducing the volume required to carry out a process. Conducting reactions in gas phase in the present work eliminates the use of toxic organic solvents. Generally one of the reactant is taken in excess (only up to a molar ratio of 20 in the present case) to get improved selectivity of a particular product. In the gas phase reactor, the catalysts can be reused continuously for hours, for the fresh reagents. High temperature treatment regenerates the deactivated catalyst (as a result of coke formation during continuous run) without altering the reaction set up.

This work deals with some industrially important Friedel-Crafts alkylation reactions of benzene and toluene that gives an idea of the activity of present PILC catalysts in acid catalyzed organic transformations such as

substitution, acetalyzation etc. In addition, construction of molecules using conjugate addition and alkoxyalkylation are reported over clay catalysts, we proposes present PILC catalysts as better three dimensional reactor for these reactions. The dual nature of PILC catalysts (both acidic and basic) are established from the formation of cyclohexanone during cyclohexanol decomposition reactions which may make PILC clay catalysts efficient in Michaeal addition and many other reactions where both sites play its own role . Solid catalysts with both basic and acidic sites are beginning to attract considerable attention.

Nanotechnology - in the guise of nanoscale-materials has already been around for a long time. Today, the term "nanotechnology" refers most broadly to the use of materials with nano scale dimensions, a size range from 1 to 100 billionths of a meter, or nanometers. Because this range includes everything from collections of a few atoms to those protein-based motors, researchers in chemistry, physics, materials science, and molecular biology all lay stake to some territory in this field.

Polymer/clay nanocomposites are formed through the union of two very different materials with organic and mineral pedigrees. The ability of clays to intercalate organic compound has been largely applied to obtain a wide family of intercalation materials exhibiting relevant properties. Due to the synergistic effects that result from adding a small amount of an inexpensive silicate, the synthesis and characterization of polymer nanocomposites has been intensely investigated in the last decade. By tailoring the clay structure in

polymers on the nanometer scale, novel material properties have been found. Another interest in developing clay/polymer nanocomposites is that the technology can be applied immediately for commercial applications, while most other nanotechnologies are still in the concept and proving stage.

Promising inorganic materials, the PILCs that will lead to fibrous morphology are introduced to the field of clay/polymer nanocomposites. In the present work PANI/PILC nanofibers with good conductivity, thermal stability with strong interaction between the organic and inorganic material of the hydride nanocomposites are prepared and characterized. The results obtained offer PILCs as the inorganic materials for nanocomposites with any other organic/polymeric material.

LIST OF PUBLICATIONS AND PRESENTATIONS

Selective formation of cumene on pillared clays by isopropylation of benzene Binitha N Narayanan and Sankaran Sugunan*, Reaction Kinetics and Catalysis Letters, 89 (2006) 45-53.

Preparation,characterization and catalytic activity of titania pillared montmorillonite clays, N.N.Binitha, S.Sugunan*, Microporous and Mesoporous Materials, 93 (2006) 82-89.

p-Cymene preparation over modified montmorillonite clays, N.N. Binitha, S.Sugunan *, Catalysis Communications, in revision.

Polyaniline/Pillared Montmorillonite Clay Composite Nanofibers, N. Narayanan Binitha, Sankaran Sugunan*, Journal of Applied Polymer Science, in revision.

Shape selective toluene methylation over chromia pillared montmorillonites, N.N.Binitha, S.Sugunan*, Communicated.

Polyaniline - montmorillonite nanocomposites using H_2O_2 as the oxidant, N.N.Binitha, S.Sugunan*, Communicated.

Alkylation of benzene with 1-octene over titania pillared montmorillonite, Binitha N Narayanan and Sankaran Sugunan*, Communicated.

N.N. Binitha and S. Sugunan, "Influence of titania pillars on the zirconia pillared Montmorillonite for Cumene cracking reactions'' National Symposium on Light and Smart Materials, Material Research Society of India, February 2004, Banaras Hindu University, Varanasi.

Binitha N. N. and Sugunan S, "Synthesis of polyaniline-pillared montmorillonite nanocomposites", Current Trends in Inorganic Chemistry, March 2004, Cochin University of Science and Technology, Kochi.

N.N Binitha & S. Sugunan "Alkylation of benzene with 1-octene over pillared clays", National Seminar on Frontiers in Chemistry, March 24-25, 2006, Cochin University of Science and Technology, Kochi.

N.N. Binitha and S. Sugunan, "Selective formation of cumene on pillared clays by isopropylation of benzene", 17th National Symposium on Catalysis (January 2005, Central Salt and Marine Chemical Research Institute, Bhavnagar, Gujarat, India).

Binitha N N, Sugunan S, "Effect of mixed pillaring on the structural and textural properties of montmorillonites", Sixth International Conference on Solvothermal Reactions (ICSTR-6, 2004, University of Mysore).

★★★★★★★★★★★★★★★★★